ISSN 2313–5891 (Online)
ISSN 2304–974X (Print)

Ukrainian Food Journal

Volume 7, Issue 4
2018

Kyiv **Київ**

2018

Ukrainian Food Journal is an international scientific journal that publishes innovative papers of the experts in the fields of food science, engineering and technology, chemistry, economics and management.

Ukrainian Food Journal – міжнародне наукове періодичне видання для публікації результатів досліджень фахівців у галузі харчової науки, техніки та технології, хімії, економіки і управління.

Ukrainian Food Journal is abstracted and indexed by scientometric databases:

Ukrainian Food Journal індексується наукометричними базами:

Index Copernicus (2012)
EBSCO (2013)
Google Scholar (2013)
UlrichsWeb (2013)
CABI full text (2014)
Online Library of University of Southern Denmark (2014)
Directory of Research Journals Indexing (DRJI) (2014)
Directory of Open Access scholarly Resources (ROAD) (2014)
European Reference Index for the Humanities and the Social Sciences (ERIH PLUS) (2014)
Directory of Open Access Journals (DOAJ) (2015)
InfoBase Index (2015)
Chemical Abstracts Service Source Index (CASSI) (2016)
FSTA (Food Science and Technology Abstracts) (2018)
Emerging Sourses Citaton Index (2018)

Ukrainian Food Journal включено у перелік наукових фахових видань України з технічних наук (Наказ Міністерства освіти і науки України № 1609 від 21.11.2013)

Editorial office address:

National University
of Food Technologies
Volodymyrska str., 68
Ukraine, Kyiv 01601

Адреса редакції:

Національний університет
харчових технологій
вул. Володимирська, 68
Київ 01601

e-mail: **ufj_nuft@meta.ua**

Scientific Council of the National University of Food Technologies recommends the Journal for printing. Protocol № 5, 27.12.2018

Рекомендовано вченою радою Національного університету харчових технологій. Протокол № 5 від 27.12.2018.

Ukrainian Food Journal publishes original research articles, short communications, scientific news in the related fields and also literature reviews.

Topics coverage:

Food engineering	Food nanotechnologies
Food chemistry	Food processing
Food microbiology	Economics and management in food industry
Physical property of food	Automation of food processes
Food quality and safety	Food packaging

Periodicity of the journal – 4 isues per year.

Reviewing a Manuscript for Publication. All scientific articles submitted for publication in "Ukrainian Food Journal" are double-blind peer-reviewed by at least two academics appointed by the Editors' Board: one from the Editorial Board and one, not affiliated to the Board and/or the Publisher.

Copyright. Authors submitting articles for publication are expected to provide an electronic statement confirming that their work is not an infringement of any existing copyright and will not indemnify the publisher against any breach of legislation and/or international standards in academic publishing. For the ease of dissemination all papers and other contributions become the legal copyright of the publisher unless agreed otherwise.

Academic ethics policy. The Editorial Board of "Ukrainian Food Journal" strictly follows all internationally acknowledged rules and regulations on academic publishing and academic ethics. For more details on this see: Miguel Roig (2003, 2006) "Avoiding plagiarism, self-plagiarism, and other questionable writing practices. A guide to ethical writing". The Editorial Board suggests all potential contributors of the journal, reviewers and readers to dully follow this guidance in order to avoid misconceptions.

For a **Full guide for All Authors** please visit our website:

http://ufj.ho.ua

International Editorial Board

Contents

Size and morphological features of native starch granules of different botanical origin

Vladimir Litvyak

Scientific and Practical Centre for Foodstuffs of the National Academy of Sciences of Belarus, Minsk, Republic of Belarus

Keywords:

Starch
Morphology
Grain
Size
Shape

Article history:

Received 12.03.2018
Received in revised form 24.06.2018
Accepted 27.12.2018

Corresponding author:

Vladimir Litvyak
E-mail: besserk1974@mail.ru

DOI:
10.24263/2304-974X-2018-7-4-3

Abstract

Introduction. When developing modern technologies for deep processing of plant starch-containing raw materials, the most important aspect is the study of the size and morphological structure of starch grains.

Materials and methods. Native potatoes, corn, tapioca, wheat, rice, rye, peas, amaranth, barley, sorghum, triticale and oats starches were studied. Scanning electron micrographs of starch grains were obtained using a scanning electron microscope LEO 1420. Metallization of native starch preparations was carried out with gold in the EMITECH K 550X vacuum system.

Results and discussion. The sizes and morphological features of the grains of native starch of different botanical origin were investigated. The main structural characteristic of the structure of native starch, which determines its physicochemical properties, is starch grain (granule). There was revealed a large variety of forms of starch grains: regular and irregular oval, rounded, multi-faceted. The size of starch grains varied within 60,0–0,5 microns. Depending on the average size, starchy grains can be arranged in a descending row: potato (21,7±1,22), rye (21,2±2,36), pea (20,4±2,57), chickpea (14,8±0,93), triticale (13,2±1,75), wheat (12,4±1,90), sorghum (11,0±0,76), barley (10,9±1,15), tapioca (10,6±0,50), corn (9,8±0,42), oat (7,39±0,87), rice (5,3±0,29), amaranth (1,1±0,04). The largest size of starch grains was found in potato starch, and the smallest size in amaranth starch. It was established that in 7 native starches (sorghum, barley, oat, pea, chickpea, amaranth and corn) the distribution of starch grains is monomodal in size (1-fractional), in 4 (wheat, triticale, potato and tapioca) – bimodal (2-fractional), in 2 (rye and rice) – trimodal (3-fractional).

The source of starch-containing raw materials and the peculiarities of the structural organization of native starch largely determine the technological methods used for the most complete and gentle extraction of the seeds of native starch from the plant cell.

The main structural characteristic of the structure of native starch, which determines its properties, is starch grain. Features of the size and shape of starch grains cause the manifestation of the following properties of starch: molecular weight, the amount of bound moisture, temperature of gelatinization, the ratio of starch fractions and density of their laying in crystalline areas, the rheological characteristics of starch paste.

Conclusion. The morphology of starch grains of different botanical origin varies significantly in size (60,0–0,5 μm) and shape (round, oval, irregular shape). The size of starch granules is the main structural characteristic determining the physicochemical properties of starch pastes.

Introduction

The range of products of starch-treacle production is quite large and amounts to several hundred items [1–36]. The main raw material for the production of starch and starch products are potatoes [6, 34], corn [19, 35], wheat [12, 17], rye [2], barley [13, 22], rice [4, 21], buckwheat [2, 5], tapioca [24, 26], lentils [36], banana [31] etc. In addition to native starch, molasses of various carbohydrate compositions (low-sugared, caramel, high-sugared, maltose, dextrin-maltose) maltose, maltin, crystalline glucose, as well as glucose, glucose-fructose and fructose syrups are produced [1]. A large range of modified starches and dextrins is available [3, 20].

Starch and starch products play an important role in the national economy [1–3]. They are widely used in many branches of food industry: confectionery, bakery, canning, food concentrates, dairy, meat, as well as in other industries: textile, paper, leather, printing, pharmaceutical, metallurgy, and household. In addition, starch and its derivatives are used in chemical industry in the production of sorbitol, lactic acid, glycerol, acetone, butanol, varnishes, various films, etc.

When developing modern technologies for deep processing of vegetable starch-containing raw materials (technologies for obtaining native and modified starches), the most important aspect is the study of the size and morphological structure of starch granules.

Despite the great interest shown by the scientific community to fundamental and applied research in the field of starch and starch products, up to now there are no systematic studies of the morphological characteristics of starch granules (size and shape) isolated from plant materials of various botanical origin.

The aim is to study the size and morphological features of native starch granules of different botanical origin.

Materials and methods

Materials

The objects of the research are native starches: potato starch according to the Technical Normative Legal Act (TNPA), corn starch according to TNPA, tapioca starch according to TNPA, wheat starch according to TNPA, rice starch according to TNPA, rye starch according to TNPA, pea starch according to TNPA, amaranth starch according to TNPA, barley starch according to TNPA, sorghum starch according to TNPA, triticale starch according to TNPA, oat starch according to TNPA [37, 38].

Methods

Scanning Electron Microscopy (SEM)

Sample preparation. Metallization of native starch preparations was carried out with gold in the EMITECH K 550X vacuum unit.

Analysis. Scanning electron micrographs of native starch granules were obtained using a LEO 1420 scanning (raster) electron microscope (Germany) (Figure 1).

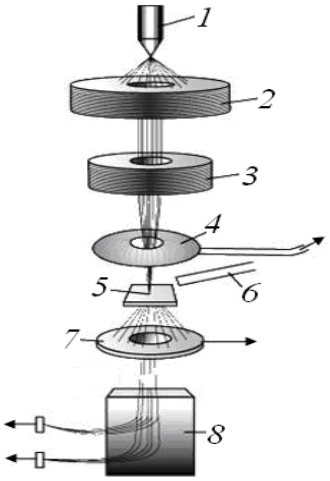

1 – electron source;
2 – accelerating system;
3 – magnetic lens;
4 – deflecting coils;
5 – sample;
6 – reflected electron detector;
7 – ring detector;
8 – analyzer.

Figure 1. Scanning electron microscope

The principle of operation of the scanning electron microscope consists in scanning the sample surface with a focused electron beam and analyzing particles reflected from it and X-ray radiation resulting from the interaction of electrons with matter. In a scanning electron microscope, an electron beam (electron probe) is focused by electromagnetic lenses of a capacitor and a lens [39, 40]. A special device – deflector deflects the electron beam (primary electrons), which slides on the surface (raster). The secondary electrons (reflected from the surface) are perceived by the detector and are focused on the screen of the scanning electron microscope creating a three-dimensional image. The scanning electron microscope allows working in a wide range of magnifications from ×10 (which is equivalent to an increase in a strong hand-held lens) to ×1000000, which is ≈ 500 times the increase limit of the best optical microscopes. The scanning surface is necessarily sprayed with metal: platinum, gold, silver, aluminum [39, 40].

Statistical Analysis

The dimensions of the starch granules were estimated using computer aids according to generally accepted procedures. Using MS Excel, the average values of starch granule size were calculated and the boundaries of the confidence interval were determined, and graphs of the distribution of starch granules by size [38] were plotted.

Results and discussion

Results

Granules of native starch, isolated from plant cells of various botanical origin, vary considerably in form and size, which largely determines the technological features of starch production, its further modification and subsequent use, if necessary [2, 9, 15].

Scanning electron micrographs of native starch granules of various botanical origin: potato, corn, tapioca, wheat, rice, rye, pea, amaranth, barley, sorghum, triticale are shown in Figures 2–5. Figures 6 and 7 give the granulometric analysis of native starch granules of

different botanical origin (the distribution of native starch granules by size). Granulometric analysis of native starch granules is based on the results given in Table 1. Table 1 shows the average, minimum and maximum granule sizes of native starches of different botanical origin with statistical processing characteristics of the sample studied.

The analysis of the morphological characteristics of native starch granules has shown that starchy granules predominantly have the following form: in rye and barley, oval and round, in wheat and triticale, regular oval and round, in pea and potato – irregular oval, in oat and tapioca – irregular round, in rice and corn – irregular polyhedral, in sorghum – oval and polyhedral, in chick pea – regular oval, in amaranth – polyhedral (Figure 2–5).

It has been established that the average granule size of native rye, wheat, triticale, sorghum, barley, rice, pea, chick pea, amaranth, tapioca, potato, corn, oat will accordingly be: 21,2 (±2,36); 12,4 (±1,90); 13,2 (±1,75); 11,0 (±0,76); 10,9 (±1,15); 5,3 (±0,29); 20,4 (±2,57); 14,8 (±0,93); 1.1 (±0,04); 10,6 (±0,50); 21,7 (±1,22); 9,8 (±0,42); 7,39 (±0,87) μm (Table 1). The minimum and maximum granule sizes of native rye, wheat, triticale, sorghum, barley, rice, pea, chick pea, amaranth, tapioca, potato, corn vary between: 4,9–42,8; 2,8–27,1; 4,0–30,7; 3,5–21,7; 3,0–21,4; 2,7–7,9; 6,1–32,3; 6,0–25,6; 0,5–1,5; 2,8–31,2; 7,7–60,0; 3,6–19,2; 3,96–14,91 μm (Table 1).

According to the average size of the starch granules all the studied native starches can be arranged in a descending series (→): potato → rye → pea → chick pea → triticale → wheat → sorghum → barley → tapioca → corn → oat → rice → amaranth. The largest size of starch granules was found in potato starch, and the smallest one – in amaranth starch.

In seven types of native starches (sorghum, barley, oat, pea, chick pea, amaranth and corn), the distribution of starch granules in size is mono modal (one fraction is clearly identified), in four types of native starches (wheat, triticale, potato and tapioca), distribution of starch granules in sizeis bimodal (two-fraction), and in two types of native starches (rye and rice), the distribution of starch granules in size is tri-modal (three-fraction) (Figures 6 and 7).

Discussion

Starch-containing raw materials for the production of native potato starch are tubers of the *Solanum tuberosum* (L.) potato plant [2, 3], native corn (maize) starch – the *Zea mays* (L.) corn [21, 23], native tapioca starch – tubers of the *Manihot utilissima* (L.) and *Manihot palmate* (L.) plants [2, 26], native sorghum starch – the waxlike *Red leoti* (L.) sorghum plant [2], native wheat starch – grains of the *Triticum* genus plants [2, 16], native triticale starch – grains of the cereal triticale plant (*Tritikale*, from Latin «*triticum*» – wheat and from Latin «*secale*» – rye) – a hybrid of wheat and rye [2], and native rye starch – grains of the *Secale cereale* (L.) plants [2], native barley starch – grains of the *Hordeum vulgare* (L.) plant [2, 13], native oat starch – grains of the *Avena sativa* (L.) oat plant [2, 5], native rice starch – grains of the *Oryza sativa* (L.) rice plants [2, 21], native pea starch – seeds of the *Pisum sativum* (L.) plants [2], native amaranth starch – the Joseph's-coat amaranth *Amaranthus tricolor* (L.) or other plants of the *Amaranthus* genus [2], native chick pea starch – the *Cicer arietinum* (L.) chick pea [2].

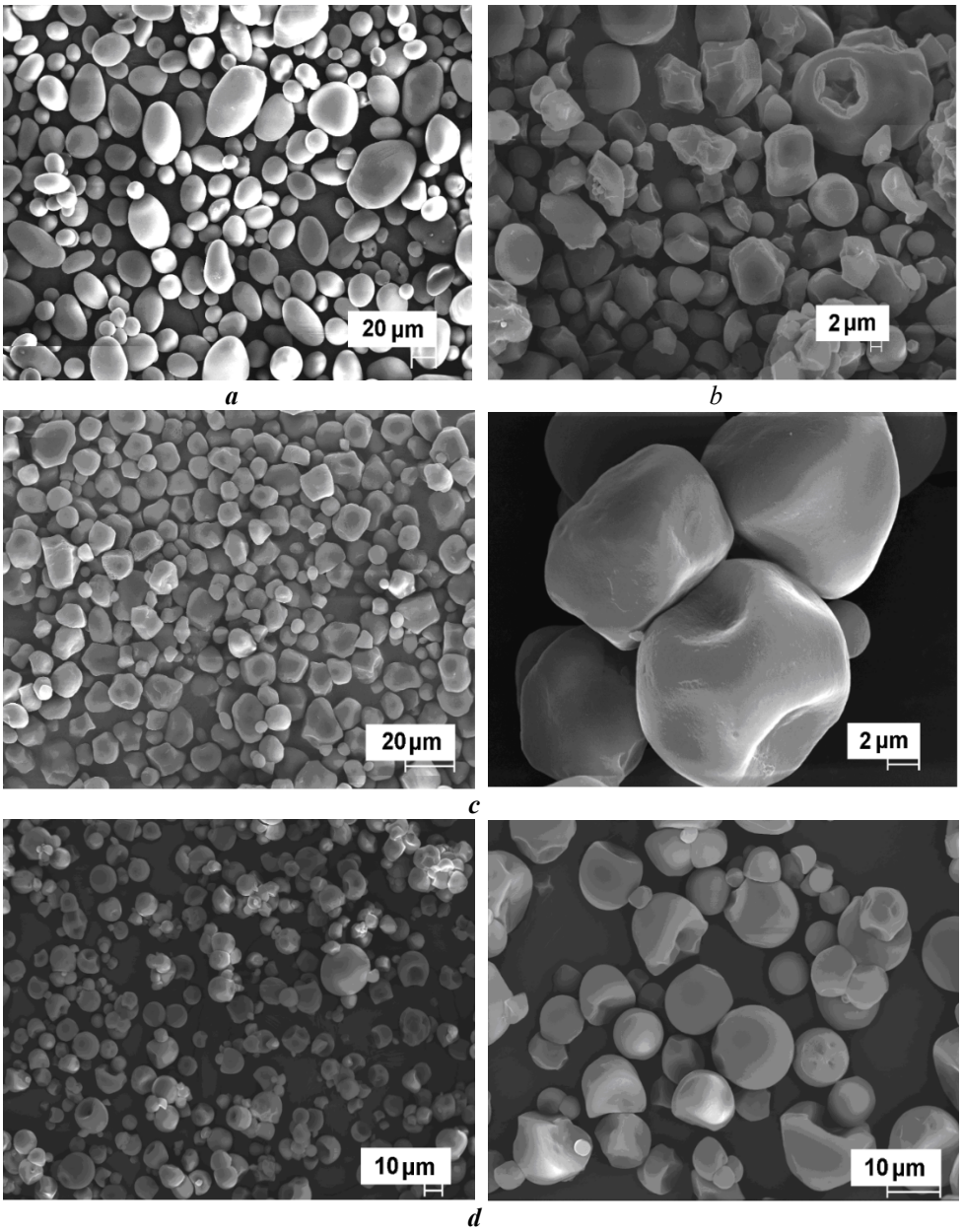

Figure 2. Scanning electron micrographs of native starch granules: *a* – potato, *b* – oats, *c* – corn, *d* – tapioca

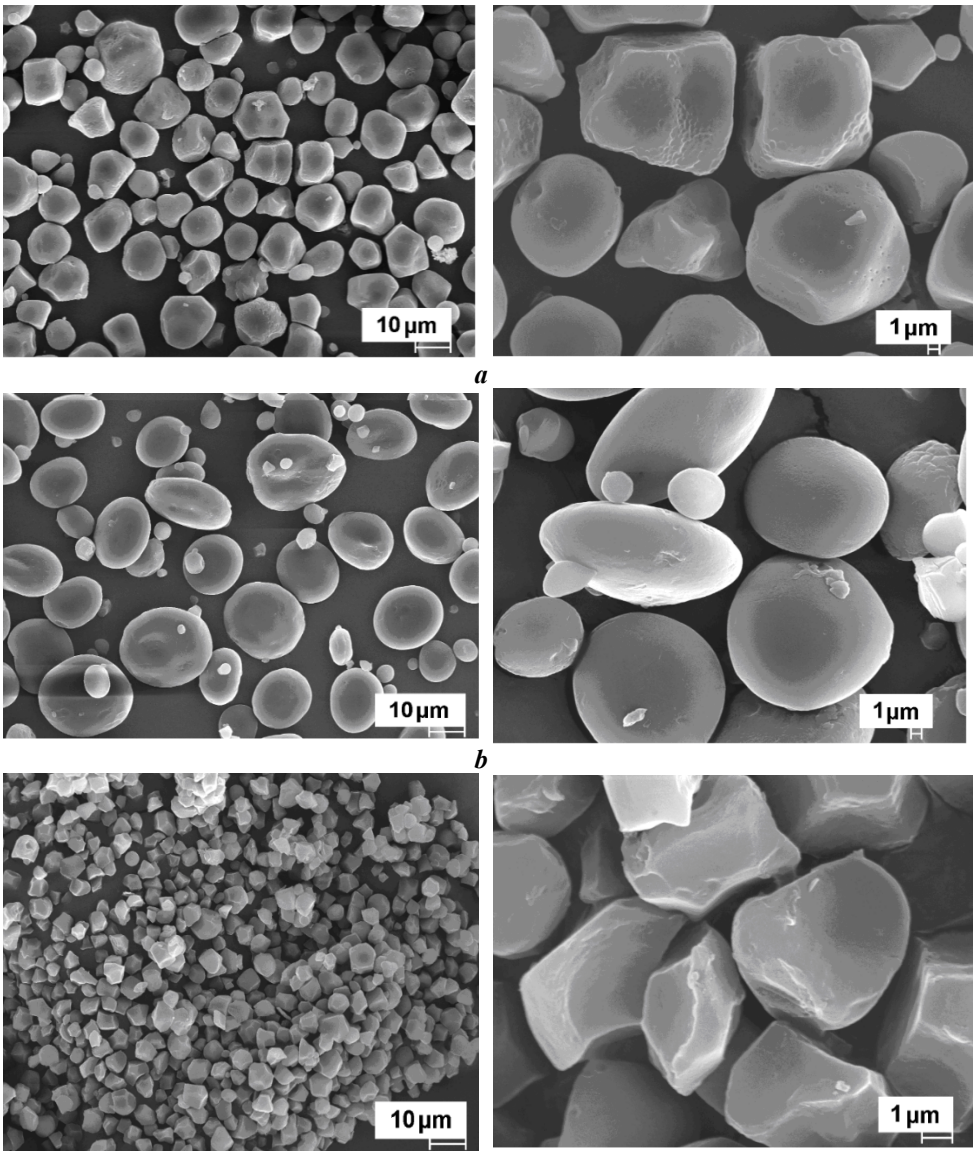

Figure 3. Scanning electron micrographs of native starch granule: *a* – sorghum, *b* – wheat, *c* – rice

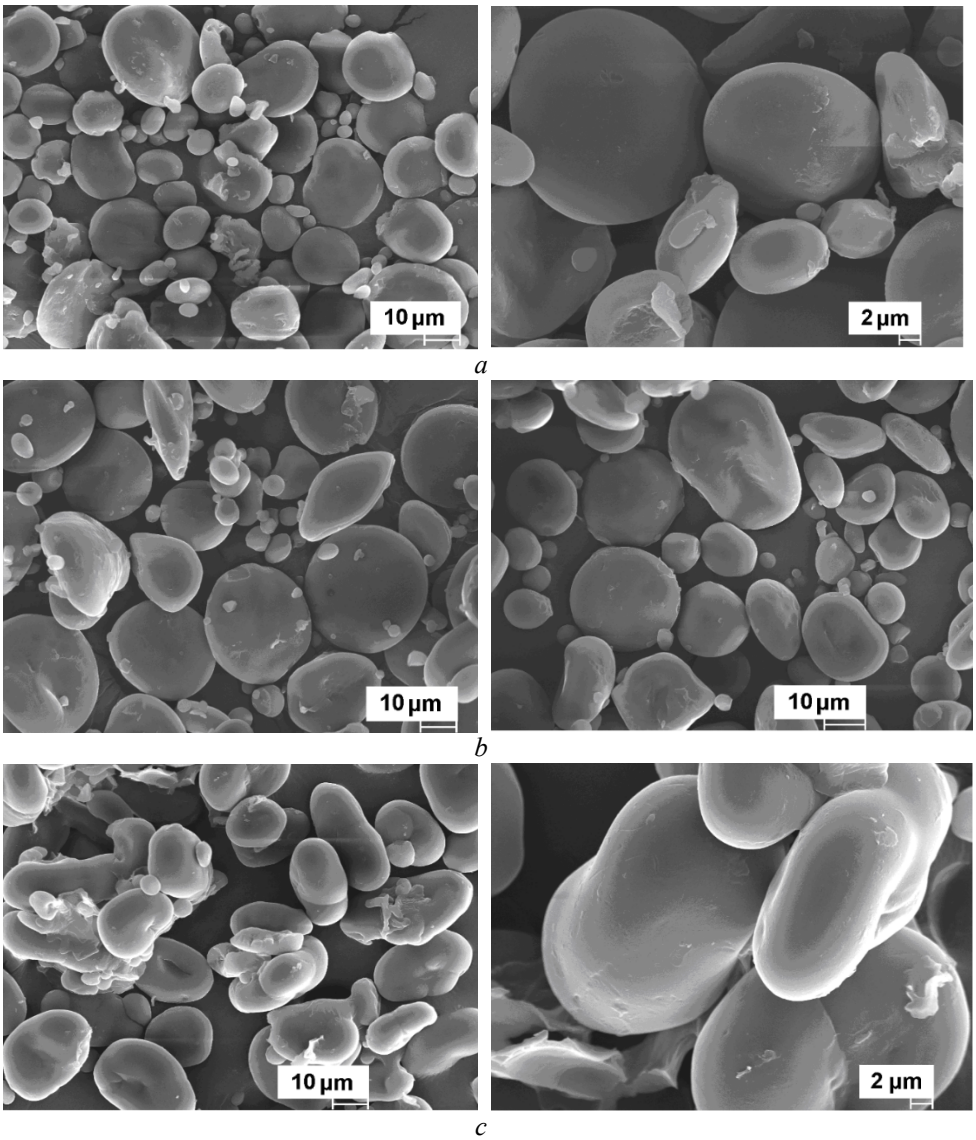

Figure 4. Scanning electron micrographs of native starch granules: *a* – triticale, *b* – rye; *c* – pea

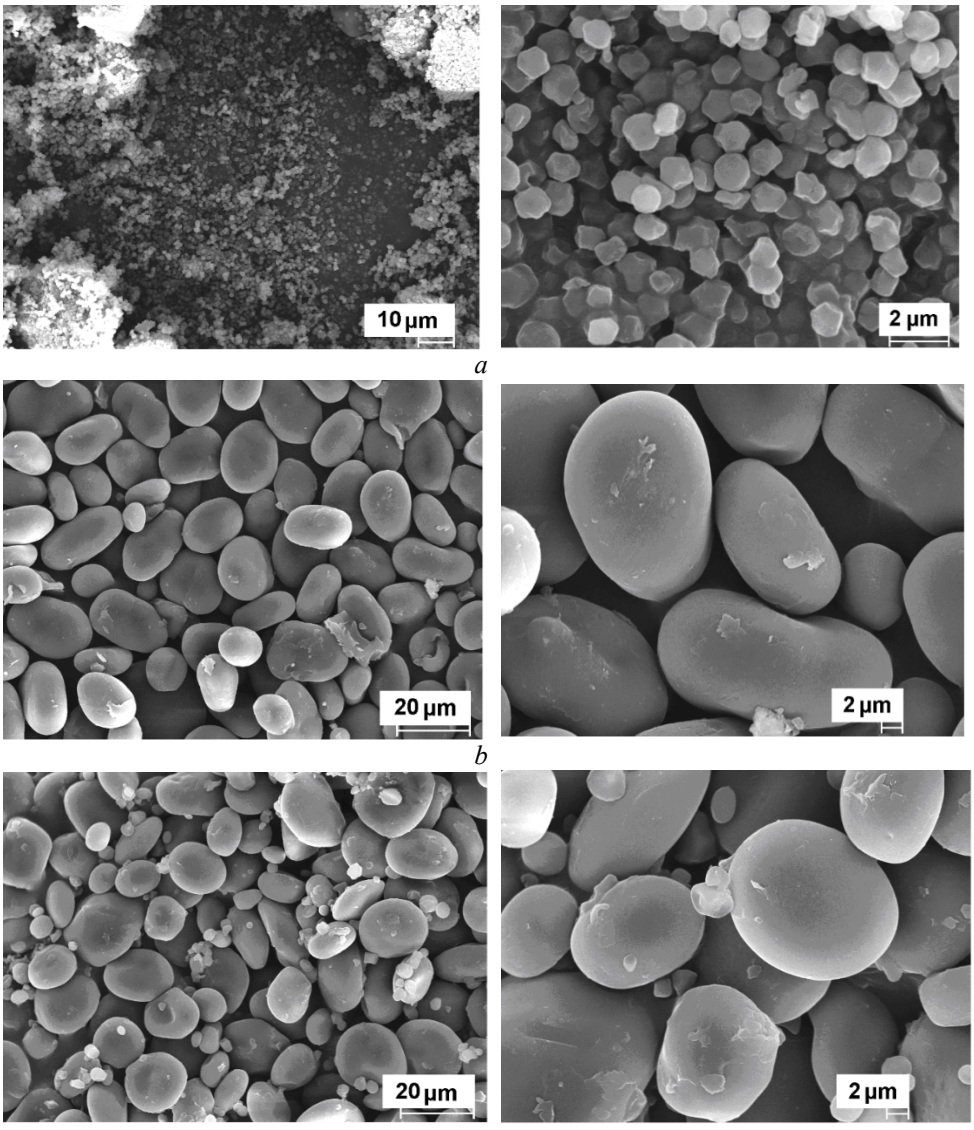

Figure 5. Scanning electron micrographs of native starch grains: *a* – amaranth, *b* – chick pea, *c* – barley

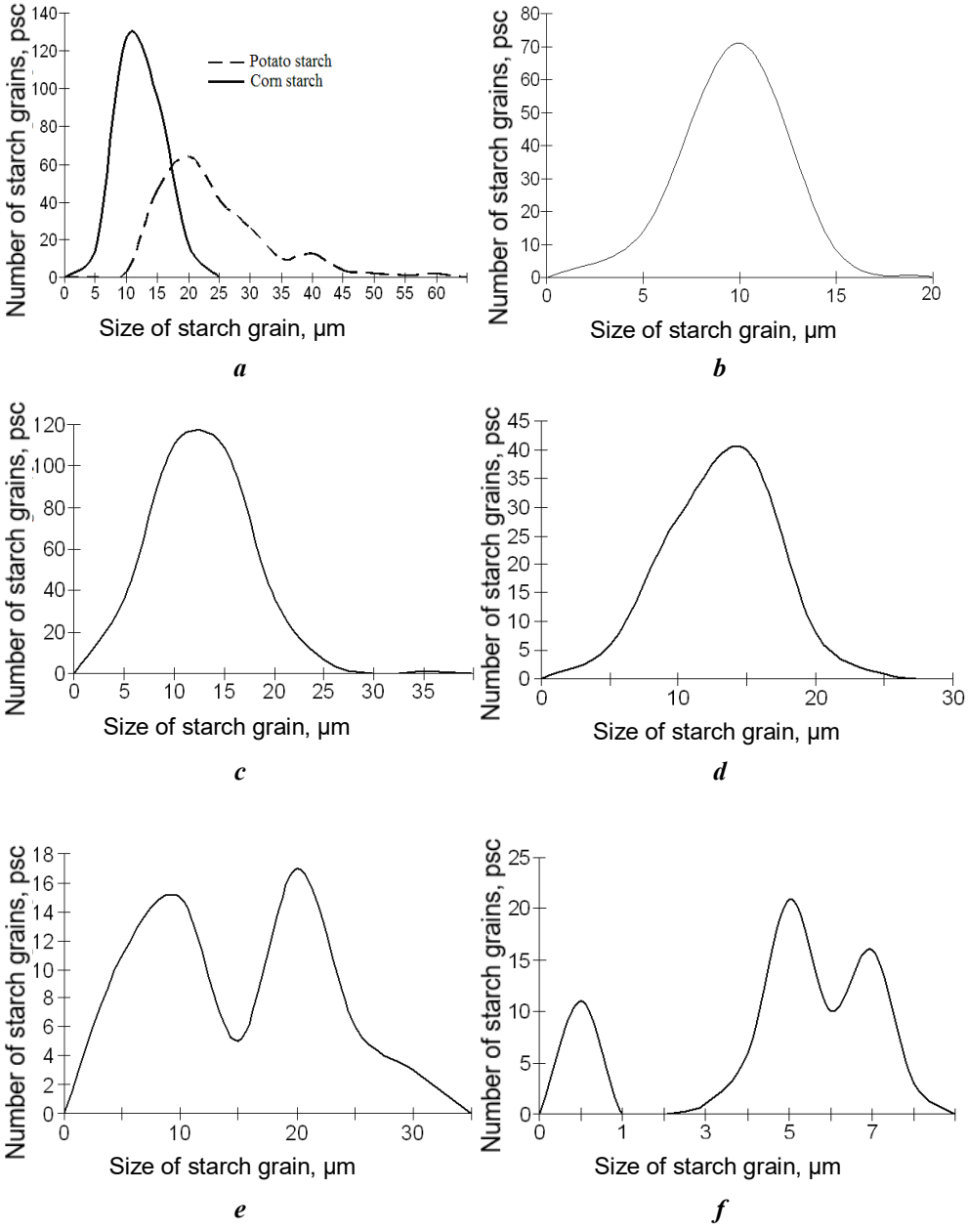

Figure 6 – Granulometric analysis of native starch grains:
***a* – potato and corn, *в* – oat, *c* – tapioca, *d* – sorghum, *e* – wheat, *f* – rice**

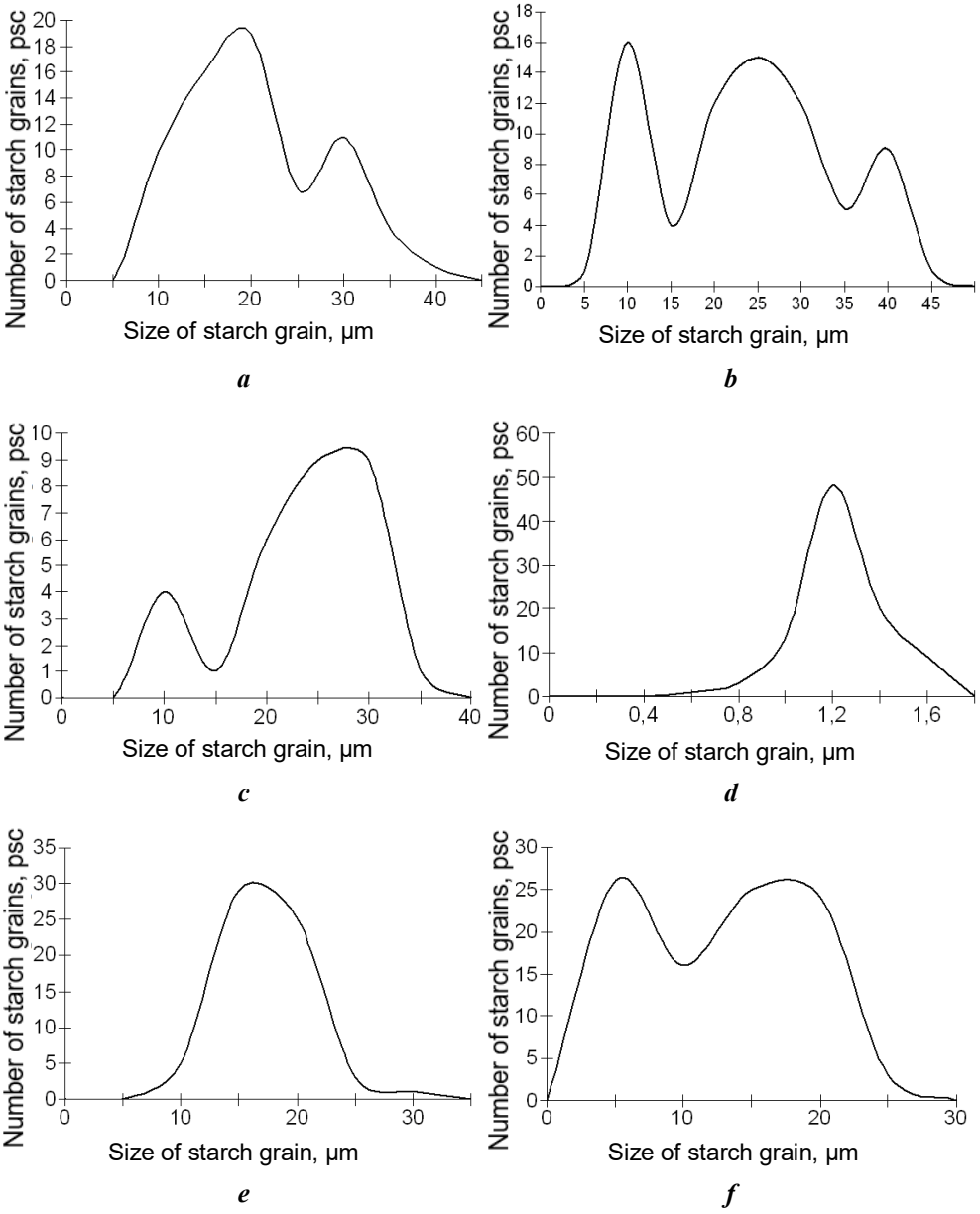

Figure 7. Granulometric analysis of native starch granules:
***a* – triticale, *b* – rye, *c* – pea, *d* – amaranth, *e* – chick pea, *f* – barley**

Table 1

Morphological characteristic of native starches of different botanical origin

Parameters	Native starches					
	1	**2**	**3**	**4**	**5**	**6**
$d_{aver.}$	21,2	12,4	13,2	11,0	10,9	5,3
Standard error	1,19	0,97	0,88	0,38	0,58	0,15
Median	21,8	11,3	12,7	11,0	11,4	5,2
Mode	22,4	2,8	13,1	12,2	4,5	4,1
Standard deviation	10,27	7,31	7,24	3,49	5,63	1,11
Sample variance	105,4	53,5	52,48	12,19	31,72	1,23
Excess	–0,9	–1,27	–0,67	0,16	–1,34	–0,59
Asymmetry	0,1	0,26	0,51	0,09	0,1	0,06
Interval	37,9	24,3	26,7	18,2	18,4	5,2
d_{min}	4,9	2,8	4,0	3,5	3,0	2,7
d_{max}	42,8	27,1	30,7	21,7	21,4	7,9
Reliability level (95,0%)	2,36	1,90	1,75	0,76	1,15	0,29
Upper limit	23,5	14,3	15	11,7	12,1	5,6
Lower limit	18,8	10,5	11,5	10,2	9,8	5

Parameters	Native starches						
	7	**8**	**9**	**10**	**11**	**12**	**13**
$d_{aver.}$	20,4	14,8	1,1	10,6	21,7	9,8	7,39
Standard error	1,25	2,46	0,02	0,26	0,62	0,21	0,43
Median	20,8	14,5	1,1	10,1	19,0	9,7	6,57
Mode	н/д	15,8	1,2	8,8	17,1	12,7	5,09
Standard deviation	6,87	3,69	0,18	4,43	8,99	3,38	2,56
Sample variance	47,22	13,59	0,03	19,63	80,88	11,44	6,57
Excess	0,02	0,17	0,71	0,66	2,2	–0,49	0,66
Asymmetry	–0,74	0,07	–0,32	0,54	1,4	0,37	1,04
Interval	26,3	19,6	1,0	28,4	52,3	15,5	10,96
d_{min}	6,1	6,0	0,5	2,8	7,7	3,6	3,96
d_{max}	32,3	25,6	1,5	31,2	60,0	19,2	14,91
Reliability level (95%)	2,57	0,93	0,04	0,50	1,22	0,42	0,87
Upper limit	23,0	15,7	1,2	11,1	22,9	10,2	8,25
Lower limit	17,8	13,9	1,1	10,1	20,5	9,3	6,52

Note: **1** – rye, **2** – wheat, **3** – triticale, **4** – sorghum, **5** – barley, **6** – rice, **7** – pea, **8** – chick pea, **9** – amaranth, **10** – tapioca, **11** – potato, **12** – corn, **13** – oat

Native starch is a natural polymer in which monomers (the residues of α-D-glucopyranose) are bound by α-(1→4)- and α-(1→6)-glucoside bonds to form amylose (a linear polysaccharide) and amylopectin (a branched polysaccharide structure). Starch fractions (amylose and amylopectin) are compactly packaged into starch grains (or granules) [9, 15].

The source of starch-containing raw materials and the peculiarities of the structural organization of native starch largely determine the technological methods used for maximally complete and gentle extraction of the granules of native starch from the plant cell. To obtain native starch it is necessary to prepare vegetable starch containing raw materials for processing, to destroy the plant cell, to extract the native starch, to wash it with pure water to

remove the accompanying impurities, to dehydrate, to dry, to prepack and pack. It is known that there exist generally accepted methods of processing potatoes to obtain starch using a variety of technological schemes and various types of technological equipment. However, regardless of the equipment design, each of these methods includes the production stages that are characteristic of all modern technologies for the obtaining of potato starch: the preparation of potatoes for processing, grinding, the isolation of potato (cell) juice and pulp, the purification of starch, its dehydration and drying [2].

At present, the most rational method is the preparation of native potato starch, which involves preparation for processing and shredding of starch-containing raw materials, the use of a multistage hydro-cyclone unit which separates finely ground starch-based raw materials into a starch suspension and a mixture of pulp with other by-products. Subsequently, a partial thickening of the starch suspension is carried out, followed by dehydration, drying and removal of the metal-magnetic impurities, prepacking, packaging, labeling and transportation of the starch [2].

Methods of corn grain processing to obtain starch include five obligatory steps: preliminary softening of the corn grain structure by soaking it in an acid medium, isolating and washing the embryo, isolating and washing the pulp, isolating and concentrating the protein, washing the starch and drying it [2].

It is possible to improve the technology of native starch extraction in the most optimal way and also to abandon the technology of chemical modification in many respects. For that purpose it is necessary to apply the fundamental scientific principle that «the structure of a substance determines its properties» to the deep processing technologies for starch-containing plant raw materials.

According to our results, as well as the data obtained by other researchers [42, 43], starch granules have an oval, spherical or irregular shape, their diameter varies from 0,001 to 0,2 mm. Starchy granules are divided into simple and complex: simple granules are homogeneous formations; complex ones are a combination of smaller particles. The density of starch is an average of 1,5 kg/m^3.

The analysis of the peculiarities of the structure of native starch makes it possible to assume that the main structural characteristic of the native starch which determines its properties is starch grain (granule). Therefore the features of the size and shape of starch granules determine the manifestation of the following properties (characteristics) of starch:

1. The amount of bound moisture (the larger the starch granule is, the more bound moisture there is in starch and vice versa).
2. The temperature of gelatinization (the larger the starch granule is, the less its gelatinization temperature is and vice versa).
3. The ratio of starch fractions of the branched fraction of amylopectin and linear amylose (the formation of a starch granule is due to the interaction of linear sections of amylopectin with each other or with amylose).
4. Rheological characteristics of starch paste (viscosity of starch paste is due to the ratio of starch fractions of amylopectin and amylose).

Conclusions

1. The main structural characteristic of native starch, which determines its physical-chemical properties, is a starch granule.
2. A wide variety of forms of starch granules has been revealed. Starchy granules were found to be of a regular and irregular oval form, of a round form and a polyhedral one.

3. The sizes of starch granules range within the following limits: 60,0–0,5 microns. Depending on the average size of the starch granules the studied native starches can be arranged in a descending series: potato (21,7 ±1,22), rye (21,2 ±2,36), pea (20,4 ±2,57), (14,8 ±0,93), triticale (13,2 ±1,75), wheat (12,4 ±1,90), sorghum (11,0 ±0,76), barley (10,9 ±1,15), tapioca (10,6 ±0,50), corn (9,8 ±0,42), oat (7,39 ±0,87), rice (5,3 ±0,29), amaranth (1,1 ±0,04). The largest size of starch granules was found in potato starch, and the smallest one – in amaranth starch.
4. It was found that in 7 native starches (sorghum, barley, oat, pea, chick pea, amaranth and corn) the distribution of starch granules in size is mono modal (1-fractional), in the four of them (wheat, triticale, potato and tapioca) – bimodal (2-fractional), in the two of them (rye and rice) – tri modal (3-fractional).

References

1. Gliuk N.G., Zhushman A.I., Ladur T.A., Shtyrkova E.A. (1985), *Krakhmal i krakhmaloprodukty*, Agropromizdat, Moscow.
2. Andreev N.R. (2001), Osnovy proizvodstva nativnykh krakhmalov, *Pishchepromizdat*, Moscow.
3. Zhushman A.I. (2007), Modifitsirovannye krakhmaly, Pishchepromizdat, Moscow.Nikhil K. Chrungoo, Ayam Gangarani Devi. (2015), Morphological and Rheological Properties of Starches Separated from Cultivars of Rice (*Oryza sativa* L.) from North East India, ***American Journal of Plant Sciences***, 6, pp. 2019–2031.
4. Makella M.J., Laakso S. (2006), Studies on Oat Starch with a Celloscope: Granule Size and Distribution, *Starch/Starke*, 36, pp. 159–163.
5. Sylvia de Pater, Martien Caspers, Marijke Kottenhagen, Henk Meima, Renaldo Ter Stege, Nick de Vetten (2006), Manipulation of starch granule size distribution in potato tubers by modulation of plastid division, *Plant Biotechnology Journal*, 4, pp. 123–134.
6. Jane J-L., Kasemsuwan T., Leas S., Zobel H., Robyt J.F. (1994), Anthology of starch granule morphology by scanning electron microscopy, *Starch/Starke*, 46, pp. 121–129.
7. Malinski E., Daniel J.R., Zhang X.X., Whistler R.L. (2003), Isolation of small starch granules and determination of their fat mimic characteristics, *Cereal. Chem.*, 80, pp. 1–4.
8. Pérez S., Bertoft E. (2010), The molecular structures of starch components and their contribution to the architecture of starch granules: a comprehensive review, *Starch/Starke*, 62, pp. 389–420.
9. Buleon A., Colonna P., Planchot V., Ball S. (1998), Starch granules: structure and biosynthesis, *Int. J. Biol. Macromol.*, 23, pp. 85–112.
10. Sahlstrom S., Brathen E., Lea P., Autio K. (1998), Influence of starch granule size distribution on bread characteristics, *J. Cereal. Sci.*, 28, pp. 157–164.
11. Yonemoto P.G., Calori D.M.A., Franco C.M.L. (2007), Effect of granule size on the structural and physico- chemical characteristics of wheat starch, *Ciênc. Tecnol. Aliment.*, 27, pp. 761–771.
12. Takeda Y., Takeda C., Mizukami H., Hanashiro I. (1999), Structures of large, medium and small starch granules of barley grain, *Carbohyd. Polym.*, 38, pp. 109–114.
13. Swinkels J.J.M. (1985), Composition and Properties of commercial Native Starches, *Starch/Starke*, 37. – pp. 1–5.
14. Zobel H.F. (1988), Molecules to Granules: A Comperehensive Starch Review, *Starch/Starke*, 40, pp. 44–50.
15. Dengate H., Meredith P. (1984), Variation in size distribution of starch granules from wheat grain, *J. Cereal. Sci.*, 2, pp. 83–90.
16. Stoddard F.L. (1999), Survey of starch particle-size distribution in wheat and related species, *Cereal. Chem.*, 76, pp. 145–9.
17. Lindebloom N, Chang P.R., Tyler R.T. (2004), Analytical, Biochemical and Hysiochemical Aspects of Starch Granule Size, with Emphasis on Small Granule Starches: A Review, *Starch/Starke*, 56, pp. 89–99.
18. Uarrota V.G., Amante E.R., Demiate I.M., Vieira F., Delgadillo I., Maraschin M. (2013), Physicochemical, thermal, and pasting properties of flours and starches of eight Brazilian maize landraces (*Zea mays* L.), *Food Hydrocolloid*, 30, pp. 614–624.
19. Neelam K., Viajay S., Lalit S. (2012), Various techniques for the modification of starch and the application of its derivatives, *Int. Res. J. Pharm*, 3, pp. 25–31.

20. Hebeish A., El-Rafie M.H., El-Sisi F., Abdel Hafiz F., Abdel–Rahman A.A. (1994), Oxidation of maize and rice starches using potassium permanganate with various reductants, *Polym. Degrad. Stab*., 43, pp. 363–372.
21. Halal S.L.M., Colussi R., Pinto V.Z., Bartz J., Radunz M., Carreño N.L.V., Dias, A.R.G., Zavareze E.R. (2015), Structure, morphology and functionality of acetylated and oxidised barley starches, *Food Chem*., 168, pp. 247–256.
22. Ribeiro L.S., Cordoba L.P., Colman T.A., Oliveira C.S., Andrade M.M.P., Schnitzler E. (2014), Influence of some sugars on the thermal, rheological and morphological properties of "pinhão" starch, *J.Therm. Anal. Calorim*., 117, pp. 935–942.
23. Malucelli L.C., Lacerda L.G., Carvalho Filho M.A.S., Fernández D.E.R., Demiate I.M., Oliveira C.S., Schnitzler, E. (2015), Porous waxy maize starch, *J. Therm. Anal. Calorim*., 120, pp. 525–532.
24. Colman T.A.D., Demiate I.M., Schnitzler E. (2014), The effect of microwave radiation on some thermal, rheological and structural properties of cassava starch, *J. Therm. Anal. Calorim.*, 115, pp. 2245–2252.
25. Beninca C., Colman T.A.D., Lacerda L.G., Carvalho-Filho M.A.S., Demiate I.M., Schnitzler E. (2013), Thermal, rheological, and structural behaviors of natural and modified cassava starch granules, with hypochlorite solutions, *J. Therm. Anal. Calorim.,* 111, pp. 2217–2222.
26. Oliveira C.S., Andrade M.M.P., Colman T.A.D., Costa F.J.O.G., Schnitzler E. (2014), Thermal, structural and rheological behaviour of native and modified waxy corn starch with hydrochloric acid at different temperatures, *J. Therm. Anal. Calorim*, 115, pp. 13–18.
27. Beninca C., Demiate I.M., Lacerda L.G., Carvalho Filho M.A.S., Ionashiro M., Schnitzler E. (2008), Thermal behavior of corn starch granules modified by acid treatment at 30 and 50 °C, *Ecletica Quim.,* 33, pp. 13–18.
28. Liu X., Ma H., Yu L., Chen L., Tong Z., Chen P. (2014a), Thermal–oxidative degradation of high–amylose corn starch, *J. Therm. Anal. Calorim*., 115, pp. 659–665.
29. Pietrzyk S., Fortuna T., Królikowska K., Rogozínska E., Labanowska M., Kurdziel M. (2013), Effect of mineral elements on physicochemical properties of oxidised starches and generation of free radicals, *Carbohydr. Polym.* 97, pp. 343–351.
30. Carmona-Garcia R., Sanchez-Rivera M.M., Mendez-Montealvo G., Garza-Montoya B., Bello-Perez L.A. (2009), Effect of the cross–linked reagent type on some morphological, physicochemical and functional characteristics of banana starch (*Musa paradisíaca*), *Carbohydr. Polym*., 76, pp. 117–122.
31. Liu J., Wang B., Lin L., Zhang J., Liu W., Xie J., Ding Y. (2014b), Functional, physicochemical properties and structure of cross–linked oxidized maize starch, *Food Hydrocolloids*, 36, pp. 45–52.
32. Kuakpetoon D., Wang Y.J. (2001), Characterization of different starches oxidized by hypochlorite, *Starch/Stärkë*, 53, pp. 211–218.
33. Zhou F., Liu Q., Zhang H., Chen Q., Kong B. (2016), Potato starch oxidation induced by sodium hypochlorite and its effect on functional properties and digestibility, *Int. J. Biol. Macromol*., 84, pp. 410–417.
34. Spier F., Zavareze E.R., Silva R.M., Elias M.C., Dias A.R.G. (2013), Effect of alkali and oxidative treatments on the physicochemical, pasting, thermal and morphological properties of corn starch, *J. Sci. Food Agric*., 93, pp. 2331–2337.
35. Joshi M., Aldred P., McKinight S., Panozzo J.F., Kasapis S., Adhikari R., Adhukari, B. (2013), Physicochemical and functional characteristics of lentil starch, *Carbohydr. Polym.*, 92, pp. 1484–1496.
36. Joint FAO/WHO Expert Committee on Food Additives (JECFA) (1992), *Compendium of food additive specifications, vol. 1 and 2. FAO Food and Nutrition Paper 52/1,* Food and Agriculture Organization of the United Nations, Rome.
37. National Academy of Sciences (1996*), Food chemicals codex, 4th edn., National Academy Press,* Washington.
38. McMullan D. (1988), Von Ardenne and the scanning electron microscope, *Proc Roy Microsc Soc*, 23, pp. 283–288.
39. Mignot, Christophe (2018), Color (and 3D) for Scanning Electron Microscopy, *Microscopy Today*, 26(3), pp. 12–17.
40. Rokitskii P.F. (1973), *Biologicheskaia statistika*, Minsk.
41. Litviak V.V., Ospankulova G.Kh., Shaimerdenova D.A., Iurkshtovich N.K., Butrim S.M., Rosliakov Iu.F. (2016), *Atlas: morfologiia polisakharidov*, EDIGE, Astana.
42. Litviak V.V., Rosliakov Iu.F., Butrim S.M., Kozlova L.N. (2013), *Krakhmal i krakhmaloprodukty: monografiia*, Krasnodar.

Chemical composition and application of flowers of false acacia (*Robinia pseudoacacia* L.)

Stanko Stankov[1], Hafize Fidan[1], Tanya Ivanova[1], Albena Stoyanova[1], Stanka Damyanova[2], Mykola Desyk[3]

1 – University of Food Technologies, Plovdiv, Bulgaria
2 – University of Russe, Branch - Razgrad, Bulgaria
3 – National University of Food Technologies, Kyiv, Ukraine

Keywords:

Robinia
pseudoacacia
Flower
Extracts
Chemical
Composition

Article history:

Received 13.06.2018
Received in revised form 27.08.2018
Accepted 27.12.2018

Corresponding author:

Hafize Fidan
E-mail:
hafizefidan@abv.bg

DOI: 10.24263/2304-974X-2018-7-4-4

Abstract

Introduction. The study was carried out to determine the chemical composition and biological activity of false acacia flowers and their products (concrete and syrups) grown in Bulgaria.

Materials and methods. Concrete was obtained by extraction with n-hexane and its chemical composition was determined by GC-MS. Syrups with different concentrations have been obtained and their polyphenols content, antimicrobial and antioxidant activity were established.

Result and discussion. The yield of concrete was 1.06% and the major constituents of the concrete are as follows: n-nonacosane (25.18%), n-heptacosane (20.10%), α-linolenic acid (5.97%), n-pentacosane (4.98%), palmitic acid (4.92%), diisooctyl phthalate (4.05%), hexahydrofarnesyl acetone (3.86%), linoleic acid (3.64%), isopropyl myristate (3.47%), and n-hentriacontane (3.39%). The total aliphatic hydrocarbons constituted the highest percentage of the component of the concrete constituting 61.50%. *The minerals identified as biggest content in the tested samples of false acacia flowers are* nickel, copper, calcium and chromium.

Higher values of phenolic compounds in the flowers (0.77 mg GAE/mL) than those of the syrup 60 °Brix (0.06 mg GAE/mL) and *R. pseudoacacia* syrup 70 °Brix (0.14 mg GAE/mL) were found. The syrup samples exhibit antimicrobial properties against foodborne pathogenic bacteria as *Salmonella, E. coli* and *L. monocytogenes.*

Conclusion. Based on the chemical and biochemical properties of false acacia flowers, it could be recommended as a potential raw material for food, pharmaceutical and cosmetic products.

Introduction

Robinia pseudoacacia L. (black locust, false acacia), belonging to the family of Fabaceae, originally native to the south-eastern USA, is widely distributed as wild and cultivated species growing in temperate regions throughout the world [1]. The genus *Robinia* commonly known as locust comprises 10 species of trees and shrubs characterized by white or pink flowers with intensive, distinctive, sweet aroma [1, 2]. The flowers are white, borne in pendulous racemes of 10-15 cm long and are edible, with high nutrient and functional values. The flowers of false acacia are used in traditional medicine as diuretic, spasmolytic, sedative and cholagogic agents and relieve inflammation of the kidneys and biliary ducts [3, 4].

The investigation for chemical composition of *R. pseudoacacia* showed that flowers were rich in proteins and microelements which could be used for additives in foods [5, 6]. Its flowers also contained an important bioactive compound called robinin which had a lot of medicinal usage.

The review of the scientific literature indicated that flowers of false acacia, have been attracting a special interest due to their gentle fragrance, containing essential oil which composition depends on geographical region. Volatile compounds of flowers have been studied by several researchers, as well as aroma profiles in honey made from these flowers. In 1994, Kandem et al. [7] used Tenax tube cartridges to trap the floral fragrance of fresh false acacia and analyzed these volatile compounds using GC-MS. δ-3-carene (54.6%), linalool (21%), (Z)-*β*-farnesene (3.0%) and anthranilate aldehyde (3.9%) were found to be the major components. Xie et al. [8] analyzed the chemical constituents of top fragrance from fresh flowers of false acacia growing in China using solid phase microextraction followed by GC-MS analysis and the main components were linalool (33.1%), (E)-*β*-ocimene (26.6%), (E)-*α*-bergamotene (8.9%) and formanilide (7.4%).

The main bioactive components existed in false acacia flowers include flavonoids, phenolics, ascorbic acid, *etc.* [9, 10, 11, 12]. Flowers of false acacia contain volatile compounds, flavonoids, proteins, robinin, polysaccharide and some microelements [13].

Flavonoids content of false acacia is also of increasing interests to researchers. In 2000, five flavonoids including acacetin, secundiflorol, mucronulatol, isomucronulatol and isovestitol were isolated from ethanolic extracts of acacia, following an activity-guided fractionation [14, 15]. Different parts of acacia have wide application in different areas. Its flowers could be eaten and are generally used for honey production. The flowers are also used for preparation of cakes. Series of findings support the consumption of edible flowers of the false acacia as functional food and their usage as sources of natural antioxidants in the food industry.

Recently, many investigations have been concerned with antioxidant properties of different nutritional products [16]. Antioxidant ability has usually been attributed to the activity of antioxidant enzymes as well as to the content of low-molecular antioxidants such as carotenoids, tocopherols, ascorbic acid, phenolic substances [3, 17, 18].

According to Marinas et al. [19], the alcoholic extracts of false acacia showed antimicrobial activity towards the tested strains belonging to the Gram-positive (*Staphylococcus aureus, Bacillus subtilis* and *Enterococcus faecalis*) and Gram-negative (*Pseudomonas aeruginosa, Escherichia coli, Klebsiella pneumoniae* and *Acinetobacter baumannii*) bacterial and the yeasts (*Candida* sp.) strains. Talas-Ogras et al. [20] studied the in vitro antibacterial activity of isolated from *R. pseudoacacia* seed and it had been found that the *Staphylococcus aureus* was the most sensitive strain compared with others strains

(*Corynebacterium michiganense, Bacillus subtilis, Erwinia carotovora, Pseudomonas syringae, Xanthomonas campestris and Escherichia coli*).

Bhalla and Bajpai [21] reported significant antimicrobial effects against some of the selected foodborne pathogens such as *Staphylococcus aureus* KCTC 1621, *Bacillus subtilis* KCTC 3569, *Listeria monocytogenes* KCTC 3569, *Escherichia coli* O157:H7 and *Salmonella enterica* ATCC 4731 with diameters of the zones of inhibition (15.2±0.3-17.3±2.0 mm).

As unpretentious species regarding the environmental requirements, it has also adapted successfully to a diverse range of natural habitats in Bulgaria. Data relating to the pharmacological and botanical features of the species have been found in the literature. No detailed data for the composition and application of acacia flowers in the food industry have been found.

The aim of this study is to determine the chemical composition of false acacia (*Robinia pseudoacacia* L.) flowers and their potential application in the food, cosmetic and pharmacological industries.

Materials and methods

Plant material

False acacia flowers (*R. pseudoacacia*) were collected in May 2018 from a ten-fifteen - years - old black locust tree, naturally growing in the foot of the Eastern Balkan Mountains, in the lands of the village of Topolchane, Sliven, Bulgaria. Samples were identified by an expert in Agricultural University of Plovdiv, Bulgaria.

The moisture content of the raw material (83.7±0.03%) was determined by drying up to constant weight, at 105 °C and all results have been presented on a dry weight basis [22].

Obtaining and GC-MS analysis of concrete

Concrete was obtained by two-stage, static batch extraction of 75 g flowers with n-hexane under the following conditions: hydro module (raw material: solvent) – 1:10 (w/v); duration of the first and second extraction stage – 1 h and 0.5 h; temperature 40 °C. The solvent was evaporated on a rotary vacuum evaporator at water bath temperature of 35 °C [23].

The GC-MS analysis was carried out with an Agilent 5975C MSD system coupled to an Agilent 7890A gas chromatograph (Agilent Technologies Inc., Santa Clara, CA). Agilent J&W HP-5MS column (0.25 μm, 30 m x 0.25 mm) was used with helium as a carrier gas (1.0 mL min^{-1}). The operational conditions were: oven temperature 35 °C/3 min, 5 °C/min to 250 °C for 3 min, total run time 49 min; injector temperature 260 °C; ionization voltage 70 eV; ion source temperature 230 °C; transfer line temperature 280 °C; solvent delay 4.25 min and mass range 50 - 550 Da. The MS was operated in scan mode. One μL of the sample diluted with n-hexane (10%, v/v) was injected into the GC/MS system at split ratio 30:1. The GC analysis was carried out using an Agilent 7890A GC system; FID temperature 270 °C. In order to obtain the same elution order with GC/MS, simultaneous triplicate injections were done by using the same column and the same operational conditions.

The identification of compounds was made by comparing their mass spectra with those from mass spectra libraries [24] and by comparing the literature and estimated Kovat's (retention) indices that were determined using mixtures of homologous series of normal

alkanes from C_8 to C_{40} in hexane, under the conditions described above. The percentage ratio of volatile components was computed using the normalization method of the GC/FID peak areas.

Mineral composition of flowers

Content of selected elements was measured by ICP-AES spectrometer: SPECTROFLAME MODULA-FTMOA81A. 1 g of air dried sample flowers was weighed with precision up to 0.001 g, and was poured on with 2 cm^2 concentrated nitric acid. Mixture was cooled in freezer until end of foaming process, homogenized on vortex at 3000RPM, and was heated on thermoreactor KUTESZ type 656 at 120 °C until dissolution of solid phase, and clarification of solution. After mineralization, the samples were filled up to 20 mL with 2% solution of nitric acid.

Acacia syrup preparation

For the preparation of the acacia syrups with different concentrations, anhydrous citric acid Parafarm (Saporiti, Argentina) was used to regulate the pH, food grade sucrose, potable bottled water, each from the same batch, were bought from the local market.

The acacia flowers were stored at 5 °C for 24 h. Acacia syrups are produced in two different concentrations.

For the obtaining of the lower concentration syrup the acacia flowers were extracted with a boiling 50% aqueous sugar solution for 10 minutes. Then, cooled in a cold water bath to 5 °C. The extraction takes 24 hours under refrigeration conditions (4 °C) in the presence of flowers in the sugar syrup. Citric acid (1% by the weight of the final product) was added to the syrup. Total soluble solids (TSS) were up to 60 °Brix; water activity – 0.69±0.01 (LabSwift-a_w, Novasina, Switzerland); pH – 3.23±0.02.

For the obtaining of the higher concentration syrup from acacia flowers, the common steps for preparation of extract were followed with the difference that they were subjected to extraction with a boiling aqueous solution of sugar (50%) for 30 min. Citric acid (1% by the weight of the final product) was added to the syrup. Total soluble solids (TSS) content reached 70 °Brix; water activity – 0.67±0.01 (LabSwift-aw, Novasina, Switzerland); pH – 3.19±0.02.

The prepared syrups were filtered, cooled properly and poured into sterile glass bottles.

Total phenolic contents

Total phenolic content was measured using a Folin-Ciocalteu reagent. Briefly, 1 mL five times diluted Folin-Ciocalteu reagent was mixed with 0.2 mL sample and 0.8 mL 7.5% disodium carbonate. The reaction was performed for 20 min at room temperature in dark. Then the absorbance was measured at 765 nm against blank. The results were expressed as mg equivalent of gallic acid (GAE) per mL extract, according to calibration curve [25].

Total flavonoids content

The total flavonoids content was analyzed by aluminum trinitrate ($Al(NO_3)_3$) reagents [26]. The absorbance was measured at 415 nm against blank. The results were presented as mg equivalents quercetin (QE) per g dry extract according to the calibration curve with quercetin as a standard.

DPPH radical scavenging ability

To conduct the assay, 0.15 mL from extract was mixed with 2.85 mL freshly prepared 0.1 mol solution of DPPH in methanol. The sample was incubated for 15 min at 37 °C in darkness. The reduction of absorbance was measured at 517 nm in comparison to the blank containing methanol and% inhibition were calculated [25].

Ferric reducing antioxidant power (FRAP) assay

The assay was performed according to Benzie and Strain [27] with slight modification by Kivrak et al. [26]. The FRAP reagent was freshly prepared by mixing 10 parts 0.3 M acetate buffer (pH 3.6), 1 part 10 mM 2,4,6- tripyridyl-s-triazine (TPTZ) in 40 mM HCl and 1 part 20 mM $FeCl_3{}^x6H_2O$ in distilled water. The reaction was started by mixing 3.0 mL FRAP reagent with 0.1 mL of investigated extract. The reaction time was 10 min at 37 °C in darkness and the absorbance was measured at 593 nm against blank prepared with methanol. Antioxidant activity was expressed as mM Trolox® equivalents (TE) per mL extract [25].

Microbiological analyses

For the microbial analyses a crude extract was obtained under aseptic surroundings by mashing fresh flowers after preliminary washing under tap water, sterilized distilled water and soaking for 5 min with ethanol and exposing under the influence of ultraviolet illumination for 20 min.

Antibacterial activity was tested against Gram-positive bacteria - *Listeria monocytogenes* NCTC 11994 and *Staphylococcus aureus* ATCC 25093, and Gram-negative bacteria – *Escherichia coli* ATCC 8739 and *Salmonella enterica* subsp. *enterica* serovar Abony NCTC 6017. The selective growth media, were: *Listeria* Oxford Agar Base /Merck/; Baird Parker Agar Base with Egg Yolk Tellurite emulsion supplement /Merck/, Rapid' E.coli 2 Agar /BioRad/ and Mac CONKEY Agar /Merck/, respectively. The media were inoculated with 24-hour suspension of the bacterial species.

Antimicrobial assay by agar diffusion method

The used inoculums have resulted as actual concentration cells of - *Listeria monocytogenes, Staphylococcus aureus, Escherichia coli, Salmonella enterica* into the responding selective medium about 1.10^4 CFU/mL. Melted and cooled to 45 °C selective media were inoculated with the tested microorganisms and next equally dispensed into Petri dishes. After setting of the media, sterile rings (Ø 6 mm) were placed on, and different amounts of each sample (0.05; 0.10 and 0.15 mL) were put into the rings. Petri dishes were incubated at 37 °C for 24 or 48 h according to the bacterial spices, and then the distinct zone of growth inhibition around the rings was measured. The total plate count was estimated by the conventional plate-counting technique using appropriate dilution.

Statistical analysis

All experiments were performed in triplicate. All data were presented as mean±standard deviation (SD).

Results and discussion

Chemical composition of concrete

The yield of concrete was 1.06% (in abs. dry mass). The concrete was yellow waxy pastes and had sharp odor. Chemical composition of the concrete was shown in Table 1.

The concrete was composed by 34 components representing 99.02% of its total content. Sixteen of them were in concentrations over 1% and the rest 18 constituents were in concentrations under 1%.

Table 1

Chemical composition of concrete

№	Compound	RI	Content,%
1	*trans*-Linalyl Oxide	1074	0.48
2	*cis*-Linalyl Oxide	1088	0.65
3	Methyl salicylate	1175	1.06
4	*p*-Anisic acid	1399	0.81
5	n-Pentadecane	1500	1.12
6	n-Hexadecane	1600	0.37
7	Methyl veratrate	1602	0.78
8	*cis*-Methyl dihydrojasmonate	1654	0.69
9	n-Heptadecane	1700	0.58
10	(E,E)-farnesol	1722	0.41
11	(E,Z)-farnesol	1744	0.51
12	n-Octadecane	1800	0.33
13	Isopropyl myristate	1814	3.47
14	Hexahydrofarnesyl acetone	1833	3.86
15	Diisobutyl phthalate	1862	1.52
16	Methyl isopalmitate	1891	0.59
17	Dibutyl phthalate	1914	1.38
18	Palmitic acid	1942	4.92
19	Isopropyl hexadecanoate	1989	0.72
20	Linoleic acid	2098	3.64
21	α-Linolenic acid	2106	5.97
22	Tributyl acetylcitrate	2259	0.84
23	n-Pentacosane	2500	4.98
24	Diisooctyl phthalate	2589	4.05
25	n-Hexacosane	2600	0.63
26	n-Heptacosane	2700	20.10
27	n-Octacosane	2800	1.05
28	all-trans-Squalene	2835	0.59
29	n-Nonacosane	2900	25.18
30	n-Triacontane	3000	1.86
31	n-Hentriacontane	3100	3.39
32	n-Dotriacontane	3200	0.72
33	*β*-Amyrin	3290	0.84
34	*α*-Amyrin	3320	0.93

As could be seen the major constituents (up 3%) of the concrete are as follows: n-nonacosane (25.18%), n-heptacosane (20.10%), α-linolenic acid (5.97%), n-pentacosane (4.98%), palmitic acid (4.92%), diisooctyl phthalate (4.05%), hexahydrofarnesyl acetone (3.86%), linoleic acid (3.64%), isopropyl myristate (3.47%), and n-hentriacontane (3.39%). The difference in chemical composition of our investigations and the reported data may be due to environmental conditions under which the plant has grown as well as the variation in conditions of the analysis.

The classification of the identified compounds, based on functional groups, is presented in Figure 1.

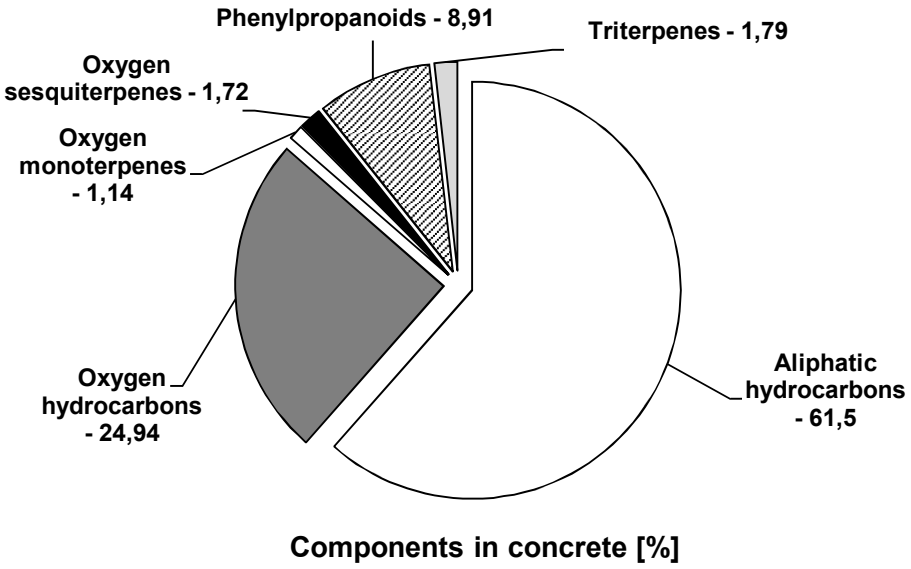

Figure 1. Groups of components in concrete

The total aliphatic hydrocarbons constituted the highest percentage of the component of the concrete constituting 61.50%. The concrete consisted above 10% concentration oxygen hydrocarbons (24.94%). The percentage of phenylpropanoids, triterpenes, oxygen sesquiterpenes and oxygen monoterpenes are under 9%.

Mineral composition of flowers

The minerals identified in the tested samples of false acacia flowers are as follows: boron – 182.64 nm, arsenic – 188.98 nm, zinc – 213.86 nm, manganese – 257.61, iron – 259.54 nm, and magnesium – 279.81 nm, and chromium – 283.56 nm, calcium – 317.93 nm, copper – 324.75 nm and nickel – 341.48 nm.

Differences in identified elements relative to other researchers may be due to environmental factors (geographical, climatic and seasonal). The relatively high levels of microelements, iron 259.54 nm is found in the active sites of many redox enzymes and

electron carriers such as hemoglobin and myoglobin, and therefore may have potential functional benefits in the human body. Copper (324.75 nm) has an important role in the active site of many redox enzymes and electron carriers, the production of hemoglobin or bone formation. Manganese (257.61 nm) activates many enzymes.

Content of polyphenolics and flavonoids

The extract of flowers presented the highest phenolic content (0.77 mg GAE/mL), followed by the acacia syrup 70 °Brix (0.14 mg GAE/mL) (Figure 2). Among the samples, false acacia flowers have the highest value for flavonoids (0.17mg QE/mL), the total phenolic content was 0.77 mg GAE/mL. With regard to the heating in the extract and syrup could rapidly flow inactivation of polyphenol oxidases, presented in flowers. Cooking with heat may lead to a higher extraction efficiency of total phenolics through destroying of the cell structure, which may lead to better solvent access and extraction.

Acacia flowers presented the highest flavonoids content (0.17 mg QE/mL), followed by the acacia syrup 60 °Brix (0.07 mg QE/mL), and syrup 70 °Brix (0.04 mg QE/mL), respectively (Figure 2).

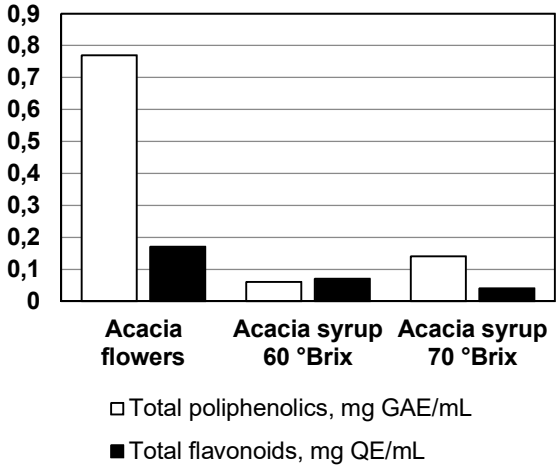

*[1]GAE - Gallic Acid Equivalents, [2]QE - Quercets Equivalents

Figure 2. The total polyphenolics and flavonoids on *R. pseudoacacia* flowers and syrups

The results obtained in this study showed that the flowers are rich in phenolic compounds and have significant antioxidant activity. Flowers of false acacia as a natural additive in food, cosmetic and pharmaceutical products could be used as effective strategy to improve their nutritional and medical value while ensuring consumer safety.

Antioxidant activity

There have been few reports on the antioxidant activity of false acacia extracts. The antioxidant activity of lyophilized extracts of acacia leaves had a lower antioxidant capacity (1940 μmol Trolox equivalent g^{-1}) compared with *Rhus typhina* (4651 μmol Trolox

equivalent g^{-1}), *Acer rubrum* (3805 μmol Trolox equivalent g^{-1}), and *Rosa multiflora* (2533 μmol Trolox equivalent g^{-1}) [28]. Recently, Marinas et al. [19] reported that the highest content of polyphenols (GAE) was found in the leaf extract (266.7 μg GAE mL^{-1} extract), followed by the extract of the seeds (232.2 μg GAE mL^{-1} extract), respectively. In addition, the content of polyphenols presented in the flowers creates a strong antioxidant potential [29]. Differences in the distribution of the polyphenols and flavonoids arise from various factors that can be biological e.g., the part analyzed and the vegetative stage of the plant [30] and technical such as the extraction method, the solvents and their concentrations [31, 32] and there are also differences in the structure and properties of the phenolic compounds presented in the different samples analysed. False acacia flowers have the highest antioxidant activities – radical scavenging activity (DPPH – 2.25 mM TE/ml) and metal reducing ability (CuPRAC – 4.52 mM TE/mL) (Figure 3).

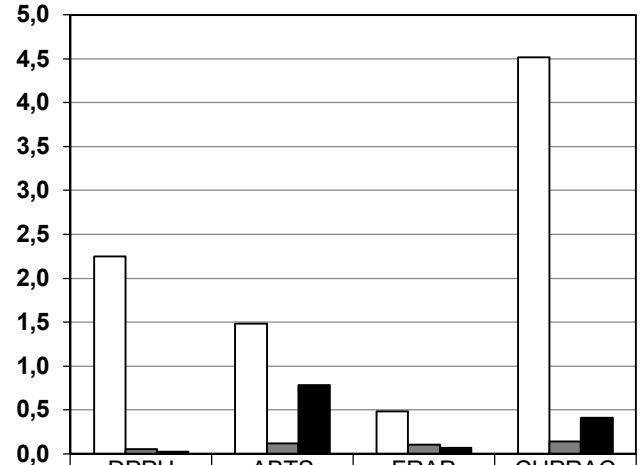

	DPPH	ABTS	FRAP	CUPRAC
Acacia flowers, mM TE/ml	2,25	1,48	0,48	4,52
Syrup 60 °Brix, mM TE/ml	0,05	0,12	0,10	0,14
Syrup 70 °Brix, mM TE/ml	0,02	0,78	0,07	0,41

Figure 3. Antioxidant activity of acacia flowers and syrups

Higher values of isolated metals as copper – 324.75 nm and nickel – 341.48 nm are directly related to the antioxidant properties of acaci flowers.

Microbiological analyses

The results of antibacterial testing are presented in Table 2.

Table 2

Diameter of zones of growth inhibition (mm) of tested pathogenic bacteria

Sample \ Bacteria		*E.coli*	*Salmonella*	*L. mono cytogenes*	*S. aureus*
		Zones of growth inhibition (mm)			
Flowers	0.15 mL	25.00	16.00	21.00	0.00
	0.10 mL	24.00	8.00	19.00	0.00
	0.05 mL	4.00	4.00	0.00	0.00
Syrup 60 °Brix	0.15 mL	18.00	13.00	0.00	0.00
	0.10 mL	10.00	0.00	0.00	0.00
	0.05 mL	0.00	0.00	0.00	0.00
Syrup 70 °Brix	0.15 mL	20.00	15.00	20.00	0.00
	0.10 mL	14.00	7.00	12.00	0.00
	0.05 mL	5.00	6.00	5.00	0.00

The crude extract of false acacia, applied in an amount of 0.15 mL, possessed the most pronounced antibacterial activity with inhibition zones: 25.00 mm against *E. coli*, 21.00 mm against *L. monocytogenes* and 16.00 mm against *Salmonella enterica*. False acacia crude extract had no inhibitory activity against *S. aureus.*

It is obvious that *S. aureus* was most resistable bacterium. False acacia syrup 60 °Brix, applied in an amount of 0.15 mL showed highest antibacterial potential against *E. coli* with a zone of inhibition of 18 mm and at the lowest sample concentration (0.05 mL) is ineffective. False acacia syrup 60 °Brix was effective against Gram-negative bacteria and didn't inhibit the growth of the Gram-positive. False acacia syrup 70 °Brix showed antibacterial activity against *E. coli, Salmonella* and *L. monocytogenes* in all applied concentrations. The antibacterial activity of false acacia syrups with different Total Soluble Solids content is considered to be due to the high sugar content in their composition.

It is obvious from the results that the activity of the false acacia extract depended on its concentration and the tested bacteria. This affirmation could be confirmed by the concluded results of Cioch et al. [33] reported that the type of the extract (ethanol, methanol or water) and the concentration of black locust displayed distinction in the level of inhibition the growth of microorganisms used in their experiments. In the case of most microorganisms, it is reported that their growth was inhibited by concentration of 2.00 mg/mL. Rosu et al. [34] reported that extracts from different parts of the plant had different antibacterial activities. Extracts of false acacia flowers and seeds were efficient antibacterials for Gram positive cocci. Bark and leaf extracts were active against *E. coli, Pseudomonas, Proteus, Salmonella choleraesuis, Candida albicans*.

Conclusion

The present study shows that flowers of false acacia (*R. pseudoacacia* L.) were with high levels of phenolic compounds and minerals that have pronounced antioxidant properties. Probably, most of the phytochemicals have preserved during the heat treatment of the syrup.

Higher values of phenolic compounds in the flowers (0.77 mg GAE/mL) than those of the false acacia syrup 60 °Brix (0.06 mg GAE/mL) and false acacia syrup 70 °Brix (0.14 mg GAE/mL) were found. The aromatic substances and phenolic compounds passing through the extracts exhibit antimicrobial properties against foodborne pathogenic bacteria as *Salmonella, E. coli* and *L. monocytogenes.* This is a reason for more thorough examination and extensive research of the chemical and biochemical properties of false acacia flowers as a potential raw material for usage in the food, pharmaceutical and cosmetic industries.

References

1. Hegi G. (1924), *Illustrierte Flora von Mittel Europa. Bd. IV/3*, Lehmanns, Munchen.
2. Tutin T., Heywood V., Burges N., Moore D., Valentine D., Walters S., Webb D. (1968), Flora Europea, University Press, Cambridge.
3. Pietta P., Simonetti P., Mauri P. (1998), Antioxidant activity of selected medicinal plants, *Journal of Agricultural and Food Chemistry*, 46, pp. 4487–4490.
4. Strzelecka H., Kowalski J. (2000), *The Encyclopedia of Herbs and Herbalism,* PWN, Warszawa.
5. Robards K., Prenzler P., Tucker G., Swatsitang P., Glover W. (1999), Phenolic compounds and their role in oxidative processes in fruits, *Food Chemistry*, 66, pp. 401–436.
6. Song Y., Luo J., Xie H. (1992), Study on the chemical composition of *Robinia pseudoacacia* flowers, *Chemistry and Industry of Forest Products*, pp. 1–4.
7. Kandem D., Gruber K., Barkman T., Gage D. (1994), Characterization of black locust floral fragrance, *Journal of Essential Oil Research*, 6, pp. 199–200.
8. Xie J., Sun B., Yu M. (2006), Constituents of top fragrance from fresh flowers of *Robinia Pseudoacacia* L. occurring in China, *Flavour and Fragrance Journal*, 21, pp. 798–800.
9. Jing L., Qiu H., Yang L., Liu M., Gao Z. (2002), Nutrition in the Pagoda flower (in Chinese), *Chinese Journal Spectroscopy. Lab.,* 19, pp. 36–38.
10. Li Y., Chu Z., Zhai Y., Kang T. (2011), Preparation technique of total flavone of *Robinia psendoacacia* (in Chinese), *Journal of Liaoning University*. TCM, 13, pp. 87–88.
11. Wang X., Tang L., Zhao L., Luan Y., Zhang Z. (2010), Determination of polyphenols in flowers of *R. pseudoacacia* L. by Folin–ciocaileu method (in Chinese), *Food Drug*, 12, pp. 332–334.
12. Wang X., Tang L., Zhao L. (2011), Optimization of ultrasound–assisted extraction of phenolic compounds from *R. pseudoacacia* L. flowers by response surface methodology, *Food Science*., 32, pp. 66–40.
13. Giet C., Ziegler H. (1980), Distribution of carbohydrate–binding proteins in different tissues of *Robinia pseudoacacia* L., *Biochemie und Physiologie der Pflanzen*, 175, pp. 58–66.
14. Tian F., McLaughlin J. (2000), Bioactive flavonoids from the black locust tree, *Robinia pseudoacacia, Pharmaceutical Biology*, 38, pp. 229–334.
15. Vinson J., Hao Y., Su X., Zubik L. (1998), Phenol antioxidant quantity and quality in foods: vegetables, *Journal of Agricultural and Food Chemistry*, 46, pp. 3630–3634.
16. Velioglu Y., Mazza G., Gao L., Oomah B. (1998), Antioxidant activity and total phenolics in selected fruits, vegetables and grain products, *Journal of Agricultural and Food Chemistry*, 46, pp. 4113–4117.
17. Bartosz G. (1997), Oxidative stress in plants, *Acta Physiologiae Plantarum*, 19, pp. 47–64.
18. Larson R. (1988), The antioxidants of higher plants, *Phytochemistry*, 27, pp. 969–978.
19. Marinas I., Oprea E., Geana E.I., Chifiriuc C., Lazar V. (2014), Antimicrobial and antioxidant activity of the vegetative and reproductive organs of Robinia pseudoacacia, *J. Serb. Chem. Soc.,* 79, pp. 1363–1378.

20. Talas–Ogras T., Ipekci Z., Bajrovic K., Gozukirmizi N. (2005), Antibacterial activity of seed proteins of *Robinia pseudoacacia, Fitoterapia,* 76, pp. 67–72.
21. Bhalla P., Bajpai V. (2017), Chemical Composition and antibacterial action of *Robinia pseudoacacia* L. flower essential oil on membrane permeability of foodborne pathogens, *Journal of Essential Oil–Bearing Plants*, 20, pp. 1–14.
22. Russian Pharmacopoeia,11th Edition, Moscow. (1990),
23. Stoyanova A., Georgiev E., Atanasova T. (2007), Handbook for Laboratory Practice in Essential Oils, *Acad. Publ. House of the University of Food Technologies*, Plovdiv (in Bulgarian).
24. Adams R. (2001), *Identification of Essential Oil Components by Gas Chromatography Quadrupole Mass Spectroscopy*. Carol Stream, Illinois.
25. Ivanov I., Vrancheva R., Marchev A., Petkova N., Aneva I., Denev P., Georgiev V., Pavlov A. (2014), Antioxidant activities and phenolic compounds in Bulgarian *Fumaria* species, *International Journal of Current Microbiology and Applied Sciences,* 3, pp. 296–306.
26. Kivrak I., Duru M., Öztürk M., Mercan N., Harmandar M., Topçu G. (2009), Antioxidant, anticholinesterase and antimicrobial constituents from the essential oil and ethanol extract of *Salvia potentillifolia, Food Chemistry,* 116, pp. 470–479.
27. Benzie F., Srain J. (1996), Ferric reducing ability of plasma (FRAP) as a measure of "antioxidant power": The FRAP assay, *Analytical Biochemistry,* 239, pp. 70–76.
28. Katiki L., Ferreira J. , Gonzalez J., Zajac A., Lindsay D., Chagas A., Amarante A. (2013), Anthelmintic effect of plant extracts containing condensed and hydrolyzable tannins on Caenorhabditis elegans, and their antioxidant capacity, *Vet. Parasitol.,* 192, pp. 218–227.
29. Zhang L., Ji H., Du A., Xu C., Yang M., Li F. (2012), Effects of drying methods on antioxidant properties in *Robinia pseudoacacia* L. flowers, *J. Med. Plants Res*., 6, pp. 3233–3239.
30. Ksouri R., Megdiche W., Falleh H., Trabelsi N., Boulaaba M., Smaoui A., Abdelly C. (2008), Influence of biological, environmental and technical factors on phenolic content and antioxidant activities of Tunisian halophytes, *Comptes Rendus Biologies*, 331, pp. 865–873.
31. Gallego M., Gordon M., Segovia F., Skowyra M., Almajano M. (2013), Antioxidant properties of three aromatic herbs (rosemary, thyme and lavender) in oil–in–water emulsions, *J. Am. Oil Chem. Soc*., 90, pp. 1559–1568.
32. Santas J., Carbó R., Gordon M., Almajano M. (2008), Comparison of the antioxidant activity of two Spanish onion varieties, *Food Chemistry*, 107, pp. 1210–1216.
33. Cioch M., Satora P., Skotniczny M., Semik–Szczurak D., Tarko T. (2017), Characterisation of antimicrobial properties of extracts of selected medicinal plants, *Polish Journal of Microbiology*, 66, pp. 463–472.
34. Rosu A., Bita A., Calina D., Rosu L., Zlatian O., Caliva V. (2012), Synergic antifungal and antibacterial activity of alcoholic extract of the species *Robinia pseudoacacia* L. (Fabaceae), *European Journal of Hospital Pharmacy: Science and Practice,*19, p. 216.

Effect of technological properties of pea seeds and processing modes on efficiency of its dehulling

Yevgen Kharchenko[1], Andrii Sharan[1], Valentyn Chornyi[1], Olena Yeremeeva[2]

1 – National University of Food Technologies, Kyiv, Ukraine,
2 – Uman's National University of Gardening, Uman, Ukraine

Keywords:

Pea
Dehulling
Kernel
Husk
Dust middlings
Fine grits

Article history:

Received 23.04.2018
Received in revised form 29.06.2018
Accepted 27.12.2018

Corresponding author:

Yevgen Kharchenko
E-mail: a_537@nuft.edu.ua

DOI:
10.24263/2304-974X-2018-7-4-5

Abstract

Introduction. The process of dehulling grain peas is not enough researched, and there are difficulties of modeling the technological process as a whole. Presented research results of the process of pea seeds dehulling allow to understand the behavior of pea seeds during dehulling in machines with abrasive working members.

Materials and methods. Pea seeds of varying large-scale and moisture are scaly in the laboratory dehuller. The products of dehulling were cleaned in the aspiration channel from husk and dust middlings after this process the products were weighed and determined the dehulling index. By changing the moisture content (from 11,6 to 16,6%) and the size of the pea seeds (from 213 to 257 g), the speed of rotation of the working body of the dehuller (from 25 to 41,6 s^{-1}), the duration of processing (from 5 to 25 s) and the coefficient of filling the working chamber (from 0,09 to 0,48) of the machine was presented dependence of the parameters on dehulling efficiency.

Results and discussion. It is determined that the increase of processing time, the pea seeds, the speed of the working organs and filling coefficient of the working chamber of the dehuller increase the efficiency of dehulling peas by linear dependence. Increase in the size of pea seeds contributes to increase of efficiency of dehulling mainly due to increase of the yield of small. The increase in the scale of seeds leads to a decrease in the dehulling index.

Along with the increasing efficiency of dehulling, increases and yield of trinkets at the expense of the kernel. When the moisture of pea seeds increases, the yield of a fine grits increases comparing to the dehulling of dry pea. Yield of the kernel is directly proportional to the reduction of the yield of undehulling seeds. The yield of a fine grits also has linear dependencies when you change the following parameters.

In the process of dehulling reduces the ash content of the kernel, but also decreases the ash content and husk and dust middlings, which is the result of transition of low-ash content particles of kernel into the dust middlings.

Conclusions. For effective dehulling of pea seeds, it is necessary to carry out dehulling for 10–15 s, filling coefficient of the machine must be not less 0,48. Pea seeds with an absolute mass of 257 g, dehull better than pea seeds with an absolute mass of 213 g.

Introduction

Technological process of dehulling of pea seeds is carried out in abrasive grinding machines [5, 27, 35]. The process of dehulling has been researched, despite its extensive application in grain processing technologies [24, 32]. This creates an obstacle to simulate the whole technological process.

The process of dehulling in abrasive machines is a scientific problem that requires detailed research and development of the function of dehullling, which will allow to develop quantitative balances of technological processes of processing pea seeds in cereals [16].

For cereals in which the shell is firmly increased with the kernel, to assess the efficiency of the dehulling process used dehulling index [11-13, 21, 22]. On the efficiency of the process of dehulling pea seeds affect its moisture and duration of processing. Prabhakar S., Phirke P.S., Bhole N.G. [21, 22] studied the dehulling index for two different types of pigeon peas depending on different ways of handling peas. Mathematical model of dehulling process was developed and process optimization was carried out.

With the increase in moisture the efficiency of the process of dehulling of legumes decreases [15, 23, 27, 33]. Goyal R.K., Vishwakarma R.K., Wanjari O.D. [13] investigated the effects of moisture on the efficiency of the dehulling process pigeon peas. They have established that with increased moisture above 10% the efficiency of the process is reduced. Opoku A., Tabil L., Sundaram J., Crerar W.J., Park S.J. [19] investigated different ways of handling pigeon peas to increase the yield of the kernel. It has been found that heat treatment contributes to an increase in the kernel of the pea. Tiwari B.K., Jaganmohan R., Venkatachalapathy N., Tito Anand M., Surabi A., Alagusundaram K. [31] optimized the influence of the process of hydrothermic treatment of pea seeds and its drying on the efficiency of seed dehulling pigeon peas. From their studies you can trace the increase in efficiency of dehulling with the increase of duration of hydro-thermal processing.

Goyal R.K., Vishwakarma R.K., The Wanjari O.D. [11, 12] has developed a mathematical model and optimized the process of dehulling pigeon peas. The mathematical model takes into account the pea moisture and duration of dehulling. These models do not take into account the large pea seeds and the filling of the equipment. The shortcomings of these models is that they can be used only for the dehullers on which the research is carried out and do not reflect all the features of the process of dehulling on other types of machines.

On the process of dehulling also affects the rotational speed of machine working organs [3, 10, 16, 17, 33]. Mangaraj S., Singh K.P. [17] developed a mathematical model and optimized the process of dehulling in the industrial machine, taking into account the speed of rotation of the working body, machine dimensions and machine performance.

One factor that affects the efficiency of dehulling is the scale of seeds [7, 10]. Most studies were conducted without regard to this factor.

Vereshchinskii A.P. [28] investigated the impact of the load on the effectiveness of wheat dehulling in the technologies of flour milling producing production. It has found that the amount of grain loaded into the dehuller affects the effectiveness of its dehulling by curved dependence.

Singh U., Santosa B.A.S., Rao P.V. [25, 26] studied efficiency of dehulling of different genotype pigeon peas. They have determined that different gene types of pea have different efficiency of dehulling.

Studies conducted by many scientists performed on the tangential abrasive dehulling device (TADD) [6, 8, 10, 18, 19, 21, 24, 26], which are structurally different from the industrial machines of continuous action. The main difference is the absence of the tangential

abrasive dehulling device trellis, which is displayed by dehullling products: husk and dust middling.

Laboratory abrasive machines with lattice canvas [4, 8, 11-13, 15, 27, 31] are better suited for modeling the dehulling process, which occurs in industrial machines continuous action with trellis canvas [27] in the middle. The results of the studies that are obtained at the tangential abrasive dehulling device are less suitable for development of dehulling function for industrial analogues in connection with the other nature of the dehulling process. Construction of the tangential abrasive dehulling device (TADD) provides a dehulling by the force of friction of grain on the abrasive disc [24], the influence of other forces is insignificant. In the machines with trellis canvas there is dehulling due to friction on the abrasive disk, the friction of grain on the lattice canvas and friction between the seeds [16]. The tangential abrasive dehulling device does not allow to investigate the effect of filling on the efficiency of dehulling due to a limited amount of seeds, which can be covered in a machine [24].

Most of results of the research is devoted to the study of the process of dehulling pigeon peas. Information about the process of dehulling field peas is not enough. The disadvantage of many of these studies is that it is not considered a large scale of seeds of field pea, which is a factor that affects the efficiency of dehulling of pea seeds. Information on the influence of the above parameters on the efficiency of the dehulling of field pea insufficient purpose of this work was to study the influence of duration of dehulling, speed of rotation of working organs of dehuller and load on the efficiency of process dehulling field peas of different moisture and large size.

Materials and methods

Materials

The technological process of dehulling of the seeds of the field of different moisture and large size, when changing the parameters of work of dehuller and processing duration is investigated.

Methods

Grain preparation for research

Before the beginning of the research, pea seeds were cleaned from light impurities by means of transmission through a laboratory aspiration channel. The cleared pea seeds were sifted on a lattice with a diameter of holes of 5,0 mm, which was allocated by a small faction of seeds, and the east is a large faction of seeds. The selected large faction of the seeds were subjected to repeated sifting on the same lattice canvas with a diameter of holes of 5,0 mm with a view of a more complete selection of small seeds. Partially dehulled, broken, eaten seeds selected from the main mass and directed to the waste. The research was conducted only with fully whole seeds, which had the whole seed shells.

The separation of peas on large and small fractions allowed to establish the influence of large pea seeds on the effectiveness of its dehulling under all other conditions.

Method of determining the moisture content of pea seeds

We have to choose from the main mass of the selected seeds of big and small fractions which were crushed in the laboratory mill. After that the crushed product of 5 g was dried in the dryer at a temperature of 130 °C, within 60 minutes. Then cooled in ecliptic and weighed in technical scales with the subsequent recalculation of moisture [2].

Method of determination of bulk density and mass of 1000 seeds

The volume weight of seeds of peas is determined when we load 1-liter seeds of peas in a pelvic container 14, 20].

Among the large and small fractions of pea seeds picked up 1000 whole seeds, after which the selected seeds were weighed [4]. Weighted samples were recalculated on the absolbno mass of pea seeds by the formula:

$$A = \frac{100 - W}{100} \times m_{1000} \quad (1)$$

where W – moisture pea seeds,%; m_{1000} – mass 1000 seeds, g.

Method of humidisting of pea seeds

The amount of water added to the pea seeds in order to increase its moisture was calculated by the formula:

$$G_w = G_g \left(\frac{100 - W_0}{100 - W_p} - 1 \right), \quad (2)$$

where G_w, G_g – according to mass of water and mass of seeds, kg; W_0, W_p – in accordance with the moisture of seeds initial and specified,%.

After water was added to the grain, it was thoroughly stirred and left to be cut for three days in a closed container.

Technique of dehulling pea seeds

Dehulling of large and small fractions of pea seeds carried out in laboratory dehuller (model ULZ-1), by changing the speed of the working body of the machine with 25 s^{-1} (1500 rpm) to 41,6 s^{-1} (2500 rpm), and the duration of dehulling changed from 5 to 25 s with a step duration handling 5 s by using an electronic timer that is equipped with a dehuller.

The dehuller ULZ-1, is the analogue of the machine Satake Grain Testing Mill TM05 [4, 8, 34]. With the difference that in the machine ULZ-1 used trellis canvas with round holes with a diameter of 2,0 mm [16, 28]. Abrasive discs of 14A40CM mark.

The efficiency of the process of dehulling was determined by the dehulling index, which is calculated by the formula [15, 29, 30, 33, 34]:

$$I_p = \frac{m_1 - m_2}{m_1} \cdot 100 \quad (3)$$

where, m_1 – mass of seeds to dehulling, g; m_2 – mass of kernel, small and half pea seeds after dehulling, g.

During the research on the installation of the effect of processing duration on the efficiency of dehulling process, mass of gravity was 100 g. During research on the measurement of filling influence on efficiency of dehulling, mass of seeds of pea seed took 40, 80, 120, 160, 200 g.

Products of dehulling passed through the aspiration channel on the scheme, which is shown on Figure 1. Air mode of aspiration channel was installed visually with the help of frequency converter of turnovers, so that only a husk and a dust middlings were taken to the bunker. Cleaned of husk and dust middlings shredding products were weighed and calculated the dehulling index in the percentage of formula 3. After weighing, purified products of dehulling were sorted on trellis canvas with diameter of holes 5,0 mm for the purpose of selection of trinkets.

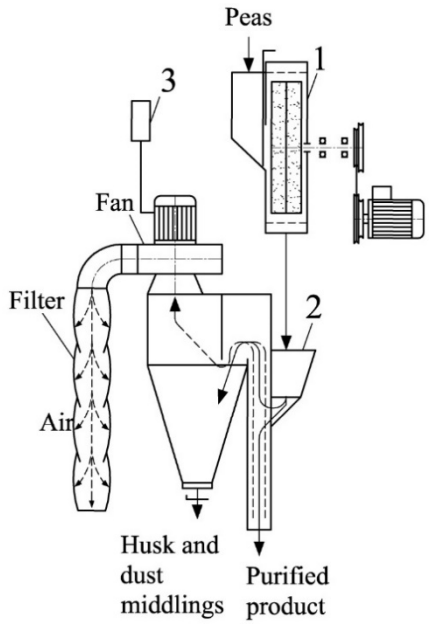

Figure 1. Scheme of research: 1 – dehuller; 2 – aspiration channel; 3 - frequency converter of revolutions

The selected trifle was also weighed and calculated its yield as a percentage, in relation to the general mass of pea seeds, which were directed on dehulling.

Method of research on the installation of influence of filling on efficiency of dehulling

Seeds of large and small fractions in the amount of 40, 80, 120, 160, 200 g separately scaly in the dehuller for 15 s. The rotation speed of the working body of the machine was 25 s^{-1} (1500 rpm).

Products of dehulling passed through the aspiration channel (Figure 1) in order to separate the light impurities, after which they weighed and counted the dehulling index on the formula 3.

After weighing the products of dehulling were sifted on a lattice with a diameter of holes of 5,0 mm in order to isolate the crushed particles, which also weighed and calculated their yield as a percentage to the masses of undehulling seeds.

The obtained research data was used to determine the coefficient of filling the working chamber of the dehuller.

The coefficient of filling of working chamber of the dehuller was calculated by the formula:

$$K = \frac{V_g}{V_m} \tag{4}$$

where K – is the coefficient of filling of working chamber of the dehuller; V_g – volume of seeds loaded in the dehuller, m³; V_m – volume of working chamber of dehuller, m³.

Amount of grain was calculated by the formula:

$$V_g = \frac{m}{\gamma} \tag{5}$$

where m – weight of seed, which is loaded into a dehuller, kg; γ – bulk density peas seeds, kg/m³.

Bulk density of large fraction amounted to 779 g/l, and weight of small fraction is 782 g/l.

The volume of the working chamber of the dehuller was calculated by the formula:

$$V_m = \left(\frac{\pi D^2}{4} - \frac{\pi d^2}{4} \right) \cdot H \tag{6}$$

where D – respectively, the diameter of the lattice fabric of the dehuller and abrasive wheel, m; H – height of the lattice of the dehuller, m.

The diameter of the gray cylinder was 0,165 m, diameter of abrasive discs – 0,15 m. Height of sieve cylinder – 0,058 m.

Methodology of the influence of moisture on the efficiency of dehulling

In six containers of 0,5 l filled with 200 g of pea seeds, added a calculated amount of water, which was calculated according to formula 2, taking into account the primary moisture of the pea. The estimated moisture step was 1,0%. After the addition of water, the tank closed the lids and moved intensively for 10 minutes and left on the drainage for three days.

After the sting of peas, from each tank was taken 40 g peas to determine the actual moisture, and 160 g peas were dehulled for 20 s and all other same conditions. The speed of the working body of the machine constituted 25 s^{-1} (1500 rpm).

The products of dehulling passed through the aspiration channel (Figure 1) with the purpose of separating the husk and the dust middlings, after which the cleaned products were weighed and calculated as a percentage of the dehulling index.

After weighing the products of dehulling sifted on a lattice with a diameter of holes of 5,0 mm in order to isolate the crushed particles, which also weighed and calculated their yield as a percentage.

The results of the researches were presented as dependence of "moisture – dehulling index". The research was carried out in three repetitions with large and small factions of peas separately.

Technique of determining the ash content product of dehulling

A large faction of pea seeds with moisture of 11,6% and an absolute mass of 257 g was scaly at the duration of 5, 10, 15, 20, 25 s, the speed of rotation of the working body of the dehuller was 25 s^{-1} (1500 rpm). After each test the cleaning machine was thoroughly cleaned of all products to avoid mixing of products of different ash content, which were obtained at different duration of processing.

The ash content was determined by the following methods. The weight of 2 g was burned in a muffle furnace at a temperature of 600...900 °C for 4 hours. The ash content indicator was determined by the dry substance by the formula [1, 9]:

$$z = \frac{m_g \cdot 100 \cdot 100}{m_p (100 - W)} \quad (7)$$

where m_z – ash content weight, g; m_p – weight of sample of product, g; W – product moisture,%.

Separately determined the ash content of the kernel and the ash content mixture of husk and dust middlings.

Results and discussion

Effect of processing duration on the efficiency of dehulling

The researches found that between the duration of treatment in the dehuller and the efficiency of dehulling of pea seeds there is linear dependence regardless of moisture and large pea. And also the speed of rotation of the working body of the dehuller. Dependence of the dehulling index of large and small fractions of peas from the duration of processing are shown in Figure 2 and 3.

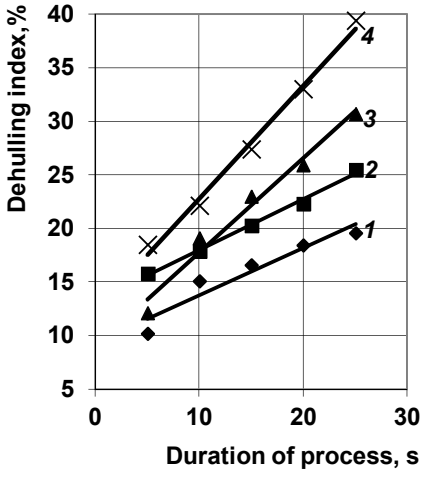

Figure 2. The dependence of the dehulling index large pea seeds faction from the duration of dehulling:
1 – W = 11,6%, ω = 25 s^{-1}; 2 – W = 11,6%, ω = 41,6 s^{-1}; 3 – W = 16,6%, ω = 25 s^{-1}; 4 – W = 16,6%, ω = 41,6 s^{-1}

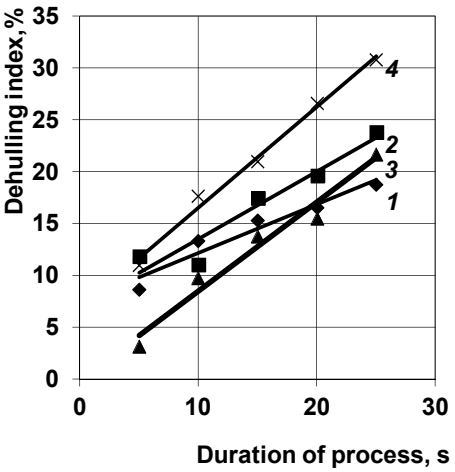

Figure 3. The dependence of the dehulling index large pea faction from the duration of dehulling:
1 – W = 11,6%, ω = 25 s^{-1}; 2 – W = 11,6%, ω = 41,6 s^{-1}; 3 – W = 16,6%, ω = 25 s^{-1}; 4 – W =16,6%, ω = 41,6 s^{-1}

From Figure 2, you can see that regardless of all other factors increase the duration of processing in the dehuller from 5 to 25 s led to the increase in the dehulling index in the processing of large fraction of pea seeds, the absolute mass of which was 257 g. The smallest efficiency of dehulling was observed at rotational speed of working body 25 s^{-1} and moisture of pea 11,6%. The index was correspondingly increased from 10,2 to 19,6%. Increase of rotation speed of working area of the dehuller from 25 s^{-1} to 41,6 s^{-1} increases the dehulling index on average by 5,0%. Increasing the speed of the working body of the machine provides a more intense impact on the efficiency of the process, which leads to its increase.

Increased pea moisture from 11,6 to 16,6% led to increased efficiency of dehulling. At the speed of rotation of the working body of the dehuller 25 s^{-1}, the dehulling index was increased from 12,2 to 30,8%. Under these same conditions increase the speed of the rotation from 25 to 41,6 s^{-1} led to an additional increase in the dehulling index, which increased from 18,5 to 39,4%.

The smallest efficiency of dehulling was observed at dehulling of dry seeds, regardless of its size. This can be explained by the fact that peas creates more resistance ripe than moist peas. With the increase in moisture of peas there is a violation of shells with the kernel, as well as the kernel becomes more plastic, which leads to a lighter abrasion in the action of abrasive bodies of dehuller and the increase of the yield of small [16].

From Figure 3 data, you can see that regardless of all other factors increase the duration of processing in the dehuller from 5 to 25 s led to the increase in the efficiency of dehulling while processing the small fraction of pea seeds, the absolute mass of which was 213 g. The dehulling index was increased from 8,7 to 18,8%. The increase in the rotation speed of the working body from 25 s^{-1} to 41,6 s^{-1} led to an additional increase in the dehulling index, which has changed from 11,9 to 23,8%.

The increase in moisture of small fraction of peas from 11,6 to 16,6% led to increased efficiency of dehulling peas only at speed of rotation of working body of dehuller 41,6 s^{-1}. At the speed of rotation of the working body of the dehuller 25 s^{-1} the reverse effect of

influence was observed. Small peas with moisture of 16,6% scaly worse than peas with moisture of 11,6%. The dehulling index was increased from 3,2 to 21,7%. This may be the result of the fact that the small peas in damp condition carries more resistance to the compressiance than dry.

The greatest efficiency of dehulling of small pea was observed at the moisture 16,6% and rotation speed of the working body 41,6 s^{-1}. Under these conditions, the dehulling index was increased from 11,0 to 30,6%.

Comparing Figures 2 and 3 can be seen that a large fraction of pea is more effective than small in all other same conditions. and the action of moisture on large seeds is more than small, resulting in greater importance of dehulling index. This can be explained by the fact that large pea seeds have less resistance to compressiance than small.

In the process of dehulling, in addition to whole seeds of pea, formed pea fine gritz. The results of the study of a fine grits yield are shown in Figures 4 and 5.

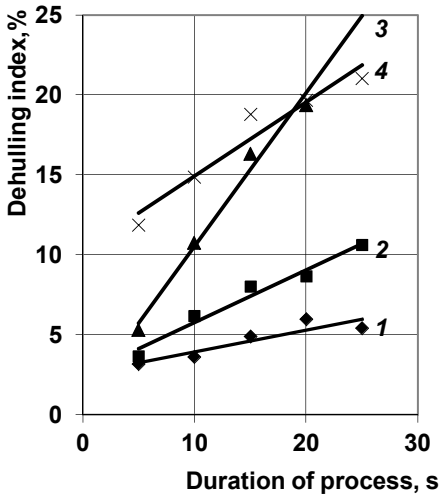

Figure 4. Dependency yield of fine grits at a different duration of dehulling of large pea fraction:
1 – W = 11,6%, ω = 25 s^{-1}; 2 – W = 11,6%, ω = 41,6 s^{-1}; 3 – W = 16,6%, ω = 25 s^{-1}; 4 – W = 16,6%, ω = 41,6 s^{-1}.

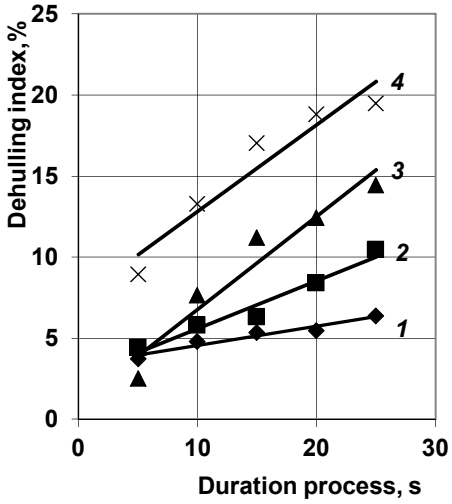

Figure 5. Dependency yield of fine grits at different duration of dehulling of small fraction of peas:
1 – W = 11,6%, ω = 25 s^{-1}; 2 – W = 11,6%, ω = 41,6 s^{-1}; 3 – W = 16,6%, ω = 25 s^{-1}; 4 – W = 16,6%, ω = 41,6 s^{-1}.

The smallest yield of fine grits at dehulling of a large fraction of peas was observed at moisture of pea 11,6% and speed of rotation of working body of dehuller 25 s^{-1}. With the increase in the duration of processing from 5 to 25 s the yield of a small scale linearly increased from 3,2 to 5,4%. Increase the rotation speed of the working body of the dehuller with 25 s^{-1} to 41,6 s^{-1}, has led to an increase in the yield of a fine grits at dehulling of a large fraction of peas with moisture of 11,6%.

Increased moisture of a large pea fraction from 11,6 to 16,6% substantially led to an increase in the yield of a fine grits. At the speed of rotation of the working body of the dehuller 25 s^{-1}, the yield of a fine grits increased from 5,3 to 25,0% duration of dehulling from 5 to 25 s. Increase the rotation speed of 25 s^{-1} to 41,6 s^{-1} led to an increase in the yield of a fine grits from 11,9 to 21,0%.

At the dehulling of small fraction of peas there is a similar effect of pea moisture and rotational speed of working body of the dehuller. The smallest yield of fine grits was observed at moisture of pea 11,6% and speed of the working body of the dehuller 25 s^{-1}, with increasing the duration of the dehulling of small pea from 5 s to 25 s, the yield of fine grits increased in accordance with 3,8 to 6,4%. The increase of rotational speed of working body of the dehuller with 25 s^{-1} to 41,6 s^{-1}, led to an increase in the yield of a fine grits, which increased depending on the duration of dehulling from 4,4 to 10,5%.

With the increase in moisture small fraction of pea seeds from 11,6 to 16,6% yield of fine grits considerably increased by linear dependence. At rotational speed of working body of dehuller 25 s^{-1}, the yield of a fine grits increased from 2,5 to 14,5%, depending on the duration of dehulling, which ranged from 5 to 25 s. With increasing speed of working body of dehull machine with 25 s^{-1} to 41,6 s^{-1} and the increase of moisture of small pea from 11,6 to 16,6%, the yield of fine grits additionally increased from 9,0 to 19,5%, with duration of dehulling from 5 to 25 s.

Comparing the Figures 4 and 5, you can see that the yield of a fine grits is bigger in large pea faction. In the dehulling of dry pea seeds with moisture of 11,6%, the yield of fine grits varies within 1,0% regardless of the fraction of the faction, and with increasing moisture up to 16,6% of the yield of fine grits is increased for both large fraction and small. Larger yield of a fine grits traced at dehulling of large fraction.

The following data can be output: increasing the duration of dehulling, the rotation speed of the working body and the pea moisture leads to an increase in the yield of small. The smallest yield of fine grits was observed at dehulling of dry seeds as large and small, and with increase of moisture yield of fine grits increases, which is the result of change of its structural-mechanical properties.

Increase of the yield of a fine grits at increasing the speed of rotation of a working body of the dehuller can be explained by the fact that the more intensive action on pea seeds due to the frictional forces [3, 10, 16, 17, 33]. The effect of moisture to increase the yield of fine grits can be explained by the fact that moisture reduces the strength of connections in the middle of the kernel peas, due to which forms a larger yield of fine grits during dehulling [5, 35].

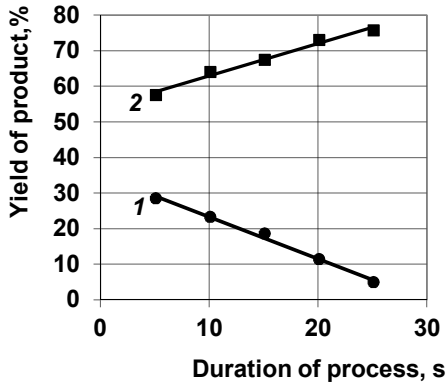

Figure 6. Yield of the kernel and undehulled seeds at fine pea dehulling: 1 – yield of undehulling seeds; 2 – yield of kernel

During the processing of peas in groats, a fine grits is a byproduct. Increasing the yield of a fine grits leads to a decrease in the yield of the whole kernel, so it is necessary to try to reduce its yield, it can be achieved by processing dry pea.

Analyzing the data of the kernel yield and undehulled seeds, it is found that the yield of undehulled seeds varies linearly inverse of the yield of the kernel, as shown in Figure 6. With the increase in the yield of the whole kernel, the yield of undehulled seeds on the same amount decreases. The moisture of the pea was 13,6% and the speed of rotation of the working body of the dehuller totalled 41,6 s^{-1}.

Effect of filling on efficiency of dehulling

In order to establish dependence of influence of the load on the efficiency of dehulling the pea was perfomed study of the dehulling of large and small fractions of pea seeds at the constant duration of dehulling 15 s, the constant speed of rotation of the working body of the dehuller, which amounted to 41,6 s^{-1} and the various pea moisture.

It is found that the dehulling of both large and small fraction of seeds of peas by moisture of 12,9%, with increase in the mass of grain loaded into the dehuller, the dehulling index increases by linear dependence. This indicates that with all the immutable parameters of the process, the efficiency of dehulling will increase by increasing the mass of pea seeds in the dehuller. The results of research are shown in Figure 7.

When dehulling a large fraction of pea seeds with 17,4% moisture (line 3 in Figure 7) was called the rotor of a dehuller, which was not observed when dehulling a small fraction with moisture of 16,8%. This can be explained by the fact that the increase in the moisture of pea seeds leads to increased friction coefficient between seeds, at the expense of which increases resistance to the working body of the dehuller.

Having expressed a mass of grain due to the coefficient of filling of working chamber of dehuller we obtain dependence of the efficiency of dehulling from filling coefficient of working chamber of the dehuller at constant time of dehulling, which totalled 15 s.

When dehulling large fraction of pea seeds with 12,9% moisture, the dehulling index was increased from 9,7 to 16,0%. The coefficient of filling of working chamber of the dehuller was increased from 0,09 to 0,48, as shown in Figure 8. In the dehulling of the small fraction of peas with moisture 12,9%, the dehulling index increased from 6,3 to 16,1% in the same conditions. This data shows that small pea fraction is less erased in the process of dehulling than large and requires greater duration of dehulling than a large fraction to achieve similar result.

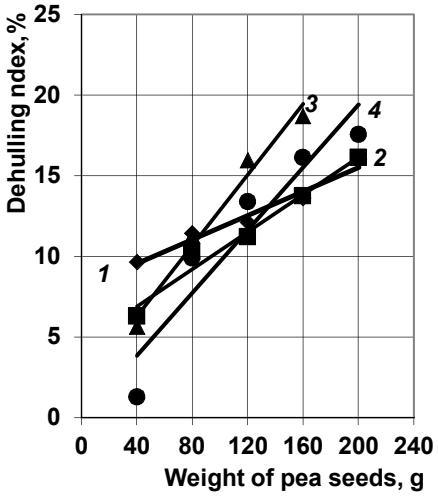

Figure 7. Dependence of the dehulling index from the amount of grain loaded in the dehuller:
1 – W = 12,9%, A = 226 g; 2 – W = 12,9%, A = 196 g; 3 – W = 17,4%, A = 226 g; 4 – W = 16,8%, A = 196 g

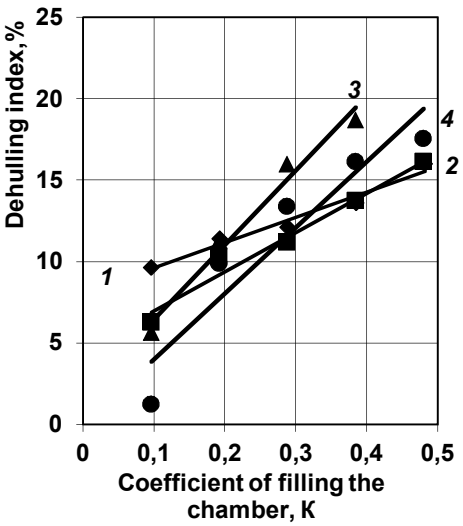

Figure 8. The dependence of the efficiency of dehulling on the fill factor of the working chamber:
1 – W = 12,9%, A = 226 g; 2 – W = 12,9%, A = 196 g; 3 – W = 17,4%, A = 226 g; 4 – W = 16,8%, A = 196 g

With increased moisture of a large pea seed fraction from 12,9 to 17,4%, the dehulling index was increased from 5,6 to 18,7% depending on the coefficient of filling the working chamber of the dehuller from 0,09 to 0,48. When the fine fraction of pea seeds with moisture 16,8%, the dehulling index increased from 1,3 to 17,6% at the same coefficients of filling the working chamber of the dehuller.

Attention is paid to the fact that at the small filling of working chamber of the dehuller (K = 0,1) with the dehulling of moist seed as large and small fractions of pea seeds The dehulling index is smaller and totalled 5,6% and 1,3% than in the processing of dry fractions pea seeds. For dry large and small fractions of pea seeds dehulling index was 9,7% and 6,3%. This indicates that when the small filling of the working chamber dehuller, moisture seed increases the resistance of friction forces operating in the working area of the machine.

The research is determined that the yield of a trifle also has increased with the increase in the coefficient of filling of working chamber of dehuller by linear dependence, as shown in Figure 9.

The yield of small pea fraction with the moisture of 12,9% increased from 0,9 to 11,2%, with the appropriate increase in coefficient of filling of working chamber from 0,09 to 0,48. With the increase in the moisture of pea seeds of large fraction from 11,6 to 17,4% and increase of filling coefficient of working chamber of dehuller from 0,09 to 0,48, the yield of small-scale increase from 1,9 to 15,9%. The increase in the pea seeds of large fraction of the faction led to an increase in the yield of small.

When the meadow small fraction of pea seeds were observed the similar dependence. With the increase in the filling coefficient of working chamber of dehuller yield of small-scale machines increased from 0,9 to 12,2%. With the increase in moisture of small fraction of pea from 12,9 to 17,4% and the corresponding change in filling coefficient of the working chamber of the dehuller from 0,09 to 0,48, the yield of a small scale is increased linearly from 1,8 to 18,2%.

The given research results show that the moisture and weight of the loaded pea seeds in the dehuller increase of the yield of a fine grits during the process of dehulling under all other conditions. This data also confirms the results of the study shown in Figure 2 and 3.

The duration of dehulling also influences the efficiency of the process. In order to establish a general effect on the efficiency of dehulling pea seeds processing duration and the coefficient of filling of working chamber of the dehuller was carried out by dehulling of large fraction of pea seeds with 12,6% moisture. The results of researches, which are shown in Figure 10 indicate a gradual increase of efficiency of dehulling under all other conditions.

Apparently from the drawing of 10 data with increase in coefficient of filling of the worker of chamber from 0.09 to 0.48 and with increase in duration of dehulling with 10 to 25 with dehulling the index while the nature of process remains invariable linearly increases.

The yield of fine grits is also subject to linear dependence, as shown in Figure 11. The largest yield of fine grits was observed at the duration of dehulling 25 s and the coefficient of filling of working chamber of the dehuller 0,48, and the smallest yield of fine grits was observed the duration of dehulling 10 s and the coefficient of filling of working chamber of the dehuller 0,09.

The given evidence indicates that the duration of finding pea seeds increases the dehulling index, but the nature of the process remains without changes.

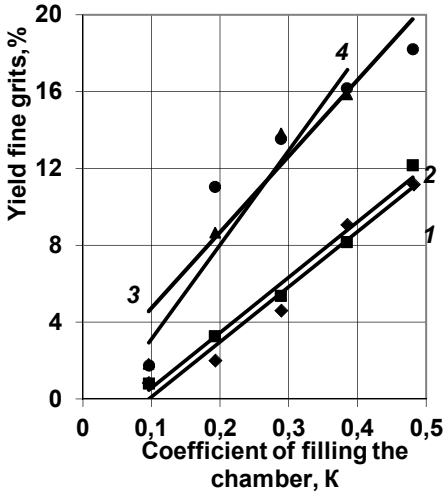

Figure 9. Dependence of a small yield depending on the coefficient of filling of working chamber of the dehuller:
1 – W = 12,9%, A = 226 g; 2 – W = 12,9%, A = 196 g; 3 – W = 17,4%, A = 226 g; 4 – W = 16,8%, A = 196 g

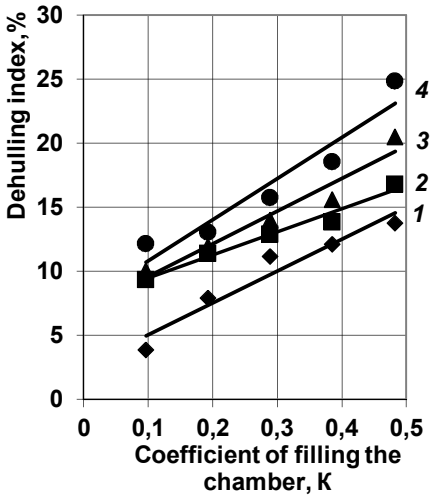

Figure 10. Influence of duration of dehulling and filling coefficient of working chamber for efficiency of dehulling:
1 – 10 s; 2 – 15 s; 3 – 20 s; 4 – 25 s

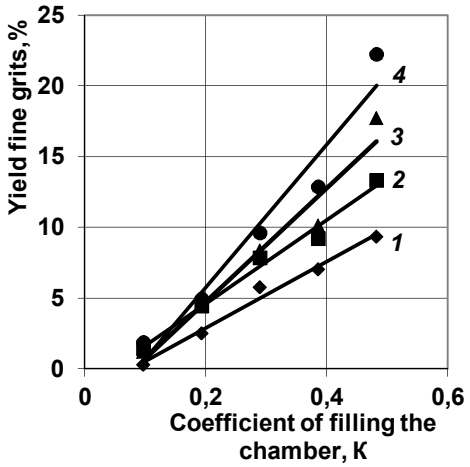

Figure 11. Yield fine grits at different duration of dehulling and coefficient of filling of working chamber of the dehuller:
1 – 10 s; 2 – 15 s; 3 – 20 s; 4 – 25 s

Investigation of moisture influence on the efficiency of dehulling peas

The data of Figures 2 and 3 indicates that the moisture affects the efficiency of the dehulling of peas, however the character of this dependence remains unknown. Conducted researches have shown that with the increase in moisture of pea seeds the efficiency also increases with all other conditions of the process of dehulling, as shown in Figure 12. During the investigation of the absolute mass of seeds of large fraction amounted to 226 g, the absolute mass of seeds of small fraction constituted 196 g.

Figure 12 shows that the large fraction of the pea change of moisture from 10,8 to 16,5% led to the growth of the dehulling index from 15,6 to 27,4%. When the small fraction was formed, the moisture was changed from 12,1 to 16,9%, the dehulling index was smaller and increased from 15,1 to 22,6%. The results obtained are consistent with the research of other researchers [13,15, 19, 23, 27].

Smaller values of the dehulling index confirm the previous research that the small peas are worse than the same for all other conditions.

With increasing the efficiency of dehulling due to the increase in the moisture of peas also increases the yield of fine grits at line dependence, as shown in Figure 13. The smallest yield of fine grits is observed at low moisture of peas, and with increased moisture of the pea, yield of small lines increases.

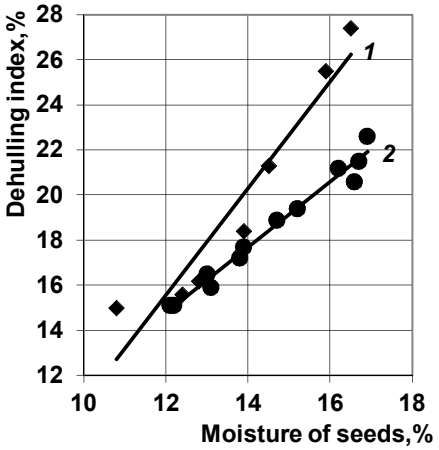

Figure 12. Effect of pea moisture on the efficiency of its dehulling:
1 – large fraction; 2 – fine fraction

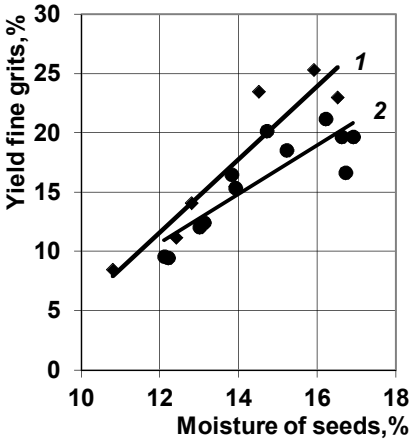

Figure 13. Yield of fine grits depending on the moisture of peas:
1 – large fraction; 2 – fine fraction

Analysis of the ash content dehulling products

By studies of ash content content of kernel, husk and dust middlings at the dehulling of a large fraction of peas found that the ash content is changing linearly depending on the duration of dehulling of pea seeds, as shown in Figure 14.

Data Figure 14 It is confirmed that the ash content content of dehulling linearly decreases with the increase of duration of dehulling. With the increase in the duration of the dehulling from 5 s to 25 s, the kernel's ash content decreased from 2,86 to 2,42%, under these conditions, the ash content content of husk and dust middlings decreased from 3,7 to 3,32%.

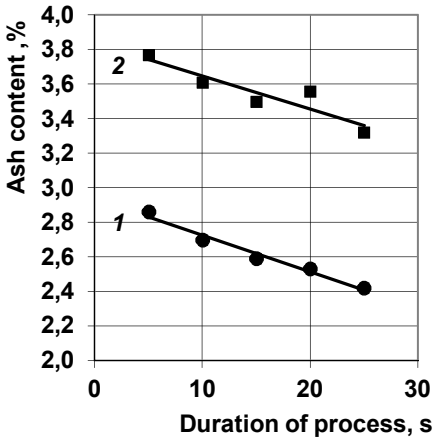

Figure 14. Change of ash content content of kernel, husk and dust middlings of large pea fraction:
1 – kernel; 2 – husk and dust middlings

From figure 14 data, you can see that the direct change in the ash content is parallel to one another. This indicates that with increasing the duration of dehulling of high-ash content products, which are separated from the kernel are transferred to products that form the flow of husk and dust middlings and have less ash content than husk and dust middlings. With a gradual decrease in the kernel of the kernel, the ash content particles are also diminished, which are sent to husk and dust middlings, which leads to a decrease in their ash content.

From these data it is possible to conclude that with the increase of duration of dehulling, the compression of a low-ash content kernel leads to decreasing of the flow of husk and dust middlings, which reduces the yield of the kernel and increases the yield of husk and dust middlings, whose ash content is also reduced.

The results of the researches give an opportunity to better understand the behavior of pea seeds in the dehulling process.

Conclusions

Scientific novelty of the results consists in the fact that it allows to understand the behavior of pea seeds in the process of dehulling during its processing at different parameters of the process.

1. Increasing the duration of dehulling from 5 to 25 and increases the efficiency of dehulling of pea seeds according to linear dependence, regardless of the size of the pea seeds.
2. Increase in the moisture of pea seeds from 11,6 to 16,8% also leads to increased efficiency of dehulling. Efficiency of dehulling with increase in moisture increases by increasing the yield of small.
3. Increase the rotation speed of the working body of the dehuller with 25 s^{-1} to 41,6 s^{-1} leads to increased efficiency of dehulling peas.
4. Big seeds of peas - a factor which reduces efficiency of dehulling..
5. At efficiency of dehulling also significantly influences the coefficient of filling of working chamber of the dehuller. Regardless of the large pea, increasing the coefficient of filling of the working chamber of the dehuller leads to increased efficiency of dehulling on linear dependence.
6. With the increase in duration of processing, the speed of the working body of the dehuller, the load factor of the working chamber of the dehuller, as well as moisture contributes to an increase in the yield of fine grits by decreasing the yield of the whole kernel. Under the same conditions, the yield of fine grits is smaller when the small fraction is at the expense of greater resistance to the joints.
7. The maintenance of ash-content of a kernel and peel and goods of average quality of dust - linearly reduction with the increasing process duration..

References

1. AACC. (2010), *Approved methods of analysis*, (11th edn.). AACC International, St. Paul: American Association of Cereal Chemists.
2. AOAC. (2016), *Official Methods of Analysis of AOAC International*, (20th edn.). AOAC International, Maryland , USA.
3. Baltabaev U.N., Tursunkhodzhaev P.M. (2011), Issledovanie vliianiia konstruktivnykh parametrov i tekhnologicheskikh protsessov shelushitelia na effektivnost shelusheniia iachmenia, *Khranenie i pererabotka zerna*, 11, pp. 65–67.
4. Black R.G., Singh U., Meares C. (1998), Effect of genotype and pretreatment of field peas (*Pisum sativum*) on their dehulling and cooking quality, *Journal of the Science of Food and Agriculture*, 77(2), pp. 251–258.
5. Dexter J.E., Sarkar A.K. (2003), Encyclopedia of food science and nutrition (Second Edition), Academic Press.
6. Ehiwe A.O.F., Reichert R.D. (1987), Variability in dehulling quality of cowpea, pigeon pea and mung bean cultivars determined with TADD, *Cereal Chemistry*, 64, pp. 81–93.
7. Erskine W., Williams P.C., Nakkoul H. (1991), Splitting and dehulling lentil (*Lens culinaris*): effects of seed size and different pretreatments, Journal of the Science of Food and Agriculture, 57, pp. 77–84.
8. George E., Rentsen B., Tabil L.G., Meda V. (2014), Optimization of wheat debranning using laboratiry equipment for ethanol production, *International Journal of Agricultural and Biological Engineering*, 7(6), pp. 54–66.
9. Ghavidel R.A., Prakash content J. (2007), The impact of germination and dehulling on nutrients, antinutrients, in vitro iron and calcium bioavailability and in vitro starch and protein digestibility of some legume seeds, *LWT*, 40, 1292–1299.
10. Ghermezgoli K.M., Ghassemzadeh H.R., Moghaddam M. (2017), Optimization of Kabuli chickpea dehulling process, *Journal of Biodiversity and Environmental Sciences*, 10(2), pp. 115–125.
11. Goyal R.K., Vishwakarma R.K., Wanjari O.D. (2008), Optimisation of the pigeon pea dehulling process, *Biosystems Engineering,* 99, pp. 56–61.
12. Goyal R.K., Vishwakarma R.K., Wanjari O.D. (2009), Optimization of process parameters and mathematical modelling for dehulling of pigeon pea, *International Journal of Food Science & Technology*, 44, pp. 36–41.
13. Goyal R.K., Vishwakarma R.K., Wanjari O.D. (2010), Effect of moisture content on pitting and milling efficiency of pigeon pea grain, *Food and Bioprocess Technology*, 3(1), pp. 146–149.
14. ICC (2009), The ICC Handbook of cereals, flour, dough & product testing. Methods and applications. (Stanley P. Cauvain, et al., eds), DEStech Publications, Inc.
15. Joyner J.J., Yadav B.K. (2015), Optimization of continuous hydrothermal treatment for improving the dehulling of black gram (*Vigna mungo L*), *Journal of Food Science and Technology*, 52(12), pp. 7817–7827.
16. Kharchenko Y.I., Sharan A.V. (2017), Shelushenie zerna iachmenia, *Khranenie i pererabotka zerna*, 9, pp. 28–31.
17. Mangaraj S., Singh K.P. (2009), Optimization of machine parameters for milling of pigeon pea using RSM, *Food and Bioprocess Technology*, 4(5), pp. 762–769.
18. Oomah B.D., Ward S., Balasubramanian P. (2010), Dehulling and selected physical characteristics of Canadian dry bean (*Phaseolus vulgaris L.*) cultivars, *Food Research International*, 43, pp. 1410–1415.
19. Opoku A., Tabil L., Sundaram J., Crerar W.J., Park S.J. (2003), Conditioning and dehulling of pigeon peas and mung beans, *CSAE*, paper №03-347, pp. 2–17.

20. Ponce-Garcia N., Ramirez-Wong B., Escalante-Aburto A., Torres-Chavez P.I., Serna-Saldivar S.O. (2017), Wheat improvement, management and utilization, *IntechOpen*, pp. 275–291.
21. Phirke P.S., Prabhakar S., Bhole N.G. (2000), Pretreatment of pigeon pea grain for improvement of dehulling characteristics, *International Journal of Food Science and Technology*, 35, pp. 305–313.
22. Phirke P.S., Bhole N.G., Adhaoo S.H. (1996), Response surface modeling and optimization of dehulling of pigeon pea with different pre-treatments and conditions, *Journal of Food Science Technology*, 33, pp. 47–52.
23. .Ramakrishnaian N., Kurien P.P. (1983), Variabilities in the dehulling characteristics of pigeon pea (*Cajanus cajan L.*) cultivars, *Journal of Food Science Technology*, 20, pp. 287–291.
24. Reichert R.D., Tyler R.T., York A.E., Schwab D.J., Tatarynovich J.E., Mwasaru M.A. (1986), Description of a production model of the tangential abrasive dehulling device and its application to breeders samples, *Cereal Chem*., 63(3), pp.201–207.
25. Singh U. (1995), Methods of dehulling of pulses: a critical appraisal, *Journal of Food Science Technology*, 32, pp. 81–93.
26. Singh U., Santosa B.A.S., Rao P.V. (1992), Effect of dehulling methods and physical characteristics of seeds on dhal yield of pigeon pea (*Cajanus cajan L.*) genotypes, *Journal of Food Science Technology*, 29, pp. 350–353.
27. Sokhansanj S., Patil R.T. (2003), Dehulling and splitting pulses. In: Handbook of Post Harvest Technology (Chakraverty A., et al., eds), Marcel Dekker, New York.
28. Vereshchinskii A.P. (2011), Svoistva i osobennosti vzaimodeistviia shlifovalnykh krugov s zernom v protsesse shelusheniia, *Khranenie i pererabotka zerna*, 11, pp. 62–65.
29. Vishwakarma R.K., Shivhare U.S., Gupta R.K., Yadav D.N., Jaiswal A., Prasad P. (2017), Status of pulse milling processes and technologies: A review, *Critical Reviews in Food Science and Nutrition*, 58(10), 1615 – 1628.
30. Sreerama Y.N., Sash contentikala V.B., Pratape V.M. (2009), Effect of enzyme pre-dehulling treatments on dehulling and cooking properties of legumes, *Journal of Food Engineering*, 92, pp. 389–395.
31. Tiwari B.K., JaganMohan R., Venkatachalapathy N., Tito Anand M., Surabi A., Alagusundaram K. (2010), Optimisation of hydrothermal treatment for dehulling pigeon pea, *Food Research International*, 43, pp.496–500.
32. Yasmin A., Zeb A., Khalil A.W., Paracha G.M.D., Khattak A.B. (2008), Effect of processing on anti-nutritional factors of red kidney bean (*Phaseolus vulgaris*) seeds, *Food and Bioprocess Technology*, 1(4), pp. 415–419.
33. Wang N. (2005) Optimization of a laboratory dehulling process for lentils (*Lens culinaries*), Cereal Chemistry, 82(6), 671–676.
34. Wang N., Hatcher D.W., Gawalko E.J. (2008), Effect of variety and processing on nutrients and certain anti-nutrients in field peas (*Pisum sativum*), *Food Chemistry*, 222, pp. 132–138.
35. Wrigley C. (2004), *Encyclopedia of Grain Science*, Academic Press, North Ryde.

Biotechnological parameters determination for cultivation of lactic acid bacteria from goat milk

Nina Bogdan

Practical Scientific Institute of Horticulture and Food Technology, Chisinau, Republic of Moldova

Keywords:

Milk
Goat
Lactic
Acid
Bacteria
Biotechnological

Article history:

Received 23.03.2018
Received in revised form 25.05.2018
Accepted 27.12.2018

Corresponding author:

Nina Bogdan
E-mail: ninabogdaniurie@gmail.com

DOI:10.24263/2304-974X-2018-7-4-6

Abstract

Introduction. The purpose of research – to establish optimal cultivation conditions to determine of the efficacy of development lactic acid bacteria isolated from goat milk.

Materials and methods. Strains cultivation were performed in sterilized goat milk medium at the 30±2 °C. Parameters determination have been established for the periodic cultivation in bioreactor Sartorius Biostat® A plus. Count enumeration of lactic acid bacteria cells was performed using the spread count method.

Results and discussion. The slow pH decrease was observed at all selected strains during cultivation time. Lactic acid has been accumulated proportional what shows the intense development of the lactic acid bacteria up to 14 cultivation hours. The active development is characterized through moderate acidity of fermented milk.

Data of strains development dynamics and the biomass accumulation in the medium goat milk-based proved the obtaining to maximum count of lactic acid bacteria cells lg CFU/g.

At the same time the regression analysis of the pH value dinamics and viable cells count were performed for exactly describes results of the experiments. The strains CNMN-LB-73, CNMN-LB-74, CNMN-LB-77 and CNMN-LB-78 has the accurate regression line at pH dinamic and strains CNMN-LB-73, CNMN-LB-74, CNMN-LB-75, CNMN-LB-76 and CNMN-LB-78 at the dynamic of cells development. Strains development stages have observed since 10 hours of cultivation. The decline phase started after 12 hours for CNMN-LB-76, CNMN-LB-77, CNMN-LB-79 strains and after 14 hours for CNMN-LB-73, CNMN-LB-74, CNMN-LB-75, CNMN-LB-78, indicating that they are more resistant to acid conditions that isolated strains reported by other authors, cell multiplication was observed until the pH 4.7.

Conclusions. In conditions of periodic cultivation biotechnological parameters for cultivation of lactic acid bacteria from goat milk were determinated. Obtained data demonstrated important biotechnological properties of isolated strains.

Introduction

Milk is a complete and favorable medium for many microorganisms or a convenient survival medium for other microorganisms and viruses that do not multiply in milk but can pollute it.

The main source of milk contamination is the external environment; the microorganisms reach the milk from the atmosphere due to the lack of hygiene of the shelters and the animal, the way of the milk processing, milking, the way of cooling and transporting of the milk and the water that does not correspond the sanitary-veterinary requirements.

It is worth mention that goats has much lower sanitary-epidemiological risk because they do not suffer from such diseases as brucellosis, tuberculosis and other diseases affecting bovine animals, doing goat's milk consumed raw. Raw goat milk preserve its proteins, lipids, sugars, vitamins, enzymes and mineral salts which have higher antioxidant properties compared to cow's [1, 2]. That is why goat milk products have nutritional and curative properties [3, 4].

There is research demonstrated that goat milk and goat milk products contain more less pathogenic bacteria than other animals' milk [5].

Many authors have published results of the quality and safety research of cheeses made from raw goat milk. These cheeses did not contain pathogenic bacteria of the *Salmonella, Listeria, Escherichia, Staphylococcus* species compared to cheeses made from other animals' milk [6, 7].

It is well known that milk is also a natural source of lactic bacteria strains which are specific microflora and in most cases useful for the dairy industry. These bacteria have important biotechnological properties for the food industry. The starter cultures contained lactic acid bacteria are widely used for dairy products from cow's milk. At the same time goat milk products obtaining needs in the cultures from lactic acid bacteria isolated from goat milk – their natural habitat. In laboratory of food biotechnology investigations were carried at isolation and selection of perspective autochtonous lactic acid bacteria from raw goat milk and determination their biotechnological parameters of cultivation for starter culture creation.

For the industrial production of dairy products with regulation of legislation should be used pasteurized milk and chosen starter culture which can provide a high product quality and safety with a long shelf life due to active biotechnological properties.

From different regions of Republic of Moldova were studied 150 samples of raw goat milk. As result of cultural, morfological, phisiological and biochemical tests were selected 7 isolates with characteristic features to the species *Lactococcus lactis ssp. lactis*, *Lactococcus lactis* ssp. *lactis biovar diacetylactis*, *Lactococcus lactis ssp.cremoris* and *Streptococcus thermophilus.*

Strains have been characterized by valuable technological properties as protective culture to inhibit the growth of *Salmonella* and *Escherichia* population in goat cheese.

The selection of new lactic acid bacteria strains for the industrial purpose based on pure cultures that have improved organoleptic properties of the product. It is important to establish the optimal conditions for cultivation that to determine the development efficacy [8].

This paper presents the results of biotechnological parameters determination for lactic bacteria cultures, obtained at conditions of periodic cultivation.Based on the obtained data, it is determined the evolution of the pH of the fermented milk, the dynamics of strain development and count of viable lactic acid bacteria cells.

Materials and methods

Materials

Strains of the species *Lactococcus lactis ssp. lactis*, *Lactococcus lactis* ssp. *lactis biovar diacetylactis*, *Lactococcus lactis ssp.cremoris* and *Streptococcus thermophilus* have been isolated from the samples of raw goat milk from different regions of the Republic of Moldova. Also identified strains have been stored in the National Collection of Nonpathogenic Microorganisms of the Institute of Microbiology and Biotechnology.

For the cultivation of bacteria was used medium of skimmed sterilized goat milk. The skimmed milk was sterilized at 1 atm pressure up to 10 minutes [9];

Enumeration of bacterial cells was performed using the spread count method cultured on an agarified medium based on hydrolysed milk. In hydrolysed milk was added 1,5–1,8% agar-agar. After 20–30 min was soften, after that melted at 1 atm up to 15 min. Obtained medium was dispensed into the dishes and sterilized 10 min at 1 atm (121±2) °C [9].

Methods

Assessmentofacidificationactivity

Acidification activity was establish by the pH degree of the milk fermented by the strain. pH measurement was performed by using the electronic pH meter HANNA. The titratable acidity of milk was determined in accordance with ISO 11869: 2012 and measured in turner degrees (T °) [10].

Bioreactor online monitoring: During the bioreactor fermentation, online monitoring parameters of pH have been carried out in the Sartorius Biostat® A plus bioreactor under of periodic cultivation conditions at 30±2 °C. Parameters of cells count have been enumerated and recorded.

Regression analysis

Regression analysis are used to determined the relationship between one dependent variable and one or more independent variables. It is designed to find the regression model, which expresses the correct experiments results.

To find stationary points of optimal model must be determined the confidence interval calculation for the regression equation.

Confidence interval calculation

The confidence interval (CI) is a type of interval estimate, computed from the statistics of the observed data, that might contain the true value of an unknown area parameter. For CI calculation is used formula (1):

$$CI = (M - t_{\alpha,n-1}\frac{S}{\sqrt{n}}; M + t_{\alpha,n-1}\frac{S}{\sqrt{n}}), \quad (1)$$

where M – the sample mean; $t_{\alpha,n-1}$ – the t value for the desired confidence level α (from the Student's coeficient table); n – samples size; S – the area standard deviation

Statistical analysis

The mathematical processing of the obtained experimental data according to experiments matrices type x^2 was performed using Microsoft Excel and Advanced Grapher 2.2. software for graphs interpretation of the results.

Results and discussion

One of the biotechnological *properties* of lactic acid bacteria is the cells viability which plays the crucial for their applications as dairy starters and as probiotics. But the significant count of LAB cells lose activity due to the death of microorganisms during product storage.These applications are conduced to various stress conditions that affect to the biotechnological properties of the bacteria.

The maintenance of the viability presents one of the survival concept. Viability has to be demonstrated by investigation methods.

Previously, we conducted studies dedicated to evaluated the stability of biotechnological activity of strains in fermented goat milks samples for 28 days of storage at refrigeration conditions. During experiments the post-acidification was observed in time of cooling and this fact can be explained by the residual metabolic activity of lactic acid bacteria. It is known that activity of β-galactosidase for cleavage of lactose hold active even at the storage refrigeration temperature [11]. This is contributed to the accumulation of lactic acid, acetic acid, citric acid, butyric acid, acetaldehyde and formic acid produced by the starter cultures [12, 13, 14].

The viability of lactic acid bacteria has been affected by acidity. Research results indicated decreasing the count of viable lactic bacteria (CFU/ml) in the first week of storage what is related to the increase of acidity, though at 28 storage day concentrations of lactic bacteria in fermented milk were at the probiotic level (10^7 CFU/ml) [15]. Obtained result proves opportunity to obtain a high quality product with probiotic properties and a long shelf life [16]. According to the bibliographic study, the fermented milk has probiotic properties when the lactic acid bacteria in it remain at count min 10^6 UFC/g at the moments of consumption [17, 18]. The results confirm the maintain stability of biotechnological properties of goat milk strains described by other authors [19].

This research due to biotechnological properties on the dynamics of the strains multiplication and the evolution of the pH value of goats' skim milk were carried out in the bioreactor at the temperature of 30±2 °C.

The confidence intervals of the equation for the pH parameter of a milk fermented by strain CNMN-LB-73 were calculated at using MO Excel (Tabel 1–2).

Tabel 1

Confidence intervals

Time,h	***Lactococcus lactis subsp. lactis biovar. diacetilactis* CNMN-LB-73**				
	pH value				
	x1	**x2**	**xmed**	**x1-xmed**	**x2-xmed**
0	6,7	6,6	6,65	0,05	-0,05
2	6,58	6,62	6,6	-0,02	0,02
4	6,40	6,35	6,37	0,03	-0,02
6	6,17	6,22	6,2	-0,03	0,02
8	5,86	5,94	5,9	-0,04	0,04
10	5,62	5,71	5,66	-0,04	0,05
12	5,10	5,08	5,09	0,01	-0,01
14	4,77	4,88	4,82	-0,05	0,06

Tabel 2

Confidence intervals

(x1-xmed)²	(x2-xmed)²	Σ(xi-xmed)²	Variation	Confidence	Conf 1	Conf 2
0,0025	0,0025	0,005	0,05	0,016794	6,633206	6,666794
0,0004	0,0004	0,0008	0,02	0,006718	6,593282	6,606718
0,0009	0,0004	0,0013	0,025495	0,008563	6,361437	6,378563
0,0009	0,0004	0,0013	0,025495	0,008563	6,191437	6,208563
0,0016	0,0016	0,0032	0,04	0,013435	5,886565	5,913435
0,0016	0,0025	0,0041	0,045277	0,015207	5,644793	5,675207
0,0001	0,0001	0,0002	0,01	0,003359	5,086641	5,093359
0,0025	0,0036	0,0061	0,055227	0,018549	4,801451	4,838549

The results of fermentation process by selected strains during to the cultivation time are presented in Figures 1 and 2. Determined decrease pH values is closely related to high level of lactococci and streptococci, contributed to the faster development of acidity. The high rate of viable lactic acid bacteria cells was maintained during the whole fermentation period and will able to maintain in final product based on the presented mathematical data.

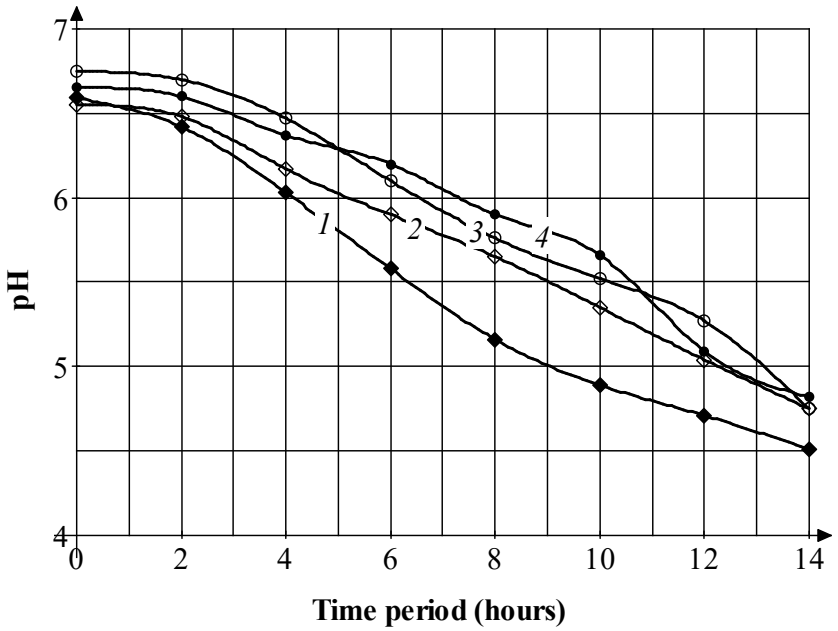

Figure 1a. Modification of pH value of goat milk fermented by lactic acid bacteria at a temperature of 30±2 °C
1 - CNMN-LB-79; 2 - CNMN-LB-78; 3 - CNMN-LB-75; 4 - CNMN-LB-73

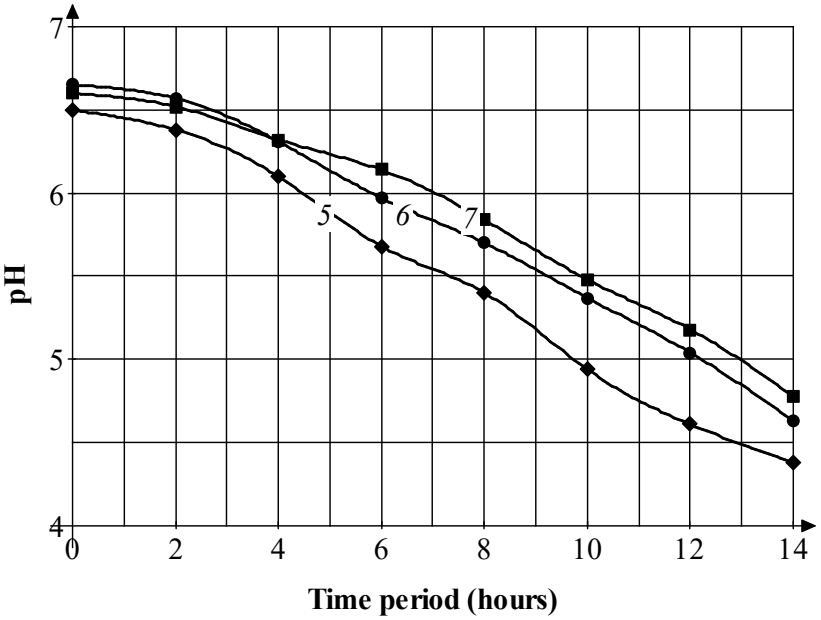

Figure 1b. Modification of pH value of goat milk fermented by lactic acid bacteria at a temperature of 30±2 °C

5 - CNMN-LB-76; 6 - CNMN-LB-77; 7 - CNMN-LB-74;

Based on mathematical data processing and regression equations obtained by the order x^2 was describe the dependence of pH during of cultivation time which allow to predict the acidogenesis process. The regression analysis is presented in Figures 1-2.

As a result of the strains growth the μ pH value = 4.6 at 14 hours of cultivation.

Analyzing the data from Figure 1a and 1b, it is noted slow pH decrease during cultivation time to all strains. Thus, after 14 hours the ΔpH of the strains was 2.37 units, indicating the accumulation of lactic acid by the intense and proportional development of the lactic bacteria.

Based on regression equations shower on Figure 1a and 1b the results strongly indicate that the confidence intervals are calculated correctly. The data show the moderate acidity and sufficient biochemical activity of these strains.

Thus, the following regression equation of the pH value of goat milk fermented by selected strains is obtained:

L. lactis biovar diacetylactis CNMN-LB-73	$Y(x)=-0.0063X^2-0.0474X+6.68$
L. lactis CNMN-LB-74	$Y(x)=-0.0058X^2-0.0504X+6.6208$
L. lactis CNMN-LB-75	$Y(x)=-0.0042X^2-0.0865X+6.8125$
L. lactis CNMN-LB-76	$Y(x)=-0.0020X^2-0.1348X+6.5854$
L. cremoris CNMN-LB-77	$Y(x)=-0.0042X^2-0.0893X+6.6991$
L. cremoris CNMN-LB-78	$Y(x)=-0.0025X^2-0.0987X+6.6037$
Str. thermophilus CNMN-LB-79	$Y(x)=0.0035X^2-0.2098X+6.7079$

The next point was to determine biotechnological parameters of selected lactic strains. Date obtained on Figure 2a and 2b shows development kinetics at the beginning of the logarithmic phase through the polynomial model of *x2* order also. These graphs help to determine the absolute maximum point of the function.

Methods of mathematical analysis were used according to the optimal model. The critical points were found by formation the experimental dependencies (the cells count during cultivation time), in which the absolute maximum values of the function were determined. Extremes obtained according to mathematical models coincide with the extremes obtained in the experiment, which confirms that the experiment was performed exactly.

The comparative evaluation of the extremes of the dependency models at order (2^2) is presented in Table 3.

Tabel 3

Extreme points of lactic acid bacteria count at temperature 30±2 °C

Strain	Regression equations	Experiment extremes		Mathematical model extremes	
		x	y	x	y
CNMN-LB-73	$y = -0,0253x^2 + 0,7473x + 3,2583$	14,78	8,89	14,77	8,77
CNMN-LB-74	$y = -0,0221x^2 + 0,6435x + 4,1985$	14,31	8,92	14,56	8,88
CNMN-LB-75	$y = -0,0285x^2 + 0,7941x + 3,1202$	13,71	8,66	13,93	8,65
CNMN-LB-76	$y = -0,0237x^2 + 0,5796x + 4,7508$	11,69	8,30	12,23	8,29
CNMN-LB-77	$y = -0,0251x^2 + 0,6437x + 3,8808$	12,49	8,06	12,82	8,00
CNMN-LB-78	$y = -0,0236x^2 + 0,6299x + 4,5895$	13,29	8,75	13,34	8,79
CNMN-LB-79	$y = -0,0596x^2 + 1,3449x + 1,3035$	11,31	9,00	11,28	8,89

The strain development and biomass accumulation are presented on Figures 2a and 2b. Also at the these figures the regression equations obtained to each strain were used to determine the extremes. Knowing the factors that influence to the lactic acid bacteria growth, according to the table it can be chosen an optimum. Based on showed regression equations the results strongly indicate that the confidence intervals are calculated correctly.

Thus, the following regression equation of the lactic acid bacteria growth is obtained:

L. lactis biovar diacetylactis CNMN-LB-73	$Y(x)=-0.0253X^2+0.7473X+3.2583$
L. lactis CNMN-LB-74	$Y(x)=-0.0221X^2+0.6435X+4.1985$
L. lactis CNMN-LB-75	$Y(x)=-0.0285X^2+0.7941X+3.1202$
L. lactis CNMN-LB-76	$Y(x)=-0.0237X^2+0.5796X+4.7508$
L. cremoris CNMN-LB-77	$Y(x)=-0.0251X^2+0.6437X+3.8896$
L. cremoris CNMN-LB-78	$Y(x)=-0.0236X^2+0.6299X+4.5895$
Str. thermophilus CNMN-LB-79	$Y(x)=-0.0596X^2+1.3449X+1.3035$

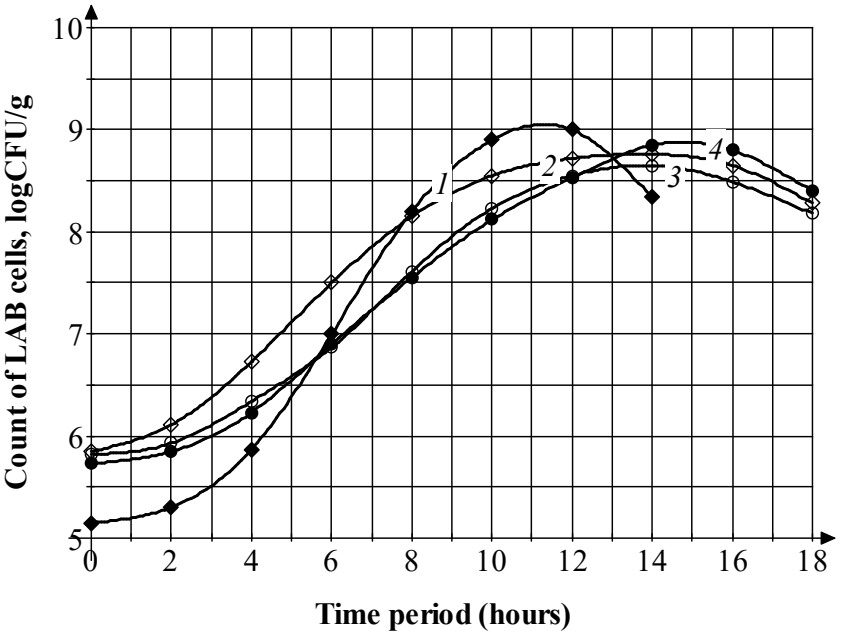

Figure 2a. Lactic acid bacteria growth at temperature 30±2 °C
1 - CNMN-LB-79; 2 - CNMN-LB-78; 3 - CNMN-LB-75; 4 - CNMN-LB-73

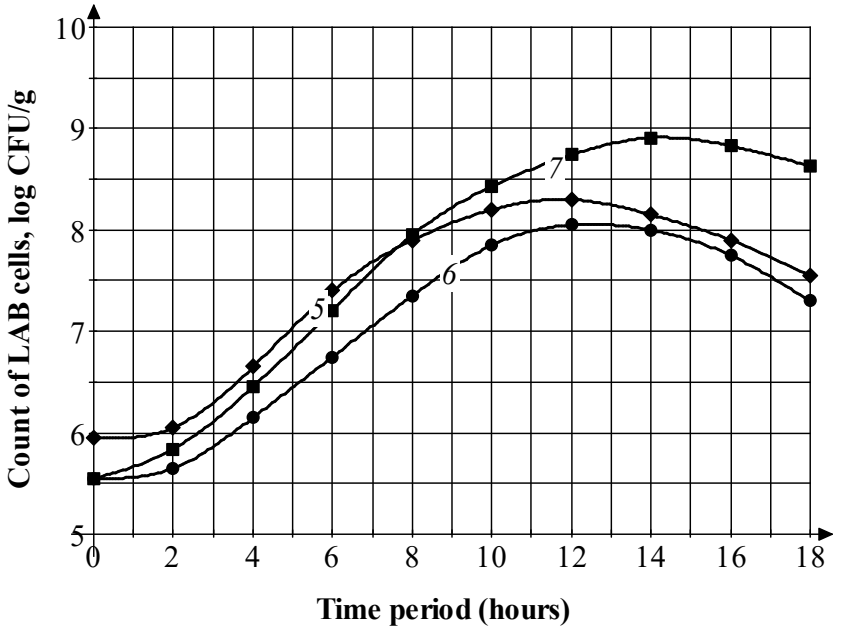

Figure 2b. Lactic acid bacteria growth at temperature 30±2 °C
5 - CNMN-LB-76; 6 - CNMN-LB-77; 7 - CNMN-LB-74

The obtained regressions showed on Figure 2a and 2b described enabled accurate determination of fermentation process related to biological activity of the strains. The CNMN-LB-74, CNMN-LB-75 and CNMN-LB-78 amount the maximum of the logarithmic phase of growth at 14 hours of cultivation, CNMN-LB-73 at 15 hours, CNMN-LB-76 and CNMN-LB-77 at 12 hours of cultivation and the strain CNMN-LB-79 amount the maximum of the logarithmic phase of growth at 11,5 hours of cultivation, what is characterized to the cultures of this specie.

Figure 2a and 2b showed the graphs of parameters monitoring for growth of selected lactic cultures, respectively, that have been carried out for 18 h of fermentation. The cultivation of the strains showed exactly the phase of the exponential multiplication and the phase of decline. According to mathematical models, the extremes have been obtained, which can determine the number of viable cells during cultivation - the absolute maximum of the function in the researched area at the moment (Table 3).

Although the technologically important parameters like optimal pH and temperature for industrially used strains are well known, the behaviour of the quantitative growth characteristics like specific growth rate, lactic acid production rate and growth with changing pH, temperature and other environmental factors are relatively poorly studied. Methods based on the measurement of pH or acid formation are used to determine the temperature optimum and acidifying activity of LAB.The method is optimal and convenient to determination technological parameters the acid formation rate and biomass concentration in food environment.

Several authors have studied the capacity of lactic bacteria to survive at low pH values. They have demonstrated the resistance of lactococcus at the environment with pH no lower that 4.8 [20, 21].

The obtained results showed that the decline phase of the selected strains started after 12 hours to the CNMN-LB-76, CNMN-LB-77, CNMN-LB-79 strains, after 14 hours CNMN- LB-74, CNMN-LB-75, CNMN-LB-78 and after 15 hours to the CNMN-LB-73 indicating that the selected strains are more resistant to acidic conditions and cell multiplication is observed until the pH = 4.7.

Conclusion

In conclusion, from the parameters controlled during the fermentation in the bioreactor, showed high count of viable cells even at influence factor of pH value with acidic condition. The process become more productive in periodic cultivation condition in goat milk based medium. After storage period at refrigeration conditions selected strains demonstrated high regeneration capacity in goat milk medium rich in nutrients and exhibit specific biochemical properties. Obtained data allow to modificate cultural medium which will have a significant stimulating effect on viability of strains isolated from goat milk. Defining of cultivation conditions allow the production of autochthonous cultures will be used as starters in traditional dairy-making from goat milk.

References

1. Bogdan N. (2017), Analysis of high biological properties of goat milk, *Annals of the 83 International scientific conference of young scientist and students "Youth scientific achievements to the 21st century nutrition problem solution",* p. 339.

2. Bogdan N. (2017), Goat milk – actual direction in dairy industry. *Annals of the Vth edition of Scientific Conference with International participation of PhD students "Contemporary trends of science development: visions of young researchers "*, p. 171–176.
3. Radulović Z. et al. (2011), Lactic acid bacteria in white brined cheese production. *Mljekarstvo Dairy*, 61(1), pp.15–25.
4. RyzhkovaT.(2013),Vliyaniyekombinatsionnykhsochetaniyzakvasochnoymikroflorynakach estvoivykhodkoz'yegotvoroga. *Scientific works of National Academy of food technologies*, 38(2), pp.185–190.
5. De reu K. et al. (2000), Hygienic parameters, toxins and pathogen occurrence in raw milk cheeses, *Journal of Food Safety*, 22(3), pp.183–196.
6. Jakobsen R.A. et al. (2011), Staphylococcus aureus and Listeria monocytogenes in Norwegian raw milk cheese production, *Food Microbiology Journal*, 28(3), pp. 492–496.
7. Yemtsev V.T.(2012), *Mikrobiologiya: uchebnikdlyabakalavrov*, Yurayt, Moscow.
8. *Sbornikinstruktsiyposelektsiimolochnokislykhbakteriyibifidobakteriyipodboruzakvasokdlya kislomolochnykhproduktov*,(1986), VNIIMS, Moscow.
9. ISO/TS 11869:2012 *Fermented milks. Determination of titratable acidity. Potentiometric method*, IDF/RM 150:2012, p. 7.
10. Kailasapathy K., Sultana K. (2003), Survival and galactosidase activity of encapsulated and free Lactobacillus acidophilus and Bifidobacteriumlactis in ice-cream, *Australian Journal of Dairy Technology*, 58, pp. 223–227.
11. Adolfsson O., Meydani S., Russell R.(2004), Yogurt and gut function, *American Journal of Clinical Nutrition*, 80(2), pp.45–56.
12. Novak L., Loubiere P.(2000), The metabolic network of Lactococcuslactis: distribution of 14C-labeled substrates between catabolic and anabolic pathways, *Journal of Bacteriology*, 182(4), pp. 1136–1143.
13. Ostlie H., Treimo J., Narvhus J.A.(2003), Effect of temperature on growth andmetabolism of probiotic bacteria in milk, *International Dairy Journal*, 15, pp. 989–997.
14. Bogdan N.(2018), Mixed culture of lactic acid bacteria strains for goat milk fermentation, *Fruit growing, viticulture and winemaking Journal*, 1-2(73-74), pp. 68-71, ISSN 1857-3142(in Romanian).
15. Homayouni A. et al.(2008), Growth and survival of some probiotic strains in simulated ice cream conditions, *Journal of Dairy Science*, 8, pp. 379–382.
16. Kurmann J., Rasic J. (1991), The health potential of products containing bifidobacteria, *Therapeutic Properties of Fermented Milks ed. Robinson, R.K. Elsevier Applied Food Sciences,* pp. 117–158.
17. Saxelin M., Korpela R., Mayra-Makinen A.(2003), Introduction: classifying functional dairy products, *T. Mattila-Sandholm, M. Saarela(Eds.), Functional Dairy Products, Woodhead Publishing Limited, Cambridge*, pp. 1–16.
18. Widodo H. et al.(2013), Fermented goat milk and cow milk produced by different starters of lactic acid bacteria: quality studies, *Journal of Agricultural Science and Technology*, A(3), pp. 904–911.
19. Adamberg K. et al.(2003), The effect of temperature and pH on the growth of lactic acid bacteria: a pH-auxostat study, *International Journal of Food Microbiology*, 85, pp. 171–183.
20. Nomura M., Kobayashi M., Narita T., Kimoto-NiraH,m Okamoto T.(2006), Phenotypic and molecular caracterization of Lactococcuslactis from milk and plants, *Applied Microbiology*, 101(2), pp. 396–405.
21. Dilanyan Z.(1982), Faktory, opredelyayushchiye vid ikachestvosyra, *Scientific works of Scientific Conference "Increasing the efficiency of production and quality of dairy products*, 1, pp. 77–78.

Characteristics of changes of the chemical composition of cranberry marsh in the process of obtaining puree

**Vira Obolkina, Olena Kokhan,
Ivanna Syvnii, Iryna Krapyvnytska**

National University of Food Technologies, Kyiv, Ukraine

Keywords:

Cranberry
Puree
Flavonoids
Anthocyanins
Preservatives

Article history:

Received 30.05.2018
Received in revised form 29.08.2018
Accepted 27.12.2018

Corresponding author:

Vira Obolkina
E-mail:
vobol_ipdo@ukr.net

DOI: 10.24263/2304-974X-2018-7-4-7

Abstract

Introduction. Studies have been carried out to determine the impact of technological processing, in particular, on the processes of blanching and deaeration on the chemical composition of cranberry marsh puree.

Materials and methods. Puree of marsh cranberry was investigated for identification of bioflavonoid; methods of high-performance liquid chromatography, electron spectrometry, gas chromatography with mass detector of initial and hydrolyzed samples were used.

Results and discussion. It was established that as a result of technological reprocessing of cranberry into puree, the amount of ascorbic acid decreased by 13.5 times; the content of phenolic substances in puree from cranberry fruits is 983 mg%, anthocyanins – 160 mg%; the content of water-soluble pectin is increased to 3.0%, which is associated with partial hydrolysis of protopectin, fiber – 3.1% of the mass fraction of dry matter of puree. In puree from cranberries, 36.6% of sugars are contained in the mass fraction of dry matter of puree, of which 28.8% are reductive, namely glucose and fructose, the increase of which is due to partial acid hydrolysis of sucrose during the processing of berries in puree.

In puree, the presence of anthocyanin compounds found in the original sample is in a bound state with citric acid, as well as mono-oxycarboxylic acids. A number of organic acids have been identified: 3-hydroxybutyric acid; ferulic acid; amber, apple, citric acids. When processing cranberry into puree, it preserves natural preservatives contained in fresh berries. Thus, in cranberry puree there is benzoic acid in the amount of 122.2 mg%±15% and a small amount of sorbic acid is available up to 2.5 mg%. The positive effect of cranberry on growth retardation of the yeast of the genus *Candida* was investigated.

Conclusions. Cranberry puree is a natural source of biologically active substances and natural preservatives and is recommended for use in long-term storage functional foods.

Introduction

An analysis of the current world trends in the creation of a new range of foods with high nutritional value has shown the feasibility of using berry raw materials [1]. Such raw materials include berries of cranberry marsh (*Oxycoccus palustris Pers*). This is a high-yielding wild berry, rich in various groups of nutrients, which is dominated by a group of biologically active substances [2]. The value of wild berries is that the content of biologically active substances significantly exceeds the one that the cultivated berries contain [3].

In recent years, throughout the world, much attention has been paid to the study of the chemical composition and useful properties of this berry [3,4,6]. It is characterized by low demanding conditions of cultivation, high yields, rapid recoupment of costs, considerable nutritional value and rich chemical composition [1].

The chemical composition of the cranberry is unique. The cranberry contains mono -, di – and polysaccharides to 4.8–8.1% per 100 g of fruit pulp, of which mono- and disaccharides are up to 3.8%, and pectin substances – up to 2.8% [2].

The cranberries are rich in organic acids (benzoin, citric, apple, oxalic, quinic), according to data [6], the total amount of those is up to 3.5%, and high content of ursolic acid is noted in the pulp of berries [6]. By structure and genetic this ursolic acid is close to many physiologically important hormones, it has mineralocorticoid activity and is capable of delaying the development of aseptic inflammation [7].

The presence of mono- and disaccharides in combination with organic acids form the taste qualities of berries, and hence – the source product as well [1, 2]. High acidity of pulp of berries creates conditions for prolonged storage of raw materials in fresh state (8–10) months, in frozen – throughout the year [4]. The nutritional and medicinal quality of the berries depends on the degree of maturity of the cranberries. Unripe berries contain little benzoic acid, which is why they quickly deteriorate [7].

The content of vitamins, and especially vitamin C, varies significantly (12–35 mg%) depending on the season. In the berries of the autumn harvest, this vitamin breaks quickly, and in the snow gathering is almost absent [4]. Of vitamins, in addition to vitamin C, thiamine, riboflavin, nicotinic acid, there are routine (0.53–1.28 mg%), pantothenic acid, pyridoxine. Recently, the value of cranberries as an important source of phyllohitone (vitamin K1) has been proved, the deficit of which leads to processes of formation of prothrombin of blood, its share in cranberry berries makes 0,8-1,0 mg% [8].

There are a lot of flavonoids in berries of cranberry that own a powerful antioxidant effect and are useful in the fight against the major ailments of the present – cardiovascular diseases, malignant tumors, infections [9, 10]. Bioflavonoids have a wide range of pharmacological effects. Being powerful natural antioxidants, bioflavonoids protect the cells of our body from the destructive effects of free radicals [11].

In addition to physiological activity, phenolic compounds have important functional and technological properties – these are natural dyes, antioxidants, preservatives. Polyphenols also contain aromas that determine the taste in many foods.

Cranberries contain polyphenolic compounds: anthocyanins – up to 180 mg%, leucoanthocyanins – up to 160 mg%, catechins – up to 260 mg%, paints and tannins – up to 1200 mg% [1, 12]. Antioxidant, especially polyphenolic components of cranberries, inhibit the growth of cancerous and tumor cells. In addition, polyphenolic compounds cause the coloring properties of semi-finished cranberries, that is, they are natural dyes [13].

The colors of the cranberries are represented by chlorophyll, carotenoids and anthocyanins; when berries are ripening, the chlorophyll content is significantly reduced, and the anthocyanin content increases [4]. The average value of the content of anthocyanins in

cranberries in terms of cyanidin-3-glucoside is 80 mg of crude weight of berries [14]. Therefore, the use of puree from cranberries as a dye component, along with its other properties, is a promising solution.

Proanthocyanidins contained in the cranberry also act as antioxidants [12]. Due to the increased content of proanthocyanidins and antioxidants per 1 gram of berries (more than in any other fruit), cranberry strengthens the body's defenses in the fight against antiradicals, which are the cause of many chronic diseases [15, 16]. Therefore, the identification and quantification of phenolic compounds in cranberries must be accompanied by multilateral research.

From literary data it is known that cranberries contain natural antimicrobial components, including benzoic acid [17]. The first mentions of the presence of benzoic acid in the cranberry berries were brought to their articles by the American scientist G. F. Mason [17]. Later, a number of scientists, with the help of modern methods of analysis, determined the quantitative content of this natural preservative. It is known that a significant influence on the amount of benzoic acid is made by conditions of growth, weather characteristics of the growing season, etc. [2, 4]. Thanks to its antiseptic properties benzoic acid in a cranberry, provides long-term storage of fresh berries. The conducted studies [18, 19] of antimicrobial action of cranberry juice have shown that the concentration of juice in the amount of 5.33% is sufficient to stop the growth of fungi of the genus *Candida*.

The increase in interest in natural phytonutrients is due both to the rigid regulation of their use in food products, and to the desire of manufacturers to provide products with the status of natural ones [13].

The above information makes cranberry a promising raw material for use in food technology. To date, a large number of studies have been carried out on the study of the chemical composition of cranberry, which confirms the content of a wide range of biologically active substances [20, 21]. Many studies have been carried out on the chemical composition of cranberry, depending on climatic conditions, degree of ripeness, duration and storage conditions [3, 4, 24, 25]. But the berries undergo a certain technological treatment and are used in the form of puree, the chemical composition of which can significantly differ from the initial chemical composition of fresh berries [22].

The purpose of the research is to determine the influence of technological treatment of blanching and deaeration on the chemical composition of cranberry puree.

Materials and methods

Materials that are studied

Investigated cranberry marsh puree, collected in the Volyn region of Ukraine. The production of cranberry puree was carried out by blasting the berries with sharp steam for 5–6 minutes, their rubbing and deaeration. Blanching reduced microbial contamination, contributed to the destruction of the membrane, which prevents the penetration of steam into berries, partial denaturation of skin proteins and increase the penetration of tissue. Blanched fruits were rubbed and sent to deaeration. The deaeration process was carried out under vacuum to remove the residual moisture and air to prevent the oxidation of biologically active substances and preserve the color of puree [13].

Description of techniques

The **mass fraction of dry substances** was determined by the refractometric method, the essence of which is to determine the mass fraction of dry matter by the refractive index of its solution [1].

The **mass fraction of total sugars and reducing agents** was determined by hot titration [2].

Actual acidity was determined by potentiometric pH method by Lur'ye [3].

Pectin substances were determined by the titrimetric method, which is based on the titration of the alkaline pre-selected and prepared pectin substances before and after hydrolysis. The titration results are proportional to the number of free and esterified carboxyl groups [2, 3, 30].

The **content of food fibers** was investigated by the method of hydrolysis of readily soluble carbohydrates with a mixture of concentrated acetic and nitric acids [1, 3].

The **content of vitamin thiamine (B_1)** was determined by the method based on oxidation of thiamine in thiohrum, its extraction in an organic solvent and measuring the intensity of fluorescence.

The **method of determining vitamin riboflavin (B_2)** is based on fluorescence measurement spectrophotometrically in hydrolyzate with 4M KH_2RO_4 and the addition of standard riboflavin.

The **determination of vitamin niacin (PP)** is based on a reaction that takes place in two stages. At the first stage, the interaction of the peridine ring of nicotinic acid with the bromide rodanum occurs. At the second stage, the coloring of the derivative glutacone aldehyde is formed, which is directly proportional to the mass fraction of vitamin and is measured colorimetrically [3].

The **amount of ascorbic acid (C)** was determined by spectrophotometrically extracted and centrifuged sample with citrate-acetate buffer and 2, 6-dichlorophenylphenol solution, read adsorption at a wavelength of 520 nm [26].

The **mass concentration of phenolic substances** was determined by the colorimetric method [26].

To determine the **content of bioflavanoid**, the following methods were used:

- Ultrasonic high-performance liquid chromatography (UPLC) with diode-matrix detection (PDA), which simultaneously records the electronic absorption spectrum of compounds. The results are obtained on the device of brand WATERS (USA). The analysis was carried out in the gradient mode of changing the composition of the mobile phase (acetonitrile-water). Column ACQUITY UPLC®BEHC$_{18}$ 1.7 μm, 50 * 2.1 mm;
- Electronic spectroscopy. The results were obtained on the device of brand Specord 210 Plus (Germany);
- Gas chromatography with mass-selective detection and a library of mass spectra before and after acid hydrolysis of source and modified (TMS derivatives) forms. The results were obtained on the Agilent GC/MSD 7890A/5975C with a capillary column of HP-5MS [28, 29].

High-performance liquid chromatography (UPLC) [26] was used in this work. To identify compounds with mobile atoms, the method of derivatization (getting derivatives) [26] was used to increase the molecular weight of the starting compound at a known value, to carry out a higher quality chromatography, and also to increase its initial molecular weight – reliable identification. In studies, N-methyl-N-trimethylsilyl-trifluoroacetamide (TMS) reagent was used for this purpose.

The production of ethanol concentrate (organic compounds) was carried out as follows

[26]: 3,087 g of cranberry puree are transferred to a 100 cm^3 flat bottom flask, filled with 60 cm^3 of 96% ethyl alcohol, and added to the reflux condenser and kept in a boiling water bath for 90 minutes. After that, the water bath is cooled, the condenser is washed with 5 cm^3 of ethyl alcohol, and the contents of the flask are transferred (filtered) into a volumetric flask of 100 cm^3. Then 35 cm^3 of ethanol was added to the flask and the procedure was repeated. The volume of ethanol concentrate was adjusted to 100 cm^3.

When conducting an acid hydrolysis [26], the weight of the raw material (approximately 0,992 g) weighed to the fourth mark to the nearest quarter is transferred to a 100 cm^3 flat bottom flask, 20 cm^3 of ethanol, 20 cm^3 of distilled water and 10 cm^3 of concentrated hydrochloric acid are added. After attaching the flask to the reflux condenser, the mixture is kept in a boiling water bath for 90 minutes. After that, the condenser is washed with 20 cm^3 of distilled water, the flask is cooled. The contents of the flask are transferred into a separating funnel through a paper filter of 100 cm^3, adding 25 g of sodium chloride, mixing thoroughly and removing the organic compounds with ethyl acetate (pre-adding water to it), two times for 30 cm^3. After drying the ethyl acetate extracts with anhydrous sodium sulfate, the organic solvent is distilled in vacuo. The residual after distillation is dissolved in 50 cm^3 of ethanol.

To obtain TMS derivatives, 5 cm^3 of ethanol concentrate of the sample is placed in a beaker and at 80 °C ethanol is removed. To the dry residue, 300 μg of anhydrous pyridine and 100 μg of N-methyl-N-trimethylsilyl-trifluoroacetamide reagent are added. Beaker is closed and put in UZB for 30 minutes. After this, 1 cm^3 of acetonitrite is added to the beaker, mixed and GC/MS is tested according to the procedure described.

The study of the content of natural preservatives (benzoic and sorbic acid) was carried out according to the method described in work [30] and using the high-performance liquid chromatograph Varian 920-LC, the spectrophotometric detector.

To study the **microbiological criteria** as well as the microbiological stability of the cranberries purée, a research by counting the number of colonies formed as a result of sowing on the nutrient medium was carried out [31]. To determine the diameters of zones of growth retardation of microorganisms, preparations using cranberry puree of different concentrations were used.

Results and discussion

Chemical composition of cranberries berry puree

Table 1 shows the main organoleptic characteristics of the obtained puree.

Table 1

Organoleptic characteristics of cranberry puree

Indicator	Characteristic of the indicator
Appearance and consistency	Homogeneous, puree-like, rubbed mass
Color	Homogeneous throughout the mass, dark red
Scent and taste	Inherent in cranberries, sour

Preparation of puree is accompanied by a short-term effect of high temperature during blasting of berries, which may lead to the destruction of biologically active compounds [32]. Therefore, it was advisable to conduct a study of the chemical composition of puree of cranberries, the results of which are given in Table 2.

It was found that vitamin C is most susceptible to destruction, in berries of cranberry its amount was 35 mg%, in puree it remained 2.6 mg%, that is decreased by 13.5 times. This is due to the high thermal stability of ascorbic acid and its degradation under the influence of heat, which accompanies the process of blanching berries with cranes when processed in puree [32].

The content of water-soluble pectin in puree has increased and makes up almost 3.0% of the mass fraction of dry matter of puree; it is probable [32] during the heat treatment process under the influence of organic acids there was a partial hydrolysis of the protopetyte of plant tissues, as a result of this process, the amount of water-soluble pectin has increased. The increased amount of pectin in puree should have a positive effect on the formation of the composition of the produced and foamy-gelatanious like structures and to prevent the intensive removal of moisture from the product, which will extend the shelf life [23, 33].

The fiber content was 3.1% to the mass fraction of dry matter with cranberry puree, the total content of dietary fiber in puree exceeded 6.1%. Although they are not absorbed by the body [34], however, they contribute to the implementation of many positive functions: remove toxic metals and radionuclides from the body, inhibit the development of rotting microorganisms, prevent excessive boiling of carbs, and promote the binding of endogenous and exogenous toxins [35].

Table 2

Chemical composition of cranberry puree

Indicator	Content of substances per 100 g of puree	Content of substances to mass fractions of dry matter of puree
Total mass fraction of dry substances,%	24,0±1,5	
Mass fraction of water-soluble dry substances,%	12,5±1,5	
Actual acidity, pH	4,37±0,1	
Organic acid content,%	3,6±0,5	15,0±0,5
Total sugar content,%	8,8±0,5	36,6±0,5
The content of reductive sugars,%	6,9±0,5	28,8±0,5
Pectin content, г/100 г	0,72±0,1	3,0±0,1
Fiber content, г/100 г	0,75±0,1	3,1±0,1
Total content of phenolic substances, mg%	235±9,9	983±9,9
Incl. mass concentration of anthocyanins, mg%	38,4±0,25	160±0,25
Vitamin content, mg%		
Vitamin C	2,64±0,3	11±0,3
Thiamine (B_1)	0,035±0,3	0,14±0,3
Riboflavin (B_2)	0,018±0,3	0,43±0,3
Niacin (PP)	0,08±0,3	0,43±0,3
Ash,%	0,32	1,3±0,3

That is, it is possible to predict [30] that the adding cranberry puree in the production of food products may partially increase their nutritional value by adding to the product of useful nutritious fibers.

It was determined that in cranberry, 36.6% of sugars are contained in the mass fraction of dry matter of puree, of which 28.8% are reductive, namely glucose and fructose, the increase of which is due to partial acid hydrolysis of sucrose during processing berries in puree.

The most common class of organic compounds in plants are acids. Lemon and apple cranberry juice is preferred in puree. The total content of organic acids is 15% to the mass fraction of dry matter of puree.

Also vitamins – thiamine (B1), riboflavin (B2), niacin (PP) were identified in puree. The amount of ash elements was 1.3% of the mass fraction of dry matter of cranberry puree.

Identification of bioflavonoids in cranberry puree

Special attention to the cranberries has recently been crocheted due to the presence of a significant amount of bioflavonoid in it. Therefore, it was advisable to investigate the content of this class of compounds in the investigated berry.

The separation of the ethanol concentrate of cranberry purée using UPLC-PDA method confirms the presence of phenolcarboxylic acids in the sample (the mixture, since the chromatographic peak is highly blurred) – 4.38 minutes (Figure 1, A); Fennel compounds - 5.74; 6.23 min (Figure 1, B); as well as the mixture of anthocyanins -5.29 min (Figure 1, C).

The quantitative correlation between these compounds is determined (Table 3).

Table 3

Quantitative correlation between compounds according to Figure 1 a, b, c

Duration of detention	Mass fraction of the amount,%	Duration of detention	Mass fraction of the amount,%	Duration of detention	Mass fraction of the amount,%
PDA 335.0 nm		**PDA 350.0 nm**		**PDA 315.0 nm**	
4,384	88,39	5,738	39,38	5,287	100
5,193	11,61	6,229	37,19		
		6,639	23,43		

After acid hydrolysis, the chromatogram (Figure 2) is characterized by the presence of three anthocyanins with the same nature of the electron spectra, which indicates one nature of the aglucone [12]. It should be noted about the increase in the time of anthocyanins' coming out. This is due to the fact that in the original sample they were glycosylated, that is, they are connected with carbohydrates. Flavonoids, in addition to catechins and leukoanthocyanins, are relatively rare in the free state. Most of them are presented in the form of various O- and C-glycosides. The diversity of flavonoid glycosides is due to a significant amount of sugars (glucose, arabinose, xylose, etc.) and the ability to attach them to a number of positions of aglycones, as well as the fact that sugars may have different configuration of glycoside bonds and the order of the connections between them [12].

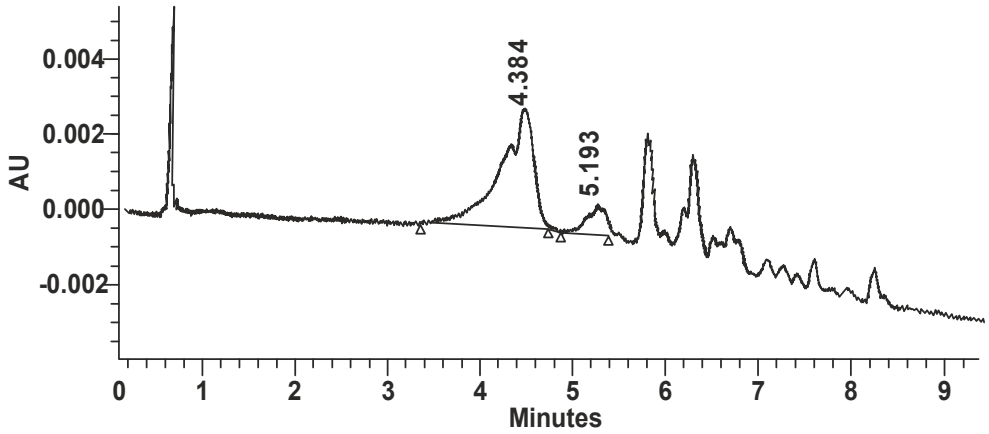

Figure 1a. Chromatogram of the source ethanol concentrate (PDA 335.0 nm)

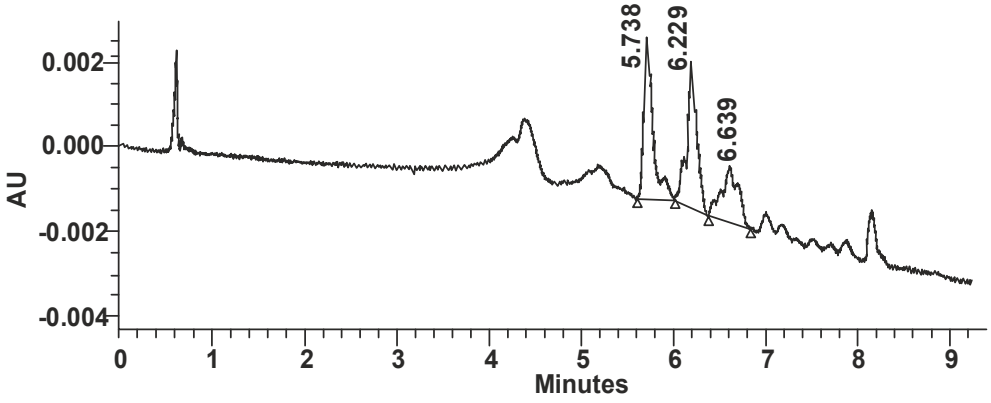

Figure 1b. Chromatogram of the source ethanol concentrate (PDA 350.0 nm)

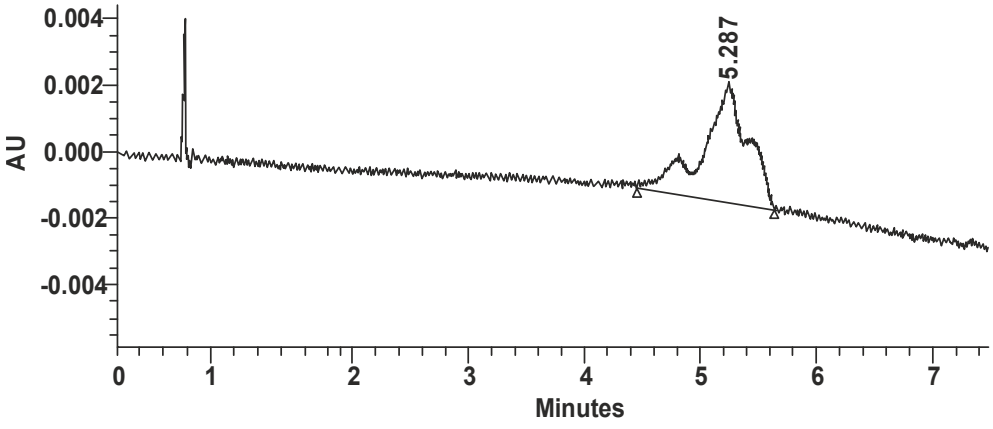

Figure 1c. Chromatogram of the source ethanol concentrate (PDA 315.0 nm)

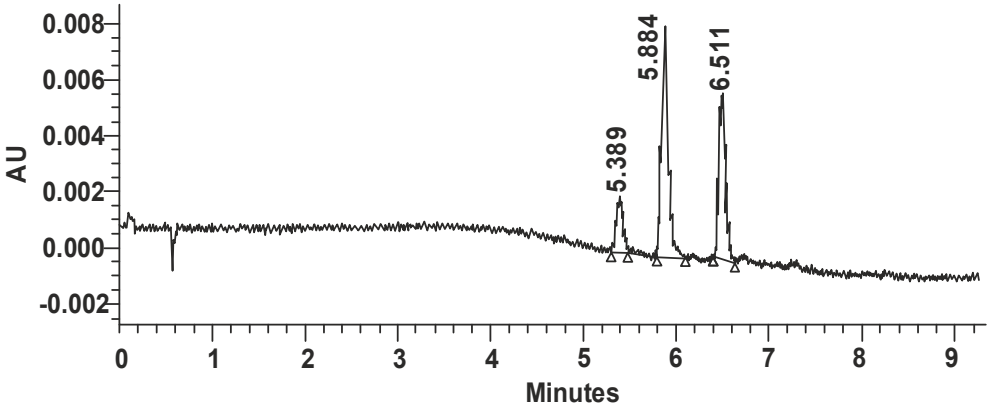

Figure 2. Acid hydrolyzate chromatogram (PDA 350.0 nm)

The quantitative correlation between these compounds is determined (Table 4).

Table 4

Quantative correlation of compounds in accordance with Figure 2 (PDA 350.0 nm)

№	Volume of sample, cm^3	Duration of detention, min	Mass fraction of the amount,%
1	1,0	5,389	10,81
2	1,0	5,884	52,39
3	1,0	6,511	36,60

Conducting the TMS derivatization reaction allowed to identify many more compounds: formaldehyde; 3-hydroxybutyric acid; fumaric acid; citric acid. In addition, a number of carbohydrates have been identified: sorbosis, glucose, butanic acid derivatives; dictone propanoic acid; malonic acid; ethyl ether and free citric acid. The total content of phenolic substances in puree of cranberries is up to 235 mg%, therefore, cranberries may be recommended for use in the creation of food products for health purposes [36].

The data of scientific literature [27] indicates the expressed antimicrobial action of cranberries isolated from the fruits of biologically active substances.

Antimicrobial action of benzoic acid and its salts is based on the ability to suppress the activity of enzymes [5]. Specific antibacterial and antifungal efficacy against Escherichia coli and Candida is active 24 hours after use [19]. Benzoic acid is able to block succinate dehydrogenase and lipase, the enzymes that break down fats and starch [19]. It suppresses the growth of yeast and bacteria of butyric fermentation, weakly acts on bacteria of vinegar fermentation and quite slightly – on lactic acid flora and mold [19].

Since berry purees have the optimal composition of nutrients, they are a good environment for the development of microorganisms of damage that can come from the surface of the skin of berries into pulp [37]. Particularly dangerous is the development of some species of fungi of the genus *Penicillium*, which are capable of secretion of mycotoxin patulin, which has a carcinogenic and mutagenic effect [37]. But in the sources [1, 3, 5, 17], there are discrepancies regarding the data on the quantitative content of preservative in wild

berries. From a scientific point of view, it was of interest to determine the amount of natural preservatives in puree, which was made from cranberries.

In cranberry puree, benzoic acid was identified in the amount of 122.2 mg%±15% and a small amount of sorbic acid – up to 2.5 mg%. Preservation of these natural preservatives in cranberry puree after the technological processing of berries, confirms preliminary studies of the preservation of the antimicrobial capacity of cranberry juice after autoclaving, are given in [32].

An experiment was conducted to investigate the effect of cranberries on puree yeast of the genus *Candida*. The genus *Candida* – the shape of cells is spherical, oval, cylindrical, elongated. Propagated by multilateral budding, as well as by agamous way – blastospores. It forms a pseudo-mycelium, and sometimes a true mycelium. On the surface of liquid substrates forms films: young – white, smooth, old – wrinkled. Assimilates glucose, sucrose, maltose, lactose. After growing in the thermostat, yeast growth retardation zones were observed, which proves the positive effect of cranberries on the growth retardation of the yeast of the genus *Candida*. Cranberries may be used as a source of natural preservatives, which will help lengthen the shelf life of food products, the dominant factor for which is microbiological damage in the process of storage [35, 36].

On the content of nutrients, cranberry puree is a promising raw material for use in creating a wide range of nutritional products for health and functional purposes of extended shelf-life.

Conclusions

1. Technological reprocessing of cranberry into puree leads to a decrease in the content of ascorbic acid by 13.5 times and to an increase of the content of water-soluble pectin up to 3.0% to the mass fraction of dry matter of puree.
2. The content of phenolic substances in puree of cranberries is 983 mg%, anthocyanins – 160 mg%. The presence of anthocyanin compounds found in the sample is in bound state with citric acid, as well as mono-oxycarboxylic acids.
3. During the processing of cranberry into puree, it preserves natural preservatives contained in fresh berries. Thus, in cranberry puree there is benzoic acid in the amount of 122.2 mg%±15% and a small amount of sorbic acid is available up to 2.5 mg%. The positive effect of cranberry on growth retardation of the yeast of the genus *Candida* was investigated.

References

1. Ruse K., Rakcejeva T. (2104) Physical and chemical parameters of latvian fresh cranberries,*FOODBALT*, pp. 167–171.
2. Khomych G., Matsuk Y., Nakonechnaya J., Oliynyk N., Medved N. (2017), Research of cranberry main indicators of chemical composition and its processing products, *EUREKA: Life Sciences*, 6, pp. 29–36.
3. Dolly Jean Watson (1997), *Chemical Characterization of Wild Maine Cranberries*, University of Maine

4. Celik, H., Ozgen, M., Serce, S., Kaya, C. (2008), Phytochemical accumulation and antioxidant capacity at four maturity stages of cranberry fruit, *Scientia Horticulturae*, 117 (4), pp. 345–348.
5. Puupponen-Pimia R., Nohynek L., Meier C., Kahkonen M., Hoinonen M., Hopia A., Oksman-Caldentey K.M. (2001), Antimicrobial properties of phenolic compounds from Finnish berries, *Journal of Applied Microbiology*, 90, pp. 494–507.
6. Jensen D., Krogfelt A., Cornett C. (2002), Hydrophilic carboxylic acids and iridoid glycosides in the juice of American and European cranberries, lingoberries, and blueberries, *Journal of Agricultural and Food Chemistry,* (50),pp. 6871–6874.
7. Su X., Howell A.B., D'Souza D.H. (2010), The effect of cranberry juice and cranberry proanthocyanidins on the infectivity of human enteric viral surrogates, *Food Microbiology*, 27, pp. 535–540.
8. Thimoteo, N. S. B., Scavuzzi, B. M., Simao, A. N. C., Dichi, I. (2017), The impact of cranberry (*Vaccinium macrocarpon*) and cranberry products on each component of the metabolic syndrome: a review. *Nurture*, 42 (1), pp. 25–36.
9. Caillet, S., Cote, J., Doyon, G., Sylvain, J.-F., Lacroix, M. (2011), Antioxidant and antiradical properties of cranberry juice and extracts, *Food Research International*, 44 (5), pp. 1408–1413.
10. Wang L., Tu Y.C., Lian T.W., Hung J.T., Yen J.H., Wu M.J. (2006), Distinctive antioxidant and antiinflammatory effects of flavonols, *Journal of Agricultural and Food Chemistry*, 54(26), pp. 9798–9804.
11. Majewska E., Skrzycki M., Podsiad M., Czeczot H. (2011), Evaluation of antioxidant potential of flavonoids: an in vitro study, *Acta Poloniae Pharmaceutica and Drug Research*, 68(4), pp.611–615.
12. Jankowski K., Jocelyn Pare J.R. (1983), Trace glycoside from cranberries (*Vaccinium oxycoccus*), *Journal of Natural Products,* (46), pp. 190–193.
13. Jackman R.L., Smith J.L. (1996), Natural Food Colourants. *Glasgow: London,* pp. 244–309.
14. Pazmiño-Durán A.E., Giusti M.M., Wrolstad R.E., Glória B.A. (2001), Anthocyanins from oxalis triangularis as potentital food colorants. *Journal of Food Chemistry*, 75(2), pp.211–216.
15. Yuan W., Zhou L., Deng G., Wang P., Creech D., Li Sh.(2011), Anthocyanins, phenolics and antioxidant capacity of Vaccinium L. in Texas, USA., *Pharmaceutical Crops*, 2, pp. 11–23.
16. Johnson-White B., Buquo L., Zeinali M., Ligler F.S. (2006), Prevention of nonspecific bacterial cell adhesion in immunoassays by use of cranberry juice, *Analytical Chemistry*, 78. pp. 853–857.
17. Mason G. F. (1905), The Occurrence of Benzoic Acid Naturally in Cranberries, *Journal of the American Chemical Society*, 27(5), pp. 613–614.
18. Côté J., Caillet S., Doyon G., Dussault D., Sylvain J.-F., Lacroix M. (2012), Antimicrobial effects of fractions from cranberry products on the growth of seven pathogenic bacteria, *Food Control*, 23, pp. 419–428.
19. Lacombe A., Vivian C.H. Wu, Tyler S., Edwards K.(2010), Antimicrobial action of the American cranberry constituents;phenolics, anthocyanins, and organic acids, against Escherichia coli, *International Journal of Food Microbiology*, 139, pp. 102–107.
20. Kaisu R., Mtt-Riihinen, Afaf Kamal-Eldin, Pirjo H. Mattila et all.(2004), Distribution and Contents of Phenolic Compounds in Eighteen Scandinavian Berry Species, *Journal of Agricultural and Food Chemistry*, (52), pp. 4477–4486.
21. Määttä-Riihinen K.R., Kähkönen M.P., Törrönen A.R., Heinonen I.M. (2005), Catechins and Procyanidins in Berries of Vaccinium Species and Their Antioxidant Activity, *Journal of Agricultural and Food Chemistry*, (53), pp. 8485–8491.

22. Cailleta S., Côtéa J., Doyonb G., Sylvainc J.-F., Lacroixa M. (2011), Antioxidant and antiradical properties of cranberry juice and extracts, *Food Research International,* 4(5), pp. 1408–1413.
23. Kalinovska T., Obolkina V. (2013), Substantiation of using wine-making secondary products as alternative raw material for confectionery industry, *Ukrainian Journal of Food Science*, l(1), pp. 77-80.
24. Wang S.J., Stretch A.W. (2001), Antioxidant capacity in cranberry is influenced by cultivar and storage temperature, *Journal of Agricultural and Food Chemistry*, 49, pp. 969–974.
25. Gurbuz G., Watkins B. (2002), Controlled-atmosphere effects on postharvest quality and antioxidant activity of cranberry fruits, *Journal of Agricultural and Food Chemistry,* 50, pp. 5932–5938.
26. Lee H.S. (1993), HPLC method for separation and determination of nonvolatile organic acids in orange juice, *Journal of Agriculture and Food Chemistry*, 41, pp. 1991–1993.
27. Zuo Y., Wang Ch., Zhan J. (2011), Separation, characterization, and quantization of benzoic acid phenolic antioxidants in American fruit by GC-MS, *Journal of Agricultural and Food Chemistry*, (50), pp. 3789–3794.
28. Prior R. L., Lazarus S. A., Cao G., Muccitelli H., Hammerstone, J. F. (2001), Identification of Procyanidins and Anthocyanins in Blueberries and Cranberries (*Vaccinium Spp.*) Using High-Performance Liquid Chromatography/Mass Spectrometry, *Journal of Agricultural and Food Chemistry*, 49(3), pp. 1270–1276. doi: 10.1021/jf001211q
29. Chen H., Zuo Y., Deng Y. (2001), Seperation and determination of flavonoids and other phenolic compounds in cranberry Juice by high-performance liquid chromatography, *Journal of Chromatography*, 913(1–2), pp. 387–395.
30. Kalinovska T., Kyianytsia S., Obolkina V. (2013), Doslidzhennia vmistu pektynovykh rechovyn napivfabrykativ z vynohradnykh vychavok ta vyznachennia yikh sorbtsiinykh vlastyvostei, *Kharchova nauka i tekhnolohiia*, 4(25), pp. 69—74.
31. Oleksiyenko N., Obolkina V., Syvnyi I. (2011), Mikrobiolohichna bezpeka kharchovykh produktiv, *Prodovolcha industriia APK*, 6, pp. 38–41.
32. Côté J., Caillet S., Dussault D., Sylvain J.-F., Lacroix M.(2011), Effect of juice processing on cranberry antibacterial properties, *Food Research International*, 44, pp. 2922–2929
33. Syvnyi I., Obolkina V. (2011), Pryrodni konservanty v ozdobliuvalnykh napivfabrykatakh z podovzhenym terminom zberihannia, *Prodovolcha industriia APK,* 4, pp. 20–22.
34. Artemio Z., Tulio Jr., Jablonskia J., Jacksona L., Lauren S., Changa C., Edirisinghec I. Burton-Freemanc B. (2014), Phenolic composition, antioxidant properties, and endothelial cell function of red and white cranberry fruits, *Food Chemistry*, 157, pp. 540–552.
35. Syvnyi I., Oleksiyenko N., Obolkina V. (2012), Vykorystannia piure z zhuravlyny pid chas pryhotuvannia ozdobliuvalnykh napivfabrykativ z podovzhenym terminom zberihannia, *Khlibopekarska i kondyterska promyslovist Ukrainy,* 10(95), pp. 6–8.
36. Syvnyi I., Obolkina V., Krapyvnytska I. (2016), Osoblyvosti zberihannia bilkovo-zbyvnoho kremu z dodavanniam horobynovoho ta zhuravlynovoho piure, *Prodovolcha industriia APK,* 5, pp.27–31.
37. Lipson S.M., Sethi L., Cohen P., Gordon R.E., Tan I.P., Burdowski A., Stotzky G. (2007), Antiviral effects on bacteriophages and rotavirus by cranberry juice, Phytomedicine, 14, pp. 23–30.

Optimization of extraction parameters of phenolic antioxidants from defatted grape seeds flour by response surface methodology

Sergey Gubsky, Maksym Labazov, Olga Samokhvalova, Nataliya Grevtseva, Olena Gorodyska

Kharkiv State University of Food Technology and Trade, Kharkiv, Ukraine

Keywords:

Antioxidant
Polyphenols
Flavonoids
Grape seeds
Coulometry

Article history:

Received 23.02.2018
Received in revised form 04.06.2018
Accepted 27.12.2018

Corresponding author:

Sergey Gubsky
E-mail:
s.gubsky@
hduht.edu.ua

DOI: 10.24263/2304-974X-2018-7-4-8

Abstract

Introduction. The optimization results of the conditions of liquid-solid extraction by wine industry waste water in the form of the defatted grape seeds flour in order to obtain the extract with high antioxidant capacity are conducted in this report.

Materials and methods. Total antioxidant capacity (TAC) and total phenolic content (TPC) of the samples were determined by the method of galvanostatic coulometric titration with electrogenerated bromine and spectrophotometric method using Folin-Ciocalteu reagent, respectively. TAC and TPC experimental values were presented in terms of the equivalent of gallic acid content (GAE) per unit mass of dry powder (DW).

Results and discussion. Response surface methodology (RSM) is used to search for optimal condition of solid-liquid extraction of phenolic compounds from defatted grape seeds flour under the influence of three factors: the temperature (60–100 °C), extraction time (90–150 min) and liquid to solid ratio (60-100). The result showed that the phenolic substances yield in the set ranges is 1.20–2.64% with total antioxidant capacity of 17.71–36.78 mg GAE/g DW. Due to optimization procedure, it was determined that under optimal conditions (the temperature of 100 °C; the extraction time is 131 min.; and the ratio of the extractive agent volume to the mass of the powder is 85) the maximum TAC of the extract of 37.04 mg GAE/g DW is achieved. The maximum yield of phenolic substances of 2.646% was obtained under the following conditions: temperature of 100 °C; extraction time is 117 min.; and the ratio of extraction agent volume to the mass of the powder is 93. When optimization is used with two TAC and YPC response functions, the following optimal conditions were obtained: the temperature of 100 °C, the extraction time is 123 minutes and the ratio of extractive agent volume to the mass of powder is 89, at which 36.91 mg GAE/g DW TAC and YPC values and 2.633% were obtained, respectively. The validation of obtained results showed their compliance within 3% with experimental values.

Conclusion. The obtained results indicate the perspective of wine industry waste recycling in order to obtain the solid extract from defatted grape seeds flour as a source of biologically active substances of a phenolic nature with high antioxidant potential.

Introduction

Plant objects are considered to be promising natural sources of antioxidants, and therefore, the number of studies on the development of plant-based additives technologies in the form of pastes, extracts and powders has recently increased. The supplementation of such additives allows obtaining functional nutrition products with high antioxidant potential as well as high biological and nutritional value.

Grape seeds are produced in large amounts as the wine industry waste products and are increasingly used to create food ingredients. This occurs due to the fact that it is a source of polyphenolic antioxidants – flavonoids, such as monomeric flavanols, dimeric, trimeric and polymeric procyanides and phenolic acids [1–3].

The extraction from raw plant materials is an important stage in phytochemical processing in order to optimize the concentration of biologically active compounds. The selection of a suitable solvent for the standardization of plant products is highly important in this process. Differences in the compounds structure determine their solubility in solvents of different polarity. Therefore, the type of extractive solvent can have substantial impact on the yield of the desired extracted compounds from the plant material. However, the selection of solvent is normally limited to water and ethanol or their mixture when using extracts for food purposes.

The selection of an appropriate withdrawal process and the optimization of various parameters are crucial for purposes of scaling and moving from the laboratory experiment to the industrial scale. According to the numerous data indicating that the optimal conditions for the extraction of phenolic compounds of some plant products are usually different for various plant matrices [4]. Extraction methods that are most commonly used include standard convection methods (maceration, percolation, infusion, decoction, hot continuous extraction) and non-convection methods (ultrasonically extraction (UEA), microwave radiation (MEA), pulse electrical discharge (PAED) and supercritical fluid extraction (SFE) [5]. Specified methods in different options of the experiment were used to conduct numerous studies on the extraction of polyphenols from grape waste for example, including grape seed [6–15].

The purpose of this study was the selection of optimal conditions for effective water solid-liquid extraction (SLE) of polyphenolic compounds from defatted grape seed flour in order to obtain an extract with the maximum antioxidant potential.

Materials and methods

Chemicals

The following chemicals used in this study are as follows: potassium bromide, sodium hydroxide, sodium carbonate (Reachim, Russia); sulphur acid (Sumychimprom, Ukraine); gallic acid (Sigma Aldrich, USA). All the chemicals used in this experiment were of analytical grade. The synthesis of Folin-Ciocalteu reagent was done according to the procedure [16]. All the chemicals used in this procedure were of analytical grade. For analysis 2 M solution was used. For preparation of the solutions distilled water with electric conductivity no more 0.55 mS/m was used. The conductivity was measured by a conductometer CEL-1M2 (Analitpribor, Georgia).

Raw Material

Defatted grape seeds flour (Oleo Vita trademark, Orion, Ukraine) was made from fresh grape seeds of unfermented squeezing in industrial conditions. A mixture of four grape varieties in equal proportions in mass, grown in the southern regions of Ukraine

(Odessa region) was used as the raw material. Gently dried grape seeds at a temperature not more than 60 °C were subject to the thorough cleaning (separation).

Grape seed cake was obtained in the form of solid plates with its further fine grinding and crushing to fine powder (flour) in the process of cold pressing. The residual fat content in the flour was 8-9%.

Extraction Process

Accurately weighted dried powder (according to ratio liquid to solid) were extracted with the solvent by 10 ml in glass test tubes (total volume 15 ml) with screw caps. Distilled water was used as the extractive agent. All the time the tubes were shaken. The extraction was performed in the dark and at corresponding temperature, a solid-liquid ratio and the extraction time. The tubes were placed in a thermostat at a set temperature for the extraction time. The liquid after extraction was separated from solids by centrifugation at 6.0 g for 10 min (OPn-8UHL4.2, Russia).

The solutions were kept at a constant temperature using the thermostat 1TZH-0.03 (Russia). The temperature in this device was maintained at an accuracy of 0.2 °C and determined by the sensor SM60-Pt1000 (Yokogawa Europa, Holland) with a precision of 0.1 °C.

The samples were weighed on laboratory scales balance CBA-300-0.005 (T-Scale, China) with accuracy of 5 mg and on analytical laboratory scales balance VLR-200 (Gosmetr, Russia) with accuracy up to 0.1 mg.

Determination of the Total Antioxidant Capacity

TAC of simples was determined by the reaction with electronegative bromine [17]. In this research using the same method that was detailed [18, 19]. The experimental data of coulometric titration were used to calculate the TAC, as the electricity quantity Q, spent for titration per 100 g of the sample and it were calculated by expression:

$$TAC = \frac{100\ Itm_{solution}}{m_{al}\ m_{sample}}, \quad (1)$$

where m_{sample} is the weight of the sample (dry powder of plant or candy caramel), $m_{solution}$ is the total weight of the solution for candy caramel or of the extract for powder of plant. Values of TAC in gallic acid equivalent (mg GAE/100 g sample) were calculated. For aqueous solutions of gallic acids the coefficients of the linear regression were determined in [18].

Determination of the Total Phenolic Content

The concentration of phenolic compounds in samples was estimated using a modified spectrophotometric Folin-Ciocalteu method according Singleton and Rossi [16] with the transition from volume to weight of the aliquot portion. Briefly, 0.1 g of extract, standard or blank solution was mixed with 0.5 g of Folin-Ciocalteu's reagent and 2.0 g water. A sample of extracts was previously diluted in 10 times. After 8 min, 1.5 g of sodium carbonate 20% (w/w) solution was added to the mixture and adjusted to 10.0 g with distilled water. Mixture was incubated for 30 min in thermostat at 45 °C temperature. Finally, measurement of absorbance was carried out in spectrophotometer SF-46 (Lomo, Russia) and modernized and connected with a computer Specord UV-VIS (JenaAnalytik, Germany) at wavelength of 765 nm against a blank sample.

Gallic acid was used as a standard. The TPC values were expressed as mg of gallic acid equivalents (GAEs) per g of dry weight (DW) of plant. A 1000 mg/kg stock solution of gallic

acid was prepared by dissolving 0.1 g of gallic acid in 100 g of distilled water. Working standard solutions of gallic acid at five different concentration levels (25, 50, 100, 250 and 500 mg/kg) were prepared by dilution of the stock solution. The gallic acid calibration curve was constructed in the range of 25–500 mg/kg and used to calculate linear regression models [18].

The yield (%) of the extraction of phenolic compound (gram to gram dry weight of powder) was defined as :

$$YPC = \frac{TPC}{1000}100\%, \quad (2)$$

Experimental Design

A response surface methodology (RSM) as a tool for optimization in this research was applied [20]. A tree level, three variable Box–Behnken design [21] was applied to determine the best combinations TAC and TPC (maximum value) of extraction variables for the extraction from defatted grape seeds flour.

Table 1

Independent variables and their levels employed in a Box–Behnken design for optimization of defatted grape seed flour extracts

Independent variables	Symbol	Coded levels		
		-1	0	1
		Natural levels		
Temperature, °C	Temp	60	80	100
Time, min	Time	90	120	150
Ratio volume of liquid to weigth of solid powder (v/w), ml/g	R L/S	60	80	100

Three independent variables selected for this study were the extraction temperature (T), the extraction time (t), and ratio volume of liquid to weight of solid powder (R L/S) (Table 1).

Preliminary trials showed as the values of responses changed with increasing temperature, time and ratio L/S; therefore, the optimal levels were selected as center points in the designed experiment. The factorial design consisted of requires an experiment number according to N=2k(k−1)+cp, where k is the number of factors (k=3) and (cp) is the number of the central points eight factorial points, and three center points leading to 15 sets of experiments [20].

Regression analysis was performed on the data of dependent variables as effected by the extraction conditions and was fitted into an empiric second order polynomial model as shown in the following equation:

$$Y = \beta_0 + \sum \beta_i X_i + \sum \beta_{ii} X_i^2 + \sum \beta_{ij} X_i X_j \,, \quad (3)$$

where Y is the predicted response; $\beta_0, \beta_i, \beta_{ii}, \beta_{ij}$ are the interception coefficient, the linear terms, the quadratic terms and the interaction terms, respectively; X_i, X_j are the actual levels of the independent variables.

Statistical analysis

Determination of the experimental values were done for a number of parallel measurements (n=4). The Student's t-test permitted us to check the statistical significance of the regression coefficients. A $p < 0.05$ was considered as statistically significant. The Fisher's test for analysis of variance (ANOVA) was performed on experimental data to evaluate the

statistical significance of the model. The the Design Expert software trial version 11.0 (Stat-Ease, USA) were employed for the regression analysis and the graphical optimization, respectively.

The models of each response for full-factorial design were expressed in terms of actual variables and without taking into account the statistically insignificant terms.

Results and discussion

Fitting the model of the extraction process from defatted grape seed flour

The experimental data of dependence of TAC and YPC water extract of grape seeds flour from the investigated factors are shown in Table 2.

These experimental data were processed in the framework of analysis of variance (ANOVA) using the model of the average, linear, mixed and quadratic models. As it is commonly known that, ANOVA is a statistical analysis method for assessing the significance of experimental data and for adequacy analysis of the fitting model [20]. Analysis of obtained calculations showed that the most adequate description of TAC and YPC experimental values is achieved in a quadratic model. ANOVA data results for a quadratic model describing the dependence of total antioxidant capacity from the investigated factors are given in Table 3.

Table 2

Experimental of the three-level and three-variable Box–Behnken design and TAC, TPC and yield of polyphenolic compound of defatted grape seed flour extracts

Run	Code pattern			Temp, °C (A)	Time, min (B)	R L/S (C)	Experimental values	
	Temp	Time	R L/S				YPC, %	TAC, GAE mg/ g DW
1	0	1	–1	80	150	60	1.625	22.93
2	–1	1	0	60	150	80	1.492	19.62
3	0	–1	–1	80	90	60	1.522	21.89
4	–1	0	–1	60	120	60	1.394	17.71
5	1	0	1	100	120	100	2.550	35.51
6	1	1	0	100	150	80	2.526	36.78
7	0	0	0	80	120	80	1.882	25.98
8	–1	0	1	60	120	100	1.428	20.19
9	0	–1	1	80	90	100	1.757	24.95
10	0	0	0	80	120	80	1.893	26.02
11	0	0	0	80	120	80	1.914	26.02
12	–1	–1	0	60	90	80	1.144	18.14
13	1	–1	0	100	90	80	2.600	35.72
14	1	0	–1	100	120	60	2.288	35.73
15	0	1	1	80	150	100	1.940	27.20

The coefficients $R^2$and $R^2_{adjusted}$ are equal to 0.9944 и 0.9843, respectively, according to the results from Table 3. These values indicate that the model adequately describes the experimental data obtained and that they are well coordinated with their predicted values. The model is statistically significant because the p value is less than 0.0001. The obtained value of the variation coefficient (C.V. = 3.19%) is quite low and indicates the reliability of the experimental data.

Table 3

Analysis of variance (ANOVA) of the fitted quadratic polynomial model for the TAC of defatted grape seed flour extracts

Source	Sum of squares	df	Mean square	F-value	p-value	*Resume*
Model	624.95	9	69.44	98.56	< 0.0001	*significant*
Residual	3.52	5	0.7045			
Lack of Fit	3.52	3	1.17	1954.98	0.0005	*significant*
Pure Error	0.0012	2	0.0006			
Cor Total	628.47	14				
Estimated regression coefficients						
Term	**Coefficient estimate**	**df**	**Std error**	**F-value**	**p-value**	
A	26.01	1	0.4846	822.55	< 0.0001	
B	8.51	1	0.2968	6.03	0.0575	
C	0.7289	1	0.2968	16.30	0.0099	
AB	1.20	1	0.2968	0.0618	0.8136	
AC	-0.1043	1	0.4197	2.60	0.1677	
BC	-0.6769	1	0.4197	0.5161	0.5047	
A^2	0.3015	1	0.4197	27.76	0.0033	
B^2	2.30	1	0.4368	2.89	0.1500	
C^2	-0.7423	1	0.4368	5.44	0.0669	
Model summary statistics						
Std. Dev.	0.8394		**R^2**	0.9944		
Mean	26.29		**Adjusted R^2**	0.9843		
C.V.%	3.19		**Predicted R^2**	0.9103		
PRESS	56.35		**Adeq Precision**	28.8892		

The Fisher criterion value of F at 98.56 level implies that the model is statistically significant. The obtained values of p criterion that are less than 0.0500 indicate the significance of the calculated coefficients A, C, A^2 of equation (3).The calculated F values for Lack of Fit are also statistically significant. The predicted value of Predicted R^2=0.9103 is in necessary compliance with Adjusted R^2 =0.9843, since their difference is less than 0.2. The value of AdeqPrecision, expressing the signal-to-noise ratio, and equal to 28.8892 is greater than the indicative value 4, which indicates data adequacy.

Similar conclusions can be made with respect to the model describing the phenolic compounds output in the extraction process (Table 4). The adequacy of the experimental data description on the phenolic substances output is achieved by indicated model, as evidenced by the high correlation coefficients R^2 and $R^2_{adjusted}$ that are equal to 0.9874 и 0.9646, respectively, and the p value that is equal to 0.0003.The reliability of the experimental data was also confirmed by the value of factor at the level of C.V.=4.59%.

The adequacy of the experimental data description on the phenolic substances output is achieved by indicated model, as evidenced by the high correlation coefficients R^2 and $R^2_{adjusted}$ that are equal to 0.9874 и 0.9646, respectively, and the p value that is equal to 0.0003.The reliability of the experimental data was also confirmed by the value of factor at the level of C.V.=4.59%.

The value of Fisher's criterion F at the level of 43.37 is lower than in the previous review, and it demonstrates better statistical significance. The obtained values of p criterion are less

than 0.0500 and they indicate the significance of the calculated coefficients A, C, A^2 of equation (3).

The calculated F values for Lack of Fit are also statistically significant. The predicted value of Predicted R^2 0.8001 is in reasonable compliance with Adjusted R^2 0.9646. The value of Adeq Precision, which represents a signal-to-noise ratio, is 20.6011 greater than the indicative value 4, which indicates data adequacy.

Table 4

Analysis of variance (ANOVA) of the fitted quadratic polynomial model for the YPC of of defatted grape seed flour extracts

Source	Sum of squares	df	Mean square	F-value	p-value	*Resume*
Model	2.86	9	0.3175	43,37	0,0003	*significant*
Residual	0.0366	5	0.0073			
Lack of Fit	0.0361	3	0.0120	45,55	0,0216	*significant*
Pure Error	0.0005	2	0.0003			
Cor Total	2.89	14				

Estimated regression coefficients					
Term	**Coefficient estimate**	**df**	**Std error**	**F-value**	**p-value**
A	1.90	1	0.0494	346,84	< 0.0001
B	0.5634	1	0.0303	5,35	0,0687
C	0.0700	1	0.0303	12,21	0,0174
AB	0.1057	1	0.0303	6,10	0,0566
AC	-0.1056	1	0.0428	1,76	0,2417
BC	0.0568	1	0.0428	0,2210	0,6581
A^2	0.0201	1	0.0428	7,76	0,0386
B^2	0.1241	1	0.0445	3,22	0,1325
C^2	-0.0800	1	0.0445	5,62	0,0639

Model summary statistics			
Std. Dev.	0.0856	**R^2**	0.9874
Mean	1.86	**Adjusted R^2**	0.9646
C.V.%	4.59	**Predicted R^2**	0.8001
PRESS	0.5785	**Adeq Precision**	20.6011

The Pearson's correlation coefficient for actual and predicted TAC and YPC values at a level of 0.9972 and 0.9936, respectively, indicates the possibility of using the models obtained to predict data on antioxidant capacity and polyphenolic compounds output for defatted grape seed flour when conducting solid-liquid extraction with water.

The following forecast models for describing the properties studied at the code level, which are described by expressions (4) and (5), are subject to proceed to, summarizing all the above:

$$\text{TAC (mg/g DW)} = 26.01 + 8.51A + 0.7289B + 1.20C - 0.1043AB - \\ -0.6769AC + 0.3015BC + 2.30A^2 - 0.7423B^2 - 1.02C^2, \quad (4)$$

$$\text{YPC (mg/g DW)} = 1.90 + 0.5634A + 0.0700B + 0.1057C - 0.1056AB + \\ + 0.0568AC + 0.0201BC + 0.1241A^2 - 0.0800B^2 - 0.1056C^2, \quad (5)$$

Effect of process variables on Total Antioxidant Capasity

The effect of independent variables of temperature, extraction time and ratio on the total antioxidant activity is shown in Figure 2. As seen from the scan, TAC value under the effect of independent variables varies within 17.71–36.78 GAE mg/g DW.

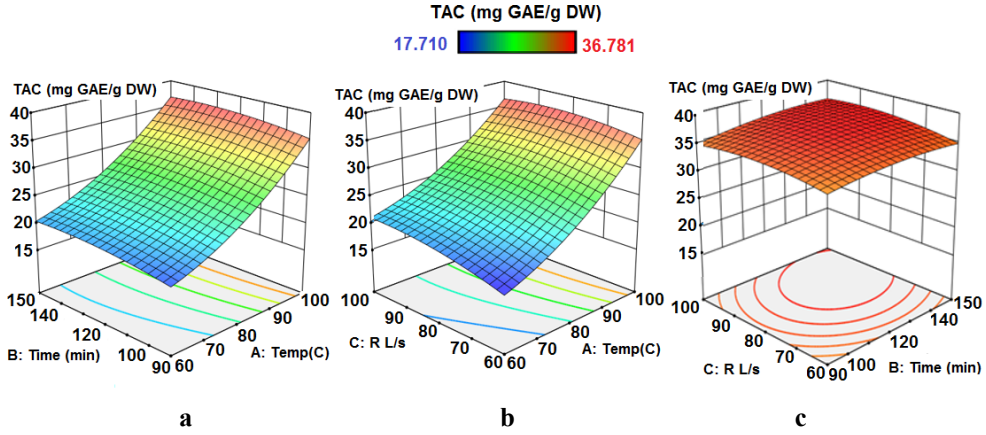

a **b** **c**

Figure 2. The 3D and 2D response surfaces profiles of TAC as affected by independent variables at optimal conditions:
ratio S/L 85 (a), time 131 min (b) and temperature 100 °C (c)

The analysis of three-dimensional surfaces of the basic property dependence on a pair of variables at a fixed optimal value of the third parameter has allowed establishing the following consistent pattern:

- an increase in temperature from 60 to 100°C leads to steady increase in TAC value regardless of the nature of the second independent parameter and the fixed value of the third parameter (Figure 2, a, b) and the achievement of the maximum TAC=36.78 GAE mg/g DW at a temperature of 100 °C
- when fixing the temperature and considering the dependence of TAC value on extraction time and R L/S, a surface with strongly pronounced single point of extremum, which corresponds to the maximum TAC value at a fixed temperature of 100 °C (Figure 2, c) is obtained.

Effect of process variables on Total Phenolics Content

The effect of temperature independent variables, extraction time and ratio L/S on the phenolic compounds yield is shown in Figure 3. As can be seen from the scan, the output value of phenolic compound varies under the effect of independent variables within 1.14–2.60%.The effect of temperature, as in the case of the total antioxidant capacity, leads to a monotonic increase in the YPC value on the entire studied variation interval from 60 to 100 °C, regardless of the variation of the second parameter (Figure 3, a, b). When the temperature is fixed at the optimal level and the other two parameters variation, the pronounced extreme dependence on the extraction time on all curves, regardless of the value of R L/S (Figure 3, c) is obtained.

The monotonous growth of YPC with an increase in the extraction time without reaching an extremum is observed on projection curves up to R L/S 90 values. The pronounced extreme dependence is weakly detected only after the value of 90.

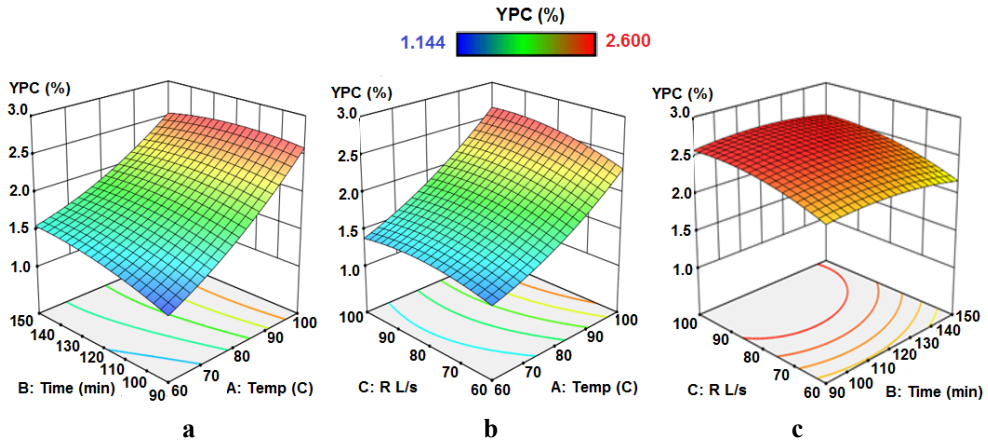

Figure 3. The 3D and 2D response surfaces profiles of YPC as affected by independent variables at optimal conditions:
ratio S/L 93 (a), time 117 min (b) and temperature 100 °C (c)

Optimum conditions for SLE from defatted grape seeds flour by water

The regression models obtained from Eqs. 4 and 5 were used to determine optimum values of extraction temperature, time and ratio liquid to solid by using optimization procedures. The objective function (Q) in this optimization was defined to maximize simultaneously the TAC as well as to maximize the yield of phenolic compounds extract with subject to temperature range (A), time (B), and ratio solid to liquid (C):

$$\max Q = \begin{cases} \text{TAC} \\ \text{YPC} \\ \text{TAC} + \text{YPC} \end{cases}, \quad \text{TAC, YPC} = f(A, B, C), \quad -1 < A, B, C < 1. \tag{6}$$

The optimal conditions are fairly simply and efficiently determined using the RSM methodology mentioned above for a single-response function [20]. TAC and YPC 37.04 and 2.646 values were obtained as a result of carrying out the optimization procedure, respectively (Table 4).

It should be noted that the completed optimization procedure using models (equations 4 and 5) makes it possible to obtain more than ten sets of optimal parameters at which the values of the optimal function are in the 1% interval of variation from the maximum value. Although, the differences in the optimal values of the parameters A, B and C are also practically in the same variation interval.

Table 4

Estimated optimum conditions of responses TAC and YPC

	T, °C	t, min	R L/S	TAC, mg GAE/g DW	YPC,%	Desirability
TAC	100	131	85	37.04		0.9585
YPC	100	117	93		2.646	0.9537
TAC+YPC	100	123	89	36.91	2.633	0.9504

It should be noted that the completed optimization procedure using models (equations 4 and 5) makes it possible to obtain more than ten sets of optimal parameters at which the values of the optimal function are in the 1% interval of variation from the maximum value. Although, the differences in the optimal values of the parameters A, B and C are also practically in the same variation interval.

Under multivariate consideration, the Derringer function or the desirability function (Desirability) were used, preferring a set with larger value (Figure 4) as a final selection criterion of the optimal conditions set.

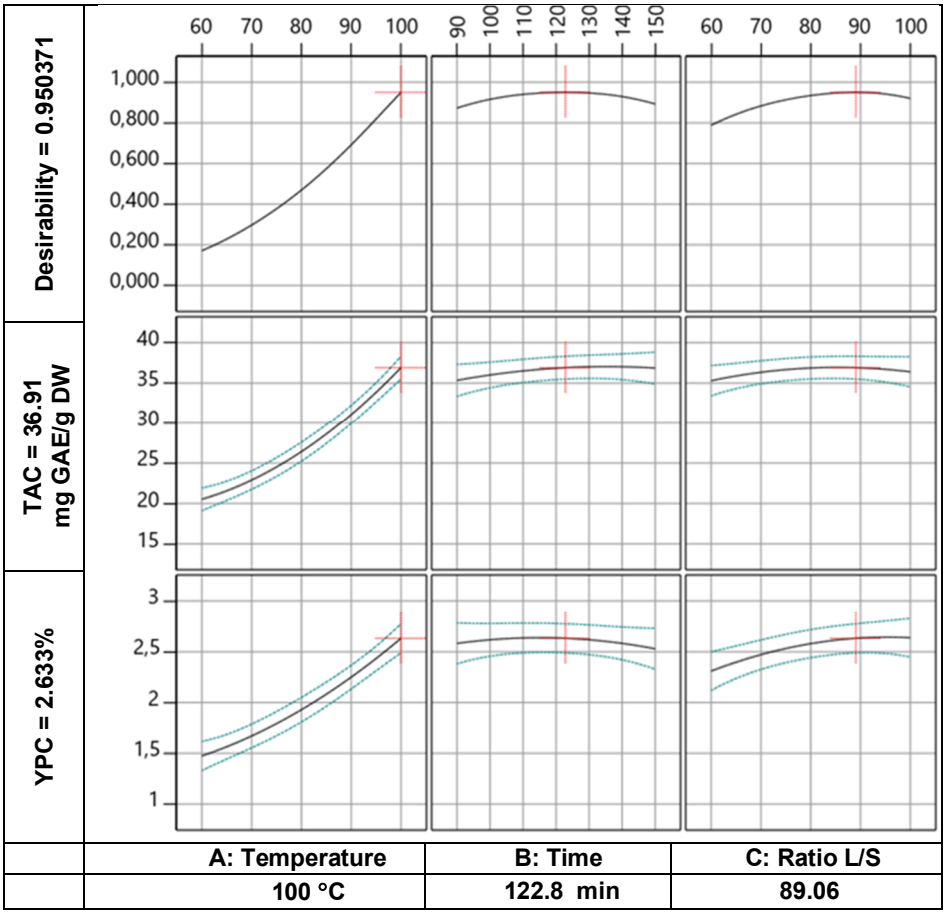

Figure 4. Overall optimum conditions of solid-liquid extraction of phenolic antioxidants from defatted grape seed flour

This function was used as a selection criterion of compromise solution in the multi-criteria optimization technology, in our case with two TAC and YPC response functions. It should be noted that the desirability function is the most important and most frequently used in optimization procedures with multiple response functions [20]. The corresponding optimization algorithm of extraction procedure conditions is effective and economical, when solving the tasks of the output maximization of necessary components from the plant matrix based on several response functions [22].

The results of optimization process of the combination of TAC and YPC values within the variation range of independent extraction variables are presented in Figure 4. The maximum value of the desirability function (0.9504) is reached at a temperature of 100 °C, extraction time of 123 minutes and the ratio of the volume of water to the mass of powder 89 (Table 4).The obtained values of antioxidant capacity and total content of phenolic compounds yield is 36.91mg GAE/g DW and 2.633% less than the similar for each of the properties optimal conditions are only at the level of 0.5%.

Table 5

Comparison between predicted and experimental values in optimal conditions of extractive process (temperature 100 °C, time 123 min, ratio L/S 89)

Value	Predicted	Experimental	δ,%
TAC, mg GAE/g DW	36.91	36.45	1.2
YPC,%	2.633	2.705	2.7

Model validation

The obtained models of TAC and TPC were verified by comparing the predicted data with experimental data. Table 5 shows the comparison between the predicted and experimental values for each response studied at conditions: temperature – 100 °C, time 123 min and ratio L/S 89.

As show Table 5, Experimentally, the values in all three cases are in good agreement with theoretical values within 3%. This can be considered a satisfactory result.

Correlation TAC and TPC values

The various mechanisms of oxidation-reduction reactions, simulating the effect of radical oxidation are used in methods for studying antioxidant properties [23, 24]. The method of galvanostatic coulometry with electrogenerated bromine was used as a method for evaluating antioxidant capacity in this study. The procedure is based on the interaction of antioxidants with bromine and allows evaluating the integral antioxidant capacity of a wide range of materials, including plant materials and materials of a biological nature [25]. The methodology for determining the total content of polyphenols is widely used to estimate the total content of polyphenolic antioxidants, unlike the previous one [24]. Although the different mechanism of reactions effect on which these methodologies are based, there is a quite high positive correlation between the obtained data (Figure 5).

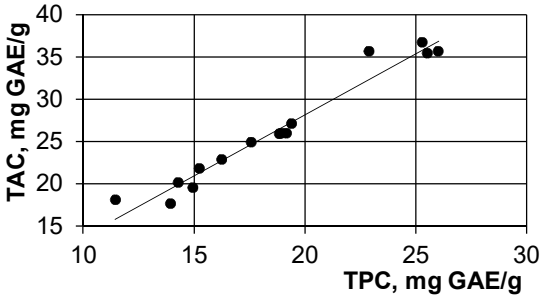

Figure 5. Correlation plots for TAC vs. TPC of water extracts from defatted grape seed flour, R^2=0.9587

Similar regularities were obtained for confectionery products with plant extracts [18]. Data concerning the correlation of TAC and TPC values is another proof that the coulometric titration methodology with electrogenerated bromine is sufficiently adequate for the purposes of determining the total antioxidant capacity in extracts and food samples based on them, with the prevailing content of phenolic compounds as antioxidants.

Conclusion

The following conclusions can be drawn, based on the results obtained:

1. As a result of optimization procedure, it has been determined, that upon optimal conditions, in particular the temperature of 100 °C, the extraction time of 131 minutes and the ratio of the extractive agent volume to the mass of powder of 85, the maximum total antioxidant capacity of the extract, that is equal to 37.04 mg GAE/g DW can be obtained. The maximum output of phenolic substances of 2.646% was obtained under the following conditions: the temperature of 100 °C, the extraction time of 117 minutes and the ratio of the extractive agent volume to the mass of powder of 93.
2. The usage of Derringer function as a selection criterion of compromise solution in a multi-criteria optimization technology with two TAC and YPC response functions, makes it possible to quickly and effectively predict the optimal conditions of the extraction procedure: the temperature of 100 °C, the extraction time of 123 minutes and the ratio of the extractive agent volume to the mass of powder of 89 – the conditions under which the values of TAC and YPC 36,91 mg GAE/g DW and 2,633%, were obtained. The validation of obtained results showed their compliance within 3% with experimental values.
3. The high correlation value between the total antioxidant capacity and the total content of phenolic substances indicates that the galvanostatic coulometric titration with electrogenerated bromine is an appropriate procedure for the purpose of quantitative evaluation of total antioxidant potential of the phenolic compounds in plant extracts.

References

1. Ma Z., & Zhang H. (2017), Phytochemical Constituents, Health Benefits, and Industrial Applications of Grape Seeds: A Mini-Review, *Antioxidants*, *6*(3), pp. 71. doi:10.3390/antiox6030071
2. Li L., & Sun B. (2017), Grape and wine polymeric polyphenols: Their importance in enology, *Critical Reviews in Food Science and Nutrition*, pp. 1–17. doi:10.1080/10408398.2017.1381071
3. Guendez R., Kallithraka S., Makris D. P., & Kefalas P. (2005), Determination of low molecular weight polyphenolic constituents in grape (Vitis vinifera sp.) seed extracts: Correlation with antiradical activity, *Food Chemistry*, *89*(1), pp. 1–9. doi:10.1016/j.foodchem.2004.02.010
4. Watson R. R. (2014), *Polyphenols in Plants: Isolation, Purification and Extract Preparation*, Elsevier. doi:10.1016/C2011-0-08711-2
5. Lebovka F., Vorobiev N., & Chemat E. (2011), *Enhancing Extraction Processes in the Food Industry* (Vol. 20114942), CRC Press. doi:10.1201/b11241
6. Casazza A. A., Aliakbarian B., De Faveri D., Fiori L., & Perego P. (2012), Antioxidants from winemaking wastes: A study on extraction parameters using response surface methodology, *Journal of Food Biochemistry*, *36*(1), pp. 28–37. doi:10.1111/j.1745-4514.2010.00511.x
7. Casazza A. A., Aliakbarian B., Mantegna S., Cravotto G., & Perego P. (2010), Extraction of phenolics from Vitis vinifera wastes using non-conventional techniques, *Journal of Food Engineering*, *100*(1), pp. 50–55. doi:10.1016/j.jfoodeng.2010.03.026
8. Ma-Hock L., Gamer A. O., Landsiedel R., Leibold E., Frechen T., Sens B., … Van Ravenzwaay

B. (2007), Generation and characterization of test atmospheres with nanomaterials, *Inhalation Toxicology*, *19*(10), pp. 833–848. doi:10.1080/08958370701479190

9. Casazza A. A., Aliakbarian B., & Mura M. (2015), Polyphenols from Grape and Apple Skin : a Study on Non- Conventional Extractions and Biological Activity on Endothelial Cell Cultures, *44*(Young 1995), pp. 205–210. doi:10.3303/CET1544035
10. Tarley C. R. T., Silveira G., dos Santos W. N. L., Matos G. D., da Silva E. G. P., Bezerra M. A., Ferreira S. L. C. (2009), Chemometric tools in electroanalytical chemistry: Methods for optimization based on factorial design and response surface methodology, *Microchemical Journal*, *92*(1), pp. 58–67. doi:10.1016/j.microc.2009.02.002
11. Garcia-Salas P., Morales-Soto A., Segura-Carretero A., & Fernández-Gutiérrez A. (2010), Phenolic-compound-extraction systems for fruit and vegetable samples, *Molecules*, *15*(12), pp. 8813–8826. doi:10.3390/molecules15128813
12. Vorobiev E., & Lebovka N. (2016), *Application of Pulsed Electric Energy for Grape Waste Biorefinery* (D. Miklavcic, Ed.), *Handbook of Electroporation*, Cham: Springer International Publishing. doi:10.1007/978-3-319-26779-1
13. Ghafoor K., Choi Y. H., Jeon J. Y., & Jo I. H. (2009), Optimization of ultrasound-assisted extraction of phenolic compounds, antioxidants, and anthocyanins from grape (Vitis vinifera) seeds, *Journal of Agricultural and Food Chemistry*, *57*(11), pp. 4988–4994. doi:10.1021/jf9001439
14. Ashraf-Khorassani M., & Taylor L. T. (2004), Sequential Fractionation of Grape Seeds into Oils, Polyphenols, and Procyanidins via a Single System Employing CO2-Based Fluids, *Journal of Agricultural and Food Chemistry*, *52*(9), pp. 2440–2444. doi:10.1021/jf030510n
15. Saykova I., Tylkowski B., Popovici C., & Peev G. (2018), Extraction of phenolic and flavonoid compounds from solid wastes of grape seed oil production by cold pressing, *Journal of Chemical Technology and Metallurgy*, *53*(2), pp. 177–190.
16. Singleton V. L., Orthofer R., & Lamuela-Raventós R. M. (1999), [14] Analysis of total phenols and other oxidation substrates and antioxidants by means of folin-ciocalteu reagent, In: *Methods in Enzymology* (pp. 152–178). doi:10.1016/S0076-6879(99)99017-1
17. Ziyatdinova G. K., Nizamova A. M., & Budnikov G. K. (2010), Galvanostatic coulometry in the analysis of natural polyphenols and its use in pharmacy, *Journal of Analytical Chemistry*, *65*(11), pp. 1176–1180. doi:10.1134/S1061934810110146
18. Mazur L., Gubsky S., Dorohovych A., & Labazov M. (2018), Antioxidant properties of candy caramel with plant extracts, *Ukrainian Food Journal*, *7*(1), pp. 2313–5891. doi:10.24263/2304-974X-2018-7-1-3
19. Gubskyi S., Nikitin S., Evlash V., & Nemirich O. (2015). Iodine content determination in dried talli of laminaria by galvanostatic coulometry, *Ukrainian Food Journal*, 4(2), pp. 320–327.
20. Bezerra M. A., Santelli R. E., Oliveira E. P., Villar L. S., & Escaleira L. A. (2008), Response surface methodology (RSM) as a tool for optimization in analytical chemistry, *Talanta*, *76*(5), pp. 965–977. doi:10.1016/j.talanta.2008.05.019
21. Box G. E. P., & Behnken D. W. (1960), Some New Three Level Designs for the Study of Quantitative Variables, *Technometrics*, *2*(4), pp. 455–475. doi:10.1080/00401706.1960.10489912
22. Krishnaswamy K., Orsat V., Gariépy Y., & Thangavel K. (2013), Optimization of Microwave-Assisted Extraction of Phenolic Antioxidants from Grape Seeds (Vitis vinifera), *Food and Bioprocess Technology*, *6*(2), pp. 441–455. doi:10.1007/s11947-012-0800-2
23. Apak R., Gorinstein S., Böhm V., Schaich K. M., Özyürek M., & Güçlü K. (2013), Methods of measurement and evaluation of natural antioxidant capacity/activity (IUPAC Technical Report), *Pure and Applied Chemistry: International Union of Pure and Applied Chemistry Journal*, *85*(5), pp. 957–998. doi:10.1351/PAC-REP-12-07-15
24. Prior R. L., Wu X., & Schaich K. (2005), Standardized methods for the determination of antioxidant capacity and phenolics in foods and dietary supplements, *Journal of Agricultural and Food Chemistry*, *53*(10), pp. 4290–4302. doi:10.1021/jf0502698
25. Budnikov G. K., & Ziyatdinova G. K. (2005), Antioxidants as analytes in analytical chemistry, *Journal of Analytical Chemistry*. doi:10.1007/s10809-005-0146-2

Cold press in oil extraction. A review

Büşra Çakaloğlu, Vasfiye Hazal Özyurt, Semih Ötleş

Ege University, Bornova, Izmir Turkey

Keywords:

Oil
Extraction
Cold
Press

Article history:

Received 19.05.2018
Received in revised form 12.07.2018
Accepted 27.12.2018

Corresponding author:

Semih Ötleş
E-mail:
semih.otles@gmail.com

DOI: 10.24263/2304-974X-2018-7-4-9

Abstract

Introduction. The aim of this review is to explain the working principle of the cold press machine and discuss the effect of the extraction efficiency. The advantages and disadvantages of the extraction by means of cold press were explained by referring to other extraction methods.

Material and method. The oil extraction from oilseeds by cold press method investigated for this study. The studies related with cold press were examined and the comparison of cold press with other methods used in oil production from oily seeds was compiled.

Results and discussion. Cold press extraction is one of the methods of mechanical extraction as well as required less energy than other oil extraction techniques and also environmental friendly. It is used to extract oil from a range of matrices and is produced especially in the oil production from oilseeds. High-quality oils can be obtained by performing production at low temperatures using cold press method. It has an environmentally friendly use with no solvents. In other words, the cold-press extraction does not involve either heat or chemical extraction. The soybean, sunflower, rapeseed, corn, grapeseed, hemp, flaxseed, rice bran, olive and pumpkin oils were obtained by cold press extraction method. Moreover, these oils are interesting for consumers due to their natural and safe as well as prevent certain diseases and improve human health due to including a higher level of lipophilic phytochemicals such as antioxidants. These oils have better nutritive properties than refined oils. However, they have a lot of advantages, one of the disadvantages of this technique is low productivity. Another disadvantage of this technique is hard to extract same quality product. The cold pressed oils can add to food as natural antioxidative additives due to phytochemicals and as fatty acid supplements due due to invaluabile double bond fatty acid. There are several studies to investigate the other chemical compounds in the oils and try to use in food products.

Conclusion. While observing the studies, it was generally focused on cold press extraction.

Introduction

Considering the disadvantages of the solvent extraction method using solvent is toxic and expensive and the damage to the environment is quite excessive, alternative methods of extraction are applied. The desire to obtain high-quality crude oil, ecological reasons and the adaptability of the system to continuous processes are the reasons for the use of mechanical systems [1].

The advantages of mechanical oil extraction include simple use, rapid realization of the process and that leads to the short duration of the process, use of small quantities of raw materials, application of different oilseeds and low cost. Also as a by-product protein, rich press cake is obtained [2].

The disadvantages are that the yield is not as high as the solvent extraction, although it is possible to reduce up to 4–6% by using pre-heat treated seeds, approximately 7% of the oil remains in the seed [3].

Mechanical press method is often defined as a solid-liquid phase separation system used for oil extraction from oilseeds with oil content below 20% [4]. Pressure is used in the separation of the mentioned phase separation. And depending on whether or not the temperature is applied, it is called hot or cold press extraction [5].

Cold press machine has one inlet that seeds were feed and two exits that obtained oil and a non-oiled cake was exit.

Pre-treatment and process parameters applied to the raw material in the cold pressing method play a major role in terms of oil yield. The pre-processes mentioned may be peeling, drying, solvent or enzymatic treatment of raw material; the process parameters are feeding rate, the diameter of the restriction dye, temperature, cold rotation speed [6, 7].

Cold presses can be classified as expellers, expanders and twin-cold systems. Twin-cold systems are currently used in laboratory and pilot scale, optimization studies have gained weight. Soybean and cottonseed oil are also used in the production of oil from raw materials that are not considered very high in the amount of oil. Expellers are the name of the first press made by Anderson in 1902. It is the most common type of cold press. In accordance with cold or hot press usage, the heating system has increased the use of being adaptable. The oil separated from the cake is removed from the slot between the metal bars placed at regular intervals with the rotating cold [8].

According to the Turkish Food Codex [9], cold press oils are defined as oils obtained only by mechanical means which are suitable for direct consumption and without heat treatment. In other words, cold pressed oil is generally ready for consumption without needing to be refined, high-quality oil. Many temperature sensitive phenolic compounds are not lost and there are no oxidation reactions occurring along with the heat treatment, which is referred to as a higher quality oil. In the purifying of cold press oils, only washing with water, filtration and centrifugation can be carried out.

In addition to the main functions in human metabolism of vegetable oils, the fact that they are getting much more information about their positive contribution to human health through their bioactive components has led to an increasing interest of consumers in vegetable oils produced by cold pressing and consumed without being refined. Cold press oils with itself characteristic intense taste, color, and special aroma are gaining the appreciation of consumers. Cold press oil production techniques are simple, ecological and do not cost much investment, but the oil yield from raw material is low and the product standard is very difficult to capture [10, 11, 12].

1. Parameters that affect product yield in cold press extraction

Critical parameters in extraction with cold press; characteristics of the raw material (shell-shellless, moisture content, oil content, and type of raw material), feed rate, temperature (hot or cold), cold rotation speed, the diameter of restriction dye, pre-treatment. In the ongoing paragraphs, the studies which investigated the parameters affecting oil yield in cold press method were located.

Dalgıç et al. [13] studied the effect of the roasting temperature applied to the quality of turbentine oil. For this purpose, 3 different species of *Pistacia terebinthus* were cleaned from their garbage and mixed homogeneously and pre-dried overnight at 60 °C. Then, turbentine oils were extracted from the menengiç fruit seeds, which were roasted at 100, 120 and 140 °C for half an hour, using a cold press system. Results showed that the oil extraction efficiency, a, β and a-tocopherol amounts, palmitic and palmitoleic fatty acid components, total phenolic substance and total chlorophyll, carotenoid and feofitin-a increase due to the increase in roasting temperature. Also, a decrease in oleic and linoleic acid amounts and an increase in acidity, K232, K270 peroxide number was observed. In other words, quality parameters have been negatively affected by higher roasting temperature.

Rabadan et al. [14] aim in this study that determine the effect of cold press extraction temperature on the quality parameters of almond, walnut, and peanut oils. Related the texture of raw materials there is necessary pre-treatment as peeling and drying applied. The effect of cold press extraction conditions (temperature of the device and rotation speed of the cold) on the temperature of the obtained oils were studied. The researchers carried out extraction experiments at 50, 100, 150 and 200 °C temperature and 17, 49, 96 rpm cold rotation speeds. When the results were examined, it was observed that (when study conditions were 100 °C and above) the temperature of the oil obtained decreases as the rotation speed increased. The researchers claim that as the rotation speed increased can cause decrease the time that of heating ring exposure. They also found that the temperature of the oil obtained did not exceed 84 °C even if the ring was raised to 200 °C so that the temperature of the heating ring had an effect on the oil outlet temperature but the rotational speed was the decisive factor.

Rombaut et al. [15] aimed to investigate the effects of cold press extraction on grape seed oils total phenolic content and optimize the oil yield. Grape seeds obtained from different harvest times were dried up to 7% moisture content at 40 °C. Materials and process parameters effect determined by Taguchi experiment design with 12 experiments. Variables are a grape seed, pre-heating temperature, rotational speed (20-110 rpm) and restriction dye (8, 10, 12 and 15 mm). Obtained oils were centrifuged at 3000 g for 10 minutes and moisture, ash, total phenolic contents were determined. Researchers concluded that the most effective parameter due to the determining grape seed oil phenolics is the type of the seeds. Nevertheless, by optimizing the device conditions, it was stated that the number of phenolic compounds would increase, but the increase at the moisture content in raw material had a negative effect on performance.

Burg [16] aimed evaluation of grape seed oil extraction process and 3 white (Welschriesling, Green Veltliner, Hibernal) and 2 red (Zweigelt ve Saint Laurent) grape seeds used for oil production. All seeds moisture and oil contents, 1000 grain weight, density were determined. Seeds were dried about 5-8% moisture contents at 40 °C. Variables for cold press extraction were grape varieties, rotational speed (20, 40 60 80 rpm), press performance and oil yield. Press performance increase as the rotational speed was an increase but oil yield was decreased. Results of this study showed that extraction 1000g seeds can produce 67.5- 98.5 g seed oil and this approved oil yield has related with seed varieties.

Hazelnut, pistachio, walnut, apricot, caju, peanut, almonds, pecan walnut samples were dried and waited at +4 °C until analysis. Extraction was performed in cold press device with 2-6 liters/H capacity. The oil obtained was left to collapse for 1 week and was recovered from the impurities by applying filtration and kept in the hermetic closed brown bottle under nitrogen gas at +4 °C. In the solution extraction (petroleum ether) 5 hours extraction time was determined and rotary evaporator 50 °C was flipped. The oil obtained was preserved in brown glass bottles at -18 °C. Carotenoid, flavonoid, anthocyanin, fatty acid composition, tocopherol content, total phenolic content, phenolic content composition, antioxidant activity analysis were applied to obtained oils. The oleic acid contents of the cold pressed oils were higher than the oils extracted by Soxhlet method. According to the results of the analysis, the cold press method was compared with soxhlet method and it was argued that the cold press method was a more economical and safe method since it does not include the use of solvents and heat treatment. In addition to different extraction methods, the parameters affecting the quality and yield of fats; raw material type, origin, harvest time, agro-technical precautions [17].

The researchers investigated the influence of pretreatment as cooking and moisture content over the crambe seed oil by cold press extraction. Crambe is a plant species that is commercially used in the industry. Industrial oil containing the high percentage of erucic acid in the seed is commercially important. The plant is produced in the USA, Canada, Italy, and Spain and is included in the radishes class. Crambe seeds are kept at 4 °C at dry weight with a moisture value of 9.9%. Some of the samples are first cooked and then dried up to the desired moisture content, while others are only dried before the cooking process is applied. In cold compression, the heating ring is set to 120 °C and the rotational speed is 20 rpm. Cold press operation took about four-five minutes. The analysis was made to determine the moisture and fat values of the seeds, and the analysis applied to the oils is the calculation of sedimentation and oil recovery. Results showed that the cooking pretreatment has a positive effect over oil yield but moisture content has a negative effect [18].

In this study which carried out by Akın [19] the contents of fatty acids, phytosterols, squalene, phenolic compounds and acids, carotenoids and phenolic bioactive substances and free radical scavenger antioxidant activities were determined from the raw pumpkin seeds grown in four different central Anatolia regions of Turkey. The oils extracted with cold press extraction method at 40 rpm and 40 °C were drained and left to collapse for 1 day at the temperature below 15 °C (sedimentation) in brown bottles, then sedimentation was removed and centrifuged for 20 minutes at 10 °C and kept at +4 °C (refrigerated) until analysis. Results showed that the cold press extraction one of the best method for obtaining quality and solvent-free pumpkin seed oil.

32-factor experimental design was used for almond and walnut oil extraction. Experimental designs include Seed Moisture Content (SMC) and restriction die (Rd) as parameters. Analysis of response variables oil yield (OY), fine solid content (FC) and oil quality parameters. Almond and walnut moisture and oil quantities are determined. All trials were carried out at 35-40 °C with a rotational speed of 20 rpm. The applied analysis was; peroxide value, FFA content, K232 and K270 coefficients, fatty acid composition, oxidative stability with rancimat. RSM was used in oil extraction. Results were showed that SMC has a positive effect on oil yield when Rd has a negative effect [20].

Singh et al.[21], examined the effect of pre-treatment on the extraction efficiency of linseed oil with the help of the cold press. In this respect, some of the linseeds were only established and some of them were subjected to steam pre-treatment and some to enzyme pre-treatment. Oil yield, residual oil in the cake, rotational speed rate and sediment content were measured as a function of pretreatments and moisture content for cold pressing of

linseed. Results showed that the pretreatments had a significant effect on residual oil and press rate, no significant effect on oil recovery and sediment content. The researchers find out that the seed which low moisture content has provided better oil recovery from enzyme and steam pretreatments.

In the study of Teh [22], tomatoes, grapes and pomegranate seeds examined the parameters that affect oil extraction by cold press method. The parameters studied within the study are; pre-heating conditions, particle sizes, cold rotation speed, the moisture content of seeds and diameter of restriction dye. It has been concluded that the oil is barely separated from the seeds without pre-heating and the device is heated and facilitates the oil outlet when waiting for a certain period of time. When the effect of particle size was examined, the best result was achieved in the processing of seeds as a whole. As the cold rotational speed increases. Press capacity and speed increases. However, oil efficiency was found to be higher at low cold rotational speeds because of the contact time with the device is more. When the effect of different sizes on oil yield was examined using restriction dye, it was concluded that lower diameter molds increased the oil output (with high pressure) in the seed structure. Moisture content negatively affected oil yield.

2. Other studies related with cold press extraction

There are lots of studies related with the cold press extraction. It is hard to classify these studies into groups. But here we mentioned different aimes and how these studies done. Several researchers investigate the different seed cultivars effect on the oil yield;

Walnut oils obtained from 3 different walnut varieties by cold press extraction with 30 rpm rotational speed and 50 °C temperature. Also, 5 different walnut oils purchased from markets. In this way, 8 different walnut oils have been analyzed for characterization. Moisture, ash, oil, tocopherol, total phenolic contents, antioxidant activity (DPPH, ORAC), volatile content (SPME), pigment (chlorophyll carotenoid), color values (L, a, b) were determined [65]

8 different grape varieties have been chosen and all grape seeds were dried 5-10% moisture content. Cold press extraction process parameters were flow rate (constant) and rotational rate 40 rpm. Seeds moisture and oil contents were determined. Also, total oil contents determined by the solvent extraction method. Obtained oils fatty acids analyzed with gas chromatography [66]

This study [47] was conducted to determine the physicochemical properties of pomegranate seed oils obtained by cold pressing with Torche Malas Iran (TMOI) type and two commercial oils of Iran (COI) and Turkey (COT). Analysis of pomegranate seeds was the determination of moisture, fat, protein, carbohydrates and ash. Thermal properties (DSC), refractive index, determination of viscosity, color values, peroxide value, iodine value, amount of non-anhydrous substance, free fatty acid quantity, total phenolic substance amount, fatty acid composition composition, rapid gas chromatography - surface acoustic wave (GC-saw) and flavor assessment analysis were carried out with obtained pomegranate seed oils.In this study [67] quality and physicochemical properties of 7 different flaxseed oils sold in the market were analyzed. Fatty acid content, moisture content, volatile components, non-saponifying content, free fatty acids, chlorophyll pigment, total phenolic acid and flavonoids, tocopherol composition, color values, peroxide value, conjugated dienoic acids, K230-K270 values were determined. Statistical analysis was performed. The results were compared in accordance with the literature and the law.

Volatile components of grape seed oil obtained from different grapes were investigated. Grapeseed oil was purchased from the market. With solid phase micro-extraction (SPME),

volatile components were determined in GC/MS. Tag (triacyl glycerol) composition, total phenol content, antioxidant capacity determination (TEAC) was performed [69].

Several researchers tried to optimise the process conditions, add pretreatment for increase the oil yield.

Rice germ oil obtained from the mechanical press. Specific roasting temperatures and durations have been tried, the samples have been prepared as a control. Determination of color, fatty acid composition, phosphorus and phospholipid analysis, γ-Oryzanol content, tocopherol, and tocotrienol analysis were applied to the obtained oil [68].

In order to perform sesame oil extraction by using Box-Behnken design (50 °C at low temperature), the cold press extraction method was optimized. Experimental designs include Seed Moisture Content (SMC), pressing speed (PS) and restriction dye (Rd) as the main processing parameters. Cold-squeezing was carried out first on a pilot scale and then on an industrial scale. Pilot-scale; seed moisture content (SMC 7, 12 and 17% w.b), press speed (PS 20, 40 and 60 rpm); restriction dye (rd 4, 5 and 6 mm). Industrial-scale experimental design includes SMC (8-14% w.b), PS (20-40 rpm range) and RD (10-14 mm) parameters. The fat content of sesame seeds and pressed cakes were determined by using Soxhlet devices, as solver with n-hexane extraction (10 hours). The solvent was removed at 40 °C using a rotary vacuum vaporizer. Fat content was determined as gravimetric and expressed as percentages by weight on the dry basis (AOCS 2009). The oil obtained by cold press extraction method was subjected to centrifuge for 11000g, 30 minutes. Finally, the analysis applied to the oil obtained; peroxide value, free fatty acid value, K232, K270 values, GC help to determine the composition of fatty acid, total lignan content, radical scavenger capacity (DPPH), determination of oxidative stability by rancimat. The pilot plant-scale extraction showed a peak in oil efficiency (or, 71.1±2.8%) at 12.3% SMC, 4mm Rd, and 20 rpm PS. In order to evaluate the proposed extraction method on an industrial scale, theoretical models were scanned against experimental data. A model fitted for oil recovery showed a maximum estimated value similar to the highest experimental value (74.4±1.2%) under the following conditions: 8,03 SMC, 10 mm Rd and 20 rpm PS. The chemical quality parameters of both pilot and industrial oils have been in the ranges specified in Codex (FAO/WHO) standards for unrefined sesame oil [70].

Several researchers aimed to obtain different oil and their characterization.

Parry [71]; cold pressed onions, parsley, cardamom, cattle, roasted pumpkin, and milk thistle seed oils were taken from the outside. Fatty acid, carotenoid compositions were determined, tocopherol profile was examined, total phenolic matter quantity, ORAC, DPPH, oxidative stability, refractive index, and density analysis were performed.

Siger [72]; antioxidant properties of soybean, sunflower, rapeseed, corn, grapeseed, hemp, flaxseed, rice bran, olive and pumpkin oils obtained by cold press extraction method were studied. Methanol extracts were obtained by solid phase extraction and separation. These oils were purchased from the market. Total phenolic content, determination of phenolic acids (HPLC), antioxidant activity with DPPH were performed.

3. The role of cold press in food production different than the oil extraction from oil seeds

Although cold press method is widely used in the oil extraction, there is an area where it is used too much to be underestimated, it is fruit juice production. Different methods such as diffusion method or different press types are also possible to produce juice. However, since we decided to examine the use of only cold presses under this heading of our study, we found

it appropriate to give information about the screw pressing place during the production phase of fruit juice.

The fruit mass obtained with the crushing of the mill takes the name of mayşe or cake. It is possible to produce clear and fuzzy fruit juices by pressing the cake.

In fruit juice production, screw presses, packaged presses, tape presses, pneumatic presses are used. Cake and press auxiliary material (only if necessary) enters the press feed input, at this stage with the help of sieve free juice leaves and the remaining cake starts to be pressed with the rotating screw. There is a much softer material than the oil extraction from the oil seeds, and there is a possibility that the screw will return to its shape together. To prevent this, press sets have been placed. Thus, the efficiency of this advance has been achieved. The last thing to do is to get out of the restriction dye, water in the structure of the cake is gone and no longer called cake. Here the cake is subjected not only to pressure, but to friction and buckling forces [23].

In addition, pekmez production, wine production, is also used in the production of pestil or in other words fruit leather. These products are produced by juice which obtained cutting and pressing treatments of fruit and than juice concentrated (pekmez), fermenting (wine), concentrated and dried (fruit leather/ pestil) [24, 25, 26].

Different Press types can be used depending on the physical structure of the fruit during pressing stage; it is common to use screw presses because it is suitable for hard fruits such as apples and allows many fruits to be pressed.

4. The other techniques for oil extraction from seed

Oil extraction based on basic principles like not damage the oil during the operation, oil extraction with the least possible impurity, reduction of the amount of fat remaining in the cake, to obtain as much oil as possible from the raw material [27]. The principles mentioned are common to all extraction methods, although their technologies are different. Figure 1 in below schematize the basic methods for oil extraction from oilseed materials. In the scope of the study the oil extraction methods, working principles of them and the studies related with them were mentioned and compared with the cold press method which is the main subject of this review.

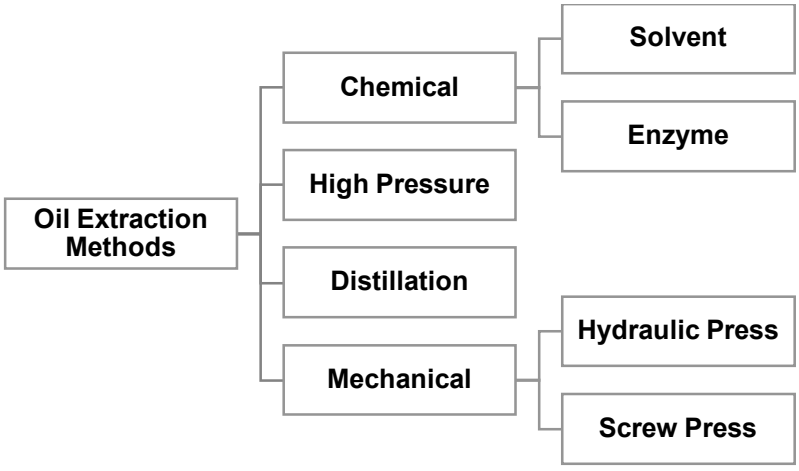

Figure 1. Basic oil extraction methods [28].

4.1. Solvent extraction

First solvent extraction was carried out in France in 1855, Deiss used carbon disulfide as solvent [29]. Although a large number of different solvents are used over time, hegzan is commonly used as a solvent.

Solvent extraction has a multicomponent solid, a solvent which solves the desired material in the medium. The principle of this extraction method is to dissolve the oil with solvent and remove it from the environment. Diffusion is slow in solids, so it is very difficult to reach equilibrium in this process [30].

The parameters affecting solvent extraction are the contact of oil with solvent (oil is usually localized between cells, therefore the size reduction pre-treatment is required, so the surface area is increased, the contact area is also increased), the structure and amount of solvent to dissolve oil, the solution can easily be removed from the environment (lower boiling points ones preferred), temperature (diffusion rate increases as temperature increases) [31].

The advantages of solvent extraction are low cost, simple equipment use, no need to filtration the oil obtained, and high efficiency. However, the too much toxic solution to release the environment and high-temperature application disadvantages [32].

Pradhan et al. [34] examined the chemical composition of the oil obtained from the flax seed with supercritical carbon dioxide extraction, solvent extraction and cold press method. According to this, the highest oil yield was achieved in solvent extraction with hegzan, followed by supercritical CO_2 extraction and the minimum efficiency was achieved by cold press method. However, when the quality criteria were examined, the quality of the oil obtained by cold press method was considered to be better than the other techniques. The difficulty of removing the solvent from the oil, the presence of the solvent in the obtained oil, and the fact that it is ecologically harmful, reduces the use of solvent extraction. Instead, the eco-friendly supercritical CO_2 and cold press method should be considered. However, when evaluated in terms of yield, supercritical CO_2 extraction method can be used between cold press and solvent extraction.

Yılmaz and Gökmen [35] obtained oil from the seed by solvent extraction in their study for the characterization of sour cherry kernels. In addition, they obtained oil by supercritical fluid extraction method and examined the effect of these extraction methods on the composition of the cherry kernel oil. The results of the study showed that the amount of carotene extracted in solvent extraction was higher and the amount of phenolic compounds was lower. In addition, the effect of hexan and hexan ethanol mixture on oil composition was investigated in solvent extraction and it was observed that oil has a positive effect on the extraction of phenolic compounds, antioxidant activity and carotene composition.

Studies have shown that the solvent extraction method in low and medium fat seeds provides higher oil yield by 11.5% compared to cold press method [36, 37].

4.2. Enzyme-assisted extraction

The disadvantages of solving extraction have resulted in the search for alternative methods. Water has been tried as a cheap and non-toxic solvent in order to eliminate the use of toxic solvents. However, no acceptable yield was achieved. On the other hand, with the addition of enzyme, the cost increased more than when the cell wall was broken and the extraction of oil was performed and high efficiency was achieved. Water is used as a separation medium by using the rule that the oil is not dissolved in water, the cell walls are

broken and the oil extraction is performed so that the amount of enzyme used is reduced as much as possible [38, 39, 40].

Enzymes used in the aforementioned method have an effect on those in their own structure from the components that make up the cell wall, such as cellulose, hemicellulose, lignin, pectin compounds [41].

The Table 1 shows the enzymes used for enzyme-assisted aqueous extraction from some oilseeds.

Table 1

Enzymes used for enzyme-assisted aqueous extraction

Materials	Used enzymes	References
Ground peanuts	Alcalase	[42]
	As1398	
	Protizyme	
	Papain	
	Chymotrypsin	
	Nutrias	
	Protamex	
	Trypsin	
Ground sesame seeds	Alcalase 2.4L	[43]
	Protex 7L	
	Viscozyme L	
	Natuzyme	
	Kemzyme	
Minced yellow horn seed kernels	Cellulase	[44]
	Hemicellulase	
	Pectinase	
Jatropha seed kernels	Protizyme	[45]
	Cellulase	
	Pectinex Ultra SP-L	
	Promozyme	
Watermelon seeds	Protex 6L	[46]

Arslan [47] used an enzyme-assisted aqueous extraction method to extract grape seed oil. According to this, it is proven that the enzyme type, enzyme concentration, hydrolysis time and solvent effect to oil yield and optimum conditions are reached to maximise oil yield.

Jung [48] obtained fat from soybean seeds by aqueous extraction method and enzyme-assisted aqueous extraction methods. The cold press method, which is thought to have an effect on oil yield, was pre-treated and its effect on the said extraction was investigated. Accordingly, it was revealed that a greater amount of oil was obtained from the samples subjected to cold pressing as the pretreatment. In particular, the efficiency of cold press was increased from 62.8 to 95.7% in enzyme-assisted aqueous extraction.

Szydłowska-Czerniak et al. [49] applied to enzyme support to increase the efficiency of cold press method in the extraction of flax seed oil. It was concluded that enzymatic extraction increased the oil yield from 5 to 16.4%.

Cold press method; simple to use, environment-friendly and fatty seeds are the most commonly used method in the oil field, but its efficiency is low while enzyme-assisted extraction is high but difficult in terms of cost and processing steps are difficult. For these reasons, enzyme extraction can be applied as a pre-process [50, 51, 52, 49].

4.3. High-pressure extraction

In this study, high-pressure extraction is relatively new technology than other extraction methods which mentioned. Contrary to popular belief, it is not a homogenization method or supercritical fluid extraction [53].

In high-pressure extraction, the solid samples are usually used and the solution is discharged to high temperatures up to 200 °C above the boiling point by the short-term high-pressure application. Mentioned high pressure to reduce solvent consumption is about 1000-1500 psi [54].

The advantages are that the obtained product is far away from impurities, that it saves energy, that it is a safe method and that it reduces the use of solvents as much as possible [55, 56].

The difference between the pressure inside and outside the seed cells is based on the principle of breaking the cell wall and the release of the localized oil between them. Therefore, it can be considered as a suitable method for oil extraction from oilseeds. Contact with the solvent can sometimes be interrupted by blocking the solvent passage from the pores with the amount of air and water sample has, but this problem can be solved by applying higher pressure [57, 58].

Previous studies indicate that reducing the emulsion capacity of proteins with high pressure increases the yield of fat extraction. This change in the structure of proteins is facilitated by hydrolysis and denaturation, which is possible with the high-pressure application. With decreasing protein solubility, in addition to denaturation, peptide bonds in proteins facilitate hydrolysis with proteolytic enzymes. This has lead to studies that use the high-pressure method as a pretreatment [59].

Jung and Mahfuz [60] performed enzyme extraction after high-pressure application and increased soybean oil yield by up to 3%.

Andreou et al. [61] studied the effect of high pressure and pulsed electric fields on oil yield and oil quality parameters in olive oil. According to this, the high pressure application of olive oil has increased oil yield by 6 to 8% (although it varies according to Olive cultivars). The researchers pointed out that the high pressure application did not cause any negative effects on the sensory properties and quality parameters of olive oil, even better caused an increase in oxidative stability of the oil and emphasized that its use in the oil industry with its advantages such as low processing times and low costs could have positive results.

4.4. Distillation

Distillation method is a commonly used method in the extraction of essential oils. Aromatic plants contain highly volatile components and therefore, in other extraction methods, a large portion of these components are lost. In distillation, volatile oils released from the plant's structure together with Steam have transported through steam again. When they pass through the back cooler, it intensifies and returns to the liquid form. Thus, it is possible to obtain pure essential oil. Most important advantages of essential oil obtained by steam distillation is that process temperature lower than 100 °C, so included essential oils temperature sensitive other materials can be distilled [28, 62]. In this study we focused on

oil extraction from oilseeds, for this reason, it is considered appropriate to give only brief information about distillation method.

4.5. Hydraulic press

First in 1785 J. Bramah discovered hydraulic press for oil extraction from oilseeds. In the 1800's, hydraulic presses with 16 press boxes and 400 tons of pressure force were used [29]. The principle of Hydraulic Press is that the oil that comes out of the filter is obtained by pressing the seeds that are filled in the filter cloth inside the boxes. Press cake remains in filter cloth, then manually emptied. The most important parameters are pressure and temperature [63]. Although the hydraulic press cages that did not require filter cloth in the 1900s provided great convenience, in 1950, methods such as cold extractors, solvent extraction, which were able to be applied to continuous systems, maintained high-efficiency, worked faster, required less labor, and the remaining oil amounts were relatively low begin to use. The hydraulic press is still used in olive oil production today.

Gros et al. [33] in their study of the purpose of obtaining the oil from flax seed in cold press method used in their work. In order to increase the oil yield, subjected the flax seeds to the hydraulic press as pretreatment but concluded that there was no significant effect on the yield.Owolarafe et al. [64] compared the hydraulic press and cold press method in palm oil extraction. The yield and quality parameters of the oils obtained by these two extraction methods were compared. According to this, it is suggested that the cold press method is superior to the hydraulic press, because the required labor force and cost are lower during the process, oil yield is higher and the processing time is shorter, in other words extraction is faster and obtained oil has better quality.

Conclusion

In this review, brief information about oil extraction was given and traditional extraction methods were evaluated in terms of advantages, disadvantages and working principles. Since extraction is a very wide and has a very long history separation method, it is limited to working oil extraction and especially with the help of cold press cold squeezing or cold pressing. Cold press is preferred due to its wide usage areas, simple use, lack of manpower, low cost, environmentally friendly, lack of harmful organic solvents and high-quality production possibilities. In addition, generally the product is not applied to heat treatment (cold press), therefore, as mentioned in the study, high-quality oils are obtained. These oils are generally suitable for direct consumption and do not require refining. In this review, the studies which are working on the optimization of the oil extraction with the cold press and the parameters affecting the oil quality and efficiency, and the studies that have applied the pre-treatment before the cold press and examines the effect of the pre-treatment on the oil yield are included. Generally, when the amount of seed moisture content is 10% and above, the efficiency is negatively affected, the product type has a significant effect on the yield, contrary to the thought that the speed of the cold rotation does not increase the yield.

References

1. Richter B. E., Jones B. A., Ezzell J. L., Porter N. L., Avdalovic N., Pohl C. (1996), Accelerated solvent extraction: A technique for sample preparation, *Analytical Chemistry*, 68, pp. 1033.
2. Singh J., Bargale P. C. (2000), Development of a small capacity double stage compression cold press for oil expression, *Journal of Food Engineering*, 43(2), pp. 75–82.
3. Arslan M. (2010), *Üzüm çekirdeklerinden enzim destekli sulu ekstraksiyon yöntemi ile yağ eldesi. Doctoral dissertation*, İstanbul Technical University.
4. Zuorro A., Lavecchia R., Medici F., Piga L. (2014), Use of cell wall degrading enzymes for the production of high–quality functional products from tomato processing waste, *Chemical Engineering Transactions*, 38, pp. 355–360.
5. Kiritsakis A.K. (2002), Virgin olive oil composition and its effect on human health, *Inform*., 13, pp. 237–241.
6. Savoire R., Lanoisellé J. L., Vorobiev E. (2013), Mechanical continuous oil expression from oilseeds: a review, *Food and Bioprocess Technology*, 6(1), pp. 1–16.
7. Chemat F., Strube J. (Eds.). (2015), Green extraction of natural products: theory and practice, *John Wiley & Sons*, pp. 108–113.
8. Uitterhaegen E., Evon P. (2017), Twin–cold extrusion technology for vegetable oil extraction: A review, *Journal of Food Engineering*, 212, pp. 190–200.
9. T.G.K., (2012), *Türk Gıda Kodeksi Bitki Adıyla Anılan Yağlar Tebliği, Tebliğ no: 2012/29.*
10. Matthaus, B. and Brühl, L. (2003), Quality of cold–pressed edible rapeseed oil in Germany, *Food*, 47(6), pp. 413–419.
11. Gürpınar G.Ç., Geçgel Ü., Taşan m., (2011), *Soğuk presyon tekniği ile üretilen bitkisel yağların özellikleri ve sağlık üzerine etkileri. 7. Gıda Mühendisliği Kongresi*, Ankara.
12. İmer Y., Taşan M., (2018), Çeşitli soğuk pres yağların bazı mikro ve makro element içeriklerinin belirlenmesi, *Tekirdağ Ziraat Fakültesi Dergisi*, 15(1), p. 15.
13. Dalgıç L., Sermet O. S., Özkan G. (2011), Farklı kavurma sıcaklıklarının menengiç yağ kalite parametreleri üzerine etkisi, *Academic Food Journal/Akademik GIDA*, 9(3), pp. 26–36.
14. Rabadán A., Pardo J. E., Gómez R., Álvarez–Ortí M. (2018), Influence of temperature in the extraction of nut oils by means of cold pressing, *LWT*, 93, pp. 354–361.
15. Rombaut N., Savoire R., Thomasset B., Castello J., Van Hecke E., Lanoisellé J. L. (2015), Optimization of oil yield and oil total phenolic content during grape seed cold cold pressing, *Industrial Crops and Products*, 63, pp. 26–33.
16. Burg P., Mašán V., Rutkowski, K. (2017), Evaluation of the pressing process during oil extraction from grape seeds, *Potravinarstvo*, 11(1).
17. Al Juhaimi F., Özcan M. M., Ghafoor K., Babiker E. E., Hussain S. (2018), Comparison of cold–pressing and soxhlet extraction systems for bioactive compounds, antioxidant properties, polyphenols, fatty acids and tocopherols in eight nut oils, *Journal of food science and technology*, 55(8), pp. 3163–3173.
18. Singh K. K., Wiesenborn D. P., Tostenson K., Kangas N. (2002), Influence of moisture content and cooking on cold pressing of crambe seed, *Journal of the American Oil Chemists' Society*, 79(2), pp. 165–170.
19. Akin G., Arslan F. N., Elmasa S. K., Yilmaz I. (2018), Cold–pressed pumpkin seed (Cucurbita pepo L.) oils from the central Anatolia region of Turkey: Characterization of phytosterols, squalene, tocols, phenolic acids, carotenoids, and fatty acid bioactive compounds, *Grasas y Aceites, International Journal of Fats and Oils*, 69(1), pp. 232.
20. Martínez M. L., Bordón M. G., Bodoira R. M., Penci M. C., Ribotta P. D., Maestri D. (2017), *Walnut and almond oil cold–press extraction at industrial scale: Effects of process parameters on oil yield and quality*, Instituto de la Grasa; Grasas y Aceites, pp. 68–4.
21. Singh K. K., Jhamb S. A., Kumar R. (2012), Effect of pretreatments on a performance of cold pressing for flaxseed, *Journal of Food Process Engineering*, 35(4), pp. 543–556.

22. Teh H. E. (2016), Extraction and characterization of functional components from fruit and vegetable processing waste. Ph.D. thesis, University of California, Davis.
23. Cemeroğlu B. S. (2013), Meyve ve Sebze İşleme Teknolojisi. 1. Cilt, 5. Baskı. Ankara.
24. Batu A., Kaya C., Çatak J., Şahin C. (2007), *Pestil üretim tekniği, Teknolojik Araştırmalar*, Gıda Teknolojileri Elektronik Dergisi, 1, pp. 71–81.
25. Genç S. (2017), Endüstriyel Pekmez Üretim Sürecinde Enerji Analizi, *Akademik Gıda*, 15(1), pp. 51–59.
26. Özdemir S. (2017), *Farklı maya suşlarının narince ve papazkarası (vitis vinifera) üzüm çeşitlerinden üretilen şarapların kaliteleri üzerine etkileri. Master's thesis*, Namık Kemal Üniversitesi, Tekirdağ.
27. Ionesu M., Vladut V., Ungureanu N., Dınca M., Zabava B. S. Stefan, M. (2017), Methods for oil obtaining from oleagınous materials, *Annals of the University of Craiova–Agriculture, Montanology, Cadastre Series*, 46(2), pp. 411–417.
28. Sarı P., (2006), *Preliminary design and construction of a prototype canola seed oil extraction machine, Doctoral dissertation*, Middle East Technical University, Ankara.
29. Kirschenbauer H. G., (1944), *Fats and Oils*, Reinhold Publishing, New York, pp. 122–123.
30. McCabe W.L., Smith J.C., Harriott P. (2001), *Unit operations of chemical engineering (6th Edition),* McGraw–Hill, Singapore.
31. Balcıoğlu, (2015), *Kabak çekirdeğinden enzimatik sulu ekstraksiyon ile yağ eldesi ve yanıt yüzey yöntemiyle optimizasyonu. Masters thesis*. İstanbul Technical University.
32. De Castro M. L., Priego–Capote F. (2010), Soxhlet extraction: Past and present panacea, *Journal of Chromatography A*, 1217(16), pp. 2383–2389.
33. Gros C., Lanoisellé J. L., Vorobiev E. (2003), Towards an alternative extraction process for linseed oil, *Chemical Engineering Research and Design*, 81(9), pp. 1059–1065.
34. Pradhan R. C., Meda V., Rout P. K., Naik S., Dalai A. K. (2010), Supercritical CO_2 extraction of fatty oil from flaxseed and comparison with screw press expression and solvent extraction processes, *Journal of Food Engineering*, 98(4), pp. 393–397.
35. Yılmaz C., Gökmen V. (2013), Compositional characteristics of sour cherry kernel and its oil as influenced by different extraction and roasting conditions, *Industrial crops and products*, 49, pp. 130–135.
36. Aguilera J.M. (2003), *Solid–Liquid Extraction. Extraction optimization,* in: Food Engineering. Tzia, C. and Liadakis, G. (eds.), Marcel Dekker Inc, New York, USA. pp. 35–55.
37. Kayahan M. (2006), Yağlı tohumlardan ham yağ üretim teknolojisi, *TMMOB GıdaMühendisleri Odası, kitaplar serisi,* 7, Ankara, 244p.
38. Niranjan K., Hanmoungja P. (2004), *Nutritionally Enhanced Edible Oil and Oilseed Processing, Chapter 5– Enzyme–Aided Aqueous Extraction*, AOCS Press, USA.
39. Moura J. M., Campbell K., Mahfuz A., Jung S., Glatz C. E., (2008), Enzyme–assisted aqueous extraction of oil and protein from soybeans and cream de–emulsification, *Journal of The American Oil Chemist' Society*, 85, pp. 985–995.
40. Do L. D., Sabatini D.A. (2010), Aqueous extended-surfactant based method for vegetable oil extraction: proof of concept, *Journal of the American Oil Chemists' Society*, 87(10), pp. 1211–1220.
41. Wu J., Johnson L.A., Jung S., (2009), Demulsification of oil–rich emulsion from enzyme–assisted aqueous extraction of extruded soybean flakes, *Bioresource Technology*, 100, pp. 527–533
42. Jiang L., Hua D., Wang Z., Xu S. (2010), Aqueous enzymatic extraction of peanut oil and protein hydrolysates, *Foods and Bioproducts Processing*, 88, 233e238.
43. Latif S., Anwar F. (2011), Aqueous enzymatic sesame oil and protein extraction, *Food Chemistry*, 125, pp. 679–684.

44. Li J., Zu Y. G., Luo M., Gu C. B., Zhao C. J., Efferth T. (2013), Aqueous enzymatic process assisted by microwave extraction of oil from yellow horn (Xanthoceras sorbifolia Bunge.) seed kernels and its quality evaluation, *Food Chemistry*, 138, 2152-2158.
45. Shah S., Sharma A., Gupta M.N. (2005), Extraction of oil from Jatropha curcas L. seed kernels by the combination of ultrasonication and aqueous enzymatic oil extraction, *Bioresource technology*, 96(1), pp. 121–123.
46. Sui X., Jiang L., Li Y., Liu S. (2011), The research on extracting oil from watermelon seeds by aqueous enzymatic extraction method, *Procedia Engineering*, 15, pp. 4673–4680.
47. Khoddami A., Man Y. B. C., Roberts T. H. (2014), Physico-chemical properties and fatty acid profile of seed oils from pomegranate (Punica granatum L.) extracted by cold pressing, *European journal of lipid science and technology*, 116(5), pp. 553–562.
48. Jung S. (2009), Aqueous extraction of oil and protein from soybean and lupin: a comparative study, *Journal of food processing and preservation*, 33(4), pp. 547–559.
49. Szydłowska–Czerniak A., Karlovits G., Hellner G., Szłyk E. (2010), Effect of enzymatic and hydrothermal treatments of rapeseeds on quality of the pressed rapeseed oils: part II. Oil yield and oxidative stability, *Process Biochemistry*, 45(2), pp. 247–258.
50. Rosenthal A., Pyle D. L., Niranjan K. (1996), Aqueous and enzymatic processes for edible oil extraction, *Enzyme and Microbial Technology*, 19(6), pp. 402–420.
51. Sineiro J., Domınguez H., Nunez M. J., Lema J.M. (1998), Optimization of the enzymatic treatment during aqueous oil extraction from sunflower seeds, *Food Chemistry*, 61(4), pp. 467–474.
52. Passos C. P., Yilmaz S., Silva C.M., Coimbra M.A. (2009), Enhancement of grape seed oil extraction using a cell wall degrading enzyme cocktail, *Food Chemistry*, 115(1), pp. 48–53.
53. Shouqin Z., Junjie Z., Changzhen W. (2004), Novel high–pressure extraction technology, *International Journal of Pharmaceutics*, 278(2), pp. 471–474.
54. Bernal J. L., del Nozal M. J., Jimenez J.J. (1992), Use of a high–pressure Soxhlet extractor for the determination of organochlorine residues by gas chromatography, *Chromatographia*, 34(9–10), pp. 468–474.
55. Rostagno M.A., Villares A., Guillamon E., Garcia–Lafuente A., Martinez J.A. (2009), Sample preparation for the analysis of isoflavones from soybeans and soy foods, *Journal of Chromatography A*, 1216(1), 2.
56. Büyüktuncel E. (2012), Gelişmiş ekstraksiyon teknikleri I, *Hacettepe Üniversitesi Eczacılık Fakültesi Dergisi*, 32(2), pp. 209–242.
57. Bjorklund E., Bowadt S., Nilsson T., Mathiasson L. (1999), Pressurized fluid extraction of polychlorinated biphenyls in solid environmental samples, *Journal of Chromatography A*, 836(2), p. 285
58. Adil I.H. (2006), *Pressurized liquid extraction of phenolic compounds from fruit pomaces. Doctoral dissertation*, Middle East Technical University, Ankara.
59. Yusoff M. M., Gordon M. H., Ezeh O., Niranjan K. (2017), High–pressure pre–treatment of Moringa oleifera seed kernels prior to aqueous enzymatic oil extraction, *Innovative food science & emerging technologies*, 39, pp. 129–136.
60. Jung S., Mahfuz A. A. (2009), Low–temperature dry extrusion and high–pressure processing prior to enzyme–assisted aqueous extraction of full–fat soybean flakes, *Food Chemistry*, 114(3), pp. 947–954.
61. Andreou V., Dimopoulos G., Alexandrakis Z., Katsaros G., Oikonomou D., Toepfl S., Taoukis P. (2017), Shelf–life evaluation of virgin olive oil extracted from olives subjected to nonthermal pretreatments for yield increase, *Innovative Food Science & Emerging Technologies*, 40, pp. 52–57.
62. Ranjitha J., Vijiyalakshmi S. (2014), Facile methods for the extraction of essential oil from the plant species–a review, *International Journal for Pharmaceutical Sciences and Research*, 5(4), pp. 1107–1115.

63. Lanoiselle´ J. L., Bouvier J. M., (1994), Le pressage hydraulique des ole´agineux, *Mise au point, Rev Franc¸ Corps Gras*, 41(3), pp. 61–72.
64. Owolarafe O. K., Faborode M. O., Ajibola O. O. (2002), Comparative evaluation of the digester–screw press and a hand–operated hydraulic press for palm fruit processing, *Journal of food engineering*, 52(3), pp. 249–255.
65. Ojeda–Amador R. M., Salvador M. D., Gómez–Alonso S., Fregapane G. (2018), Characterization of virgin walnut oils and their residual cakes produced from different varieties, *Food Research International*, 108, pp. 396–404.
66. Mašán V., Burg P., Rutkowski K., Burgová J., Lampíř L., Višacki V. (2017), Seed oil content and selected qualitative parameters of oils from grape seeds, *Potravinarstvo Slovak Journal of Food Sciences*, 11(1), pp. 629–633.
67. Choo W. S., Birch J., Dufour J.P. (2007), Physicochemical and quality characteristics of cold–pressed flaxseed oils, *Journal of Food Composition and Analysis*, 20(3–4), pp. 202–211.
68. Kim I. H., Kim C. J., You J. M., Lee K. W., Kim C. T., Chung S. H., Tae B. S. (2002), Effect of roasting temperature and time on the chemical composition of rice germ oil, *Journal of the American Oil Chemists' Society*, 79(5), pp. 413–418.
69. Bail S., Stuebiger G., Krist S., Unterweger H., Buchbauer G. (2008), Characterization of various grape seed oils by volatile compounds, triacylglycerol composition, total phenols, and antioxidant capacity, *Food Chemistry*, 108(3), pp. 1122–1132.
70. Martínez M. L., Bordón M.G., Lallana R. L., Ribotta P. D., Maestri D.M. (2017), Optimization of sesame oil extraction by cold–pressing at low temperature, *Food and Bioprocess Technology*, 10(6), pp. 1113–1121.
71. Parry J., Hao Z., Luther M., Su L., Zhou K., Yu L. (2006), Characterization of cold-pressed onion, parsley, cardamom, mullein, roasted pumpkin, and milk thistle seed oils, *Journal of the American oil chemists' society*, 83(10), pp. 847–854.
72. Siger A., Nogala-Kalucka M., Lampart-Szczapa E. (2008), The content and antioxidant activity of phenolic compounds in cold-pressed plant oils, *Journal of Food Lipids*, 15(2), pp. 137–149.

Internal mechanisms of establishment of the equilibrium state of water-alcohol mixtures in vodka technology

Oleg Kuzmin[1], Valentyna Zubkova[2], Tatiana Shendrik[3], Yurii Korenets[4], Anton Kuzmin[5], Pavlo Bilenkyi[1]

1 – National University of Food Technologies, Kyiv, Ukraine
2 – Jan Kochanowski University in Kielce, Kielce, Poland
3 – L.M. Litvinenko Institute of Physical-Organic Chemistry and Coal Chemistry of the NAS, Kyiv, Ukraine
4 – Donetsk National University of Economics and Trade named after Mykhailo Tugan-Baranovskyi, Kryvyi Rih, Ukraine
5 – National Aviation University, Kyiv, Ukraine

Keywords:
Alcohol
Water
Mixture
Na-cationization
Electrochemical
Activation
^1H *NMR*

Article history:
Received
29.01.2018
Received in
revised form
26.07.2018
Accepted
27.12.2018

Corresponding author:
Oleg Kuzmin
E-mail:
kuzmin_ovl@
nuft.edu.ua

DOI:
10.24263/2304–
974X-2017–6–1–
10

Abstract

Introduction. The aim of the publication is to study the mechanism of the establishment of relaxation of water-alcohol mixtures (WAM) in the main stages of creating vodka in the application of electrochemical activation (ECA) at the stage of *Na*-cationization process water softening.

Materials and methods. ^1H *NMR* analysis was performed using: *FT-NMR* Bruker Avance II spectrometer (400 MHz); special capillary with acEtOHe-d_6; high accuracy ampoules № 507-HP; dispenser; ethyl alcohol rectified (EAR); water softened by *Na*-cationization; WAM from EAR and softened water.

Results and discussion. In this work, the equilibrium state of vodkas in the creation of WAM in the process of ECA of softened water by *Na*-cationization is investigated. It has been established that electrochemical reactions lead to a change in the system of intermolecular interactions. Charging states of molecules in anolyte and catholyte lead to differences in the electron distribution, which affects the chemical displacements of hydroxyl protons. In relation to the softened water (δ_{H2O}=4.65 ppm), the anolyte with δ_{H2O}=(4.23; 4.22) ppm has a displacement of the hydroxyl proton in the «strong field» at Δf=170 Hz. The catholyte with δ_{H2O}=(4.56; 4.54) ppm has a displacement in the «strong field» at Δf=40 Hz. It has been proved that the WAM on anolyte (pH=2.43) and EAR has an acidic medium (pH=3.10), WAM in a catholyte (pH=11.08), and EAR has a meadow medium (pH=11.75). These polar ratios of H_3O^+ to OH^- for anolyte and catholyte lead to a restructuring of the structure in the alcohol/water system. It can be assumed that the proton exchange is accelerated, while there is one general signal of mobile protons $EtOH+H_2O$.

On the basis of the study a fundamental difference between the behavior of the WAM and the vodka prepared on softened water and water after ECA treatment was established. Found systems (alcohol/water) with a stable equilibrium, which are characterized by a high degree of generalization of protons, as well as characteristic rates of exchange for it.

Conclusions. The experimental data obtained prove the dependence of the speed and nature of the establishment of the thermodynamic equilibrium due to the relaxation of the WAM. It is shown that relaxation occurs at the simultaneous stabilization of the hydroxyl group of water and ethanol protons.

Introduction

Today, ^1H *NMR* spectroscopy is the most popular among spectroscopic methods due to its simplicity (Rutledge, 1996) [26] and completeness of information (Majumdar et al., 2017; Richards, Hollerton, 2011) [23, 27], thus accelerating chemical research, especially in the food industry (Abraham, Mobli, 2008) [20]. A large number of articles discuss the use of *NMR* for research of food products: honey, fruits, juices, vegetables, pastry, cheese, meat, fish, dairy products, starch and alcohol products (Zuriarrain et al, 2015; Minoja, Napoli, 2014; Zhu, 2017; Campo et al, 2016; Pinto et al, 2018; Oh et al, 2018; Shi et al, 2018; Youssouf et al, 2017; Li et al, 2018; Kuballa et al, 2018; Yuan et al, 2017) [1, 2, 5, 6, 9, 10, 11, 17, 25, 28, 32]. This method provides comprehensive information with relatively simple obtaining spectra, thus greatly facilitating and accelerating chemical research (Hu et al, 2010; Nose et al, 2005; Roberts, 2002; Richards, Hollerton, 2011) [8, 18, 24, 27].

Since the first ^1H *NMR* spectra of water and ethanol have been obtained more than 60 years, today there are many works (Batta et al, 1997; Albert, 2002; Meusinger, 2010; Rutledge, 1996; Holzgrabe et al, 2008) [7, 12, 21, 26, 29] in which the spectra of water and ethanol are given – which are understandble from the analytical point of view of the substance. But these relatively simple molecules have a large variety of details that occupy a deserved place both in works (Arnold, 2002; Becker et al, 2002; Oliveira et al, 2007; Ababneh, 2018; Richards, Hollerton, 2011; Xu et al, 2012; Mori et al, 2018) [3, 4, 19, 22, 27, 30, 31] and are of interest to our work (Kuzmin et al, 2017) [15, 16].

We will consider a complex of issues related to intermolecular proton exchange. The hydroxyl protone of ethanol can be exchanged with free H^+ ions in the matrix, which are generated by the introduced water or by residual quantities of acid (Arnold, 2002; Becker et al, 2002; Abraham, Mobli, 2008) [3, 4, 20]. The rate of exchange is proportional to the number of free ions H^+, so the actual location of the center of the signal depends on the availability of an alternative exchange point (water), as well as on the difference in chemical changes in the protons of the two milieus (Arnold, 2002; Richards, Hollerton, 2011) [3, 27].

Previously, we have conducted primary research of ^1H *NMR* of water-alcohol mixtures (WAM), which were described in the work of Kuzmin et al, 2017 [15, 16]. The obtained results give grounds to assert a fundamental difference in the behavior of the WAM prepared from the alcohol and water passing through various processes. This may indicate the presence of such features as separate signals of *OH*-protons of H_2O and *EtOH*. Also abnormal waveforms of CH_3 and CH_2 characterize a product with a lowered tasting properties. The presence of the combined signal of H_2O+*(EtOH)* and a «clear» form of CH_3 and CH_2 signals (triplet – for CH_3, quartet – for CH_2) – characterizes the WAM with the best tasting properties.

Thus, in the work of Kuzmin et al, 2017 [15, 16] established experimental evidence or instilment nature/(non- installment) of thermodynamic balance, taking into account the organoleptic characteristics of WAM in dependence on water treatment method and time of system's functioning. However, the questions related to internal mechanism's specification and the rate of establishment of thermodynamic balance depending on type of water used in the process of creating the WAM are remain unsolved.

Therefore, the additional research is required for a detailed study of internal mechanism of thermodynamic balance and insurance in obtaining high quality vodka products – for each type of water separately.

Conducting a set of technical solutions at the main stages of production of vodka, due to electrochemical activation (ECA) of technological water, will allow us to study the mechanism for establishing the equilibrium state of WAM by stabilizing the position of *OH*-protons of ethanol and water, using ^1H *NMR* spectroscopy. Since there is no such information

in the literature, the purpose of the work was to study the mechanism of establishing the thermodynamic equilibrium – the relaxation of the WAM at the major stages of creating vodka when applying ECA at the stage of *Na*-cationization softening of technological water to predict the quality of the final product.

For the set goal, the following tasks were solved:

– to obtain experimental evidence of the rate and nature of the establishment of the thermodynamic equilibrium of WAM;

– to establish a mechanism of thermodynamic equilibrium – the relaxation of WAM;

– to investigate the stabilization of the hydroxyl group of water and ethanol protons.

Materials and methods

Scheme of conducting research (basic scheme of the experimental stand, the scheme of sample preparation for the ^1H *NMR* study and block diagram of the ^1H *NMR* spectrometer) is presented in Figure 1.

The following devices, materials and raw materials were used for research:

- dispenser (15); ampoules 5 mm (400 MHz) with specimens (16); capillaries with deuteroacEtOHe (DAC) (17); ampoules with capillary (18) (Figure 1, b);
- drinking water (0.0) with characteristics: hydrogen index 6.91 unit pH; redox potential (ORP) «+»269.0 mV; mass concentration (MC) MC_{Ca} – 104.342 mg/dm^3; MC_{Mg} – 22.835 mg/dm^3; MC_{Na} – 91.966 mg/dm^3; total hardness – 8.04 mmol/dm^3; total alkalinity – 5.38 mmol/dm^3;
- softened water (1.0) with characteristics: hydrogen index 7.18 unit pH; ORP «+» 288.0 mV; MC_{Ca} – 0 mg/dm^3; MC_{Mg} – 0 mg/dm^3; MC_{Na} – 266.131 mg/dm^3; total hardness – 0.05 mmol/dm^3; total alkalinity – 4.12 mmol/dm^3;
- anolyte (1.2) with characteristics: hydrogen index 2.43 unit pH; ORP «+» 451.0 mV; MC_{Ca} – 0 mg/dm^3; MC_{Mg} – 0 mg/dm^3; MC_{Na} – 156.626 mg/dm^3; total hardness – 0.90 mmol/dm^3; total alkalinity – 0.00 mmol/dm^3;
- catholyte (1.1) with characteristics: hydrogen index 11.08 unit pH; ORP «+» 44.0 mV; MC_{Ca} – 0 mg/dm^3; MC_{Mg} – 0 mg/dm^3; MC_{Na} – 380.009 mg/dm^3; total hardness – 0.15 mmol/dm^3; total alkalinity – 10.85 mmol/dm^3;
- ethyl alcohol rectified (EAR) of the class «Lux» (2.0): volume fraction of ethanol – 96.37%, at T=293 K; $MC_{aldehydes}$ – 1.28 mg/dm^3; $MC_{fusel\ oil}$ – 1.47 mg/dm^3; MC_{esters} – 1.30 mg/dm^3; volume fraction of methanol – 0.0022%;
- WAM for EAR of a class «Lux» and water softened by *Na*-cationization (3.0): volume fraction of ethanol – 39.90%; hydrogen index 7.84 unit pH; ORP – «–»35 mV; $MC_{aldehydes}$ – 1.31 mg/dm^3; $MC_{fusel\ oil}$ – 1.41 mg/dm^3; MC_{esters} – 1.41 mg/dm^3; volume fraction of methanol – 0.0020%; alkalinity – 2.40 ml; tasting score – 9.49 points;
- WAM on softened water – anolyte (3.2): volume fraction of ethanol – 39.91%; hydrogen index 3.10 unit pH; ORP – «+»146 mV; $MC_{aldehydes}$ – 1.80 mg/dm^3; $MC_{fusel\ oil}$ – 1.26 mg/dm^3; MC_{esters} – 1.55 mg/dm^3; volume fraction of methanol – 0.0022%; alkalinity – 0.00 ml; tasting score – 9.51 points;
- WAM on softened water – catholyte (3.1): volume fraction of ethanol – 39.95%; hydrogen index 11.75 unit pH; ORP – «–»174mV; $MC_{aldehydes}$ – 1.43 mg/dm^3; $MC_{fusel\ oil}$ – 1.20 mg/dm^3; MC_{esters} – 1.42 mg/dm^3; volume fraction of methanol – 0.0021%; alkalinity – 2.40 ml; tasting score – 9.42 points;

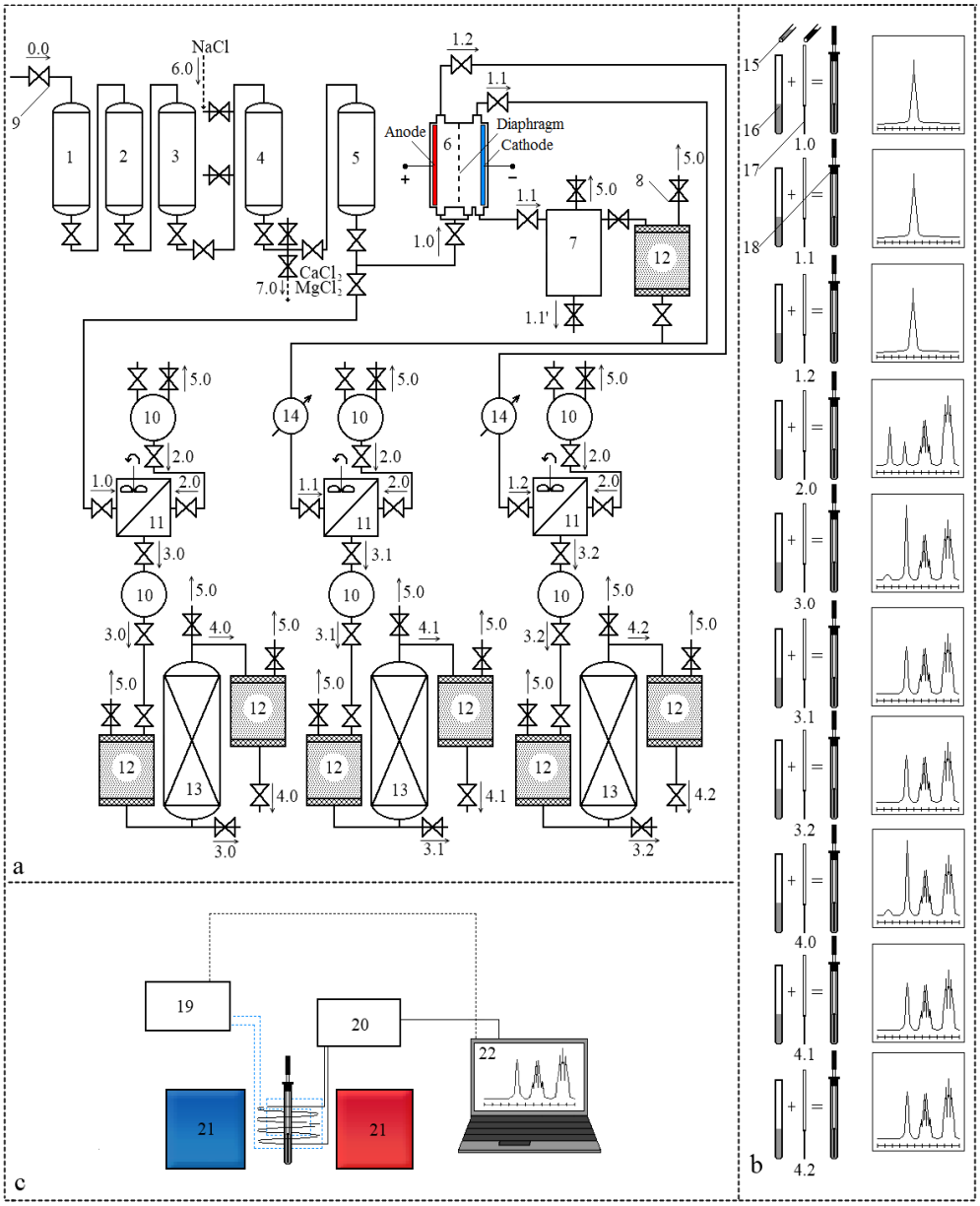

Figure 1. Scheme of research:
a – the principle scheme of the experimental stand;
b – sample preparation scheme for *^{1}H NMR* study;
c – block diagram of a *^{1}H NMR* spectrometer;
0.0–7.0 – streams; 1–14 – technological equipment; 15–22 – laboratory equipment

- WAM on EAR and water softened at the expense of *Na*-cationization after treatment with activated carbon (AC) (4.0): volume fraction of ethanol – 39.81%; hydrogen index 9.14 unit pH; ORP – «+»122 mV; $MC_{aldehydes}$ – 1.72 mg/dm^3; $MC_{fusel\ oil}$ – 1.34 mg/dm^3; MC_{esters} – 1.82 mg/dm^3; volume fraction of methanol – 0.0023%; alkalinity – 2.3 ml; tasting score – 9.63 points;
- WAM on softened water – anolyte after AC (4.2): volume fraction of ethanol – 39.82%; hydrogen index 3.12 unit pH; ORP – «+»360 mV; $MC_{aldehydes}$ – 4.54 mg/dm^3; $MC_{fusel\ oil}$ – 1.57 mg/dm^3; MC_{esters} – 3.52 mg/dm^3; volume fraction of methanol – 0.0024%; alkalinity – 0.0 ml; tasting score – 9.61 points;
- WAM on softened water – catholyte after AC (4.1): volume fraction of ethanol – 39.80%; hydrogen index 10.45 unit pH; ORP – «+»92 mV; $MC_{aldehydes}$ – 2.22 mg/dm^3; $MC_{fusel\ oil}$ – 1.44 mg/dm^3; MC_{esters} – 1.60 mg/dm^3; volume fraction of methanol – 0.0024%; alkalinity – 2.4 ml; tasting score – 9.65 points;

Methods: ^1H *NMR* spectroscopy; methods for assessing physical-chemical and organoleptic characteristics of water, EAR, WAM and vodka.

Work methodology of ^1H *NMR* (Kuzmin et al, 2017) [15, 16]: using the dispenser (15) in the ampoule (16) the test specimen is given. Necessary for the system LOCK – deuterial stabilization *NMR* spectrometer DAC – external standard, which is separated from the test substance, is introduced into the ampule (16) in the capillaries of a special form (17); in accordance with the method of recording ^1H *NMR* spectra, the spectrum of the sample in the DAC (18) is recorded and processed using the Bruker TopSpin v2.6 program.

Apparatus. For the ^1H *NMR* study, the *Fourier NMR* spectrometer Bruker Avance II 400 MHz (Figure 1, c) (19–22) was used.

In Figure 1 a, the principal scheme of the experimental stand with the diaphragm electrochemical reactor is given.

Drinking water (0.0) through the open tap (9) enters the line for preparation of technological water, which consists of the following elements:

- mechanical filter (1) of polypropylene fiber with a filtration rating of 5 μm, which removes mechanical impurities of more than 5 μm from the water;
- carbon filter (2) with porous carbon materials (PCM), which is prepared from alternative materials – food industry wastes by method of chemical activation using H_3PO_4 (Kuzmin O., Shendrik T., Zubkova V., 2017) [14], which provides clearing of active chlorine, iron;
- a mechanical filter (3) with a filtration rating of 1 μm which removes mechanical impurities from the water, which are in the form of weighted particles of varying degrees of dispersion sized by more than 1 μm;
- a filter with ion exchange resin cationic type granules (4). The installation is equipped with mechanisms of automatic regeneration of ion exchange resin *NaCl* (6.0) and a drain of water concentrate from $CaCl_2$ and $MgCl_2$ (7.0);
- a barrier filter (5), which is designed for control softened water filtration before supplying reverse osmosis with a particle lag rating of 1 μm.

Results and discussions

On the ECA preparation line, softened water enters the electrochemical reactor (6), the anodic and cathodic space of which is separated by a porous partition, a diaphragm that is permeable to ions and impervious to products of electrolysis. In this case, the arrival of electrons in water occurs near the cathode, and the removal of electrons from water – near

the anode, which leads to the formation in a cathode chamber – a catholyte (1.1), and in the anode – anolyte (1.2).

For drainage and filtration of the catholyte concentrate (1.1') there is an additional line with a receiving capacity (7), a sand-filter (12) and air cocks (8) – for air separation (5.0).

The ECA process leads to an increase in the water temperature to $T_{1.1\text{-}1.2}$=310 K, which is unacceptable for the manufacture of WAMs, so the water flows (1.1, 1.2) are additionally cooled using a chiller (14).

On the WAM preparation line from the pressure tanks (10) to the sorting tanks the EAR (2.0) and then the water (1.0–1.2) are added (11), where they are mixed by high-speed propeller mixers with the asynchronous electric motor Vemat VTB80B–8. In the process of mixing there is contractionof the total volume of the WAM with heat release. After mixing using the density analyzer «Anton Paar DMA 4500», if the strength of the WAM is determined with deviations from the given, adjust it, re-mix and carry out sampling (3.0–3.2).

After mixing, the WAM enters the pressure vessels (10), after which it is filtered on the sand filters (12) and treated with AC in adsorbers (13). AC used from pyrolyzed wood wastes, obtained by the method of alkaline activation of *KOH* (Kuzmin O., Tamarkina J., Shendrik T., Zubkova V. et al, 2017) [13]. In order to get rid of small particles of coal, WAM (vodka) is filtered again and sampled (4.0–4.2).

In Figure 2–11 shows one-dimensional ^1H *NMR* spectra of hydroxyl protons of the studied substances, taking into account the chemical shift.

The studies used EAR with a volume fraction of ethanol – 96.37% and water – 3.63%, so the ^1H *NMR* spectra of *OH*-proton WAMs are represented by two separate signals of ethanol *EtOH* and H_2O water (Figure 2). The component *EtOH* is a symmetric singlet with an expanded base and an apex of the correct form with a chemical shift δ_{EtOH}=5.65 ppm. The H_2O component is a singlet from δ_{H2O}=4.85 ppm. The difference in chemical shifts between *EtOH* and H_2O is $\Delta\delta$=0.80 ppm (Δf=320 Hz).

The ^1H *NMR* spectrum of softened water due to *Na*-cationization (Figure 3) is presented as a singlet with an expanded base and an irregular vertex and δ_{H2O}=4.65 ppm. The ^1H *NMR* spectrum of water softened by *Na*-cationization after ECA: anolyte is a singlet from δ_{H2O}=(4.23; 4.22) ppm (Figure 4); catholyte is a singlet from δ_{H2O}=(4.56; 4.54) ppm (Figure 5). In relation to the water softened by *Na*-cationization, anolyte has displacement in the «strong field» at $\Delta\delta$=0.425 ppm (Δf=170 Hz), catholyte has a displacement of the hydroxyl proton in a «strong field» with an average value of $\Delta\delta$=0.10 ppm (Δf=40 Hz).

In the process of mixing the EAR class «Lux» (Figure 2) with water softened by *Na*-cationization (Figure 3), the WAM is formed (Figure 6), whose ^1H *NMR* spectra are represented by one single singlet – $EtOH+H_2O$ with an expanded base and the vertex of the correct form and $\delta_{EtOH+H2O}$=4.41 ppm. The difference in chemical shifts between *EtOH* and H_2O is $\Delta\delta$=0.0 ppm.

When creating a WAM (Figure 7) on an EAR of the class «Lux» (Figure 2) with the anolyte (Figure 4), the proton spectra are represented by one single singlet – $EtOH+H_2O$ with $\delta_{EtOH+H2O}$=(4.82; 4.81) pmm. The form of the $EtOH+H_2O$ signal is a distorted gaussian, with an extended base and a certain asymmetry of the vertex, which has one principal peak peak and one additional low-peak peak.

When creating a WAM (Figure 8) in the catholyte (Figure 5), the proton spectra are characterized by a total singlEtOH $EtOH+H_2O$ with $\delta_{EtOH+H2O}$=(4.76; 4.75) pmm.

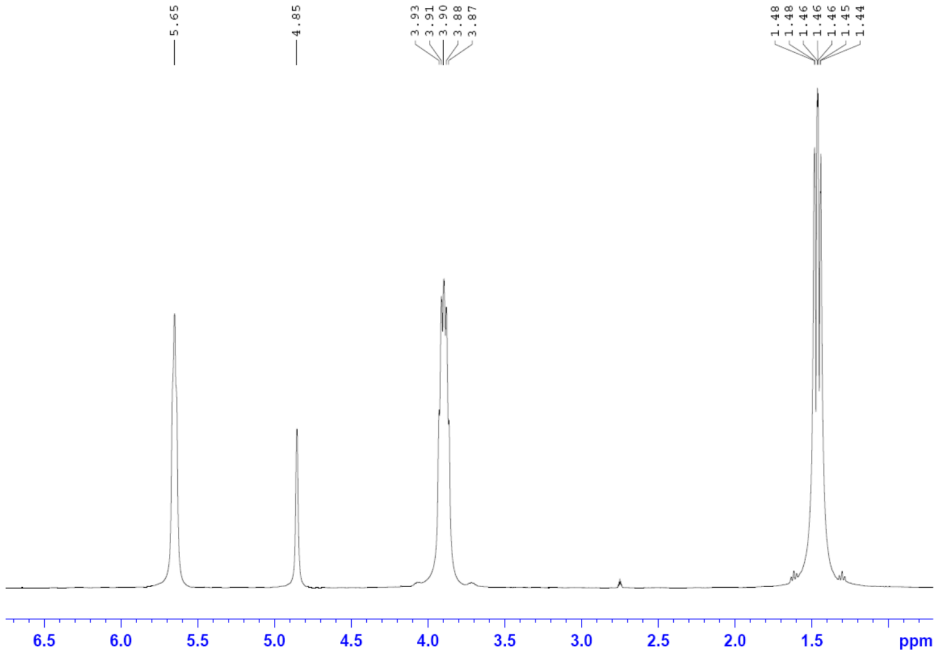

Figure 2. *^{1}H NMR* **spectra of proton groups EAR:** *CH_3*; *CH_2*; *H_2O*; *EtOH*

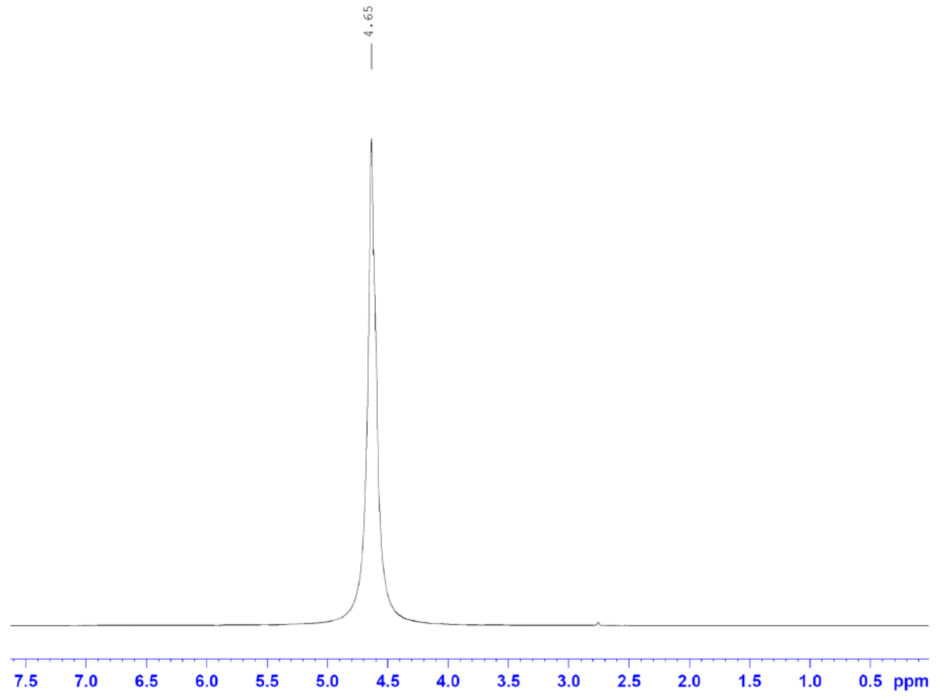

Figure 3. *^{1}H NMR* **spectra of hydroxyl proton of** *Na*-**cationization softening of technological water**

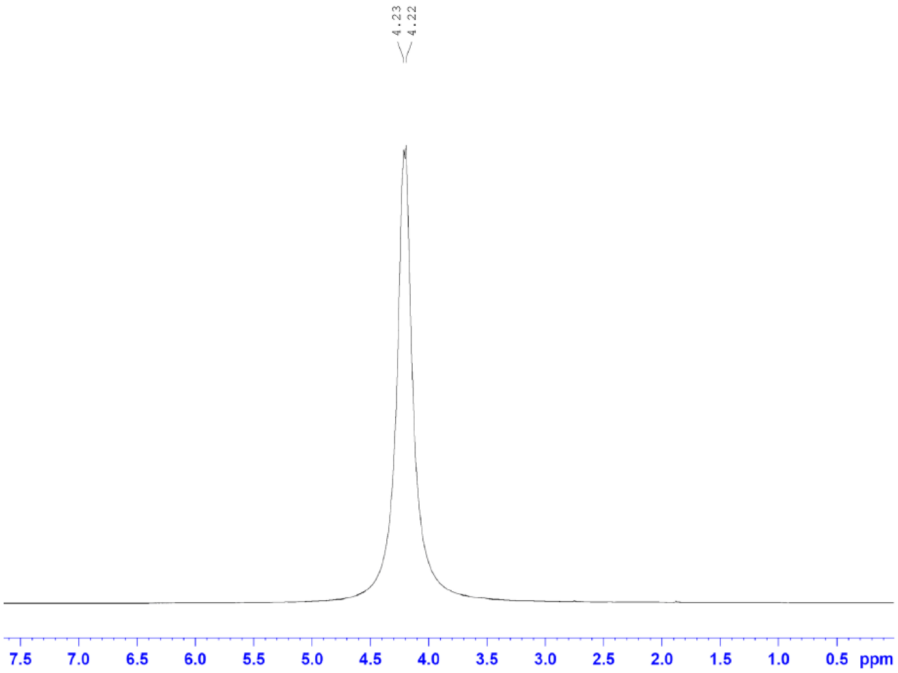

Figure 4. ^{1}H *NMR* spectra of hydroxyl proton of water softened by *Na*-cationization after ECA (anolyte)

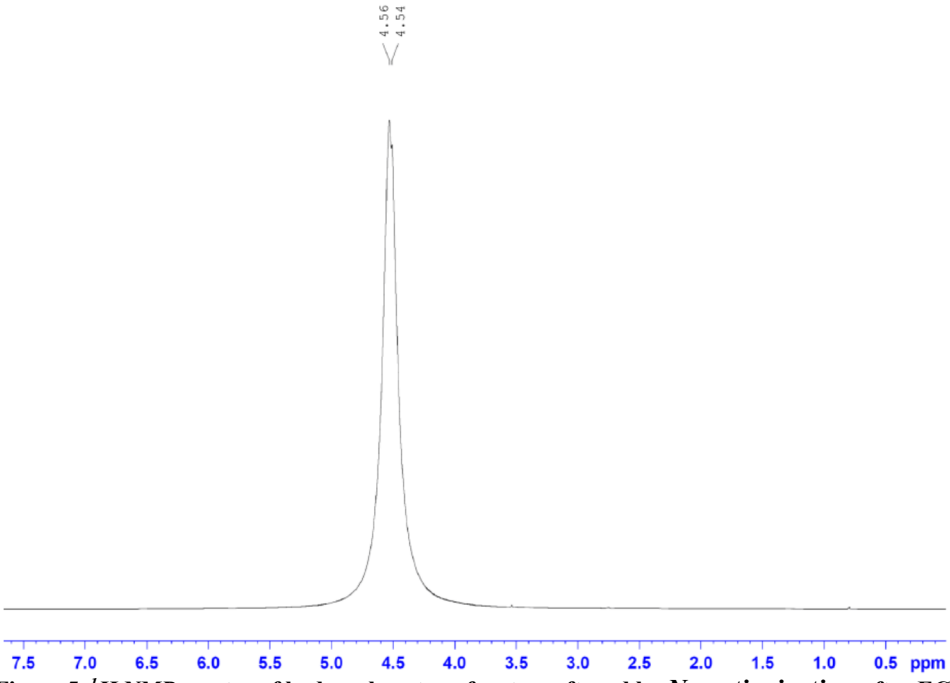

Figure 5. ^{1}H *NMR* spectra of hydroxyl proton of water softened by *Na*-cationization after ECA (catholyte)

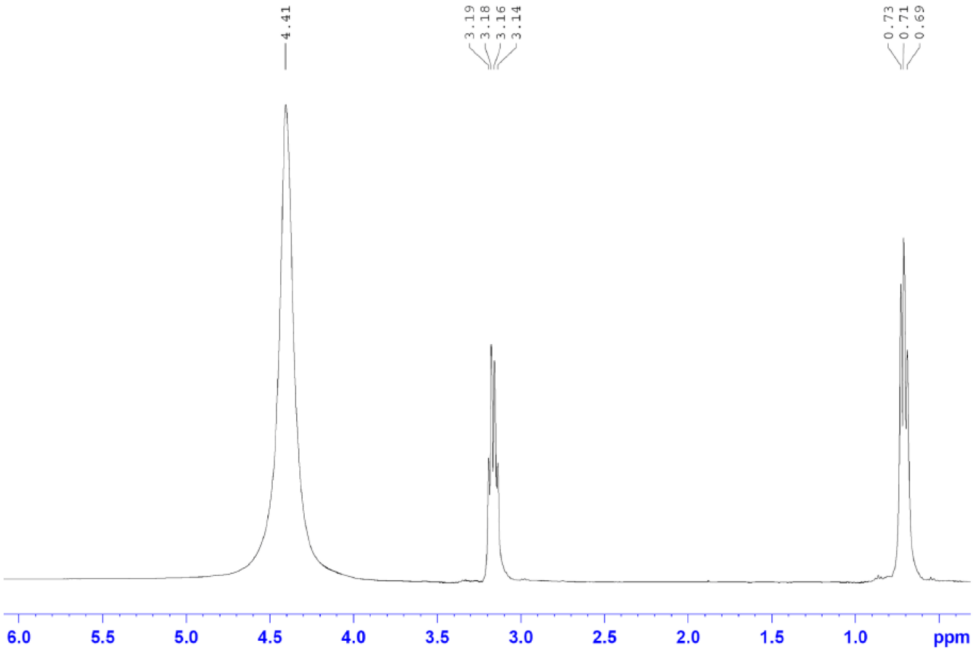

Figure 6. *^{1}H NMR* proton spectra of WAM for EAR and softening of water

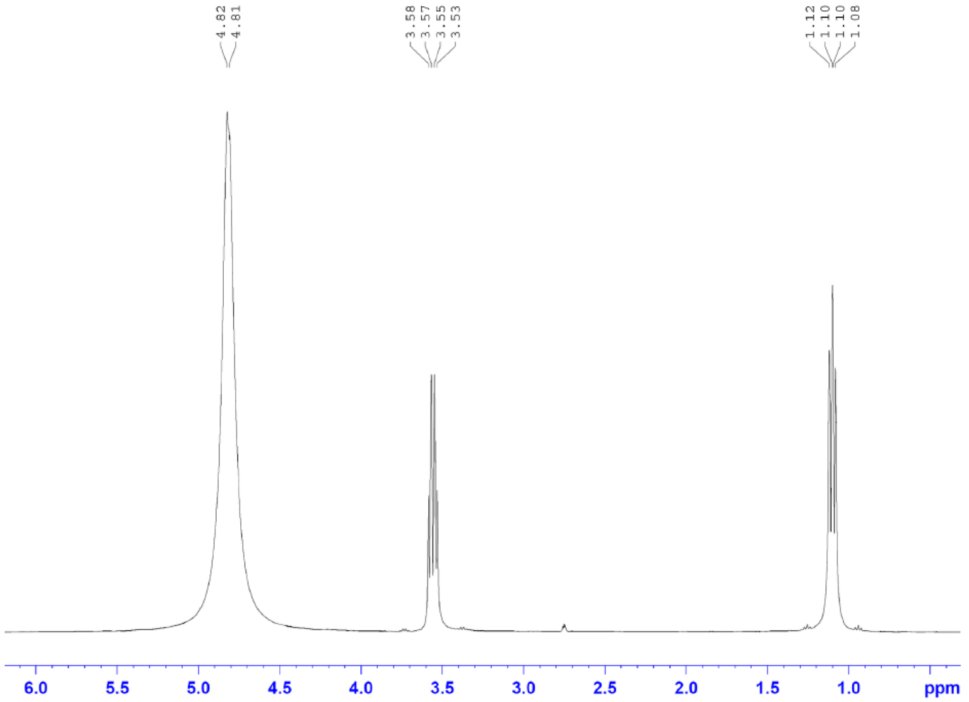

Figure 7. *^{1}H NMR* proton spectra of WAM for EAR and softening of water after ECA (anolyte)

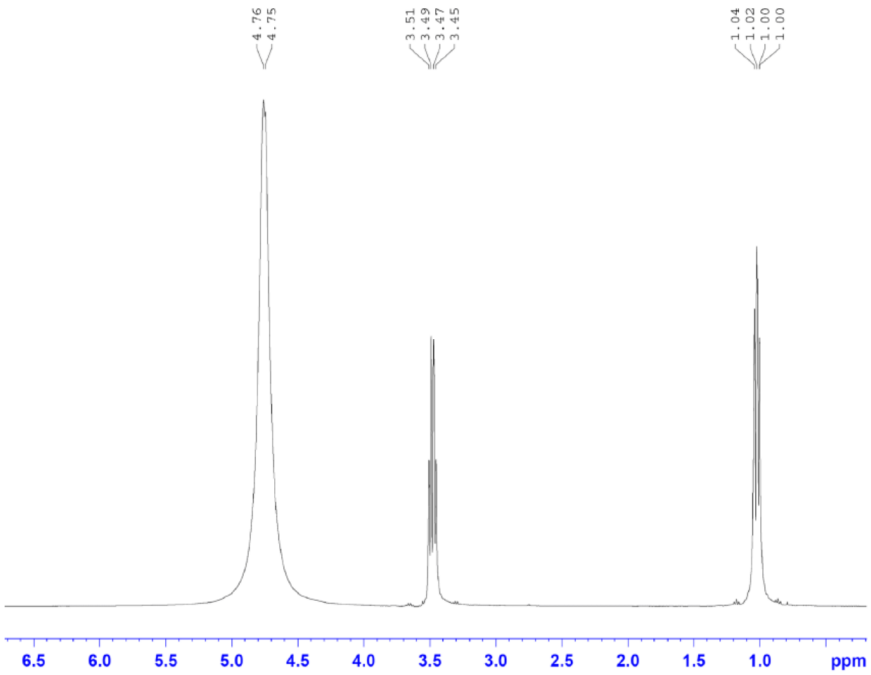

Figure 8. *^{1}H NMR* proton spectra of WAM for EAR and softening of water after ECA (catholyte)

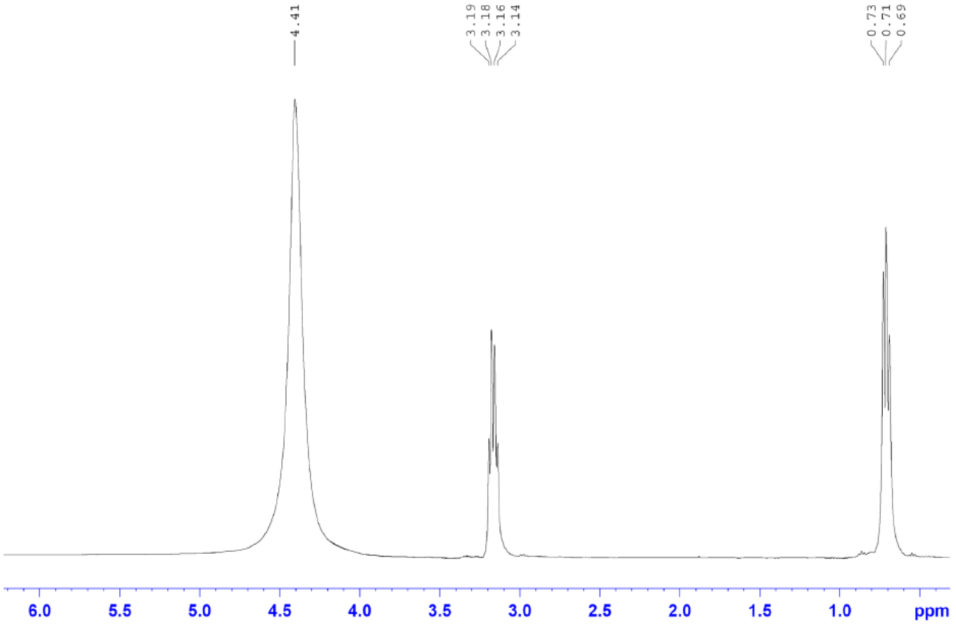

Figure 9. *^{1}H NMR* proton spectra of WAM for EAR and softening of water after treatment with AC

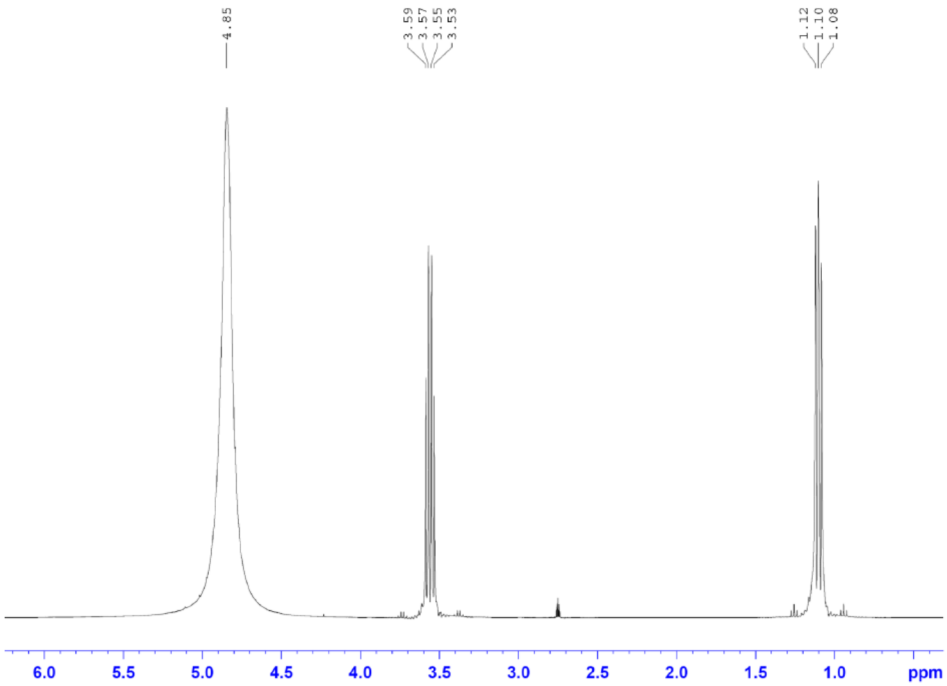

Figure 10. ***^{1}H NMR*** **proton spectra of WAM for EAR and anolyte after treatment with AC**

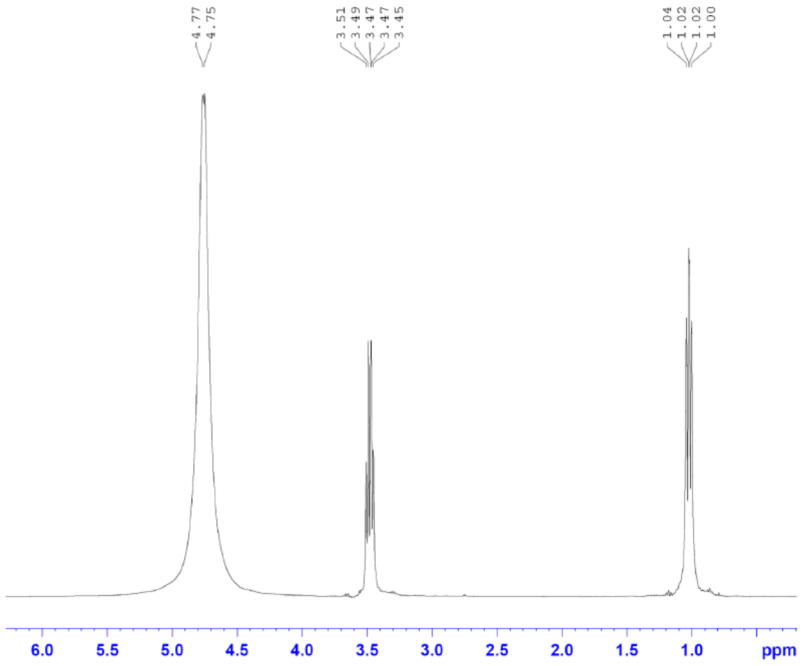

Figure 11. ***^{1}H NMR*** **proton spectra of WAM for EAR and catholyte after treatment with AC**

It can be concluded that in the process of creating a WAM in water softened by *Na*-cationization with a pH level of 7.18 and an EAR of the «Lux» class, the obtained WAM has a pH level of 7.84, which characterizes the reduced concentration of ions of hydroxonium H_3O^+ in relation to OH^- hydroxyl ions. At constant concentration of alcohol in WAM (volume fraction of ethanol – 39.94%) and thermostating system at ^1H studies (T=296.5 K) there is an instantaneous structuring of the system, the proton exchange is so fast that there is only one general signal of hydroxyl protons ethanol (*EtOH*) and water (H_2O), although with a certain asymmetry.

At the expense of the ECA when WAM is created in anolyte with a pH level of 2.43 and an EAR of the Lux class, the WAM obtained has a pH level of 3.10, which characterizes the acidic medium. WAM on a catholyte with a pH level of 11.08 has a strongly alkaline medium (pH=11.75).

These polar ratios of H_3O^+ to OH^- concentrations for anolyte and catholyte lead to a restructuring of the structure in the alcohol/water system, therefore, the proton exchange is accelerated and there is also only one general signal of mobile protons $EtOH+H_2O$ asymmetric.

In this case, the ECA water intensifies the oxidation-reduction reactions when creating WAM, due to the increase of MC aldehydes and esters. Aldehydes are acetaldehyde, which is formed by oxidation of ethanol with oxygen. Esters are represented by ethyl acetate, by oxidation of part of acetaldehyde to acetic acid by oxygen and by the interaction of acetic acid with ethanol to form ethyl acetate.

After processing AC WAM on water softened by *Na*-cationization (Figure 9), the resulting vodka is characterized by a single total signal of hydroxyl protons, $EtOH+H_2O$, represented as a symmetric singlet with a chemical shift $\delta_{EtOH+H2O}$=4.41 ppm. In the process of processing AC WAM in the anolyte (Figure 10), which is characterized by a total peak – $EtOH+H_2O$, represented as a symmetric singlet with $\delta_{EtOH+H2O}$=4.85 ppm. In the process of AC WAM treatment on the catholyte (Figure 11), ^1H *NMR* spectra of *OH*-groups are characterized by a total peak – $EtOH+H_2O$ with a chemical shift $\delta_{EtOH+H2O}$= (4.77; 4.75) ppm. The form of the total signal is a distorted Gaussian with an extended base and a vertex that has one main high-field peak and an additional low-field peak.

When producing vodka on the EAR class «Lux», technological water must meet the requirements of the organization standard and have the following characteristics: dry residue – no more than 350 mg/dm^3; hydrogen index – from 6.0 to 8.0 units pH; total hardness – not more than 0.1 mmol/dm^3; alkalinity total – from 1.0 to 2.0 mmol/dm^3; ORP is not standardized.

Due to the conducted research, water after *Na*-cationization has an elevated pH=7.18 relative to drinking water (pH=6.91), as well as elevated ORP=«+»288.0 mV for drinking water (ORP=«+»269.0 mV). Anolyte and catholyte samples are characterized by a change in the pH and ORP levels relative to the initial values: with the anode ECA, the hydrogen index becomes more acidic (pH=2.43); ORP – increased to positive (oxidative) values (ORP=«+»451 mV); at catholit – the pH=11.08 acquires a more alkaline reaction; ORP=«+»44.0 mV.

In Figure 12 is represented the dependence of hydrogen indicator of the ORP for water, WAM, WAM after AC without processing and after ECA. In this case, three areas of samples can be observed: a_0 – without treatment; a_1 – samples in the catholyte; a_2 – samples on anolyte.

It can be argued that in the process of creating vodka there is relaxation of the WAM in terms of the level of pH and ORP, which in this case are «markers» of stabilization. The values of pH and ORP tend to shift to a stationary area of values that will not undergo critical

changes throughout the «life cycle» of the finished product, while maintaining optimal storage conditions. Although in real storage conditions, there is a slight increase in pH and decrease in ORP, which are already dependent on the interaction of the product with the glass in which the product is stored.

A slight change in the value of total alkalinity in *Na*-cationization (4.12 mmol/dm^3) relative to drinking water (5.38 mmol/dm^3) is a major disadvantage of this process. Therefore, in the process of ECA on anolyte there is a decrease in alkalinity to 0 mmol/dm^3, and after ECA (catholyte) – an increase in alkalinity to 10.85 mmol/dm^3. Therefore with the help of anolyte it is possible to further acidify the water to reduce the total alkalinity of water.

It can be concluded that the electrochemical reactions occurring in the anode and cathode chambers of the diaphragm electrolyzer lead to a change in the entire system of intermolecular interactions, with different charge states of molecules in the anolyte and catholyte leading to differences in the electron distribution, which affects the values of chemical shifts hydroxyl protons.

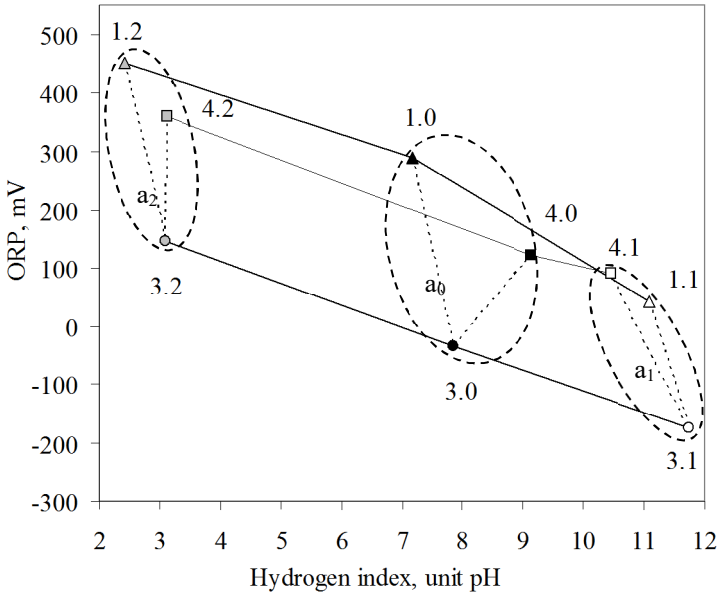

Figure 12. Dependence of hydrogen index of the ORP for water, WAM, WAM after AC without processing and after ECA:

a_0 – area of samples without processing – control (1.0 – water softened by *Na*-cationization, 3.0 – WAM on softened water, 4.0 – WAM on water softened after treatment AC);

a_1 – area of samples after ECA (catholyte);

a_2 – area of samples after ECA (anolyte)

The vodka from the EAR class «Lux» should correspond to the following indicators: MC aldehydes in terms of acetic aldehyde – no more than 4 mg/dm^3; MC of fusel oil, calculated on the mixture of propyl, isobutyl and isoamilic alcohols – not more than 4 mg/dm^3; MC esters in terms of acetic-ethyl ester – no more than 5 mg/dm^3; volume fraction of methyl alcohol – not more than 0.01%; alkalinity – from 0.5 to 3.5 cm^3.

As water is softened by *Na*-cationization and water softened after ECA – do not meet all

the requirements of the normative documentation, the vodka created on this water, conditionally meets the requirements of regulatory documentation, except for alkalinity and MC aldehydes – for vodka on anolyte. In this case there are significant changes in the level of pH and ORP in the WAM in the catholyte after processing with AC. At the primary pH=11.75 for the WAM, after the AC WAM processing at the catholyte, the pH level 10.45, with the primary ORP=«–»174 mV, after the AC WAM treatment at the ORP cathode «+» 92 mV.

It can be argued that at the stage of treatment of AC WAM in water softened by *Na*-cationization and ECA there is a relaxation of the WAM, which results in the return of the values of pH and ORP to the new equilibrium values while simultaneously stabilizing the hydroxyl groups of protons of ethanol and water, due to generalizing of signals.

Conclusions

On the basis of the study, a fundamental difference was found between the behavior of WAM and vodka prepared on water softened by *Na*-cationization and water treated by the ECA. Systems with unstable equilibrium were not detected. The system of alcohol/water with a constant equilibrium and a high degree of generalization of protons, as well as its characteristic exchange rates, is characteristic of the WAM from the EAR of the Luxury class and the water softened by *Na*-cationization as well as the water that passed the ECA in the diaphragm electrolyzer.

Thus, experimental evidence is obtained of the dependence of the rate or time and nature of the establishment of the thermodynamic equilibrium due to the relaxation of the water-alcohol systems with the simultaneous stabilization of the hydroxyl group of water and ethanol protons.

The purpose of the work is to study the mechanism of establishing the equilibrium state of vodkas during the creation of water-alcohol mixtures in the process of electrochemical activation of technological water at the stage of *Na*-cationization softening. Experimentally proved the dependence of the time and nature of the establishment of the thermodynamic equilibrium – the relaxation of the water-alcohol systems during the stabilization of the hydroxyl group of protons of ethanol and water.

Acknowledgements. The research and technical developments are executed by the international interuniversity team and are directly related to the direction of work of the target complex program of scientific, scientific and technical and innovation activity: «Creation of scientific bases of technological processes of water restoration to its natural structural and energy state» (The Ministry of Education and Science of Ukraine, № 0117U001244, 2017-2019).

References

1. Andoni Zuriarrain, Juan Zuriarrain, Mercedes Villar, Iñaki Berregi (2015), Quantitative determination of ethanol in cider by ^{1}H NMR spectrometry, *Food Control*, 50, pp. 758–762.
2. Anna Paola Minoja, Claudia Napoli (2014), NMR screening in the quality control of food and nutraceuticals, *Food Research International*, 63(B), pp. 126–131.
3. Arnold J.T. (2002), Early perceptions in nuclear magnetic resonance (NMR), *Encyclopedia of nuclear magnetic resonance*, John Wiley & Sons.
4. Edwin D. Becker, Cherie L. Fisk, C.L. Khetrapal (2002), The development of NMR,

Encyclopedia of nuclear magnetic resonance, John Wiley & Sons.
5. Fan Zhu (2017), NMR spectroscopy of starch systems, *Food Hydrocolloids*, 63, pp. 611–624.
6. Gloria del Campo, Juan Zuriarrain, Andoni Zuriarrain, Iñaki Berregi (2016), Quantitative determination of carboxylic acids, amino acids, carbohydrates, ethanol and hydroxymethylfurfural in honey by ^{1}H NMR, *Food Chemistry*, 196, pp. 1031–1039.
7. Gy. Batta, K.E. Köver, Cs. Szantaz, Jr. (1997), *Methods for structure elucidation by high-resolution NMR. Application to organic molecules of moderate molecular weight,* Amsterdam, Lausanne, New York, Oxford, Shannon, Singapore, Tokyo, Elsevier.
8. Hu N., Wu D., Cross K. and other (2010), Structurability: A collective measure of the structural differences in vodkas, *Journal of agricultural and food chemistry,* 58, pp. 7394–7401.
9. Joana Pinto, Ana Sofia Oliveira, Joana Azevedo, Victor De Freitas, Paula Guedes de Pinho (2018), Assessment of oxidation compounds in oaked Chardonnay wines: A GC-MS and ^{1}H NMR metabolomics approach, *Food Chemistry*, 257, pp. 120–127.
10. Junsang Oh, Deok-Hyo Yoon, Jae-Gu Han, Hyung-Kyoon Choi, Gi-Ho Sung (2018), ^{1}H NMR based metabolite profiling for optimizing the ethanol extraction of Wolfiporia cocos, *Saudi Journal of Biological Sciences*, 25(6), pp. 1128–1134.
11. Kemeng Shi, Christian Marcus Pedersen, Zhaohui Guo, Yanqiu Li, Yingxiong Wang (2018), NMR studies of the tautomer distributions of d-fructose in lower alcohols/DMSO-d6, *Journal of Molecular Liquids*, 271, pp. 926–932.
12. Klaus Albert (2002), On-line LC-NMR and related techniques, Chichester, John Wiley & Sons Ltd.
13. Kuzmin O., Tamarkina J., Shendrik T., Zubkova V., Koval O., Roman T. (2017), Production of active coal from pyrolyzed wood wastes by alkaline activation of KOH, *Ukrainian Food Journal*, 6(3), pp. 443–458.
14. Kuzmin O., Shendrik T., Zubkova V. (2017), Substantiation of the conditions of obtaining porous carbon materials from pyrolyzed wood wastes by chemical activation of H_3PO_4, *Ukrainian Food Journal*, 6(1), pp. 103–116.
15. Kuzmin O., Suikov S., Niemirich O., Ditrich I., Sylka I. (2017), Effects of the water desalting by reverse osmosis on the process of formation of water-alcohol mixtures. ^{1}H NMR spectroscopy studies, *Ukrainian Food Journal*, 6(2), pp. 239–257.
16. Kuzmin O., Suikov S., Koretska I., Matiyashchuk O., Poliovyk V. (2017), Identification of equilibrium state of hydroxyl protons in vodkas by ^{1}H NMR spectroscopy, *Ukrainian Food Journal*, 6(2), pp. 314–336.
17. Latufa Youssouf, Laura Lallemand, Pierre Giraud, Faiza Soulé, Joël Couprie (2017), Ultrasound-assisted extraction and structural characterization by NMR of alginates and carrageenans from seaweeds, *Carbohydrate Polymers*, 166, pp. 55–63.
18. Nose A., Hamasaki T., Hojo M. and other (2005), Hydrogen bonding in alcoholic beverages (distilled spirits) and water-ethanol mixture, *Journal of agricultural and food chemistry,* 53, pp. 7074–7081.
19. Oliveira I.S., Bonagamba T.J., Sarthour R.S. and other (2007), *NMR quantum information processing*, Amsterdam, Oxford, Elsevier.
20. Raymond J. Abraham, Mehdi Mobli (2008), *Modelling ^{1}H NMR spectra of organic compounds. Theory, applications and NMR prediction software*, John Wiley & Sons Ltd., Wiltshire.
21. Reinhard Meusinger (2010), *NMR-Spektren richtig ausgewertet : 100 Übungen für Studium und Beruf*, Heidelberg, Dordrecht, London, New York, Springer.
22. Riad Ababneh, Ahmad Telfah, Inshad Jum'h, Mohammad Abudayah, Roland Hergenröder (2018), ^{1}H NMR spectroscopy to investigate the kinetics and the mechanism of proton charge carriers ionization and transportation in hydrophilic/hydrophobic media: Methyl

sulfonic acid as a protonic ion source in water/alcohol binary mixtures, *Journal of Molecular Liquids*, 265, pp. 621–628.
23. R. Dutta Majumdar, T. Montina, O.C. Mullins, M. Gerken, P. Hazendonk (2017), Insights into asphaltene aggregate structure using ultrafast MAS solid-state ^{1}H NMR spectroscopy, *Fuel*, 193, pp. 359–368.
24. Roberts J.D. (2002), Organic chemistry applications, in Grant, D.M., Harris, R.K. (ed.) *Encyclopedia of nuclear magnetic resonance,* Chichester: John Wiley & Sons, Ltd, pp. 3386–3400.
25. Rui-Yao Li, Xiao-Wei Zheng, Xin Zhang, Zheng Yan, Bei-Zhong Han (2018), Characterization of bacteria and yeasts isolated from traditional fermentation starter (Fen-Daqu) through a ^{1}H NMR-based metabolomics approach, *Food Microbiology*, 76, pp. 11–20.
26. Rutledge D.N. (1996), *Signal treatment and signal analysis in NMR,* Amsterdam, Lausanne, New York, Oxford, Shannon, Tokyo, Elsevier.
27. Richards S.A., Hollerton J.C. (2011), *Essential practical NMR for organic chemistry*, Chichester, John Wiley & Sons.
28. Thomas Kuballa, Thomas Hausler, Alex O. Okaru, Maria Neufeld, Dirk W. Lachenmeier (2018), Detection of counterfeit brand spirits using ^{1}H NMR fingerprints in comparison to sensory analysis, *Food Chemistry*, 245, pp. 112–118.
29. Holzgrabe U., Wawer I., Diehl B. (2008), *NMR spectroscopy in pharmaceutical analysis*, edited by B. Diehl, Amsterdam, Oxford, Elsevier.
30. Yingjie Xu, Wu Qian, Qiongqiong Gao, Haoran Li (2012), Prediction of vapor–liquid equilibria of alcohol+hydrocarbon systems by ^{1}H NMR spectroscopy, *Chemical Engineering Science*, 74, pp. 211–218.
31. Yoshimasa Mori, Mitsumasa Takahashi, Yasushi Ohno, Ryuhei Okura, Hidetoshi Arima (2018), Identification of molecular-interaction sites between lowly hydrolyzed polyvinyl alcohols and indomethacin by NMR spectroscopy, *International Journal of Pharmaceutics*, 549(1-2), pp. 456–465.
32. Yunfei Yuan, Yupeng Zhao, Jiali Yang, Yueming Jiang, Bao Yang (2017), Metabolomics' analyses of banana during postharvest senescence by ^{1}H-high resolution-NMR, *Food Chemistry*, 218, pp. 406–412.

Improvement of antioxidant potential of wheat flours and breads by addition of medicinal plants

Ivan Dimov[1], Nadezhda Petkova[2], Gjore Nakov[3], Ira Taneva[1], Ivan Ivanov[2], Viktorija Stamatovska[4]

1 – Trakia University of Stara Zagora, Yambol, Bulgaria;
2 – University of Food Technologies, Plovdiv, Bulgaria;
3 – University of Ruse "Angel Kanchev" Branch Razgrad, Bulgaria;
4 – „St. Kliment Ohridski" University of Bitola, Veles, Macedonia.

Keywords:

Herb
Flour
Bread
Antioxidant
Total phenols

Article history:

Received 13.05.2018
Received in revised form 24.06.2018
Accepted 27.12.2018

Corresponding author:

Gjore Nakov
E-mail:
gnakov@
uni-ruse.bg

DOI: 10.24263/2304-974X-2018-7-4-11

Abstract

Introduction. The research aim – to determine the effect of two herbal mixtures on herb bread properties. The influence was established of the herbals on the total phenolic content and antioxidant activities of herbal mixtures, herbal-flour mixtures and herb breads.

Materials and methods. It was used two herbal mixtures (1 – thyme, oregano and lemon balm; 2 – thyme, oregano, lemon balm and fenugreek) with wheat flour for herb bread production. Total polyphenol content was determined following the *Folin-Ciocalteu* method. The antioxidant activities of sample extracts were evaluated by four methods: $ABTS^{\bullet+}$, CUPRAC, FRAP and DPPH assay.

Results and discussion. The highest total phenolic content from all investigated herbs showed oregano (30.43 mg GAE/g dw), herbal mixtures 1 and herbal mixtures 2 – 19.18 mg GAE/g dw and 17.47 mg GAE/g dw, respectively. In herbal-flour mixture and prepared breads the level of total phenolic content were in the range from 0.31mg GAE/g dw to 0.37 mg GAE/g dw. Therefore, the content of these bioactive compounds didn`t changed significantly during the baking process. The highest antioxidant activity of herbal mixtures, herbal-flour mixtures and breads were obtained by two of the used methods – ABTS and FRAP assay. The highest antioxidant potential was demonstrated by herbal mixture 1 consisted of 3 herbs – 16829.73 mM TE/100 g dw, followed by the herbal mixture 2 with 4 herbs – 14693.75 mM TE/100 g dw, respectively, both evaluated by the ABTS method. For the FRAP method, the antioxidant activity values were: 15997.65 mM TE/100 g dw for the herbal mixture 1 with 3 herbs and 14136.82 mM TE/100 g dw for the herbal mixture 2 of 4 herbs.

Conclusions. Herbs added to flour increased the total phenolics and antioxidant values of flour-mixtures and breads. Insignifiant differences in the antioxidant potentials were observed between breads with three and four herbs.

Introduction

One of the global problems among people is diseases caused by unbalanced eating. The current methods of solving these problems are to increase the nutritional and biological value of daily consumed food products, including bread. It is known that traditional types of bread that have a high energy value are characterized by an unbalanced amino acid composition, a low fiber content, vitamins and minerals. Therefore, an important task of bread-making is to strive for the production of bread enriched with physiological-functional ingredients [1].

The nutritional value of the bread depends on the type of flour used and on the variety of other ingredients added to the production. Bread is well absorbed by the body, as it has an elastic medium in which the proteins are optimally denatured, the starch is clustered and the sugars dissolved. They are thus available for the action of enzymes in the gastrointestinal tract [2].

To increase the nutritional and biological value of bread, we proposed to use medigal plants like thyme (*Thymus vulgaris* L.), oregano (*Origanum vulgare* L.), lemon balm (*Melissa officinalis* L.), fenugreek (*Trigonella foenum-graecum* L.) how are rich sources of bioactive compound, especially essential oils, terpenes, phenolic acids and flavonoids with proven antioxidant activity.

Medicinal plants present abundant sources of natural antioxidants and find enormous application in human nutrition, not only as flavoring spices but also as natural remedy. Herbal fortification of white bread is a new trend to improve its nutritional value [3]. Herbs are rich in minerals, vitamins, flavouring agents and natural antioxidants. Roots, stems, leaves or seeds of herbal plants have long been used in cooking and in naturopathy all over the world. This supplementation of herbs add a spicy flavour, greatly improved taste and sensory properties, and enhanced the level of natural antioxidants. Bulgarian culinary herbs and medicinal plants find enourmous application in nutrition, because of their healthy effect due to the bioactive compounds as essential oils, phenolic acids and antioxidants [4].

The nutritional and biological value of traditional wild herbs and spices used in food preparation has been studied. According to this study, their chemical composition (% vc) includes: crude protein (from 4.6 to 22.1%), from 7.5 to 36.0% fat, from 34.6 to 71.9% carbohydrates and from 0.1 to 5.2% essential oils that determine the flavor of the herb-spice. For wild herbs and spices, high antioxidant activity has been detected due to their biologically active components [5]. Most herbs have been shown to exhibit an antioxidant, bactericidal, fungicidal, antiviral effect and lower blood sugar levels [6, 7].

Recently, herbs are included as ingredients of herbal food supplements to enrich them with biologically active substances useful for human health. In the ancient times, human used herbs as a spice in the bread. The introduction of herbs into the bread contributes to its enrichment with biologically active substances [8]. Dried herbs can be incorporated in a larger assortment of bread and bakery products, technologies have been developed in recent years to prepare ready-made flour mixtures enriched with ground herbal dried herbs [9]. It has been found that thyme, marjoram, lemon balm and fenugreek are proper for incorporation in ready-made wheat flour mixtures due to their pleasant aroma and their easier shredding [10].

Moreover, thyme possessed strong antioxidant effect that is mainly due to flavonoids, phenolic aids as rosmarinic acid and caffeic acid [11, 12, 13]. From the volatile aromatic substances contained in the thyme, the eugenol, thymol and carvacrol exhibit a strong antioxidant activity comparable to that of the known antioxidants such as α-tocopherol and butyl hydroxytoluene [14, 15]. In addition, oregano is also herb with strong radical-

scavenging activity, due to not only to presence of rosmarinic acid, but also of phenolic compounds as apigenin, luteolin and carnosic acid [11, 13, 16, 17].

Melissa officinalis L. (known as lemon balm) belongs to the family of Lamiaceae. Its therapeutic properties include sedative, carminative, antispasmodic, antibacterial, antiviral, anti-inflammatory and antioxidative activities [18]. Various in vitro studies indicated that the extract of lemon balm, oregano and thyme possessed antioxidant properties [19, 20, 21, 12, 13, 22]. Some authors Ando et al. [23]; Brown [24]; Kassaian et al. [25]; Naidu [26] have reported antioxidant properties of fenugreek, that makes it a valuable component of healthy nutrition.

The aim of the current study is to evaluate total phenolic content and in vitro antioxidant activity of herbal-flour mixtures and prepared herbal breads.

Materials and methods

Materials

All chemicals for chemical analysis were analytical grade. Medical plants used in the current study were as follows: thyme (*Thymus vulgaris* L.), oregano (*Origanum vulgare* L.), lemon balm (*Melissa officinalis* L.) – leaves and *Trigonella foenum-graecum* L. areal parts. The plants were with Bulgarian origin and were purchased from drugstore (Yambol, Bulgaria). They were then heated to 40 °C for 1 h in a hot air oven and then ground to powder in a commercial kitchen grinder. Then they were sieved through 0.1 mm. Commercial bread-making wheat flour (type 1150 with moisture 13% and ash 11.5%), kindly delivered by AgroMel-Import Ltd (Saedinenie, Bulgaria), was used in bread preparation. Salt was purchased from the local stores of Yambol, Bulgaria. Dried baker's yeast („Pakmaya", Turkey) was used as the leavening agent. Drinking water used for bread preparation was with purity and proper for food purposes that was in accordance with the requirements of Bulgarian legislation.

Herbal mixtures (1– thyme, oregano and lemon balm) and (2 – thyme, oregano, lemon balm and fenugreek) were prepared by mixing, homogenizing and grinding of the medicinal plants in ratio 1:1:1 (herbal mixture 1) and in ratio 1:1:1:1 (herbal mixture 2).

Preparation of composite flour mixtures

Herbal-flour mixtures with 3 and 4 herbs were prepared as follow:

Herbal-flour mixture 1 contained wheat flour type 1150, 1.5% herbal mixture 1 (thyme, oregano and lemon balm), dried yeasts 1.4% and 1.5% salt.

Herbal-flour mixture 2 contained wheat flour 1150, 2% herbal mixture 2 (thyme, oregano, lemon balm and fenugreek), dried yeasts 1.4% and 1.5% salt.

Preparation of breads

The breads were prepared according to bread making methods in the Department of Technology of cereals, fodders, bread making and confectionary products (University of Food Technologies, Plovdiv). The bread formula contained wheat flour (100%), dried yeasts (1.4%), sodium chloride (1.5%), and deionized water (57%) and herbal-flour mixtures 1 and 2. Control bread sample was prepared without addition of herbal mixture, only wheat flour 1150, yeasts 1.4% and 1.5% salt. Bread dough was formed for 6 min at 29–31 ºC and fermented at 35 ºC for 34 min. Breads were baked at 230 – 240 ºC in a convection oven for 16 min. Breads were cooled to room temperature for 60 min [27, 28].

Sample extractions

Bread samples were sliced (3 cm width and 1 cm thickness) and air-dried for 24 h. The dried material was ground to obtain powdered bread samples. Powdered medicinal plants, herbal mixtures and breads (10 g) were extracted with 50 mL of 80% aqueous methanol for 24 h at 25 °C. Samples were then centrifuged at 3500 rpm for 15 min. The supernatant collected was used for further studies.

Determination of the total phenolic content (TPC)

The total phenolic content (TPC) was determined using the Folin–Ciocalteu reagent according to Stintzing et al. [29] with slight modifications. Basically, 0.2 mL extract was mixed with 1 mL Folin–Ciocalteu`s reagent diluted five times and 0.8 mL 7.5% Na_2CO_3. The reaction was carried out 20 min at room temperature in darkness and the absorbance was measured at 765 nm against blank sample. The results were expressed in mg equivalent of gallic acid (GAE) per g dry weight.

Antioxidant activity

The antioxidant activities of sample extracts were evaluated by four methods: DPPH (1,1- diphenyl-2- picrylhydrazyl) radical and ABTS+ radical scavenging ability assay based on mixed hydrogen atom transfer (HAT) and both assay based only on single electron transfer mechanism FRAP (ferric reducing antioxidant power) and CUPRAC, respectively.

ABTS assay. ABTS radical was generated by mixing aliquot parts of water solution of 7.0 mM 2,2`-azinobis(3)ethylbenzthiazoline-6-sulfonic acid (ABTS) and 2.45 mM potassium persulfate. The generated ABTS radical was stable for several days. ABTS.+ solution (2.85 mL) was mixed with 0.15 mL extracts. After 15 min at 37 °C in darkness the absorbance was measured at 734 nm against methanol.

CUPRAC assay. The reaction was started by mixing of 1.0 mL $CuCl_2 \times 2H_2O$, 1.0 ml 7.5 mM Neocuproine (Sigma) in methanol, 1.0 mL 0.1 M ammonium acetate buffer (pH 7.0), 0.1 mL of investigated extract and 1.0 mL d. H_2O. Blank sample was prepared with methanol. The reaction time was 20 min at 50 °C in darkness. After cooling the absorbance was measured at 450 nm against blank [30].

Ferric reducing antioxidant power (FRAP) assay. Three mL freshly prepared FRAP reagent (10 parts 0.3 M acetate buffer (pH 3.6), 1 part 10 mM 2,4,6- tripyridyl-s-triazine (TPTZ) in 40 mM HCl and 1 part 20 mM $FeCl_3.6H_2O$ in d. H_2O) were mixed with 0.1 mL of investigated extract [31]. The reaction time was 10 min at 37 °C in darkness and the absorbance was measured at 593 nm against blank prepared with methanol [30].

DPPH radical-scavenging ability. Each extract (0.15 mL) was mixed with 2.85 mL freshly prepared 0.1mM solution of DPPH (2,2-diphenyl-1-picryl hydrazyl radical) in methanol. The sample was incubated for 15 min at 37 °C in darkness. The reduction of absorbance at 517 nm was measured by spectrophotometer in comparison to the blank containing methanol [32].

The results from all methods for antioxidant activity were expressed as mM Trolox® equivalents (TE) per 100 g dry weight (dw).

Statistical analysis

All experiments were performed in triplicate and the results were expressed as mean ± SD (standard deviation).Statistical analysis was performed using and Excel 2010.

Results and discussion

The total phenolic content of wheat flour, medicinal plants, herbal mixtures, herbal-flour mixtures and prepared breads were summerized in Table 1.

Polyphenols are compounds known to possess the ability to capture free radicals and inhibit lipid oxidation in vitro [33].

Table 1

Total phenolic content in herbs, herbal mixtures, herbal-flour mixtures and herb bread

Sample	Total phenolic content, mg GAE/g dw
Wheat flour Type 1150	-
Thyme	12.05±0.20
Oregano	30.43±0.20
Lemon balm	15.05±0.20
Fenugreek	12.34±0.05
Herbal mixture 1 (thyme, oregano and lemon balm)	19.18±0.05
Herbal mixture 2 (thyme, oregano, lemon balm and fenugreek)	17.47±0.07
Herbal-flour mixture 1	0.31±0.05
Herbal-flour mixture 2	0.36±0.05
Bread prepared with Herbal-flour mixture 1	0.32±0.02
Bread prepared with Herbal-flour mixture 2	0.37±0.05

The highest value of total phenolic content was found in oregano – 30.43 mg GAE/g dw, followed by Lemon balm – 15,05 mg GAE/g dw. The total polyphenol content (TPC) in lemon balm was close to reported values in previous research (18.17±0.04 mg GAE/g dw) mg GAE/g dw [18]. The content of total phenolic compounds in oregano was two time more in comparision with these ones in thyme, lemon balm and fenugreek. Among thyme, lemon and fenugreek herbs, no signifiant differences in the content of common phenolic substances were observed. In this study, the obtained values for the total phenolic content in thyme and fenugreek were close to a previous report for some trademarks of these herbs commercially available in Bulgaria – from 16 to 24 mg GAE/g dw [22].

The values for the total phenolic substances content in herbal mixtures 1 and 2 were in the range of 19.18 mg GAE/g dw for herbal mixture of 3 herbs and 17.47 mg GAE/g dw for the herbal mixture of 4 herbs, as the difference was negligible and due to the involvement of fenugreek in the mixture having a lower content of common phenolic substances – 12.34 mg GAE/g dw in the comparison with oregano and lemon balm.

The values for the content of common phenolic substances in herbal-flour mixture 1 and 2 and in the breads produced from them were in very close range – a total of 0.31 to 0.37 mg GAE/g dw. Compared to individual herbs and herbal mixtures, these values were significantly lower, due to the presence of flour in herbal mixtures, respectively in bread. Moreover, wheat flour present as the main raw material in the largest content. From the results presented, it can be seen that the produced breads have a higher content of polyphenols than the mixes used. Żmijewski et al. (2015) found the same [34].

Different methods were applied for the evaluation of antioxidant activities of herbs, herbal mixtures, herbal-flour mixtures and prepared breads. The results from antioxidant activity were presented (Figure 1, 2 and 3) evaluated by four methods, based on different mechanism (DPPH, ABTS, FRAP and CuPRAC).

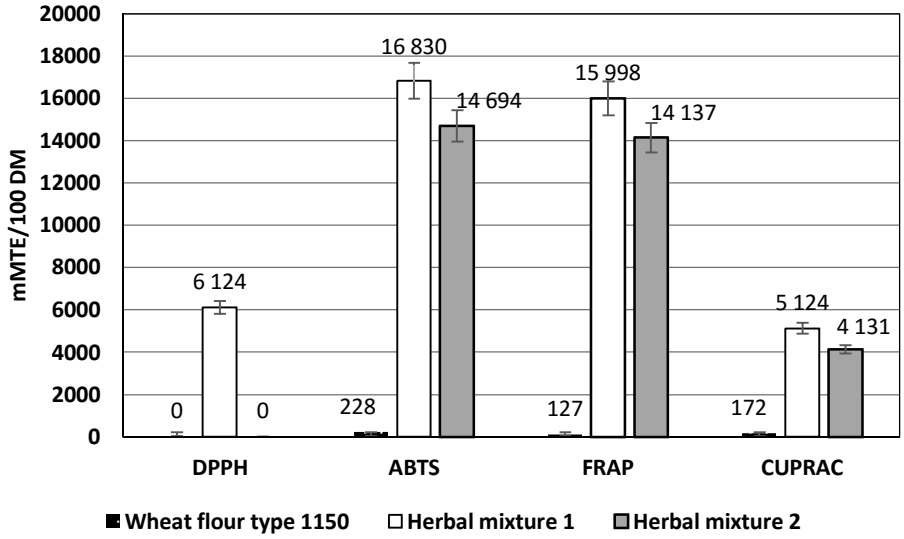

Figure 1. Antioxidant activity of flour and herbal mixtures

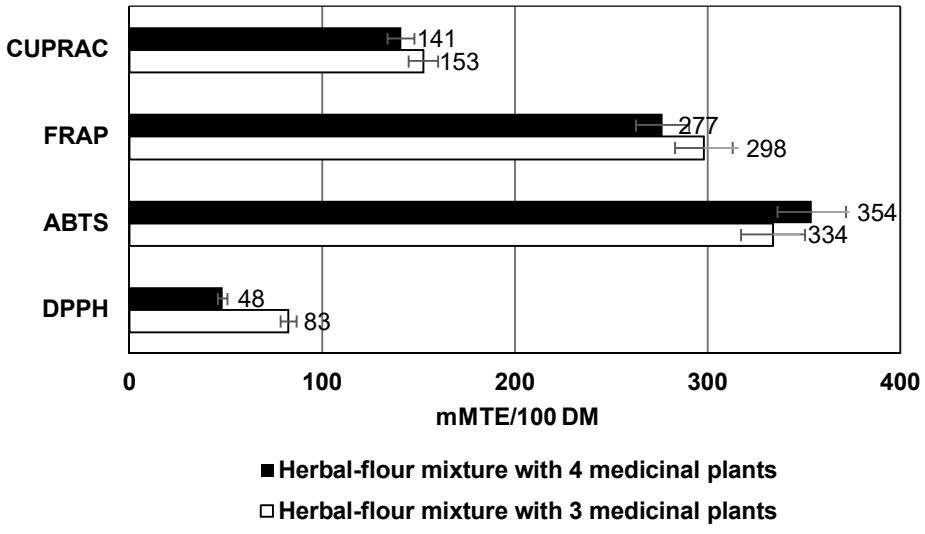

Figure 2. Antioxidant activity of herbal-flour mixtures

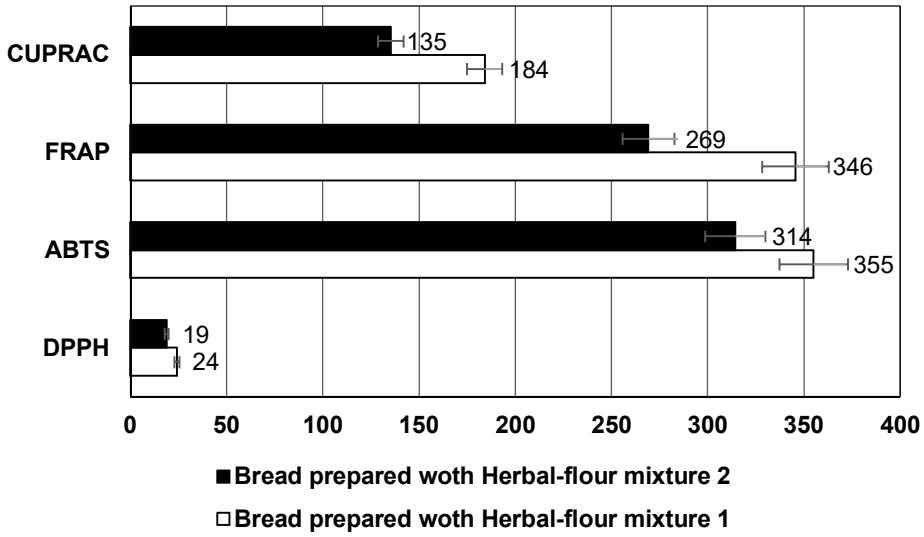

Figure 3. Antioxidant activity of herb breads

The bread production process can be divided into three leavening operations: mixing and forming the dough; fermentation; and backing. The duration of backing depends mainly on the type and mass of the bread. It has been established that the antioxidant potential of bakery products depends on the conditions of production and the raw materials used [35].

In their research, Han and Koh (2011) show that antioxidant activity and free phenolic acid content decrease when the raw materials are mixed and the dough is mixed, but they are restored after the fermentation and backing processes. This is explained by the fact that antioxidant linkages are hydrolysed during fermentation and antioxidants are released [36].

The highest antioxidant activity of herbal mixtures, herbal-flour mixtures and breads were obtained by two of the used methods - ABTS (the radical-scavanging activity against the ABTS radical - 2,2'-azino-bis) -ethylbenzothiazoline-6-sulfonic acid) and FRAP assay. The highest antioxidant potential was demonstrated by herbal mixture 1 consisted of 3 herbs - 16829.73 mM TE/100 g dw, followed by the herbal mixture 2 with 4 herbs - 14693.75 mM TE/100 g dw, respectively, both evaluated by the ABTS method. For the FRAP method, the antioxidant activity values were - 15997.65 mM TE/100 g dw for the herbal mixture 1 with 3 herbs and 14136.82 mM TE/100 g dw for the herbal mixture 2 of 4 herbs. High values of the antioxidant activity of herbal mixtures, herbal-flour mixtures and of breads were also reported in the CuPRAC method (reduction of copper ions). The lowest in the DPPH method (the radical capture activity against the DPPH radical - 2,2-difenyl- 1-picryl hydrazyl radical).

In herbal-flour mixtures and breads, the highest antioxidant activities were also evaluted by the ABTS and FRAP methods, followed by the CuPRAC method, as the insignificant differences in the different types of herbal mixtures and the breads were observed. Compared to herbal mixtures, the herbal-flour mixtures and breads demonstrated 5 times lower antioxidant activity, due to the high content of the wheat flour in herbal-flour mixtures and breads which it is the main raw material. The breads prepared with 3 herbs demonstrated slightly higher antioxidant potential compared to 4 herbal breads.

Higher values obtained from the ABTS method (conducted at neutral pH where the main mechanism is HAT) suggest that the antioxidant action of herbal mixtures is based mainly on hydrogen transfer [37]. The ability of herbs to neutralize reactive forms of oxygen through the involvement of various reaction mechanisms underlines its potential in the prevention of important diseases related with oxidative stress such as accelerated aging processes.

Some authors discussed that the heat treatment and baking process might damage or degrade the antioxidant compounds antioxidant activity that presented in different flours. The antioxidant potential in bakery products is strongly dependent on manufacturing, recipes dough mixing and kneading. Antioxidant activity of breads could be modified by active oxidative enzymes presented in ingredients of compounds used in breads production, or oxidized by atmospheric oxygen [38]. Antioxidant activity of flours was higher than in breads prepared with them (Figure 1 and Figure 3). However, the bread prepared with herbal mixtures showed good antioxidant activity evaluated by ABTS and FRAP methods (Figure 3). Antioxidant activity of breads evaluated by DPPH method showed lower results that was in accordance with tendency reported values for wheat and pseudo cereal breads [38, 39].

Many authors [34, 35, 36] are concerned with the enrichment of white bread with different ingredients containing functional components, but very few have studied the antioxidant characteristics of enriched bread. Seidel et al. (2007) have studied bread enriched with functional ingredients - green tea powder, herbs and tomato paste. The effects of bread produced on immunological and antioxidant parameters were compared with control sample of white bread.

In conclusion, the responses observed with the FRAP assay after intervention with enriched bread indicate a unique response in terms of the antioxidative potentials for this type of functional food [40].

The correlation between antioxidant activity of herbal-flour mixtures and prepared breads and addition of herbal mixtures with three and four herbs to the wheat flour was demonstrated (Table 2).

Table 2

Correlation coefficient (r^2) between antioxidant activities of herbal-flour mixtures and breads prepared with herbal-flour mixtures

Sample	Correlation coefficient (r^2)
Herbal-flour mixture 1 (with three herbs)	0.7499
Herbal-flour mixture 2 (with four herbs)	0.8071
Breads prepared with herbal-flour mixture 1	0.8067
Breads prepared with herbal-flour mixture 2	0.8186

There were significant positive correlations ranging from 0.7499 to 0.8186, which shows the significant influence of added herbal mixtures to basic wheat flour on the antioxidant activity of herbal-flour mixtures and bread made from them. Reported positive correlations showed that the antioxidant action of herbal-flour mixtures and bread could be regarded as a result of the addition of the herbal mixture to flour and enriching their effect on phenolic compounds.

Conclusion

It was found that herbs added to flours increased the total phenolics and antioxidant values of flour-mixtures and final breads. Herbal mixtures, herbal-flour mixtures and prepared breads demonstrated high antioxidant activity by radical-scavanging method ABTS and FRAP assay bease on reduction of ferric ions. The addition of herbs to the flours and breads improved the antioxidant activity of final wheat products. Therefore, the incorparation of herbal mixtures in breads enriched wheat breads of polyphenols and antioxidants, as improve the aroma, taste and healthy status of breads.

References

1. Stepankova G., Oliinyk S., Mykhaylov V., Neklesa O. (2017), Influence of maize germ oilcake on processes of wheat dough ripening and bread quality and nutritional value, *Ukrainian Food Journal*, 6(1), pp. 28–37.
2. Drobot V, Shevchenko A. (2017), Nutritional value and consumer properties of bakery products with fructose for diabetic nutrition, *Ukrainian Food Journal*, 6(3).
3. Eshetu M., Atlabachew M., Abebe A. (2018), Quality assessment of wheat bread baked in Bahir Dar City, Ethiopia. *Journal of Food Quality and Hazards Control*, 5, pp. 77–80.
4. Popova A., Mihaylova D. (2018), A review of the medicinal plants in Bulgaria–collection, storage, and extraction techniques, *Asian Journal of Pharmaceutical and Clinical Research*, 11(3), pp. 28–35.
5. Achinewhu, S.C., Ogbonna C.C., Hart A. D. (1995), Chemical composition of indigenous wild herbs, spices, fruits, nuts and leafy vegetables used as food, *Plant Foods for Human Nutrition (Formerly Qualitas Plantarum)*, 48(4), pp. 341–348.
6. Sharon Palmer, R.D. (2008), Herbs and Spices: Hot and Healthy, *Food Product Design*.
7. Small, E. (2006), *Culinary Herb*, NRC Research Press, p. 1036.
8. Dimov I. (2014), *Investigation of thechnological and sorbtional characteristics of flour-bread mixtures for bread production*, University of Food technology, Plovdiv.
9. Toplov V., Gavrailov M., Yankulov J. B. (1983), *Bilki and Bilkosybirane*, Hristo Danov Publishing Hause, Plovdiv.
10. Krasteva A., Baeva M., Gogova T., Durakova A., Bozadjiev B. (2011), Flour mixex with Herb Additives, *Food Science, Techniques and Technology, University of Food Technology*, 2, pp. 11–16.
11. Krishna Kumar I. M., Maliakel B. P. (2008), Fenugreek dietary fibre a novel class of functional food ingredient, *AgroFood industry hi-tech,* 19(2), pp. 18–21.
12. Wojdyło A., Oszmianski J., Czemerys R. (2007), Antioxidant activity and phenolic compounds in 32 selected herbs, *Food Chemistry,* 105, pp. 940–949.
13. Zheng W., Wang S.Y. (2001), Antioxidant Activity and Phenolic Compounds in Selected Herbs, *J. Agric. Food Chem.,* 49, pp. 5165–5170.
14. Anwar D.A., Hifnawy M.S., Kandeel A.M., Abdallah M.M.F. (2009), Nutritional and health-related constituents of fenugreek, sunflower and mustard sprouts as a functional food, *Annals of Agricultural Science*, 54(1), pp. 175–189.
15. Madar Z., Shomer I. (1990), Polysaccharide composition of a gel fraction derived from fenugreek and its effect on starch digestion and bile acid absorption in rats, *J.Agric. Food Chem.*, 38, pp. 1535–1539.

16. Muchuweti M., Kativu E., Mupure C., Chidewe C., Ndhlala A., Benhura M. (2007), Phenolic composition and antioxidant properties of some spices, *American journal of food technology,* 2(5), pp. 414–420.
17. Shan B., Yizhong C., Sun M., Corke H. (2005), Antioxydant capacity of 26 spice extract and characterization of their phenolic constituents, *J. Agric. FoodChem*, 53(20), pp. 7749–7759.
18. Petkova N., Ivanov I., Mihaylova D., Krastanov A. (2017), Phenolic acids content and antioxidant capacity of commercially available Melissa officinalis L. teas, *Bulgarian Chemical Communications,* 49(D), pp. 69–74.
19. Campanella L., Bonanni A., Favero G., Tomassetti M. (2003), Determination of antioxidant properties of aromatic herbs, olives and fresh fruit using an enzymatic sensor, *Anal. Bioanal.Chem*., 375, pp. 1011–1016.
20. Patora, J., Klimek B. (2002), Flavonoids from lemon balm (Melissa officinalis L., Lamiaceae), *Acta Poloniac Pllarmacculica-Drug Research,* 59(2), pp. 139–143.
21. Tóth, J., Mrlianová M. (2003), Rosmarinic acid–an important phenolic active compound of lemon balm (Melissa officinalis L.), *Acta Facult. Pharm. Univ. Comenianae,* 50, pp. 139–146.
22. Petkova N., Topuzova M., Todorova M., Ivanov I., Denev P., Polyphenolic content and antioxidant activity of eleven different aromatic plants used in bulgarian culinary, *Industrial Technologies,* V(1), pp. 40–47.
23. Ando M., Hitokoto S., Arafune Y. (1996), Effects of dough expansion rate beforenfreezing on roughness of bread crust, *Journal of the Japsanese Society for Food Science and Technology*, 43(7), pp. 812–820.
24. Brown, J. E. (1990), The Science of Human Nutrition, *HBJ Inc., NY.*
25. Kassaian N., Azadbakht L., Forghani B., Amini M. (2009), Effect of fenugreek seeds on blood glucose and lipid profiles in type 2 diabetic patients, *Int J Vitam Nutr Res.,* 79(1), pp. 34–39.
26. Naidu M.M., Shyamala B.N., Naik J.P., Sulochanamma G., Srinivas P. (2011), Chemical composition and antioxidant activity of the husk and endosperme of fenugreek seeds, *LWT Food Science and Technology*, 44(2), pp. 451–456.
27. Gogova T., Baeva M. (2012), *Aliments et boissons spéciales (fonctionnels) à la base des céréales, Gide des travaux pratiques*, Edition académique de UTA, Plovdiv.
28. Dimov I., A. Durakova, A. Krasteva (2015), Development of technology for the production of herbal bread based on a type of wheat flour, Scientific papers, XXIV *International Scientific Conference "Management and Quality"*, Yambol, Bulgaria, pp. 87–95.
29. Stintzing FC., Herbach, KM. Mosshammer, MR., Carle R., Yi W., Sellappan S., Acoh CC., Bunch R., Felker P. (2005), Color, betalain pattern, and antioxidant properties of cactus pear (Opuntiaspp.) clones, *Journal of Agricultural and Food Chemistry,* 53, pp. 442–451.
30. Ivanov I., Vrancheva R., Marchev A., Petkova N., Aneva I., Denev P., Georgiev V., Pavlov A. (2014), Antioxidant activities and phenolic compounds in Bulgarian Fumaria species, *International Journal of Current Microbiology and Applied Sciences,* 3(2), pp. 296–306.
31. Benzie F., Strain J. (1996), Ferric reducing ability of plasma (FRAP) as a measure of „antioxidant power": The FRAP assay, *Anal. Biochem,* 239, pp. 70–76.
32. Nakov G., Brandolini A., Ivanova N., Dimov I., Stamatovska V. (2018), The effect of einkorn (Triticum monococcum L.) whole meal flour addition on physico-chemical

characteristics, biological active compounds and in vitro starch digestion of cookies, *Journal of Cereal Science*, 83: 116–122.
33. Noda Y., Kaneyuka T., Mori A., Packer L. (2002), Antioxidant activities of pomegranate fruit extract and its anthocyanidins: delphinidin, cyanidin, and pelargonidin. *J Agric Food Chem.*, 50, pp. 166–171, DOI: 10.1021/jf0108765.
34. Żmijewski M., Sokół-Łętowska A., Pejcz E., Orzeł D. (2015), Antioxidant activity of rye bread enriched with milled buckwheat groats fractions, *Rocz Panstw Zakl Hi*, 66(2), pp. 115–121.
35. Dziki D., Rozy1o R., Gawlik-Dziki U., Swieca M. (2014), Current trends in the enhancement of antioxidant activity of wheat bread by the addition of plant materials rich in phenolic compounds, *Trends in Food Science & Technology* 40, pp. 48–61.
36. Han, H.-M., & Koh, B.-K. (2011), Antioxidant activity of hard wheat flour, dough and bread prepared using various processes with the addition of different phenolic acids, *Journal of the Science of Food and Agriculture*, 91, 604e608.
37. Prior, R. L.,Wu X., Schaich K. (2005), Standardized methods for the determination of antioxidant capacity and phenolics in foods and dietary supplements, *J. Agric. Food Chem.*, 53, pp. 4290–4303.
38. Chlopicka J., Pasko P., Gorinstein Sh., Jedryas A., Zagrodzki P. (2012), Total phenolic and total flavonoid content, antioxidant activity and sensory evaluation of pseudocereal breads, *LWT - Food Sci. Technol,* 46, pp. 548–555.
39. Holtekjølen A.K., Baevre A.B., Rødbotten M., Berg H., Knutsen, S. H. (2008), Antioxidant properties and sensory profiles of breads containing barley flour, *Food Chem*., 110, pp. 414–421.
40. Seidel, Ch., Boehm, V., Vogelsang, H., Wagner, A., Persin, Ch., Glei, M., et al. (2007), Influence of prebiotics and antioxidants in bread on the immune system, antioxidative status and antioxidative capacity in male smokers and non-smokers, *British Journal of Nutrition*, 97, pp. 349–356.

Investigating of artificial neural network potential to predict the properties of refined raw sugar beet juice by electrocoagulation process

Maliheh Zarifpoor, Vahid Hakimzadeh

Department of Food Science and technology, Quchan Branch, Islamic Azad University, Quchan, Iran

Keywords:

Sugar beet
Refine
Electrocoagulation
Neural network
Levenberg
Correlation

Article history:

Received 01.05.2018
Received in revised form 20.07.2018
Accepted 27.12.2018

Corresponding author:

Vahid Hakimzadeh
E-mail: v.hakimzadeh@yahoo.com

DOI:
10.24263/2304-974X-2018-7-4-12

Abstract

Introduction. In this study, based on the high potential of electrocoagulation in the removal of suspended matter and also due to high energy consumption in traditional treatment, the potential of EC was modeled by artificial neural network on purification of raw beet syrup.

Material and Methods. The potential of neural network in prediction of turbidity, color and purity of raw beet juice was investigated with different parameters as voltage (5, 10 and 15 volts) pH (6, 7 and 8) and time (regular time intervals from 1 to 60 min) during electrocoagulation process. ANN modeling was carried out by Neurosolution software v6 to determine the best type of transport function, learning rule, and determination of applied percentages for training, validation and testing stages based on their mean square errors, mean square normalized errors, mean absolute errors and correlation coefficients.

Results and discussion. The best neural network with maximum correlation coefficient for turbidity and purity obtained in Levenberg learning law and tangent transfer function which included 8 and 17 neurons respectively. Also, the best correlation coefficient and the less mean square error for color modeling related to a network with one hidden layer and 9 neurons that learned under levenberge learning law and sigmoid transfer function. Modeling was carried out with different percentages of data for training, validation and testing that the best prediction correlation for turbidity and purity obtained when 55% of the data were used for training, 40% of them were employed for validation and 5% of the data were used for testing, whereas the best percentage of learning, validation and testing for color prediction were 60, 30 and 10, respectively. The predicted values of models had suitable correlation with experimental data, so that correlation coefficient with experimental data of turbidity, color and purity were 0.999, 0.997 and 0.990, respectively. This study also addressed the model sensitivity to input data. The most model sensitivity of the model for prediction of turbidity, color and purity was related to voltage.

Conclusion. The model was able to predict the turbidity, color and purity of the syrup under various operating conditions, as the modeling data showed a high correlation with the experimental data.

Introduction

In electrocoagulation process, suspended particles, emulsions or dissolved pollutants in an aqueous medium are destabilized by electrical current. Electrocoagulation process is used to purify a wide range of water and wastewater systems, remove minerals, pollutants and pathogens (Emamjomeh, 2009). The principle of electrocoagulation process is oxidation of anodes and the production of Fe^{+2} and Al^{+3} ions. In the process, metal ions are combined with electrolysis of hydroxyl ions around the cathode and produce metal hydroxides which cause the volatility of the pollutants and the creation of suspended particles or so-called Flock. The formed flocks can be floated on the liquid surface based on density differences or with the help of hydrogen bubbles generated in the cathode, or removed by settling (Chaturvedi, 2013). In general, the mechanism of removal of impurities in the EC process involves coagulation, surface absorption, settling and floating that occurred by the following reactions on the electrodes as follows:

The reactions around anode: $Al = Al^{3+} + 3e^-$

The reaction around cathode: $3H_2O + 3e^- = 3/2H_2 + 3OH^-$

Create Aluminum flocks: $Al^{3+} + 3OH^- = Al(OH)_3$

The produced ions as Al^{3+} and OH^- during the above reactions are formed in the monomers such as $Al(OH)^{2+}$, $Al(OH)^{2+}$, $Al_2(OH)_2^{4+}$ and $Al(OH)^{4-}$ or polymers such as $Al_6(OH)_{15}^{3+}$, $Al_7(OH)_{17}^{4+}$, $Al_8(OH)_{20}^{4+}$, $Al_{13}O_4(OH)_{24}^{7+}$ and $Al_{13}(OH)_{34}^{5+}$, which eventually converted to $Al(OH)_3$ and precipitated (Kobya, 2003). Because of the insolubility of iron or aluminum hydroxides in water, the low price and availability of these two metals compared to other metals with similar properties, these are used as electrodes in the EC process (Parga, 2005). In addition, can be mentioned to the other benefits of this method such as the use of simple equipment, low initial investment and operating cost, without the need of chemicals, low sludge production, larger flocks production, stable and acid resistant flocks, faster filtration, removal of small colloidal particles and less need for repair and maintenance (Chen, 2004; Myousuf, 2001; Malakootian, 2009).

One of the studies that have been done in this area is the investigation of Shivayogimat et al (2013) who used electrocoagulation process to refine sugar industry wastewater. The results of these researchers showed that the EC process using by iron electrodes could be used as an economical process to replace the traditional process of sugar refinery wastewater treatment. Zoe et al. also used the electrocoagulation method to recover the beneficial compounds from the sewage treatment of egg processing units. The results of this study showed that electrocoagulation can be used successfully for the treatment of egg wastewater and recycle valuable compounds such as high protein digestible protein and fat. Furthermore, Bazrafshan et al. concluded that electrocoagulation is a suitable method for the removal of BOD, COD and other contaminants for the treatment of dairy wastewater. Azizi et al (2016) during purification of raw sugar beet juice using by EC process reached to better value of turbidity and purity in refined juice, but they associated the slightly increasing in color to the floatation. On the other hand, modeling can play an important role in predicting system performance, determination the impact of operational variables and design processes. Neural networks are capable of modeling nonlinear and complex systems with a large number of input and output data (Delgerange, 1998). The artificial neural network system is inspired by the brain and the neural network system of the human and the same of human brain is composed of a large number of neurons that like the human brain have ability to learning. In cases where there is a large amount of input and output information for a system and we want to provide a model for that system or when we want to obtain a structure from the available information, the use of artificial neural networks can be useful. So far, for neural networks,

various applications have been introduced with a wide range of topics (Menhaj, 2000). Therefore, researchers have shown special interest in modeling of separation processes in various industries. For example, Maskioula et al. due to membrane fouling in the ultrafiltration process in emulsion solutions introduced an experimental model for predicting the cake layer created with suitable correlation coefficient with experimental data. In 2011, Shahidi and colleagues examined the potential of nanofiltration treatment in sugar beet pulp press water, and then modeling this process with a neural network.

Therefore, in this study, based on the high efficiency of electrocoagulation in the removal of suspended matter and also due to reduce environmental problems and high energy consumption in traditional treatment of sugar beet syrup, the potential of this process was modeled on purification of raw beet syrup by artificial neural network to predict the refining properties of raw sugar beet juice that will process at another operational parameter.

Materials and methods

EC process

The data of this study were empirically and on a laboratory scale from a batch pilot. Raw sugar beet juice was produced from Chenaran sugar factory. The electrocoagulation pilot was consisted of a 5-liter reservoir. Also three electrodes made of aluminum as anode and three electrodes of iron as a cathode with a distance of 0.05 m and with a side area of 0.01875 m2 for each electrode and single-pole mode connected to an electrical power supplied (figure1). Independent variables were considered as inputs of the neural network at three levels of voltage (5, 10 and 15 volts), three pH levels (6, 7 and 8) and six equal time intervals of 1 to 60 minutes. Turbidity, color and purity of syrup were tested as dependent variables or network outputs (Azizi, 2017).

Assays

Color measurement

Measurement of syrup color after reading its absorbance at 420 nm was calculated by the UNICO 2100 model spectrophotometer and according to the ICUMSA standard on the basis of equation 1(ICUMSA, GS 9/1/2/3-8, 2011).

$$\text{Color (ICUMSA)} = 10^5 \, A/(L \times RDS \times \rho) \quad (1)$$

where A is absorption, L is the length of cell, RDS is the refractometer dry solids and ρ is density.

Turbidity

Syrup turbidity with turbidometer model AL450T-IR based on NTU unit was directly obtained.

Purity

In order to calculate the purity, after obtaining pol (sucrose percentage) with Saccharometer (Model, NIR W2) and its Brix with NAR-1T model refractometer based on equation 2 (ICUMSA, GS 1/2/3/9-1, 2011).

$$\text{Purity} = \frac{Pol}{Brix} \times 100 \quad (2)$$

Artificial neural network modeling

The modeling based on neural network was carried out using the Nerosolution software version 6. In order to evaluate different networks, data were randomly divided into three parts, so that different percentage of data for training, validation and testing of network were selected. During the training process, artificial neural networks were learnt with the data until the best of relationship between neurons in each training cycle are found so that the predicted values approach the desired output values and the error values obtained at the least. To find a suitable architecture, the Mean Error Square (MSE), Mean Absolute Error (MAE) and Correlation Coefficient (R^2) were considered (Razavi, 2003). First, the total of the data (54) was completely randomized, and then the network structure with a hidden layer and the number of different neurons was studied under the Lavenberg and Momentum learning law and the two tangent and sigmoid transfer functions. Also, the best percentage of data was determined for training, validation and testing of this network. Finally, the sensitivity of changes in purity, hardness and percentage of non-sugar compounds rejection as well as temperature, time and pressure were evaluated. For estimating the model, the correlation coefficient between predicted and experimental data was also calculated (Shahidi, 2012).

Results and discussion

To find the best configuration of the artificial neural network, different networks with the number of neurons 2 to 20 were designed, according to tables 1 to 3, the mean squares of errors, the mean square of the normalized error, the mean absolute error, and the correlation coefficient of each neuron separately in the learning laws mentioned with various functions was studied. In the following, the best percentage of data used for network training, validation and testing with the least error and the highest correlation coefficient was investigated. As shown in Table 1, the best neural network for turbidity variations was obtained based on the lowest error and the highest correlation coefficient with a hidden layer in the Levenberg learning law and with the tangent transfer function in Neuron 8.

Also for color variations, the network with the number of neurons 9 under the Levenberg learning law and the tangent transfer function showed the highest correlation coefficient and the lowest error (Table 2).

According to Table 3, the best artificial neural network structure was developed for purity of refined syrup changes in the number of neurons 17 and the Levenberge learning law and the Tangent transfer function.

Table 4 compares the best structure of artificial neural network based on the highest correlation coefficient and the lowest error under the two laws of learning Levenberg and Momentom, as well as the tangent and sigmoid transfer functions for the changes in the turbidity, color and purity of raw syrup treated by electrocoagulation.

Hakimzadeh et al. (2017) obtained the best result to predict the properties of permeate flow as refined syrup at range of 2-20 neuron under levenberg and momentum learning law during modeling of microfiltration process of raw sugar beet juice by neural network.

Table 1

Different architectures of ANN with different neurons number under the Levenberg learning law and two transfer functions to predict the turbidity of refined raw sugar beet juice by EC process

Turbidity	Levenberg							
No of neurons	Sigmoid				Tangent			
	MSE	NMSE	MAE	R	MSE	NMSE	MAE	R
2	3.386	0.634	1.578	0.628	1.267	0.237	0.951	0.948
3	3.467	0.649	1.546	0.615	1.039	0.194	0.811	0.945
4	0.310	0.058	0.462	0.947	0.965	0.181	0.829	0.965
5	4.230	0.793	1.216	0.727	0.867	0.162	0.766	0.940
6	1.733	0.324	0.894	0.830	1.727	0.323	1.080	0.854
7	0.144	0.027	0.275	0.987	0.820	0.153	0.807	0.935
8	3.596	0.674	1.709	0.924	**0.177**	**0.033**	**0.327**	**0.989**
9	0.231	0.043	0.395	0.981	0.297	0.055	0.418	0.977
10	1.485	0.278	0.847	0.858	1.362	0.255	0.964	0.929
11	2.458	0.460	1.381	0.895	1.895	0.355	1.128	0.922
12	1.135	0.212	0.825	0.947	0.649	0.121	0.639	0.946
13	0.892	0.167	0.861	0.957	0.836	0.156	0.719	0.956
14	4.828	0.905	1.736	0.917	1.065	0.199	0.771	0.959
15	0.486	0.091	0.480	0.962	0.491	0.092	0.592	0.966
16	3.598	0.647	1.606	0.784	0.188	0.035	0.326	0.982
17	0.207	0.038	0.353	0.984	0.274	0.051	0.405	0.974
18	0.945	0.177	0.779	0.949	0.261	0.049	0.434	0.986
19	5.590	1.047	1.928	0.336	0.444	0.083	0.547	0.978
20	5.545	1.039	2.054	0.787	4.760	0.892	1.543	0.654

Table 2

Different architectures of ANN with different neurons number under the Levenberg learning law and two transfer functions to predict the color of raw sugar beet juice by EC process

Color	Levenberg							
No of neurons	Sigmoid				Tanh			
	MSE	NMSE	MAE	R	MSE	NMSE	MAE	R
2	386701.6	0.642	600.833	0.641	539031.71	0.896	671.55	0.414
3	481401.7	0.800	677.616	0.518	837038.36	1.391	798.94	0.247
4	1529648.7	2.543	1034.30	0.489	494674.09	0.822	646.51	0.588
5	728191.02	1.210	640.182	0.568	439126.5	0.730	560.42	0.565
6	293851.45	0.488	416.781	0.786	792885.19	1.318	754.42	0.723
7	103790.12	0.172	184.883	0.935	941667.79	1.565	684.78	0.637
8	1170664.6	1.946	901.680	0.636	159732.29	0.265	299.67	0.914
9	**68162.75**	**0.113**	**198.121**	**0.946**	142774.3	0.237	288.32	0.888
10	1051676.8	1.748	873.264	0.483	318157.8	0.529	492.41	0.716
11	1476475.8	2.454	1028.44	0.503	525539.87	0.873	607.50	0.504
12	772007.309	1.283	721.465	0.674	400089.82	0.665	444.60	0.817
13	374009.843	0.621	526.942	0.898	675619.29	1.123	691.05	0.778
14	711061.9	1.182	736.124	0.526	737711.02	1.226	800.39	0.411
15	412772.328	0.686	499.186	0.762	468735.99	0.779	584.80	0.700
16	1206713.9	2.006	861.404	0.458	**116272.43**	**0.193**	**210.91**	**0.929**
17	111442.18	0.185	241.737	0.937	137922.04	0.229	275.75	0.911
18	1018876.13	1.694	840.285	0.695	394542.395	0.656	509.35	0.800
19	971547.29	1.615	882.676	0.831	197761.07	0.328	355.38	0.904
20	1195237.1	1.987	925.999	0.593	1141003.26	1.897	882.00	0.521

Table 3

Different architectures of ANN with different neurons number under the Levenberg learning law and two transfer functions to predict the purity of refined raw sugar beet juice by EC process

Purity	Levenberg							
No of neurons	Sigmoid				Tanh			
	MSE	NMSE	MAE	r	MSE	NMSE	MAE	R
2	0.038	0.203	0.141	0.893	0.070	0.377	0.212	0.813
3	0.069	0.370	0.224	0.802	0.083	0.448	0.235	0.791
4	0.095	0.511	0.243	0.753	0.073	0.390	0.221	0.858
5	0.227	1.216	0.312	0.540	0.076	0.408	0.233	0.777
6	0.131	0.701	0.313	0.765	0.144	0.772	0.328	0.690
7	0.049	0.263	0.163	0.879	0.330	1.764	0.454	0.427
8	0.216	1.157	0.382	0.364	0.090	0.484	0.231	0.796
9	**0.044**	**0.236**	**0.148**	**0.900**	0.038	0.207	0.145	0.902
10	0.145	0.774	0.276	0.658	0.136	0.726	0.297	0.670
11	0.162	0.868	0.302	0.616	0.039	0.208	0.151	0.895
12	0.090	0.485	0.214	0.832	0.111	0.594	0.248	0.780
13	0.056	0.300	0.168	0.856	0.049	0.263	0.164	0.923
14	0.120	0.640	0.288	0.643	0.136	0.727	0.298	0.827
15	0.096	0.515	0.263	0.724	0.073	0.389	0.240	0.855
16	0.411	2.193	0.526	0.633	0.068	0.366	0.168	0.845
17	0.069	0.370	0.224	0.861	**0.030**	**0.164**	**0.130**	**0.930**
18	0.068	0.367	0.217	0.841	0.126	0.673	0.256	0.737
19	0.159	0.853	0.342	0.843	0.063	0.338	0.173	0.877
20	0.147	0.787	0.309	0.525	0.350	1.867	0.491	0.586

Table 4

Comparison of two learning rules used for selection of the best ANN architectures to predict the Turbidity, Color and Purity in refined raw sugar beet juice by EC process

Parameter	Levenberg					
	Number of neuron	Transfer function	MSE	NMSE	MAE	r
Turbidity	8	Tangent	0.177	0.033	0.327	0.986
Color	9	sigmoid	68162.750	0.113	198.121	0.946
Purity	17	Tangent	0.030	0.164	0.130	0.930
	Momentum					
Turbidity	18	Tangent	0.701	0.131	0.682	0.983
Color	7	sigmoid	693058.41	1.152	635.673	0.668
Purity	5	Tangent	0.068	0.367	0.219	0.830

Determination of training, validation and testing percentage

Also, in ANN modeling of the turbidity, color and purity of refined syrup by electrocoagulation process different percentages of data for training, evaluation and testing was investigated. To this end, firstly, the most suitable data for training was selected according to the best correlation coefficient. Then, based on the best training percentage, the best percentages of data for validation and testing were also determinate (Tables 5 to 7).

Table5

Best percentages of data used for training, validation and testing of selected ANN architectures to model the turbidity of refined raw sugar beet juice by EC process

Training Data (%)	Validation Data (%)	Testing Data (%)	MSE	NMSE	MAE	R
55	5	40	0.362	0.063	0.507	0.978
55	10	35	0.548	0.104	0.514	0.949
55	15	30	0.276	0.048	0.460	0.981
55	20	25	0.320	0.062	0.458	0.974
55	25	20	1.450	0.252	0.835	0.890
55	30	15	0.092	0.017	0.236	0.997
55	35	10	0.023	0.006	0.137	0.998
55	**40**	**5**	**0.017**	**0.004**	**0.109**	**0.999**

Table6

Best percentages of data used for training, validation and testing of selected ANN architectures to model the color of refined raw sugar beet juice by EC process

Training Data (%)	Validation Data (%)	Testing Data (%)	MSE	NMSE	MAE	R
60	5	35	501238.39	0.556	502.473	0.775
60	10	30	38912.695	0.047	149.673	0.982
60	15	25	20725.932	0.027	120.483	0.988
60	20	20	32706.608	0.065	139.694	0.975
60	25	15	60699.965	0.124	210.322	0.962
60	**30**	**10**	**84462.280**	**0.154**	**216.560**	**0.998**
60	35	5	56360.277	0.105	170.445	0.993

Table7

Best percentages of data used for training, validation and testing of selected ANN architectures to model the purity of refined raw sugar beet juice by EC process

Training Data (%)	Validation Data (%)	Testing Data (%)	MSE	NMSE	MAE	R
55	5	45	0.062	0.309	0.198	0.873
55	10	35	0.008	0.036	0.075	0.983
55	15	30	0.015	0.068	0.095	0.974
55	20	25	0.044	0.197	0.155	0.907
55	25	20	0.036	0.182	0.168	0.924
55	30	15	0.021	0.121	0.131	0.942
55	35	10	0.014	0.053	0.116	0.992
55	**40**	**5**	**0.024**	**0.209**	**0.141**	**0.994**

Usually an effectiveness model to predict the reliable data need sufficient data for good learning that has to be over 50 percent of whole data. In other world when learning a model to get done right, the predicted values will be valuable (Jaganathan, 2017)

Investigating of neural network potential to predict data

Figure 1 shows the correlation graph of laboratory values with predicted values by the model. Accordingly, models obtained from artificial neural network to predict turbidity, color and purity were able to correlate with appropriate coefficients of 0.998, 0.996 and 0.990, respectively.

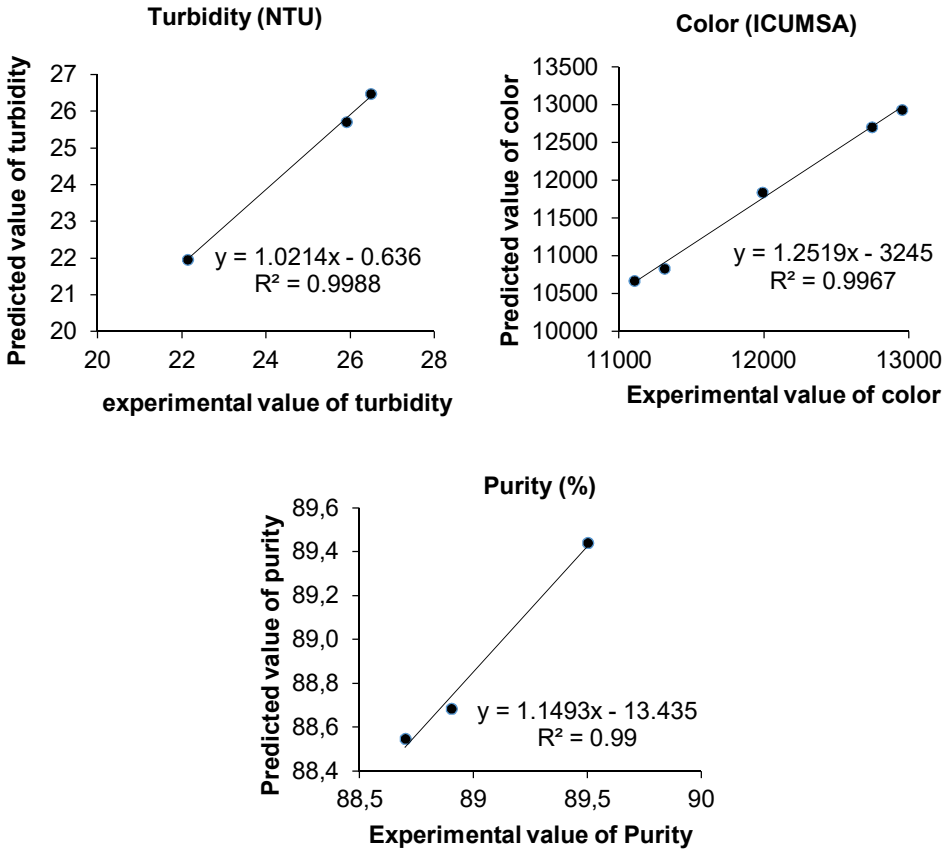

Figure 1. Correlation between experimental data and predicted values

Determine the sensitivity of the model to the input data

In this study, the susceptibility of the models to the operational variables, i.e., input data, was evaluated. According to Figure 2, the most sensitivity of model was to predict the turbidity, color and purity of the refined syrup with voltage electrocoagulation.

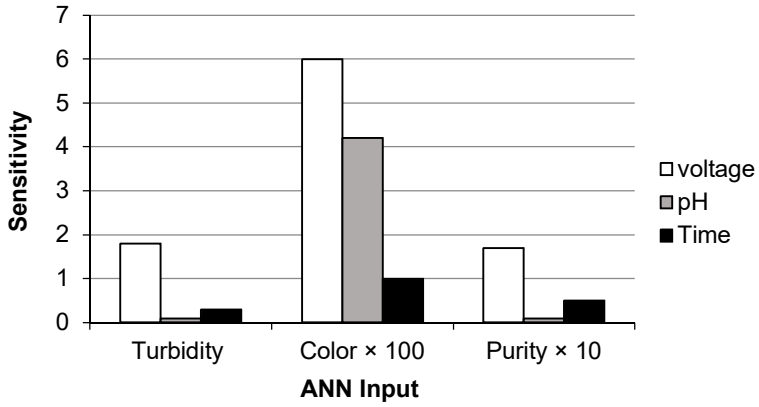

Figure 2. Models' sensitivity to prediction of turbidity, color and purity

Model's sensitivity to prediction of turbidity, color and purity due to voltage is so obvious. Because increasing of the voltage led to accelerate of anode and cathode reaction and consequently formation of flock (Ghanbari, 2013; Chaturvedi, 2013). So, with more flock forming, more impurities are absorbed on flocks and the turbidity, color and purity are improved. Shahidi et al (2011) reported the temperature as the best sensitive parameter to flux prediction during modeling of nanofiltration of sugar beet press water by artificial neural network. In membrane process increasing of temperature expand the pores diameter of membrane and the permeate flux is increased.

Conclusion

The results of electrocoagulation process modeling in purification of raw sugar beet syrup showed that the best learning law for network training to predict the Turbidity, color and purity was Levenberg law. So that the best transfer function for network design with the best prediction of the turbidity and purity value was the tangent and for prediction of color was sigmoid. The best percentage of data for learning, validation and testing of the model was obtained by predicting the turbidity and purity of the refined syrup by electrocoagulation, respectively, 55, 40 and 5, while for color 60, 30 and 10% were determined. In general, the model was able to predict the turbidity, color and purity of the syrup under various operating conditions, as the modeling data showed a high correlation with the experimental data (Table 8)

Table 8

Summarized result of modeling of turbidity, color and purity changes in purification of raw beet juice by EC process

Dependent variable	Hidden layer	Number of neuron	Transfer function	Learning rule	Percentage of learning/ validation/test	Correlation coefficient
Turbidity	1	8	Tangent	Levenberge	55/40/5	**1**
Color	1	9	Sigmoid	Levenberge	60/30/10	**1**
Purity	1	17	Tangent	Levenberge	55/40/5	**1**

References

1. Azizi H., Hakimzadeh V., Golestani H. (2016), Purification of Raw Sugar Beet Juice by Electrocoagulation, *Ukrainian Food Journal*, 5(4), pp. 667–677.
2. Bazrafshan E., Moein H., Kordmostafapour F., Nakhaie S. (2013), Application of Electrocoagulation Process for Dairy Wastewater Treatment, *Journal of Chmistry*, 64013, pp. 1–8
3. Chaturvedi S.I. (2013), Electrocoagulation: A Novel Wastewater Treatment Method, *I. J. Modern Engineering Research*, 3, 93–100.
4. Chen G. 2004), Electrochemical technologies in wastewater treatment, *Separation Purification Technology*, 38, pp. 11–41.
5. Delgrange N., Cabassud C., Cabassud M., Durand-Bourlier L., Lain J.M. (1998), Neural network for prediction of ultrafiltration transmembrane pressure application to drink water, *Journal of Membrane Science*, 150, pp. 111–123.
6. Emamjomeh M., Sivakumar M. (2009), Review of pollutants removed by electrocoagulation and electrocoagulation/flotation processes, *Journal of Environmental Management*, 90, 1663–1679.
7. Ghanbari F., Mazaheri A., Mehdipoor F., Mir Shafian S., Moradi M., Sharifi Maleksari H. (2013), Investigation of the effect of the electrocoagulation on the removal of colour from coloured sewage by using aluminium/iron and aluminium/copper electrodes, *Journal of Sabzevar University of Medical Sciences*, 20(5), pp. 716–725.
8. Jaganathan A., Kumar S.M. (2017), Artificial Neural Network Analysis in Food Science, *International Research Journal of Engineering and Technology*, 4(1), pp. 746–751.
9. Kobya M., Can O.T., Bayramoglu M. (2003), Treatment of textile wastewaters by electrocoagulation using iron and aluminum electrodes, *J. Hazardous Material*, 100, pp. 163–178.
10. Malakootian M., Yousefi N. (2009), The Efficiency of EC Process Using Aluminum Electrodes in Removal of Hardness from water, *Iran. J. Environ. Health. Sci. Eng*., 6(2), pp. 131–136.
11. Menhaj M.B. (2000), Fundamental of neural networks, *Computational illteligence*, 1.
12. Myousuf A.M., Schennach R., Parga J.R., Cocke, D.L. (2001), Electrocoagulation (EC) Science and applications, *Hazardous Materials*, 84, pp. 29–41.
13. Parga J.R., Cocke D.L., Valenzuela J.L., Gomes J.A., Kesmez M., Irwin G., Moreno H., Weir M. (2005), Arsenic removal via Electrocoagulation from heavy metal contaminated groundwater in La Comarca Lagunera Mexico, *Journal of Hazardous Material*, 124(1–3), pp. 247–5.
14. Razavi S.M.A., Mousavi S.M., Mortazavi S.A. (2003), Dynamic prediction of milk ultrafiltration performance: a neural network approach, *Chem. Eng. Sci*., 58, pp. 4185–4195.
15. Shahidi Noghabi M., Razavi S.M.A, Mousavi S.M. (2012), Prediction of permeate flux and ionic compounds rejection of sugar beet press water nanofiltration using artificial neural networks, *Desalination and Water Treatment*, 44, 1-3, pp. 83–91.
16. Shivayogimath C.B., Jahagirdar R. (2013), Treatment of Sugar Industry Wastewater Using Electrocoagulation Technique, *International Journal of Research in Engineering and Technology*, pp. 262–265.
17. Xu L.J., Sheldon B.W., Larick D.K., Carawan R.E. (2002), Recovery and Utilization of Useful By-products from Egg Processing Wastewater by Electrocoagulation, *Poultry science*, 81(6), pp. 785–792.

Development of methods of production in natural aromatic production

Natalia Frolova, Anatoly Ukrayinets

National University of Food Technologies, Kyiv, Ukraine

Keywords:

Aromatic
Essential
Oils
Natural
Chromatography

Article history:

Received
02.07.2018
Received in revised
form 21.09.2018
Accepted
27.12.2018

Corresponding author:

Natalia Frolova
E-mail:
frolovan809@
gmail.com

DOI:
10.24263/2304-
974X-2018-7-4-13

Abstract

Introduction. The analytical and experimental researches on methods of natural aroma sources separation with obtaining individual flavoring substances were conducted. Advantages of fractional distillation and preparative chromatography were demonstrated.

Materials and methods. The essential oils of Moldavian dragonhead and lemon, the model matrix (a blender of terpene hydrocarbons and their oxigen-containing derivants of both known and unknown composition) were studied. The methodologies of gas chromatographic analysis were used. The separate fractions of aimed aromatic components were obtained using preparative chromatography.

Results and discussion. The vacuum separation of essential oils into fractions under the set control regimes of temperature of the still and knob,°C, respectively on the levels: the first fraction – 67–69, 18–24; the second fraction – 112–118, 25–30; the third fraction – 130–135, 32–39; pressure value, kPa for fractions: the first – 0,92, the second – 0,62, the third – 0,33; reflux ratio for fractions: the first – 7:1, the second – 10:1, the third – 5:1 allows obtain fractions of different aroma, that significantly widens assortment of natural sources of aroma. Besides, with fractional distillation deterpenization is conducted; using it out of an essential oil the components, that discernibly worsen organoleptic properties, are separated. The deterpenization regime of lemon essential oil – temperature of the still and knob,°C, respectively 67–70, 17–19; pressure –2,64 kPa, reflux ratio – 1:3.

In order to extract essential oils preparative chromatography with development of the special column was used; a solid carrier Chromosomorb A and a stationary phase PEG-6000 were selected. The terms of preparative separation on a column filled with with a stationary phase,

In order to extract essential oils fractions in the individual mode by the method od of preparative chromatography, a special column with a number of plates 600 was developed, which makes it possible to simulate the fractionation process on the razor column of a rectification unit. During the research, a solid carrier,

The effective regimes of the process were established experimentally: the carrier gas flow rate, sm^3/min – 85–90;sample value – 0,8–1,0 $см^3$, temperature value,ºC: evaporator – 180–250, column thermostat – 120–200, detector – 220–250, fraction collector – 180–250.

Conclusion. The vacuum fractioning of essential oils allows obtaining separate fractions of different aroma. Further preparative separation of fractions provides obtaining individual flavoring substances of pure composition.

Introduction

In nature individual substances are found mainly in mixtures. The effectiveness of the separation of complex mixtures is important, both in industrial production and in scientific research of a preparative and analytical nature.

The separation process (operation) allows to receive from an original mixture of components several fractions of components with a new quantitative composition, and often, and other qualitative characteristics. Within certain tasks separation of the mixture leads to a receipt of individual components in their pure form.

Analysis of recent researchs and publications

By the nature of the process used, the operations of crystallization, freezing, forerunning, evaporation, distillation, rectification, relate to physical methods based on phase transitions over temperature changes. Difference in mass, concentration, abundance, viscosity, size, shape, polarity, charge and what is more way of conduct in fields and environments of different nature are also used.

These are processes of extraction, filtration, gel filtration, sedimentation, centrifugation, flotation, screening, electro dialysis. To this category may be attributed separation in liquids of different polarity, density, magnetic separation and others.

Usually, a difference in aggregate state allows separation mixtures into fractions. Enrichment of a fraction with a target component happens on differences in concentrations and temperatures, electrical charges or electrolytic dissociation constants (electrophoresis) with zone refining, different chemical methods [1].

However, majority of classical methods are ineffective for the production of natural or synthetic substances in pure form necessary for manufacture of numerous health and medical products. Also, research and test of the healing or therapeutic effect of complex mixtures of biologically active substances, in particular hydrocarbons, biopolymers, nucleotides, proteins, peptides, antibiotics, etc. may be conducted only after the mixture is separated into fractions and the target substances are isolated in their pure form and identified by known methods of chemistry of pure substances.

The methods of separation that are commonly used to produce biologically active substances are supercritical CO^2-extraction, usage of microwaves, isolation of natural products by ion-exchange methods, preparative chromatography. A combination of different methods is often used [2].

In the analysis published by Mc Clements [3], it is stated that in methods for the processing of aromatic sources described in 234 randomly selected works 78% primarily use forerunning. In other cases there is extraction. At the same time, in many cases, extraction is only a preliminary stage after which forerunning is used.

A rectification under high and medium vacuum [4], selective adsorption [5], fractional extraction and condensation [6], ultrasonic treatment, microwaves treatment [7], turbohydrolysis distillation [8], steam and water distillation [9] are also common. The effectiveness of the method of separation, its selectivity increases with the use of multi-stage processes, such as chromatography. This is due to the high efficiency of the selection of selective sorbents to separating components of the mixture.

A chromatographic separation of a complex mixture happens as a result of uneven distribution of components of the mixture between the stationary and moving phases, which is due to different affinity of separate components to these phases or different ability to diffuse in these phases. Chromatographic methods are classified according to the principles

underlying the separation processes. In adsorption chromatography a different adsorption capacity of even very close by structure substances is used. With the creation and physic and chemical study of new selective adsorbents, sensitive to the structural or electronic characteristics of the substances analyzed relevant task [10].

In the group of terpenes and terpenoids which are part of the essential oils there are a lot of unstable position isomers and optical isomers. Gas chromatography is most often used for their separation and research. The separation in liquid chromatography is based on different solubility of components in two mixed liquids. Specific biochemical interactions allow selectively separate substances in affinity chromatography [4].

Mixture separation by method of chromodislation [11] happens at the expense of multiple processes of condensation/evaporation of substances on the surface of an inert sorbent inside the stuffing column (or on the surface of a capillary column without a stationary phase).

To increase the effectiveness of the process, a negative temperature gradient along the column (thermal chromodistilation) or injection before the mixture a substance into the column with volatility higher than the volatility of the lightest component of the mixture (restrictive chromodislation) may be used.

To the methods of obtaining the individual components of a complex mixture can be attributed high speed counter current chromatography. This is a versatile dividing method that does not require usage of a solid fixed phase.

Specific chromatographic methods include the following: ion exclusion, longevity of ions, electronic exchange or oxidation-reduction chromatography, ligand chromatography, solubilization chromatography etc [12] .

Nowadays, more and more companies are developing constituents of modern therapies (including products for gene therapy), based on data from macromolecules and their allocation and purification are becoming increasingly important. An e xcretion of such molecules involves usage of chromatographic methods ("biochromatography") [13].

Preparative chromatography is not inferior to the indicated methods and even surpasses them in obtaining individual substances of high purity. In this case, each of the separated substances after leaving the chromatographic system gets into a separate receiver [14].

In nutrition products the concentration of substances of interest to the study may be less than one billionth of a particle, and therefore only extremely small amounts of these substances are available for analysis even after their selection and concentration [15].

A performance of preparative chromatography when separating a mixture of substances that determine the taste and aroma is well known. In such cases when the difference in vapor pressure is small and, as a result, the separation ratios for distillation are small, preparative chromatography has significant advantages over distillation through the use of highly selective sorbents [16].

It is difficult to give preference to any of the abovementioned methods. It is necessary to take into account the nature of the complex mixture, the form of its existence in separate components, the complexity, accessibility and duration of the division, the ability to combine with other stages of the process.

Production of food flavors is one of the most dynamic fields of the world food industry. For today the volume of the flavors market in the EU varies from 6 to 7.8 billion euros, according to various estimates, and this figure will increase every year [17].

Today's food industry widely uses various flavors. The problem is that the existing food flavors production in the country is not able to meet the existing demand for such products. As a result, the average annual import of flavors in the market is estimated at more than 96%. Obviously, this can be explained by the lack of domestic innovation, the high cost of foreign

technology [18].

That is why the innovative activity in the field of production of domestic natural food aromatics, the development of new technologies, the search for little-known, non-traditional sources of natural flavor for food production, the formation of fundamentally new ideas for their effective processing are relevant.

There are two decisive criteria in choosing the method of processing natural sources of aromatic substances. Firstly, taking into account, that the loss of aromatic substances even in the smallest quantities leads to a change in product flavor. Secondly, it is the complete exclusion of chemical or enzymatic adverse reactions that may alter the component composition.

Materials and methods

Materials

The materials of research is commercial essential oils of cumin and lemon. The model matrix (a blender of terpene hydrocarbons and their oxigen-containing derivants of both known and unknown composition) under boiling temperature was divided into separate factions of flavoring components.

Distillation of essential oils

Essential oils were divided into separate fractions by the target components with distillation , which were identified as the most valuable carriers of the aroma for a given nutritional basis.

Gas chromatographic studies of component composition of fractions and aromatic components

Each stage of the separation of the essential oils was accompanied by gas chromatographic studies of component composition of fractions and aromatic components with usage of an analytical column with a medium polar immobile phase dinonylphthalate.

The following devices were used for the research: chromatic mass spectrometer “HP 5890 Series II (Hewlett-Packard, USA), infrared spectrophotometer UR-20, Germany, spectrophotometer “Specord UV VIS”, Germany, spectrophotometers SF-10, SF -46.

Metrological assessment of gas chromatographic measurements was carried out with the assistance of the hardware and software complex "Chromoprocessor-5"

Preparative separation of essential oils

Preparative separation of essential oils at boiling temperature was held under such conditions: the injector temperature – 200 °C, the thermostat columns temperature – 70–200 °C, the detector temperature – 200 °C, carrier gas flow rate – 80–100 cm^3/min, sample volume– 0,8–1,0 ml, potentiometer chart bar speed – 10 or 20 cm/min, detector-catharometer. The factions were picked into an absorber, the original design of which allowed to achieve the maximum degree of enrichment of key components.

Production preparative column

To get fractions of essential oils in the individual mode of preparative distillation, were developed the basics of separate column with the number of theoretical plates – 400; solid

carrier - chromosorb A (producer "Johns Manville" (USA) and stationary phase - PMS-100 of "Реахим" production were chosen. The following process conditions are set: the injector temperature – 200 °C, the thermostat columns temperature – 70–200 °C, the detector temperature – 200 °C, carrier gas flow rate – 1,0 cm^3/min, hydrogen – 33 cm^3/min, air – 330 cm^3/min, sample volume – 0,5–0,8 mcl.

Statistical analysis

Data were expressed as means±standard deviations for triplicate determination. Differences were considered to be significant at validity of α=0.95.

Results and discussion

Vacuum separation of essential oils for getting fractions of different flavors

In our country, a number of types of spicy-aromatic raw materials is not wide enough. For the expansion of the aromatic palette it is proposed to recycle directly essential oils, complex mixtures of components with their own aroma.

The peculiarity of the classical essential oil production is that fresh essential oil may not be immediately used, because it does not meet the standard quality. It takes time and additional operations on which the oil becomes marketable. This increases the material costs.

A viable alternative to the processing of essential oils of different quality is controlled dispersion into fractions. Since this is a physical process, the resulting fractions are natural flavors. Also, the components of fast flavor modification are removed on purpose.

According to the classical laws of forerunning, when the complex mixture is heated to a boil, the components whose elasticity of steam is higher than the others, will first of all go into the steam phase. Fractional forerunning is essentially the opposite of forerunning.

In fractional forerunning, the processes of evaporation and condensation are repeated many times, and the distillate becomes the starting material for the next process every time. As a result, even low-boiling components condense [9].

As a result of fractional forerunning, a number of separated one from another fractions, boiling in the narrow temperature limits, is formed [19]. Difficulties of fractional forerunning of aromatic substances natural sources are primarily associated with a number of component composition, with a wide range of individual boiling temperatures (T_{boil}), an ability of components to chemical modification [20].

According to the classical theories, to the main controlling modes of fractional forerunning are attributed: an operating temperature and pressure [21], in particular absolute pressure from 1 to 100 mm Hg on Torr (0,13–13,33 kPa) and T_{boil} from 0 to 120˚C. When determining the operating parameters of temperature and pressure of forerunning there comes a dilemma. Typically, the pressure is chosen such that the temperature of the forerunning ensures an effective condensation of distillate vapors with the most available refrigerants, such as water or air. Taking into account the average temperature of flowing cooling water about 20 ºC, the condensation temperature of the components should not exceed 45–50 ºC. Also it is necessary to highlight the decomposition, at high forerunning temperatures, of essential oils components with the formation of connections of uncontrolled aroma.

At the same time, there are some difficulties concerning lowering the pressure of the process. First of all, tangible fluctuations of temperature within the limits of 10–15 ºC at the beginning of forerunning, decrease of general speed of mass transfer and, accordingly, increase of distillation duration are felt. At the same time, the hardware design becomes more

complicated with a need to use a powerful vacuum system [22]. Also, fractional forerunning is expedient to carry out in cases of close to T_{boil} essential oils components. The difference in T_{boil} of these components in a vacuum can be much greater than at atmospheric pressure. According to [23], a significant amount of substances that boil at atmospheric pressure at a temperature of 250 °C and above with decomposition are dispersed without changing the composition at a pressure of 1.33 kPa (10 mm Hg) and a temperature of 160–210 °C, or within the temperature range from 100 to 130 °C at a pressure of 0.00133 kPa (0.01 mm), or at temperatures from 40 to 60 °C in vacuum.

Data on the dependence of the effective parameters of fractional forerunning is limited. The table 1 lists the technological map of cumin essential oil dispersal

Table 1

Technological map of cumin essential oil dispersal

Fraction	Temperature, °C		Pressure, kPa	Reflux ratio	Content, % mass
	still	port			
Warmup of the column	50–65	-	2,64	∞	-
The first	67–69	18–24	0,92	7:1	4,5±0,1
The second	112–118	25–30	0,62	10:1	40,2±1,2
The third	130–135	32–39	0,33	5:1	19,7±1,2
Distillation residue	-	-	0,33	-	32,8±2,0
				Losses:	2,8±0,5

Fixation of losses at the level of 2.8±0.5% is due to incomplete capture of the low boiling components, loss of "clogging" the column.

Studies have shown that the vacuum separation of essential oils allows getting fractions of different flavors, which greatly extends the range of natural sources of aroma. Such technological technique does not destroy natural structural bonds of components of essential oils, preserves their naturalness and biological ability, being characteristic for natural plant raw materials.

Modes of lemon essential oil deterpenization

Under established regimes, a fractional dispersion is carried out with a deterpenization during which components, which are easily oxidized into uncontrolled compounds and significantly degrade the organoleptic properties are removed from the essential oil (Table 2).

Table 2

Working modes of lemon essential oil deterpenization

Stages of deterpenization	Temperature, °C		Pressure, kPa	Reflux ratio	Content, % mass
	still	port			
Column warmup	50–65	14–15	2,64	∞	-
Terpene fraction	67–70	17–19	2,64	1 : 3	30,0–32,0
Oxygenated fraction	84–96	30–36	0,66–0,33	1 : 14	60,0–62,0
Distillation residue	115–127	-	0,33	-	4,55±0,5
				Losses	2,0–6,0

A confirmation of the effectiveness of the essential oils separation method was made by the sensory evaluation of the obtained fractions as independent natural flavors:

- Flavor «Resinous coolness». Flavor composition: fraction 1 cumin dragonhead essential oil. Appearance: liquid. Aroma: coniferous, with a note of mint.
- Flavor «Citrus». Flavor composition: fraction 2 cumin essential oil. Appearance: liquid. Aroma: harmonious, resembles the smell of citrus.
- Flavor «Faded rose». Flavor composition: fraction 3 cumin essential oil. Appearance: liquid. Aroma: tender, of dried rose leaves.

Use of preparative chromatography for the allocation of individual aromatic substances

Obviously, in various industries, including food industry, there is a shortage of individual aromatic substances of "pure composition". "Purity" is usually considered by a degree of minimization of the amount of admixture. For usage of synthetic intermediates purity is 85-95% is believed to be enough. A level of admixtures in natural products can be considered sufficient when the concentrations reach 50-75%. The standard substances for analysis require a purity of 99% and more [24].

The use of preparative chromatography (PG) for the allocation of individual aromatic substances is motivated by the fact that the preparative selection, due to the versatility of selective fixed phase selection, significantly exceeds periodic rectification, and the specific productivity of the preparative collection of pure substances P_m is fixed within 2 ... 6 g/year, which correlates with the performance of rectification. Herewith, obtaining "pure" individual substances ($\eta = 90 ... 98\%$) is provided with significantly lower operating expenses. In order to extract essential oils fractions in the individual mode by the method od of preparative chromatography, a special column with a number of plates 600 was developed, which makes it possible to simulate the fractionation process on the razor column of a rectification unit. During the research, a solid carrier, a stationary phase, and special devices of a preparative chromatograph have been selected [25].

An effective conductor for preparative column was developed with gradient application of motionless phase PEG6000 on separate sections of solid support (SS, Hromosorb A). So, the first portion of PEG6000in amount of 25% has to be applied on the first solid support section, the second portion in amount of 20% on the second solid support section. The third solid support section is recommended to be divided into two parts. On the first solid support part PEG6000 was applied in amount of 17% and on the second part in amount of 15%. Such a sequence of application of the motionless phase on the solid support provides high selectivity of PG column and reduction of separation duration [26]. The terms of preparative separation on a column, established experimentally and are listed in Table 3

Table 3

Terms of preparative excretion and concentration of individual aromatic substances of essential oils

Indicator		**Indicator values**
Carrier gas flow rate, sm^3/min		85–90
Sample value		0,8–1,0 ml
Temprature, °C	Evaporator	180–250
	Column thermostat	120–200
	Fraction collector	180–250
	Dewar flask	(–20)– (–15)
	Detector	220–250

In researches a special trapper of individual substances, the construction of which allowed reaching the maximum degree of enrichment of the received fractions was used.

In Table 4 the value of the degree of coincidence of mass-spectras of individual substances excretioned from essential oils and their library analogues are listed.

Table 4

Degree of coincidence (% purity) mass-spectras of individual substances with the library analogues

Individual substances	% composition purity	Individual substances	% composition purity
l- linalool	96,0±0,2	Linalyl acetate	94,0±0,2
α – pinene	98,0±0,1	β-phellandrene	94,0±0,2
β – myrcene	98,0± 0,1	α-phellandrene	98,0±0,1
n– cymene	96,0±0,2	α - terpineol	99,0
d- limonene	99,0	d- carvone	99,0
Convergence of values is not less 0,95%.			

The conducted identification confirmed receipt of the expected individual substances from essential oils to 98±0.15% of the composition purity.

In Table 5 the results of sensory analysis of essential oils individual substances are listed.

Table 5

Individual substances organoleptic indexes

Individual substances	Taste	Aroma
β-myrcene	Bitterish	Resinous- citrus
Cineol	Refreshing	Citrus
l- linalool	Bitterish	Lavender with a wood tone
n- cymene	Pungent	Peppermint note
l-,α-phellandrene	Pungent	Terpene
l-,β-phellandrene	Moderately bitterish	Mint with a citrus note
d- limonene	Moderately bitterish	Earthy lemon
d- linalyl acetate		Bergamot note
d-,α- terpineol	Herbaceous	Reminds lilac
l-α- pinene	Spicy	Needle
d- carvone	Pungent	Dill note
l- cariofilen	Pungent	Wood

Received individual substances of pure composition have value as test-standards in diverse researches, including pharmacokinetic and metabolic researches of impact of natural sources of aroma on human body's organs and systems.

Individual substances organoleptic indexes are the information base for technologists in the development of formulations of flavored products of various industries, while creating compositions of aromas of stable characteristics.

Conclusion

In the development of methods of separation in the production of natural flavors, it is proposed and scientifically substantiated the treatment of essential oils by dispersal to narrow fractions of different flavors and further preparative allocation of individual substances of pure composition. The efficiency of new solutions in the manufacture of a stationary phase preparative column PEG6000 is shown in portions on the section of the solid carrier chromosorb A. The column with the number of theoretical plates 600 allows to simulate the fractionation process on the hopper column of the distillation unit.

Received individual substances of pure composition have value as test-standards in diverse researches, including pharmacokinetic and metabolic researches of impact of natural sources of aroma on human body's organs and systems.

References

1. Sarker S. D., Latif Z., & Gray A. I. (Eds.), (2006), *Natural products isolation* (Vol. 20), Springer Science & Business Media.
2. Rybkin V.V. (2010), *Analytical chemistry and physico–chemical methods of analysis*, IGHTU, Ivanovo.
3. McClements D. J. (2015), *Food emulsions: principles, practices, and techniques*, CRC Press.
4. Diosady L.X.L. (2003), Fats and Oils from Plant Materials, In: *Extraction Optimization in Food Engineering,* CRC Press.
5. Arce A., Marchiaro A., Rodríguez O., Soto A. (2006), Essential oil terpenless by extraction using organic solvents or ionic liquids, *AIChE journal*, *52*(6), pp. 2089–2097.
6. Komthong P., Katoh T., Igura N., Shimoda M., Hayakawa I. (2006), Ascending bubble extraction of terpenes from freshly squeezed orange juice, *Food research international*, 39(1), pp. 53–58.
7. Sahraoui N., Vian M. A., El Maataoui M., Boutekedjiret C., Chemat F. (2011), Valorization of citrus by-products using Microwave Steam Distillation (MSD), *Innovative food science & emerging technologies*, 12(2), pp. 163–170.
8. Herguijuela J., Pietzonka W., Wildermann A., Wolf T. (2014), *U.S. Patent No. 8,747,621*, Patent and Trademark Office, Washington.
9. Stichlmair J.G. (2010), Distillation or Rectification, *Chemical Engineering and Chemical Process Technology–Volume II: Unit Operations–Fluids and Solids*, 68.
10. Dolgonosov A.M. (2015), Polarity and hydrophilicity – principal independent characteristics of chromatographic stationary phases, *Sorption and chromatographic processes*, 15(3), pp. 316–320
11. Adams R. P., Sparkman O. D. (2007), Review of Identification of Essential Oil Components by Gas Chromatography/Mass Spectrometry, *J Am Soc Mass Spectrom*, 18, pp. 803–806.
12. Chamberlain J. (2018), The Analysis of Drugs in Biological Fluids 2nd Edition, CRC press.
13. Zhou J., Sun C., Meng L., Ye W., Luo P., Sun F., Xu X. (2017), A new PPARγ/DNA origami biochromatography and offline high performance liquid chromatography–mass spectrometry method for screening PPARγ receptor antagonists from ginsenosides, *Archives of biochemistry and biophysics*, 629, pp. 63–69.

14. Fare D.L., Adamovics J.A. (2017), High-Performance Liquid Chromatography, In: *Chromatographic Analysis of Pharmaceuticals, Second Edition,* Routledge, pp. 135–208.
15. Aklakur M., Asharf Rather M., Kumar N. (2016), Nanodelivery: an emerging avenue for nutraceuticals and drug delivery, *Critical reviews in food science and nutrition*, 56(14), pp. 2352–2361.
16. Chopel N.V., Usenko V.O., Frolova N.E., Silka I.M., Naumenko K.A. (2013), *Method for separating essential oils and their narrow fractions into pure aromatic components by preparative gas chromatography, Patent for invention No. 102171.*
17. Silva V. L., Sereno A. M., do Amaral Sobral P. J. (2018), Food industry and processing technology: on time to harmonize technology and social drivers, *Food Engineering Reviews*, pp. 1–13.
18. Ukrainian market of perfume and cosmetic products, Available at: http://apcu.ua/rinkovidoslidzhennya-ta-statistichni-dani/parfumerno-kosmetichnijrinok-ukraini.htm
19. Meirelles A.J., Batista E.A., Scanavini H.F., Batista F.R., Ceriani R., Lima Jr L.F.L. (2008), Distillation applied to the processing of spirits and aromas, *Extracting bioactive compounds: Theory and applications*, pp. 75–136.
20. Frolova N. E., Frolova N. E. (2017), *Theoretical substantiation and development of technologies of natural concentrated flavors from ethereal raw materials.*
21. Feoktistov, D.V. (2013), Experimental investigations of the efficiency of the process of distillation of binary substances, *Industrial power engineering*, 10, pp. 35–39.
22. Wiles S. (1989), *Phase equilibrium in chemical technology.*
23. Gryta M., Waszak M. (2016), Application of vacuum membrane distillation for concentration of organic solutions, *Chemical Papers*, *70*(6), 737–746.
24. Bogatyuk N.P., Danilova I.L., Pekhova O.A., Timasheva L.A. (2014), A new method of preparing vegetable raw materials for the production of essential oils, *Universum*, 9(9).
25. Frolova N.E., Usatyuk O.M. (2014), New possibilities for the processing of essential oils for the flavoring of food products, *East European Journal of Advanced Technology*, 2(12), pp. 24–29.
26. Frolova N.E., Ukrayinets A.I., Sylka I.M. (2016), Using preparative chromatography for excretion of monofactions out of complex mixtures of natural origin, *Technological audit and production reserves*, 2(4), pp. 21–26.

Mechanism of fat-binding and fat-contenting of the nanoparticles of a food supplement on the basis of double oxide of two- and trivalent iron

Iryna Tsykhanovska[1], Victoria Evlash[2], Oleksandr Oleksandrov[1], Tetiana Gontar[1]

1 – Ukrainian Engineering-Pedagogics Academy, Kharkiv, Ukraine
2 – Kharkiv State University of Food Technology and Trade, Kharkiv, Ukraine

Keywords:

Fat-binding
Fat-contenting
Iron oxide
Food
Supplement

Article history:

Received 20.04.2018
Received in revised form 28.09.2018
Accepted 27.12.2018

Corresponding author:

Iryna Tsykhanovska
E-mail: cikhanovskaja@gmail.com

DOI:
10.24263/2304-974X-2018-7-4-14

Abstract

Introduction. The mechanism of fattening and fat content of nanoparticles of a food additive on the basis of double oxide of two- and trivalent iron, which is represented by the model "Two-layer coordination", is substantiated.

Materials and methods. Nanoparticles of a dietary supplement based on bicarbonate and trivalent iron oxide, coated with linoleic acid and unrefined sunflower oil. Fat-retaining ability was investigated using IR-Fourier (FTIR) and energy-dispersive X-ray (EDX) spectroscopy, as well as scanning electron microscopy (TEM).

Results and discussion. The mechanism of fattening and fat content of nanoparticles of a food additive on the basis of double oxide of two- and trivalent iron, which is represented by the model "Two-layer coordination" is studied. The first adsorption layer is formed due to electrostatic interactions of polarized groups of lipids and ionized nanoparticles of a food additive and coordination bonds of Fe atoms, nanoparticles of a food additive with oxygenates of the COO^- group of the "hydrophilic head" of the lipid; the second adsorption layer – due to electrostatic interactions of hydrophobic centers of the first adsorption layer and hydrocarbon "tails" of lipids.

The appearance of two new bands in IR spectra at: ~1541 cm^{-1} and ~1637 cm^{-1} subsolids bidentate adsorption and the formation of a carboxylate group (–COO–) in the "lipid-nanoparticle of a food additive" composition.

Microscopic studies have established the order of the average particle size: for pure food additives – <d> 78±2,36 nm; for the particles of the supplemented linoleic acid – <d> 80±2,57 nm; for the sunflower oil-added additives – <d> 81±2,93 nm.

Energizersispersion X-ray studies have established the elemental composition of "lipid-nanoparticles of food additives": for particles of pure food additive – Fe 75,5%; O 24, 5%; for particles of the additive covered with linoleic acid – Fe 45,6%; O 34,7%; C 19,7; for particles of an additive covered with sunflower oil – Fe 39,7%; O 36,7%; C 23,6%.

Conclusions. The "Two-layer coordination" model was proposed for the first time to substantiate the mechanism of fattening and fat content of a nutritional supplement by nanoparticles on the basis of double-oxide and trivalent iron oxide.

Introduction

One of the important functional and technological properties of food raw materials and food ingredients which determine the course of the technological processes and the quality of the finished product is fat-containing ability (FCA). Knowledge of the binding mechanisms and the fat content of raw materials will allow rational use of new types of food raw materials and food additives and predict the raw ingredients behavior in food systems (test and confectionery masses, minced meat, etc.) in the process of processing and storage of finished products.

Recently for FRA improving of the food systems the various nanopowders and food additives have been used, in particular, silver, iron oxides, titanium dioxide and silicon dioxide [1–6]. It is known to use nanopowder metal oxides in innovative animal products: zinc oxide, titanium dioxide and silicon dioxide [1]; as a food additive of complex action, (Fe_3O_4) magnetite nanoparticles have been proposed [2]; nanopowders, magnetic nanoparticles of silver, silicon dioxide [3] magnetic nanoparticles of metals and metal oxides are also used in lipid, carbohydrate and protein compositions [4]; magnetite nanoparticles modifications with oleic acid [5] are used to create functional emulsions and oxide nanoparticles modifications and iron hydroxide with higher fatty acids and fats are used for aqueous suspensions [6]. The good FRA of nanopowder ingredients is associated with the high dispersion which allows not only to bind free fats, but also to keep them on the nanoparticles surface during cooking, as well as to the good availability of numerous hydrophobic sites [1–5].

In the scientific works [3–5] a single – layer adsorption model (chemisorption) of fatty acids on the metal oxide nanoparticles surface is proposed.

A model of two-layer adsorption is also considered: the first monolayer occurs on the nanoparticle surface due to the fatty acids chemisorption and makes the particles superhydrophobic; the second – due to the interaction of hydrophobic sections of the first layer with alky substituents of fatty acids [6]. However, these assumptions are controversial and require the additional experimental confirmation.

The literature analysis [1–6] showed that there is the insufficient data on the mechanism substantiation of nanopowder of food additives, in particular, Fe_3O_4 nanoparticles in the food systems. Fe_3O_4 nanopowder is the main component of the food supplement "Magnetofood" which is a scientific development of the authors of this work. Nanopowder based on iron oxides Fe_3O_4 ("Magnetofood") has the great potential and carries the new functional and technological properties (emulsifying, water-binding, water-holding, fat-binding, fat-retaining) and the advanced technological applications [2, 7, 8]. The nanoparticles interaction of Fe_3O_4 food additive ("Magnetofood") with the food systems biopolymers (proteins, proteids, carbohydrates, lipids) is a complex of complex chemical reactions. The supramolecular organization of Fe_3O_4 nanoparticles ("Magnetofood") and the of the organic matrix structure play an important role. The result is the formation of spatial nanostructures that significantly affect the functional and technological properties of raw materials and semi-finished products (confectionery and dough masses, meat stuffing systems, etc.) [7, 8].

Therefore, the work on the creation of the new functional and technological properties of food systems with the help of nanopowder of the food additives of the complex action are relevant. In this case, it is important to understand the mechanisms of fattening and fat binding and fat-containing.

To explain the mechanism of fat-containing ability (FCA) of nanoparticles (NPs) of the food additive on the basis of Fe_3O_4 iron oxides ("Magnetofood") it is necessary to determine

and understand the nature and strength of the interaction of Fe_3O_4 nanoparticles with triglycerides and higher fatty acids.

The research aim is to study the mechanism of fat binding and fat-containing with nanoparticles of a dietary supplement based on the double oxide of ferric and ferric iron.

To achieve the goal, the following tasks were set:

- to study by the IR-spectroscopy method of the of adsorption interaction mechanism of lipid molecules (in particular, linoleic acid and sunflower oil) with nanoparticles of a dietary supplement based on the double oxide of ferric and ferric iron
- to investigate by the method of transmission electron microscopy (TEM) the particle size and morphology of the experimental samples of a food additive based on the double oxide of ferrous and ferric iron pure and coated with linoleic acid and sunflower oil;
- to install energy dispersive X-ray spectroscopy (EDX) of the elemental composition of the experimental samples of a food additive based on the double oxide of two and trivalent iron pure and coated with linoleic acid and sunflower oil.

Materials and methods

Materials

Object of research: the mechanism of fat-containing ability of the powder ingredients of food raw materials, in particular nanoparticles of the food supplements based on iron oxides "Magnetofood".

Subjects of research:

- **Sample 1** – a food additive based on iron oxides ("**Magnetofood**") is a highly dispersed nanopowder of the brown or black color with a particle size ~ 80 nm. According to the chemical composition of "Magnetofood" is the double ferrous oxide ($FeO{\cdot}Fe_2O_3$ or Fe_3O_4), obtained by the method of chemical co-precipitation from aqueous solutions of two- and trivalent ferrous salts in alkaline medium [8];
- **Sample 2** – linoleic acid [company "CL Reachim" Ukraine], the storage period is 5 days before using;
- **Sample 3** – unrefined sunflower oil ["Vinnytskaia industrial company ViOil", Ukraine]. The storage period is 5 days before using;
- **Sample 4** – the food supplements nanoparticles based on iron oxides ("Magnetofood") coated with linoleic acid. We obtained dispersion of 1 g of nanoparticles of the "Magnetofood" supplement (sample 1) and 0,2 g of linoleic acid in 10 ml of dimethylformamide for 12 hours at a temperature of (50±1) °C and blowing a nitrogen stream over the reaction mixture surface. After cooling the suspension to (20–25) °C the nanoparticles of the food supplement "Magnetofood", coated with linoleic acid were isolated by magnetic filtration and washed with an aqueous-ethanol mixture (1:1) 5–7 times. The final product was dried in vacuum at (60±1) °C for 24 hours, the storage period is 1 hour to use;
- **Sample 5** – the food supplements nanoparticles based on iron oxides ("Magnetofood") coated with unrefined sunflower oil. The experimental sample was obtained in the same way as sample 4 only particles of the "Magnetofood" food supplement were coated with unrefined sunflower oil. The storage period is 1 hour to use.

Research methods

IR-Fourier Spectroscopy *(FTIR)*

The vibrational spectra of the experimental samples were obtained by FTIR spectroscopy on the Tensor 37 Fourier spectrometer from Bruker (Germany), controlled by the OPUS software package with the standard graduated capabilities in the frequency range (4000–400) cm^{-1} in the absorption format (IR Fourier spectra of samples 1, 4, 5 were removed in the tablets KBr; samples 2, 3 – in the "liquid film").

Scanning electron microscopy (TEM)

The particle size determination and morphology in the experimental samples 1, 4 and 5 were performed by using a JSM-820 scanning electron microscope (JEOL) with the increasing possibility up to 150000 times. The obtained images in a planar geometry with the electron beam falling along the hexagonal axis and perpendicular to it were processed with the help of AutoCad 2014 and MathCad 2014 programs. Based on the obtained results, the particle distribution in the experimental samples 1, 4, 5 was calculated by diameter. The particles number in the sample to determine the average values was at least 500.

Energy dispersive X-ray spectroscopy (EDX)

To establish the elemental composition of the experimental samples 1, 4, 5, a scanning electron microscope JSM-820 (JEOL) with an EDX connector was used. X-ray spectra were obtained by the bombarding experimental samples with the electrons using an acceleration voltage of 20 kV (corresponding to the lines of the characteristic spectra of the Ferrum, Carbon and Oxygen). The installation of the elemental composition of the experimental samples 1, 4, 5 was carried out by the analysis of the received spectra of characteristic X-ray radiation.

Results and discussion

The mechanism of the fat-containing abilities (FCA) of the dietary supplement nanoparticles based on the double oxide of ferric and ferric iron ($FeO{\cdot}Fe_2O_3$ or Fe_3O_4) can be represented by the model of "two-layer coordination". Figure 1 shows the ionic interactions between the ionized nanoparticles of the food additive "Magnetofood" and the charged carboxyl group (COO^-) of higher fatty acids.

Figure 1 shows how probably the interactions of the carboxyl group of free fatty acids of fats and oils with ions of NPs Fe_3O_4 which are characterized by the high binding energy (~ 500–1000 kJ/mol), take place [5].

The ability of NPs of food supplement "Magnetofood" (Fe_3O_4) to enter electrostatic (Figure 1) and coordination (Figure 2–4) interactions with hydrophilic centers of free fatty acids and triglycerides determines their chemisorption on the reactive surface of ionized nanoparticles "Magnetofood" (Fe_3O_4). As a result, the first adsorption layer is formed on surface NPs of food supplement "Magnetofood" (Fe_3O_4). Taking into account the above and previous studies of the chemical interactions of nanoparticles of metal oxides and carboxylates of higher fatty acids the interaction between hydrophilic centers of triglycerides and fatty acids with NPs of food supplement "Magnetofood" (Fe_3O_4) can be represented by four types: monodentate, bridge (bidentate), chelating (bidentate) and ionic interaction [5]. The model of ionic interactions is considered in Figure1.

Figure 2 shows the formation mechanism of the monodentate complex of NPs of food supplement "Magnetofood" (Fe_3O_4) with fatty (linoleic) acid.

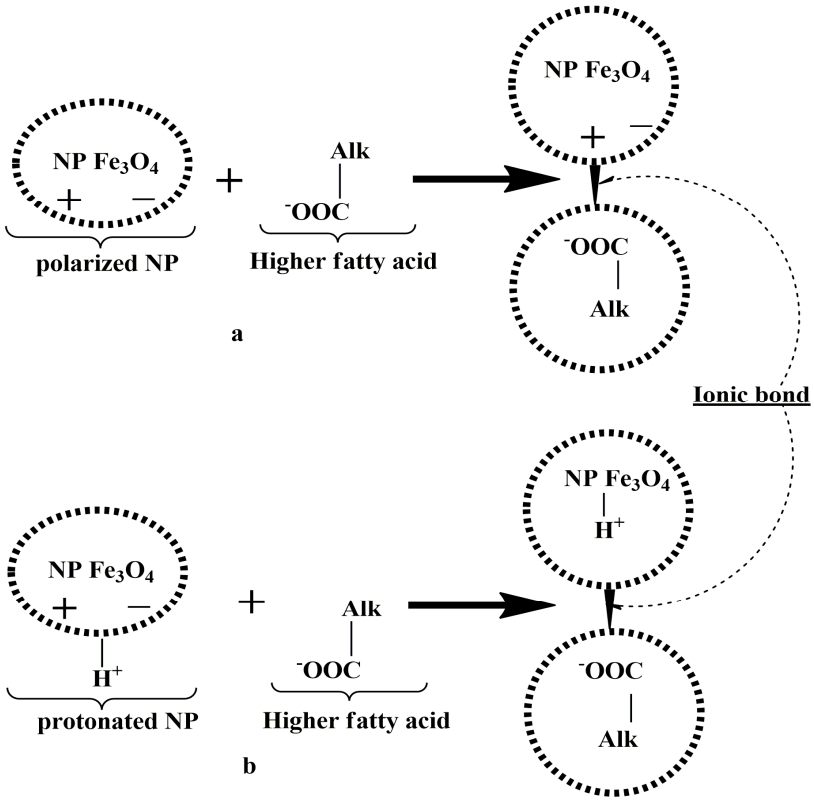

Figure 1. Ionic interactions between ionized nanoparticles of (Fe_3O_4) food supplement "Magnetofod" and COO^--a group of higher fatty acids: a – polarized NPs Fe_3O_4; b – protonated NPs Fe_3O_4

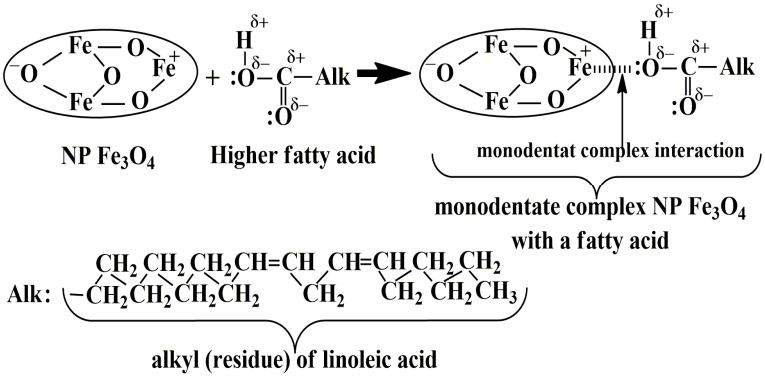

Figure 2. Formation of the monodentate complex of NPs of food supplement "Magnetofood" (Fe_3O_4) with linoleic acid

From Figure 2 it is evident that due to the complex interaction (electrostatic and coordination) one cation of the low-level iron of NPs of food supplement "Magnetofood" (Fe_3O_4) binds to one carboxylic oxygen atom of linoleic acid. As a result, a unidirectional electrostatic complex is formed.

Figure 3 shows the formation mechanism of a bidentate (chelating) NPs complex of food supplement "Magnetofood" (Fe_3O_4) with linoleic acid.

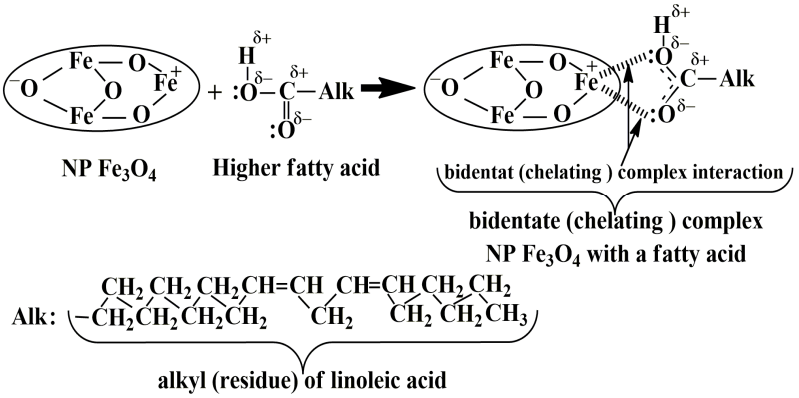

Figure 3. Shows the formation mechanism of a bidentate (chelating) NPs complex of food supplement "Magnetofood" (Fe_3O_4) with linoleic acid

This is a bidentate electrostatic complex in which one iron cation of a low-level fermentation NPs of food supplement "Magnetofood" (Fe_3O_4) binds to two oxygen atoms of the carboxyl group of linoleic acid due to the complex interaction (electrostatic and coordination).

Figure 4 shows the formation mechanism of bidentate (bridging) NPs complex of food supplement "Magnetofood" (Fe_3O_4) with linoleic acid. The interaction model shows that the formation of a bridge bidentate complex in which two iron cations of the low-level fermentation NPs of food supplement "Magnetofood" (Fe_3O_4) binds to two oxygen atoms of the carboxyl group of linoleic acid due to the complex interaction (electrostatic and coordination).

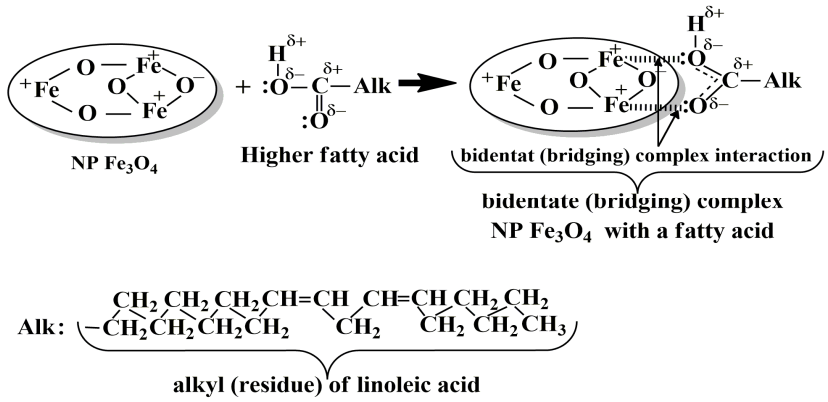

Figure 4. Formation of the bidentate (bridging**) complex of NPs of food supplement "Magnetofood" (Fe_3O_4) with linoleic acid**

As a result of the electrostatic and coordination interactions (Figures 1–4), the first adsorption layer on the NPs surface of food supplement "Magnetofood" (Fe_3O_4) which is hydrophobic due to alkyl hydrophobic residues ("tails") of fatty acids (in particular, linoleic acids) and triglycerides.

Next, a second adsorption layer is formed due to the electrostatic hydrophobic interaction. The hydrophobic matrix of the first adsorption layer enters an electrostatic hydrophobic interaction with hydrophobic aliphatic "tails" of fatty acids and triglycerides.

Figure 5 shows the formation mechanism of the lipid associate of NPs of food supplement "Magnetofood" (Fe_3O_4) due to hydrophobic interactions. From which it follows that the NPs Magnetofood food supplement (Fe_3O_4) form lipid associates with fats and higher fatty acids, in particular with linoleic acid.

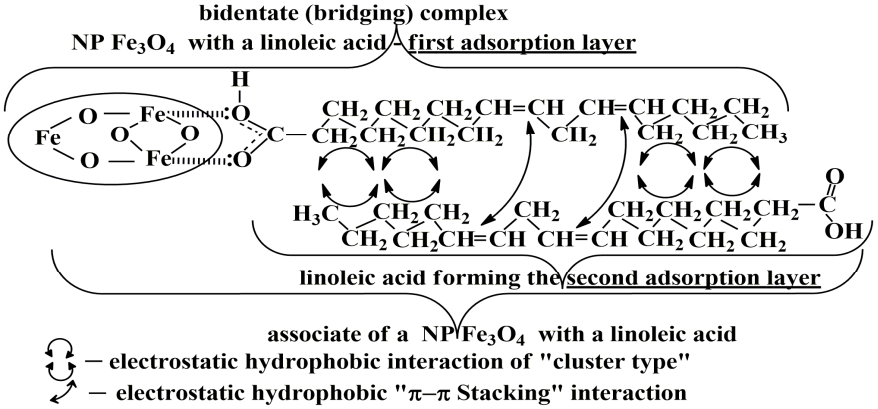

Figure 5. Formation of lipid associate of NPs of food supplement "Magnetofood" (Fe_3O_4) with linoleic acid

Consequently, the second adsorption layer is formed due to the manifestation of the dispersion forces in sufficiently extended molecules of higher fatty acids and triglycerides in which there is a possibility of multicenter dispersion interaction.

As a result, the alkyl matrix of lipids is structured according to the type of Van-der Waals complexes, forming the second layer and the associate of nanoparticles of food supplement "Magnetofood" (Fe_3O_4) with lipids.

Results of IR-Fourier Spectroscopy *(FTIR)*

To establish the adsorption interaction mechanism of the lipid molecules (in particular, linoleic acid and sunflower oil) with nanoparticles of food additive "Magnetofood" (Fe_3O_4) IR-spectroscopic studies of experimental samples 1–5 in the range 400–4000 cm^{-1} were conducted (Figure 6).

We can see in the spectrum of pure NPs of food additive "Magnetofood" Fe_3O_4. (the experimental sample 1) (Figure 6, ***a***) the absorption line of the Fe–O bond with a maximum at a value of ~ 532 cm^{-1}, is presented which agrees well with data from literary sources ~ 530 cm^{-1} [5, 9, 10].

The dislocation of the maximum of the corresponding absorption band of valence vibrations of the Fe–O bond in the experimental samples 4 and 5 (Figure 6 *d, e*) in the area ~ 584 cm^{-1} can be explained by the effect of the surface molecules of linoleic acid and sunflower oil with their interference in the near-surface a layer of nanoparticles of food

additive "Magnetofood" (Fe_3O_4) and the chemical interaction with iron cations (Figures 1–5).

In the study of compositions "lipid – NPs of food additive Fe_3O_4" the stretching frequency of the group C = O have the greatest significance. The unexcited state of these fluctuation corresponds to an absorption band of 1710 cm^{-1} (Figure 6, *b*). And in the sunflower oil in the area of 1744 cm^{-1} there is an intense peak of valence fluctuations C = O – bond (Figure 6, *c*). As you can see from Figure6, the adsorption of linoleic acid and sunflower oil on the NPs surface of "Magnetofood" food additive (Fe_3O_4) (Figure 6 *d, e*) shows the disappearance of this absorption band in the spectra of food additive (Fe_3O_4) the particles coated with the lipid. And also two new bands appear at 1543 cm^{-1} (Figure 10, *d*) and 1540 cm^{-1} (Figure 6, *e*) and 1638 cm^{-1} (Figure 6, *d*) and 1636 cm^{-1} (Figure 6, *e*) which are characterized by the valence asymmetric (ν_{as}) and valence symmetric (ν_s) of the carboxylate groups vibrations (COO^-). That is, the experimental data indicate that the lipid (carboxylic acids or triglycerides) of chemisorption on the nanoparticles surface of food additive Fe_3O_4 in carboxylate form (Figure 3, Figure 4 and Figure6, *d, e*) are using which the help of two Oxygen atoms. Which due to the electrostatic coordination interactions with Fe atoms are symmetrically coordinated with the surface of food additive Fe_3O_4 nanoparticles. The result is the formation of a monomolecular layer of a chemically adsorbed lipid (the first adsorption layer) on the nanoparticle surface of Fe_3O_4 (Figures 1–5) [11].

In the spectra of linoleic acid (Figure 6, *b*) and sunflower oil (Figure 6, *c*), the intense bands are observed with a maximum at 2926 cm^{-1}, 2856 cm^{-1} and 2924 cm^{-1}, 2854 cm^{-1} respectively. These peaks can be attributed to the asymmetric and symmetric (ν_{as} and ν_s) vibrations of the C–H bond in the CH_2 group. Also, the spectra (Figure 6, *b, c*) show the band of deformation (δ) vibrations $–CH_3$ groups about 1360 cm^{-1}, in linoleic acid, this band is very weak [9–11].

On the curves (Figure 6, ***d***) and (Figure 6, ***e***) there is a displacement of these absorption bands to a lower frequency – in the area: ν_{as} = 2904 cm^{-1}; ν_s = 2831 cm^{-1} and δ = 1350 cm^{-1}, respectively. This is due, *firstly*, to the fact that the hydrocarbon chains of linoleic acid and sunflower oil triglycerides in the monolayer (*the first adsorption layer*) surrounding the nanoparticles of food additive "Magnetofood" are under the influence of the near-surface layer of NPs of food additive "Magnetofood" Fe_3O_4 and the chemical interaction with ferrum cations; and *secondly*, due to the hydrophobic interaction of hydrophobic centers of the first adsorption layer with the hydrocarbon chains of linoleic acid and sunflower oil triglycerides due to the dispersion forces. And this contributes to the formation of *the second ad-absorption layer* on the surface of food additive Fe_3O_4 nanoparticles [12].

The unsaturated hydrocarbon chains which are a part of linoleic acid and sunflower oil triglycerides are manifested by the valence fluctuations of about 3008 cm^{-1} of the group –CH = CH– and a clear strip of deformation oscillations (δ) C–H of about 765 cm^{-1} (Figure 6 *b, c*). On the structured nanoparticles of food additive Fe_3O_4 (Figure 6 *d, e*), the displacement of these absorption bands is observed in the area: ν = 3000 cm^{-1} and δ = 752 cm^{-1}, respectively [11]. This is due, *firstly*, to the effect of NPs of food additive Fe_3O_4 on the hydrocarbon chains of linoleic acid and sunflower oil triglycerides in the formation of *the first adsorption layer*; and *secondly*, with the electrostatic interactions of the hydrophobic centers of the first adsorption layer with the alkyl matrix of triglycerides and the alkaline tail of the linoleic acid of the type "Van der Waals complexes". This contributes to the structuring of the "hydrophobic matrix" of the "NPs-lipid system of food additive Fe_3O" and the formation of the second adsorption layer on the surface nanoparticles of food additive Fe_3O_4 on which adsorbed lipids (linoleic acid or sunflower oil) have already been adsorbed in the first adsorption layer [13, 14].

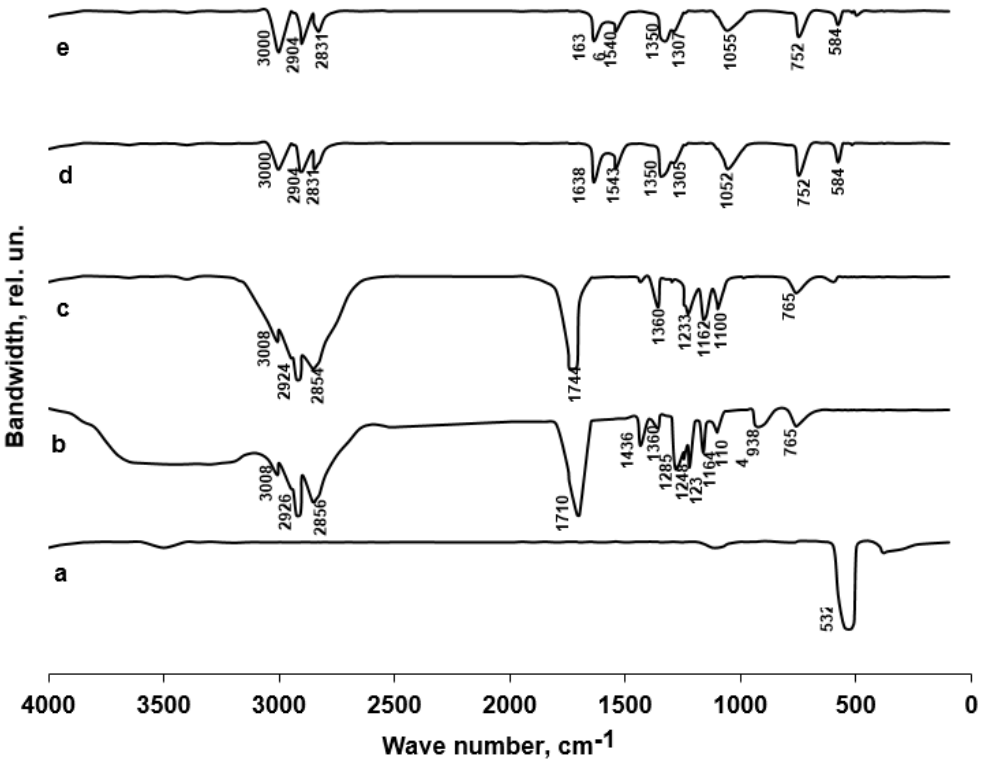

Figure 6. Fourier-IR spectra of the experimental samples of "lipid-NPs of food additive Fe_3O_4 compositions": *a* – finely-dispersed powder of food additive Fe_3O_4; *b* – linoleic acid; *c* – sunflower oil; *d* – nanoparticles of food additive Fe_3O_4 covered with linoleic acid; *e* – nanoparticles of food additive Fe_3O_4 covered with the sunflower oil

In the spectra of linoleic acid and sunflower oil (Figure 6, ***b, c***) three absorption bands are observed: a stronger band of about 1164 cm^{-1} (*b*) and 1162 cm^{-1} (*c*) and two less intensive bands of about 1236 cm^{-1} (*b*) and 1233 cm^{-1} (*c*) and 1104 cm^{-1} (*b*) and 1100 cm^{-1} (*c*). These are the valence fluctuations of the C–O group. Also, in the spectrum of linoleic acid (Figure 6, *b*), a double is noted: the first peak is at 1285 cm^{-1}, the second one is at 1248 cm^{-1}. The first arises as a result of the combination of plane deformation (δ_p) oscillations of O–H and C–O bonds. The second of the peaks refers to the symmetric valence (ν_s) oscillations of the C–O. Asymmetric valence (ν_{as}) oscillations of the C–O bond of the carboxyl group of linoleic acid appeared on the doublet on the peak form at 1436 cm^{-1} [9–11].

In the spectra (Figure 6, *d, e*) there are no such bands. And two new ones are appearing: at 1052 cm^{-1} and 1305 cm^{-1} (Figure 6, *d*) and 1055 cm^{-1} and 1307 cm^{1} (Figure 6, *e*) which are characteristic of plane deformation ($\delta_{pd.}$) and valence (ν) oscillations of C–O that interacts with polarized NPs of food additive Fe_3O_4 (Figure 1–5) [11].

The presence of the broad absorption band of average intensity for the spectrum of linoleic acid (Figure 6, *b*) in the range of 3200 – 3600 cm^{-1} associated with the characteristic

vibrations of the surface OH–groups. The non-plating ($\delta_{npd.}$) deformation vibrations of the O–H bond of the carboxyl group of linoleic acid are noted in the form of a band at 938 cm^{-1}. Also you can see from Figure 6 (*c, d, e*) in the spectrum of sunflower oil (Figure 6, *c*) and with the adsorption of linoleic acid (Figure 6, *d*) and sunflower oil (Figure 6, *e*) on the NPs of food additive Fe_3O_4 surface, these absorption bands disappear. This is confirmed by data on the absence of free hydroxy-groups on the surface of the "lipid-NPs of food additive Fe_3O_4" system. These results confirm that oleic acid and triglycerides of sunflower oil are chemisorbed on nanoparticles of food additive Fe_3O_4 (Figures 1–5).

Obtained results of IR studies of the experimental samples in combination with previous studies of the processes of adsorption of fatty acids on particles of food additive Fe_3O_4 [9–11] confirm the formation mechanisms of the first lipid adsorption layer on the NPs of food additive Fe_3O_4, which can be represented by four types: monodentate, bridge (bidentate), chelating (bidentate) and ionic interaction (Figure 1–5) [5].

The differences in the wave number values ($\Delta\nu_o$) between the asymmetric (ν_{as}) and symmetric (ν_s) stretching vibrations of the carboxylate ν_{as} ($-COO^-$–) and ν_s ($-COO^-$–) groups (in the IR spectrum – Figure 6, *d, e*) can be used for the type identification of the interaction between carboxyl (COO^-) lipids and a metal atom (in particular, Fe) of nanoparticles of food additive Fe_3O_4

The largest deviation of the wave number $\Delta\nu_o$ (200 – 320 cm^{-1}) corresponded to the monodentate interaction, and the smallest – $\Delta\nu_o$ (<110 cm^{-1}) – chelating (bidentate).

The mean average deviation $\Delta\nu_o$ (140–190 cm^{-1}) is characteristic for the bridge (bidentate) interaction. In this work, the $\Delta\nu_o$ value is ~ 100 cm^{-1} (1638 –1543 = 95 cm^{-1}, for sample *d*) 1636 – 1540 = 96 cm^{-1} for the sample *e*) and indicates the bidentate structure existence where two oxygen atoms of the carboxyl group of lipid which coordinated link with Ferum atoms surface of food additive Fe_3O_4 nanoparticles (Figures 4, 5).

Hence, the mechanism of fat-containing and fat binding capability of NPs of food additive "Magnetofood" (Fe_3O_4) consists of the chemisorption of fats on their surface and can be represented by the "two-layer coordination" model:

- The first adsorption layer – due to the electrostatic interactions of polarized groups of lipids with the ionized nanoparticles of Fe_3O_4 additive and the coordination bonds of Ferum atoms of NPs of food additive Fe_3O_4 with Oxygen COO^- – group of "hydrophilic head" of higher fatty acids and triglycerides of fat;
- The second adsorption layer – due to the electrostatic interactions of hydrophobic centers of the first adsorption layer and hydrocarbon tails of higher fatty acids and triglycerides of free fat.

Morphological analysis of experimental samples. Scanning Electron Microscopy (TEM)

Particle size and morphology of experimental samples 1, 4 and 5 have been studied by using the transmission electron microscopy (TEM). Figure 7 shows the normalized distribution function of the particle size in the experimental samples 1, 4 and 5.

It is established that the distribution function is rather narrow and symmetric which tests the systems of the experimental samples of nanoparticles of food additive "Magnetofood" Fe_3O_4 as homogeneous with a low degree of polydispersity (Figure 7 *a, b, c*). The established order of the average particle size is: for sample 1 – <d> ~ 78±2,36 nm; for sample 4 – <d> ~ 80±2,57 nm; for a sample of 5 – <d> ~ 81±2,93 nm.

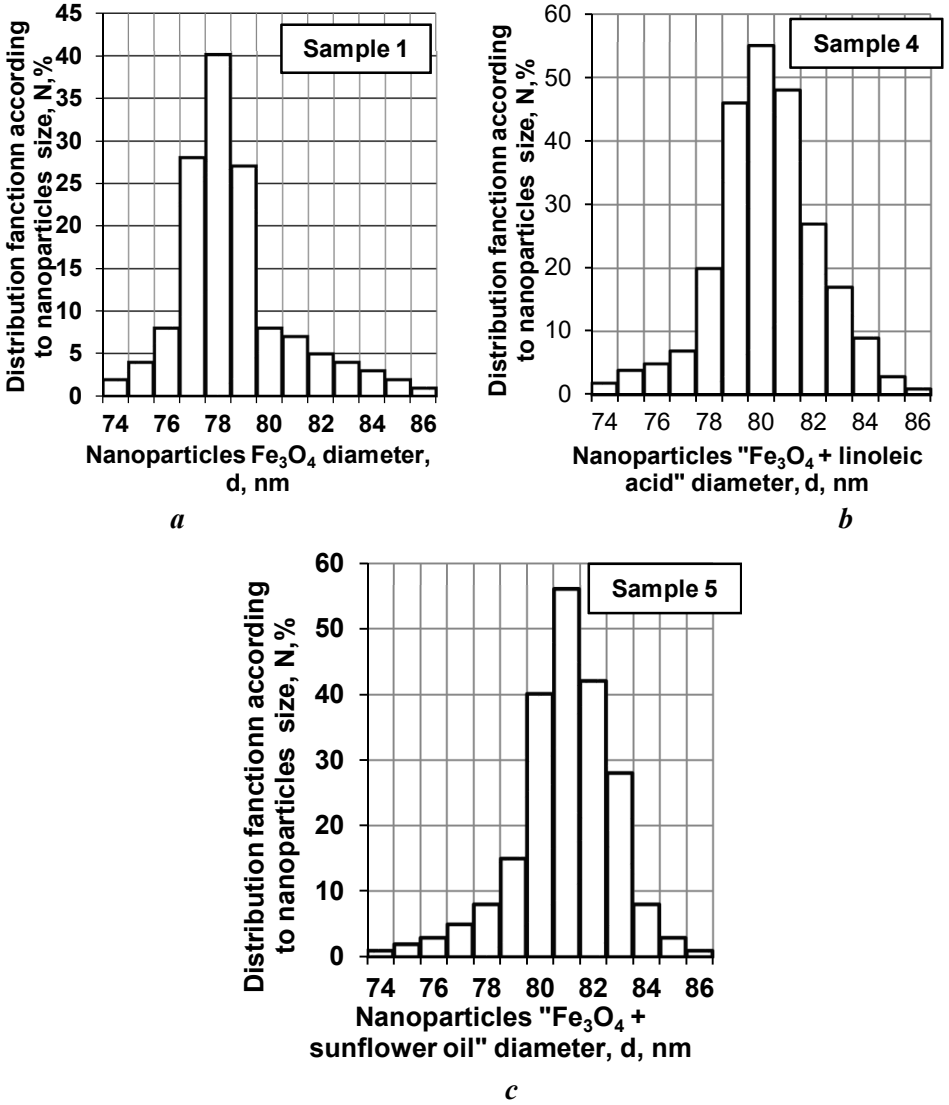

Figure 7. Diagrams of the particles distribution in order of size in the experimental samples:
***a* – synthesized fine powder of food additive Fe_3O_4;**
***b* – nanoparticles of food additive Fe_3O_4 covered with linoleic acid;**
***c* – nanoparticles of food additive Fe_3O_4 covered with sunflower oil**

The increase in the particle size of food additive Fe_3O_4 in the experimental samples 4 and 5 compared with the pure NPs of food additive Fe_3O_4 (sample 1) is due to adsorption of linoleic acid and sunflower oil on the nanoparticles surface of food additive Fe_3O_4. That is, the total thickness of the 2d lipid adsorption layer is: for linoleic acid (sample 4) – 2d = 2·(1,10 – 1,25) nm = (2,2 – 2,5)nm; for sunflower oil (sample 5) – 2d = 2·(1,4 – 1,6) nm = (2,8 – 3,2) nm.

Elemental analysis of the experimental samples. Energy dispersive X-ray spectroscopy (EDX)

Using the EDX-spectra (Table 1) the elemental composition of the experimental samples of the composition "Lipid-NPsFe_3O_4" was established.

Table 1

Elemental composition of the experimental samples

Experimental\ samples	Elemental composition					
	Fe		O		C	
	Mass%	Atomic%	Mass%	Atomic%	Mass%	Atomic%
Sample 1	75,5	42,9	24,5	57,1	–	–
Sample 4	45,6	37,5	34,7	26,6	19,7	35,9
Sample 5	39,7	35,5	36,7	29,6	23,6	34,9

On X-ray spectra of the experimental samples 1, 4, 5 the peaks are about 0,8; 6,3 and 6,8 keV and associated with the absorption of the kinetic energy of electrons by the Fe atom. The NPs spectra of food additive Fe_3O_4 which are covered with lipids contain two more peaks: about 0,27 keV and 0,47 keV. These absorption bands belong to the atoms C and O [4, 5]. Moreover, the peak at 0,47 keV, characteristic of the atom O is also present in the spectrum of pure food additive Fe_3O_4 (sample 1). EDX-spectra analysis of the experimental samples 1, 4, 5 shows that Fe, O and C (H can not be investigated) are the main components in the "lipid-NPs of food additive Fe_3O_4".

From the analysis of the experimental data (EDX-spectra) it follows that the experimental samples have the following chemical (qualitative and quantitative) composition: *sample 1* (highly dispersed powder of food additive Fe_3O_4) – Fe 75,5%; In 24,5%; *sample 4* (nanoparticles of food additive Fe_3O_4 covered with linoleic acid) – Fe 45,6%; O 34,7%; C 19,7%; *sample 5* (nanoparticles of food additive Fe_3O_4 covered with sunflower oil) – Fe 39,7%; O 36,7%; C 23,67%. In the experimental samples 4, 5 a new chemical element (C) appears that is absent in the pure of food additive Fe_3O_4 (sample 1). The result indicates that NPs of food additive Fe_3O_4 was successfully synthesized (sample 1) and lipids (samples 4, 5) which chemisorption on the particles of food additive Fe_3O_4. The absorption band of atom C appeared in the samples 4, 5, confirms the process of adsorption and chemical interaction of particles of food additive Fe_3O_4 with lipids (in particular, linoleic acid and with triglycerides of sunflower oil).

Conclusions

1. The proposed model of "Two-layer coordination" of fats and higher fatty acids, in particular, of the linoleic acid on the surface NPs of food additive Fe_3O_4: the first adsorption layer is formed due to the electrostatic interactions of polarized groups of lipids and ionized nanoparticles of food additive Fe_3O_4 and the coordination bonds of Fe atomic nanoparticles of food additive Fe_3O_4 with Oxygen COO^- – a group of "hydrophilic head" of lipids; the second adsorption layer is due to the electrostatic interactions of hydrophobic centers of the first adsorption layer and hydrocarbon "tails" of lipids.

2. Experimentally confirmed the mechanism of fat binding and fat content of nanoparticles of food additive on the basis of double oxide of two- and trivalent iron (Fe_3O_4) which is represented by the model "Two-layer coordination":

- By the IR-Fourier spectroscopy method, the chemisorption of linoleic acid and 1-linoleyl-2-oleoyl-3-linolenoylglycerol on the surface NPs of food additive Fe_3O_4 has been demonstrated: for example, in IR-spectrum of the experimental samples of NPs of food additive Fe_3O_4 covered with linoleic acid (sample 4) and sunflower oil (sample 5) appeared in two new bands at 1543 cm^{-1} (sample 4) and 1540 cm^{-1} (sample 5) and 1638 cm^{-1} (sample 4) and 1636 cm^{-1} (sample 5), which are characteristic of valence asymmetric (ν_{as}) and valence symmetric (ν_s) oscillations of the carboxylate group (COO^-). The absorption band at 1710 cm^{-1} (linoleic acid is in the sample 2) and at 1744 cm^{-1} (sunflower oil is in the sample 3), characteristic of the valence fluctuations C = O–bond, disappeared. That is, the experimental data of the IR-Fourier spectroscopy indicate that lipids (linoleic acid or triglycerides of sunflower oil) are chemisorbed on the nanoparticles surface of food additive Fe_3O_4 in the carboxylate form using two oxygen atoms. The result is the formation of a monomolecular layer of chemically adsorbed lipids on the nanoparticles surface of food additive Fe_3O_4. In the spectra of linoleic acid (example 2) and sunflower oil (sample 3) the intense bands are observed with peaks at 2926 cm^{-1} , 2856 cm^{-1} and 2924 cm^{-1} , 2854 cm^{-1} , respectively and about 1360 cm^{-1}. On the curves of the experimental samples 4 and 5 these absorption bands are shifted to a lower frequency and the region: ν_{as} = 2904 cm^{-1}; ν_s = 2831 cm^{-1} and δ = 1350 cm^{-1}, respectively. This is due to the formation not only the first adsorption layer but also the formation of the second adsorption layer on the nanoparticles surface of food additive Fe_3O_4 ;
- The method of scanning electron microscopy revealed that the established order of the average particle size is: for sample 1 – <d>78±2,36 nm; for sample 4 – <d> 80±2,57 nm; for a sample of 5 – <d>81±2,93 nm;
- The method of energy dispersive X-ray spectroscopy the elemental composition of the experimental samples of food additive Fe_3O_4 was studied: sample 1 (highly dispersed powder of food additive Fe_3O_4) – Fe 75,5%; O 24, 5%; sample 4 (nanoparticles of food additive Fe_3O_4 covered with linoleic acid) – Fe 45,6%; O 34,7%; C 19,7; sample 5 (nanoparticles of food additive Fe_3O_4 covered with sunflower oil) – Fe 39,7%; O 36,7%; C 23,67%.

The obtained results will allow to simulate the processes of fat-retaining capacity and fat-binding capability in the various food systems; the functional and technological characteristics of fat-containing compositions and the quality indicators of finished products.

References

1. Ramachandraiah K., Choi M.-J., Hong G.-P. (2018), Micro- and nanoscaled materials for strategy-based applications in innovative livestock products: a review, *Trends in Food Science & Technology*, 71, pp. 25–35.
2. Ilyukha N. G., Barsova Z. V., Kovalenko V. A., Tsikhanovskaya I. V. (2010), Tekhnologiya proizvodstva i pokazateli kachestva pishchevoy dobavki na osnove magnetita, *Vostochno-Yevropeyskiy zhurnal peredovykh tekhnologiy*, 6(10), pp. 32–35.
3. Drmota A., Kosak A., Znidarsik A. (2008), A mechanism for the adsorption of carboxylic acids onto the surface of magnetic nanoparticles, *Materials and technology*, 42, pp. 79–83.

4. Mahdavi M., Ahmad M. B., Haron M. J., Namvar F., Nadi B., Ab Rahman M. Z., Amin J. (2013), Synthesis, Surface Modification and Characterisation of Biocompatible Magnetic Iron Oxide Nanoparticles for Biomedical Applications, *Molecules*, 18, pp. 7533–7548; doi:10.3390/molecules18077533.
5. Ling Z., Rong H., Hong-Chen G. (2006), Oleic acid coating on the monodisperse magnetite nanoparticles, *Applied Surface Science, APSUSC-14301*, 7, pp. 1–7, doi:10.1016/j.apsusc.2006.05.023.
6. Chernyshova I., Ponnurangam S., Somasundaran P. (2011), Adsorption of Fatty Acids on Iron (Hydr)oxides from Aqueous Solutions, *Langmuir*, 27 (16), pp. 10007–10018, DOI: 10.1021/la2017374.
7. Tsykhanovska I., Alexandrov A., Evlash V., Lazareva T., Svidlo K., Gontar T. (2018), Investigation of the moisture-retaining power of rye-wheat gluten and flour with polyfunctional food supplement "Magnetofood", *Eureka: Life Sciences*, 2(14), pp. 67–76, doi: 10.21303/2504-5695.2018.00611.
8. (2018), *Patent UA 126502, Kharchova dobavka "Mahnetofud"*, B.12.
9. Wang L.S. (2008), Synthesis, surface modification and characterization of nanoparticles, *Advances in Nanocomposites*, 34, pp. 289–322.
10. Hajdu A., Illes E., Tombacz E., Borbath I. (2009), Surface charging, polyanionic coating and colloid stability of magnetite nanoparticles, *Colloids and Surfaces A*, 347, pp. 104–108.
11. Shen Y.F., Tang J., Nie Z.H., Wang Y.D., Ren Y., Zuo L. (2009), Preparation and application of magnetic Fe_3O_4 nanoparticles for wastewater purification, *Sep. Purif. Technol*., 68, pp. 312–319.
12. Skopenko V.V., Tsivadze A.Yu., Savranskiy L.I., Garnovskiy A.D. (2007), *Koordinatsionnaya khimiya*, Akademkniga, Moscow.
13. Steed J.W., Atwood J.L. (2000), *Supramolecular chemistry*, John Wiley & Sons Ltd, Chichester.
14. Steed J.W., Atwood J.L. (2004), *Encyclopedia of Supramolecular Chemistry*, Marcel Dekker,

Antimicrobial properties of two naphthopyrandione derivatives with cycloalkanespirohydantoins towards some phytopathogenic and beneficial microorganisms

Marin Marinov, Mladen Naydenov, Rumyana Prodanova

Agricultural University, Plovdiv, Bulgaria

Keywords:
Naphthopyrandione
Cycloalkanespiro-hydantoins
Antimicrobial
Phytopathogenic
Microorganism

Article history:

Received 14.06.2018
Received in revised form 22.09.2018
Accepted 27.12.2018

Corresponding author:

Marin Marinov
E-mail:
m_n_marinov@abv.bg

DOI: 10.24263/2304-974X-2018-7-4-15

Abstract

Introduction. Antimicrobial properties of two naphthopyrandione derivatives with cycloalkanespirohydantoins towards some phytopathogenic and beneficial microorganisms are investigated and presented in this work.

Materials and methods. The title compounds are obtained following a known procedure. The agar well diffusion test is applied to determine the antimicrobial activities of the synthesized products on bacteria and fungi. The initial cycloalkanespirohydantoins are prepared *via* the Bucherer-Lieb method. The starting compounds used in the studies, namely 6-bromo-1H,3H-naphtho[1,8-cd]pyran-1,3-dione, cycloalkanespirohydantoins, naphthopyrandione derivatives with cycloalkanespirohydantoins, namely 3-(1,3-dioxo-1H,3H-naphtho[1,8-cd]pyran-6-yl)-1,3-diazaspiro [4.4]-nonane-2,4-dione and 3-(1,3-dioxo-1H,3H-naphtho[1,8-cd]pyran-6-yl)-1,3-diazaspiro[4.5]decane-2,4-dione, are synthesized according to the methods described in the literature.

Results and discussion. The antimicrobial activity of the parent compounds and the final products is investigated against the fungi *Fusarium oxysporum* and *Trichoderma asperellum* T6, the Gram-positive bacterium *Bacillus amyloliquefaciens* 2/7 A and the Gram-negative bacterium *Xanthomonas vesicatoria*. All substances (except the initial spirohydantoins) show activity to the microorganisms studied. With regard to the test fungi, more susceptible are those of phytopathogenic species (*Fusarium oxysporum*). The effect is different in the case of bio-control agent (*Trichoderma asperellum* T6). In addition to being weaker, over time, the fungus overcomes the inhibitory effect as its growth covers inhibition zones already formed. The 3-(1,3-dioxo-1*H*,3*H*-naphtho[1,8-*cd*]pyran-6-yl)-1,3-diazaspiro[4.5]decane-2,4-dione shows the highest activity against phytopathogenic microorganisms while having a relatively lower effect against *Trichoderma asperellum* T6.

Conclusions. The 6-bromo-1*H*,3*H*-naphtho[1,8-*cd*]pyran-1,3-dione, 3-(1,3-dioxo-1*H*,3*H*-naphtho[1,8-*cd*]pyran-6-yl)-1,3-diazaspiro[4.4]nonane-2,4-dione and 3-(1,3-dioxo-1*H*,3*H*-naphtho[1,8-*cd*]pyran-6-yl)-1,3-diazaspiro[4.5]decane-2,4-dione possessed the highest biological activity to all of the tested microorganisms.

Introduction

The hydantoins (imidazolidinediones) are substances with a broad spectrum of biological activity. Different derivatives of such compounds are known as antimicrobial agents [1-34].

The antimicrobial activity of various spirohydantoins and their derivatives has been investigated and reported in previous studies of ours. Some of the products tested for the presence of such type of activity are shown in figure 1.

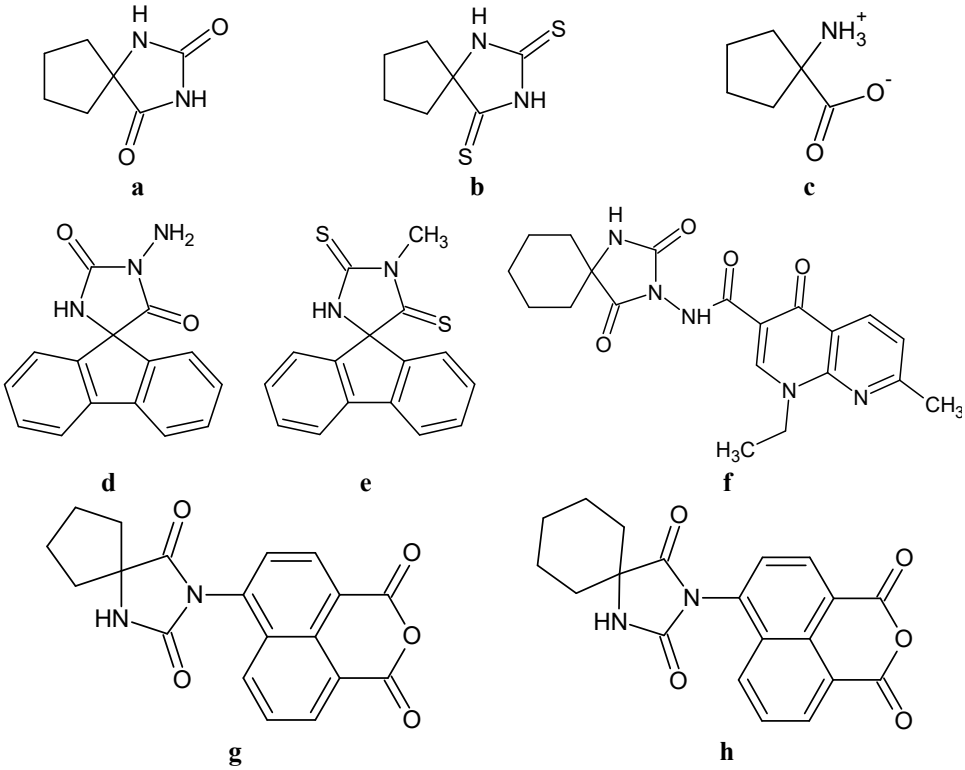

Figure 1. Some biologically active spirohydantoins and their derivatives

The cyclopentanespiro-5-hydantoin /1,3-diazaspiro[4.4]nonane-2,4-dione/ (figure 1a), cyclopentanespiro-5-(2,4-dithiohydantoin) /1,3-diazaspiro[4.4]nonane-2,4-dithione/ (figure 1b) and 1-aminocyclopentane-1-carboxylic acid (figure 1c) have shown strong fungicidal activity against *Blumeria graminis* f. sp. *tritici* (wheat powdery mildew) [35]. Other compounds with pronounced fungicidal properties are
3-(1,3-dioxo-1*H*,3*H*-naphtho[1,8-*cd*]pyran-6-yl)-1,3-diazaspiro[4.4]nonane-2,4-dione (Figure 1g) and
3-(1,3-dioxo-1*H*,3*H*-naphtho[1,8-*cd*]pyran-6-yl)-1,3-diazaspiro[4.5]decane-2,4-dione (figure 1h).

Both products completely inhibited the germination of the *Monilia fructigena* (brown rot) conidia [36]. With regard to *Plasmopara viticola* (grapevine downy mildew), only the cyclopentyl derivative (figure 1g) was found to be effective [37]. The 3-amino-9'-

fluorenespiro-5-hydantoin /3'-aminospiro[fluorene-9,5'-imidazolidine]-2',4'-dione/ (figure 1d) exhibited a distinct antibacterial activity against the Gram-negative bacterium *Escherichia coli* [38]. In contrast to the example above, it was found out that the 3-methyl-(9'-fluorene)-spiro-5-(2,4-dithiohydantoin) /3'-methylspiro[fluorene-9,5'-imidazolidine]-2',4'-dithione/ (figure 1e) showed antibacterial effect towards Gram-positive bacteria (*Staphylococcus aureus* and *Bacillus subtilis*) [39]. The *N*-(2,4-dioxo-1,3-diazaspiro[4.5]decan-3-yl)-1-ethyl-7-methyl-4-oxo-1,4-dihydro-1,8-naphthyridine-3-carboxamide (figure 1f) possessed a certain antibacterial activity against Gram-positive and Gram-negative bacteria [40].

The current work is a continuation of the biological activity research of 3-(1,3-dioxo-1*H*,3*H*-naphtho[1,8-*cd*]pyran-6-yl)-1,3-diazaspiro[4.4]nonane-2,4-dione (figure 1g) and 3-(1,3-dioxo-1*H*,3*H*-naphtho[1,8-*cd*]pyran-6-yl)-1,3-diazaspiro[4.5] decane-2,4-dione (figure 1h). Herein, we present a study of the antimicrobial activity of both compounds against bacterial and fungal cultures of phytopathogenic and beneficial microorganisms.

Materials and methods

Synthetic compounds

All chemicals used for the synthesis were purchased from Merck and Sigma-Aldrich. The melting points were determined with a SMP-10 digital melting point apparatus. The elemental analysis data were obtained with an automatic analyzer Carlo Erba 1106. The purity of the compounds was checked by thin layer chromatography on Kieselgel 60 F_{254}, 0.2 mm Merck plates, eluent systems (vol. ratio): benzene : ethanol = 5 : 1, ethyl acetate : petroleum ether = 1 : 2 and *n*-butanol : acetic acid : water = 3 : 1 : 1. The IR spectra were registered in KBr pellets on a VERTEX 70 FT-IR spectrometer (Bruker Optics) from 4000 cm^{-1} to 400 cm^{-1} at resolution 2 cm^{-1} with 25 scans. The NMR spectra were taken on a Bruker DRX-250 spectrometer, operating at 250.13 and 62.90 MHz for ^{1}H and ^{13}C, respectively, using the standard Bruker software. The chemical shifts were referenced to tetramethylsilane (TMS). The measurements in DMSO-d_6 solutions were carried out at ambient temperature (300 K). Typical conditions for ^{1}H NMR spectra were: pulse width 30º, 1 s relaxation delay, 16K time domain points, zero-filled to 64K, hard pulse with 90º pulse width of 11.8 μs; ^{13}C NMR spectra: pulse width 30º, 1 s relaxation delay, 16K time domain points, zero-filled to 32K, hard pulse with 90º pulse width of 6.4 μs at a power level of 3 dB below the maximum output.

Microorganisms

Bacterial and fungal cultures of phytopathogenic and beneficial microorganisms were used to study the biological activity of the test substances. Fungi used were the phytopathogenic *Fusarium oxysporum* and the bio-control agent *Trichoderma asperellum* T6. The Gram-positive *Bacillus amyloliquefaciens* 2/7 A, having the ability to stimulate plant growth and to restrict the development of fungal phytopathogens and plant pathogenic and the Gram-negative *Xanthomonas vesicatoria* were used as bacterial test cultures. The microorganisms used in the study were from the collection of the Laboratory of microbial technologies except *Xanthomonas vesicatoria*, kindly provided by Dr. Katia Vasileva from Maritsa Vegetable Crops Research Institute, Plovdiv.

Biological assay

The agar well diffusion method was applied to determine the antimicrobial activities of compounds 1a, 1b, 2, 3a and 3b on the bacteria and fungi [41-43]. The incubations were done on tryptic soy agar (TSA Biolife 4021552) for the bacterial isolates and potato dextrose agar (Merck 1.10130.0500) for the fungi. The agar plate surface was inoculated by spreading 100 µl of the microbial inoculum, adjusted to yield approximately 1.0 X 10^8 cfu per ml with sterile water. Then, a hole with a diameter of 10 mm was punched aseptically with a sterile cork borer and a volume of 50 µl of the dimethylsulfoxide (DMSO) solution of the synthesized compounds in concentration of 20 mg/ml was introduced into the well. The agar plates were incubated in thermostat at 28 °C for all microorganisms. The inhibition zones were recorded at 48 and 96 h. The inhibition zones were analyzed using Digimizer®4.6.1, image analysis software.

Results and discussion

The synthesis of the title naphthopyrandione derivatives with cycloalkanespirohydantoins was carried out according to Figure 1.

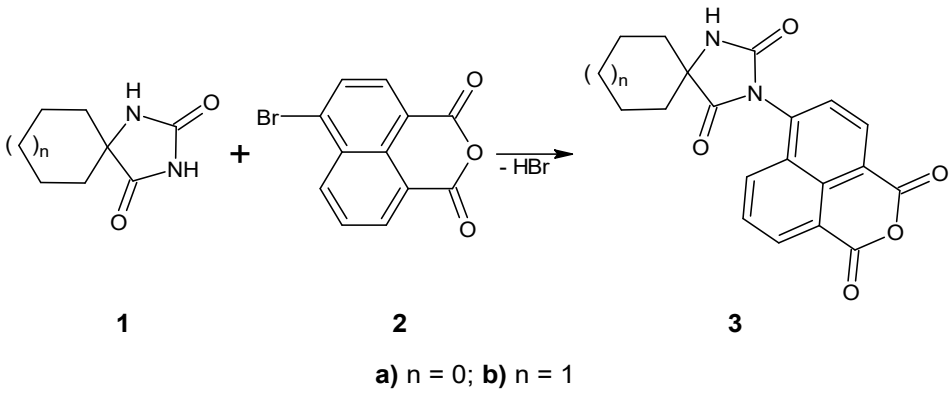

Figure 1. Synthesis of naphthopyrandione derivatives with cycloalkanespirohydantoins [36]

The cyclopentanespiro-5-hydantoin (1a) and cyclohexanespiro-5-hydantoin (1b) were prepared *via* the Bucherer-Lieb method [44]. The synthesis was performed by the reaction of cyclopentanone and cyclohexanone with sodium cyanide, ammonium carbonate and ethanol.

The 4-bromo-1,8-naphthalic anhydride (2) was obtained by the bromination of 1,8-naphthalic anhydride /1*H*,3*H*-naphtho[1,8-*cd*]pyran-1,3-dione/ in accordance with Grayshan et *al*. [45].

The interaction of cycloalkanespirohydantoins (1a and 1b) with 4-bromo-1,8-naphthalic anhydride (2) led to 3-(1,3-dioxo-1*H*,3*H*-naphtho[1,8-*cd*]pyran-6-yl)-1,3-diazaspiro[4.4]nonane-2,4-dione (3a) and 3-(1,3-dioxo-1*H*,3*H*-naphtho[1,8-*cd*]pyran-6-yl)-1,3-diazaspiro[4.5]decane-2,4-dione (3b) formation [36].

The compounds cited above (see table 1) were characterized by physicochemical parameters, elemental analysis, IR and NMR spectral data. The results obtained from these analyses match the literature data [36, 45-48].

Table 1

Compounds used for the biological tests

№	Structure	Name / IUPAC* systematic name	Synthesis procedure
1a	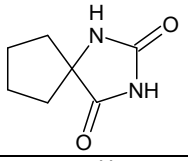	Cyclopentanespiro-5-hydantoin /1,3-Diazaspiro[4.4]nonane-2,4-dione/	[44]
1b	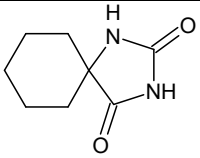	Cyclohexanespiro-5-hydantoin /1,3-Diazaspiro[4.5]decane-2,4-dione/	[44]
2	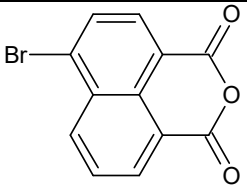	4-Bromo-1,8-naphthalic anhydride /6-Bromo-1*H*,3*H*-naphtho[1,8-*cd*]pyran-1,3-dione/	[45]
3a	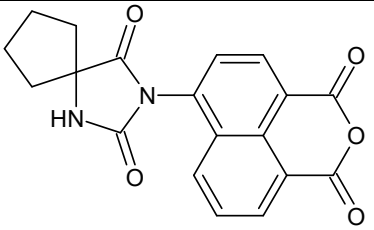	3-(1,3-Dioxo-1*H*,3*H*-naphtho[1,8-*cd*]pyran-6-yl)-1,3-diazaspiro[4.4]nonane-2,4-dione	[36]
3b	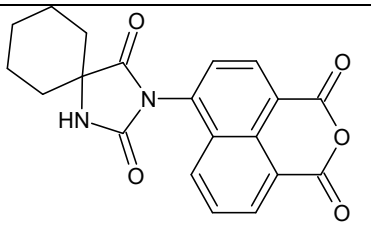	3-(1,3-Dioxo-1*H*,3*H*-naphtho[1,8-*cd*]pyran-6-yl)-1,3-diazaspiro[4.5]decane-2,4-dione	[36]

* International Union of Pure and Applied Chemistry

The research of synthesized substances, that are active against phytopathogens, requires verification of their action against microorganisms, harmful to plants, as well as useful microorganisms in combination with which they could be used.

In this preliminary study, bacteria and fungal strains important for growing quality agricultural produce are selected. Two phytopathogenic microorganisms, one fungus and one bacterium, have been selected. The other two microorganisms tested were beneficial bacteria and fungi that have the ability to control plant diseases and stimulate plant growth. This leads to an increase in the quantity and quality of the agricultural products.

Xanthomonas vesicatoria is a Gram-negative, aerobic, rod-shaped bacterium that causes leaf and fruit spots on peppers and tomatoes [49, 50]. *X. vesicatoria* occurs widely in tomato- and *Capsicum*-growing areas in different parts of the world and bacterial spot is common and

serious disease. Bacterial spot lesions can be observed on leaves, stems and fruit and occurs during all stages of plant growth. In favorable weather conditions, spots can coalesce and cause large areas of chlorosis. While fruit lesions are often only superficial, they reduce product quality in terms of fresh consumption and processing.

Fusarium oxysporum is a soilborne pathogenic fungus of worldwide importance [51]. The pathogen enters the plant through the roots and is then spread throughout the plant by the vascular system. This fungus can cause severe damages to many types of vegetables, flowers and field crops.

Fungi from the genus *Trichoderma* and bacteria from the genus *Bacillus* have been widely used in the agriculture as biocontrol agents. They possess a mycoparasitic capacity and ability to improve plant health and protection against phytopathogens, as well as to increase tolerance to biotic and abiotic stresses [52-54].

The antimicrobial activity of the parent compounds and the final products was investigated against the fungi *Fusarium oxysporum* and *Trichoderma asperellum* T6, the Gram-positive bacterium *Bacillus amyloliquefaciens* 2/7 A and the Gram-negative bacterium *Xanthomonas vesicatoria* (see the "Materials and methods" part). The results of the conducted tests are presented in figures 2-4.

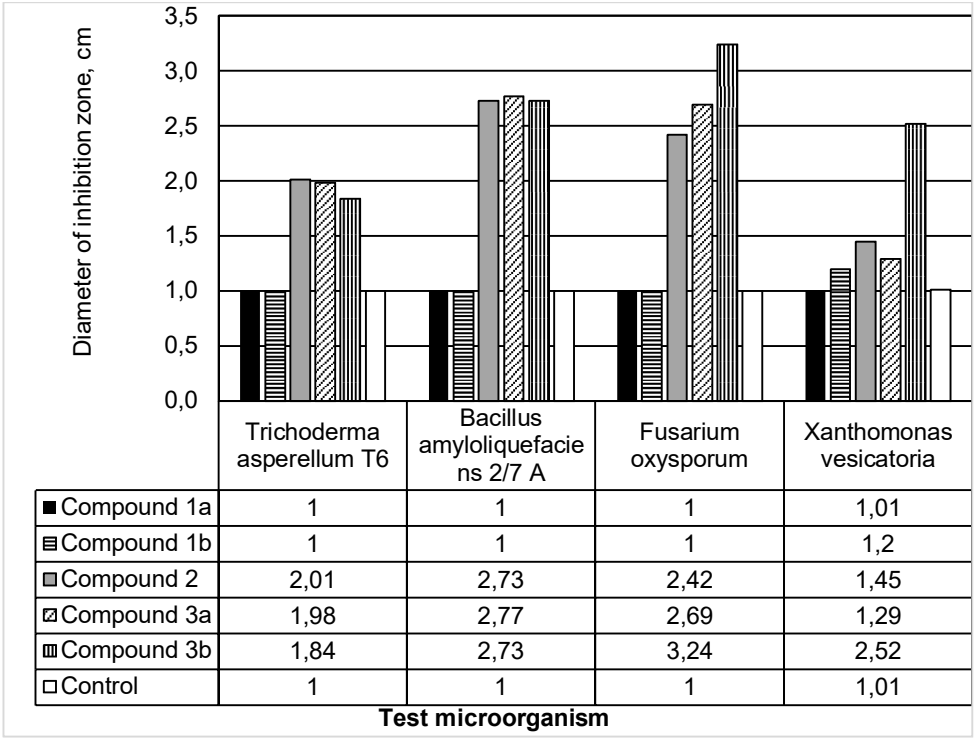

	Trichoderma asperellum T6	Bacillus amyloliquefaciens 2/7 A	Fusarium oxysporum	Xanthomonas vesicatoria
Compound 1a	1	1	1	1,01
Compound 1b	1	1	1	1,2
Compound 2	2,01	2,73	2,42	1,45
Compound 3a	1,98	2,77	2,69	1,29
Compound 3b	1,84	2,73	3,24	2,52
Control	1	1	1	1,01

Figure 2. Inhibition zones (cm) of the test substances

All substances (except the initial spirohydantoins **1a** and **1b**) show activity towards all studied microorganisms. With regard to the test fungi, more susceptible are those of phytopathogenic species (*Fusarium oxysporum*).

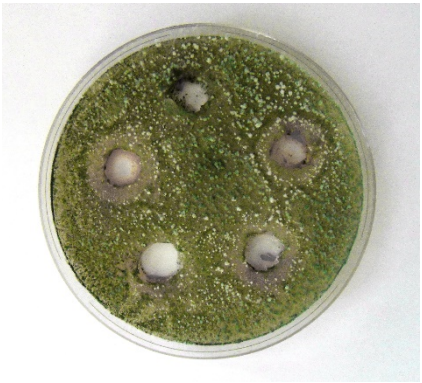

Figure 3. Overcomed inhibitory effect by *Trichoderma asperellum* T6

The effect is different in the case of bio-control agent (*Trichoderma asperellum* T6, Figure 3). In addition to being weaker, over time, the fungus overcomes the inhibitory effect as its growth covers inhibition zones already formed.

With respect to the test substances, the biological activity of compounds 2, 3a and 3b is the highest of all tested microorganisms. Compound 3b shows the highest activity against phytopathogenic microorganisms while having a relatively lower effect against *Trichoderma asperellum* T6. The remaining substances differ in their activity against various microorganisms, however, their cumulative activities to all microorganisms are approximately the same and do not differ to the control (Figure 4).

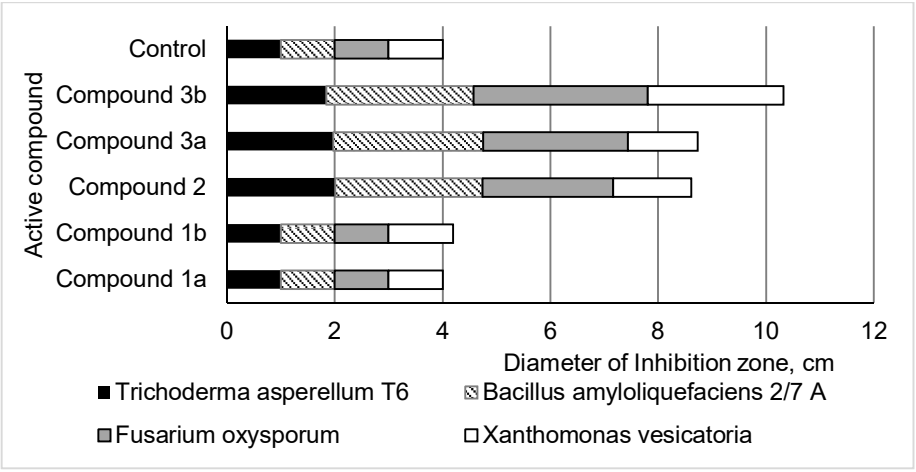

Figure 4. Cumulative activity of the compounds against test microorganisms

Conclusions

When comparing the activity of the original and the synthesized substances it is obvious that the initial materials practically do not exhibit biological activity to the test microorganisms.

The synthesized substances exhibit biological activity against all tested microorganisms. As such, these are of interest for further research. Compound **3b** depicts the highest activity, which is the only substance that has a significant activity against *Xanthomonas vesicatoria*.

Another important observation is that the activity exerted on the fungal bio-control agent *Trichoderma asperellum* T6 is expressed in temporary growth retention, which is then overcome by the fungus.

The latter can be used in the joint application of test substances together with fungal bio-control agents of the genus *Trichoderma* for the control of plant diseases in the production of safe plant produce for consumption and future processing.

Acknowledgements. Financial support by the Agricultural University – Plovdiv, Bulgaria (Contract 06-18) is gratefully acknowledged. We are also grateful to Prof. N. Stoyanov, Razgrad, for stimulating discussions.

References

1. Wolf C. N., Ligett W. B. (1960), Fungicidal composition of a hydantoin selected from the group consisting of 5,5 polymethylene and 5,5 diaryl, and 5,5 aryl, alkyl hydanton, *United States Patent № 2,920,997*.
2. Cremlyn R. J. C.-D., Elias R. S., Geoghegan M. J. A., Braunholtz J. T. (1965), *N*-Trichloromethylthiohydantoins, *United States Patent № 3,177,224*.
3. Fujinami A., Ozaki T., Horiuchi F., Yamamoto S., Akiba K., Tanaka K., Ooba S., Ooishi T., Nodera K., Kameda N. (1972), 3-(3′,5′-Dihalogenophenyl) imidazolidine-2,4-dione derivatives, *United States Patent № 3,668,217*.
4. Sauli M. (1973), Substituted 3-phenyl hydantoins useful as fungicides, *United States Patent № 3,755,350*.
5. Singer M. (1974), Herbicidal and/or fungicidal 5-poly-haloethylimino- and 5-polyhalovinylimino-2,4-imidazolidinedione, *United States Patent № 3,822,282*.
6. Hubele A. (1976), Imidazolidine-2,4-dione derivatives and their use as pesticides, *United States Patent № 3,960,883*.
7. Enders E., Frohberger P. -E. (1977), Combating fungi with l-aryl-5-alkylidene-2,4-dioxo imidazolidines, *United States Patent № 4,053,620*.
8. Sonntag N. O. V. (1978), Hydantoin derivatives and broad spectrum bactericidal/ fungicidal compositions thereof, *United States Patent № 4,073,924*.
9. Shull S. E., Bennett E. O. (1979), Antimicrobal hydanton derivative compositions and method of use, *United States Patent № 4,172,140*.
10. Rentzea C., Pommer E.-H., Mappes C. J., Zeeh B. (1980), 1,3-Bis-(trihalomethylsulfenyl)-imidazoline-2,4-diones, *United States Patent № 4,198,423*.
11. Zaidi S. M. M., Satsangi R. K., Nasir P., Agarwal R., Tiwari S.S. (1980), New anti-mycobacterial hydantoins, *Pharmazie*, 35, 755–756.
12. Asao S., Yamamoto S., Hisada Y., Nakayama Y., Takayama C. (1980), Imidazolidinedione compounds, and their production and use, *United States Patent № 4,237,22*.
13. Hubele A. (1982), Imidazolidine-2,4-dione derivatives, process for their preparation and their microbicidal application, *European Patent Application № 0043348A1*.
14. Takayama C., Fujinami A., Kirino O., Kato T. (1983), Quantitative structure-activity relationships of antifungal 1-acyl-3-(3,5-dichlorophenyl)-2,4-imidazolidinediones, *Journal of Pesticide Science*, 8(2), pp. 193–198.
15. Takayama C., Imajo H., Kirino O., Miyashita J., Sasaki S. (1983), Steric effect of acyl moiety substituents on the antifungal activity of 1-acyl-3-(3,5-dichlorophenyl)-2,4-imidazolidinediones, *Journal of Pesticide Science*, 8(4), pp. 583–586.
16. Moore J. E. (1986), 1-Substituted-3-polyhaloalkylthio hydanton fungicides, *United States Patent № 4,602,029*.
17. Takayama C., Kirino O., Hisada Y., Fujinami A. (1987), Quantitative structure-activity relationships for antifungal 3-(3,5-dichlorophenyl)-2,4-imidazolidinediones, *Agricultural and Biological Chemistry*, 51(6), pp. 1547–1552.
18. Chan H.-F. (1988), Substituted 2,4-imidazolidinediones and fungicidal compositions, *United States Patent № 4,753,957*.

19. Mohamed A. M., El-Sharief A. M., Ammar Y. A., Aly M. M. (1989), Synthesis and antimicrobial activity of some new 2,5-imidazolidinediones, *Pharmazie*, 44, 765–767.
20. Schoenberg T. G. (1991), Antimicrobial preservative system and method comprising a formaldehyde substituted hydanton, *United States Patent № 5,037,843*.
21. Goes A. J., De Lima M. C., Galdino S. L., Pitta I. R., Luu-Duc C. (1991), Synthesis and antimicrobial activity of substituted, fluorobenzyl benzylidenethiazolidinediones and imidazolidinediones, *Journal de Pharmacie de Belgique*, 46, pp. 236–240.
22. Lima M. C., Costa D. L., Goes A. J., Galdino S. L., Pitta I. R., Luu-Duc C. (1992), Synthesis and antimicrobial activity of chlorobenzyl benzylidene imidazolidinedione derivatives and substituted thiazolidinediones, *Pharmazie*, 47, pp. 182–184.
23. Marton J., Enisz J., Hosztafi S., Timar T. (1993), Preparation and fungicidal activity of 5-substituted hydantoins and their 2-thio analogs, *Journal of Agricultural and Food Chemistry*, 41(1), pp. 148-152.
24. Hsu A. C. T., Shaber S. H., Michelotti E. L. (1994), *N*-Iodopropargyl hydantoin compounds, compositions, preparation, and use as antimicrobial agents, *United States Patent № 5,346,913*.
25. Albuquerque J. F. C., Rocha Filho J. A., Brandao S. S. F., Lima M. C. A., Ximenes E. A., Galdino S. L., Pitta I. R., Chantegrel J., Perrissin M., Luu-Duc C. (1999), Synthesis and antimicrobial activity of substituted imidazolidinediones and thioxoimidazolidinones, *Il Farmaco*, 54, pp. 77–82.
26. Lin J., Winkelman C., Worley S. D., Broughton R. M., Williams J. F. (2001), Antimicrobial treatment of nylon, *Journal of Applied Polymer Science*, 81, pp. 943–947.
27. Szymańska E., Kieć-Kononowicz K., Białecka A., Kasprowicz A. (2002), Antimicrobial activity of 5-arylidene aromatic derivatives of hydantoin. Part 2, *Il Farmaco*, 57, pp. 39–44.
28. Kaziska A. J., Czuczak M. F., Lemke D. W. (2004), Sustained release antimicrobial composition including a partially halogenated hydanton and a colorant, *United States Patent Application Publication № US 2004/0043914A1*.
29. Barnes K., Liang J., Wu R., Worley S. D., Lee J., Broughton R. M., Huang T. S. (2006), Synthesis and antimicrobial applications of 5,5′-ethylenebis[5-methyl-3-(3-triethoxysilylpropyl)hydantoin], *Biomaterials*, 27, pp. 4825–4830.
30. Chen Z., Sun Y. (2006), *N*-Halamine-based antimicrobial additives for polymers: preparation, characterization, and antimicrobial activity, *Industrial & Engineering Chemistry Research*, 45, pp. 2634–2640.
31. Abdel-Aty A. H. (2009), Pesticidal effects of some imidazolidine and oxazolone derivatives, *World Journal of Agricultural Sciences*, 5(1), pp. 105–113.
32. Mandal A., Krishnan R. S. G., Thennarasu S., Panigrahi S., Mandal A. B. (2010), Two-dimensional surface properties of an antimicrobial hydantoin at the air-water interface: An experimental and theoretical study, *Colloids and Surfaces B: Biointerfaces*, 79, pp. 136–141.
33. Kocer H. B., Worley S. D., Broughton R. M., Huang T. S. (2011), A novel *N*-halamine acrylamide monomer and its copolymers for antimicrobial coatings, *Reactive & Functional Polymers*, 71, pp. 561–568.
34. Tan L., Maji S., Mattheis C., Chen Y., Agarwal S. (2012), Antimicrobial hydantoin-grafted poly(ε-caprolactone) by ring-opening polymerization and click chemistry, *Macromolecular Bioscience*, 12(12), pp. 1721–1730.
35. Marinov M., Ganchev D., Nikolov A., Marinova P., Krustev S., Madzharova V., Stoyanov N. (2013), *In vitro* fungicidal activity of cyclopentanespiro-5-hydantoin and its derivatives towards *Blumeria graminis* f. sp. *tritici*, *Agricultural Sciences*, 12, pp. 97–101.
36. Marinov, M., Ganchev D., Frenkeva M., Prodanova R., Penchev P. (2018), New naphthopyrandione derivatives with cycloalkanespirohydantoins: synthesis, characterization and fungicidal activity towards *Monilia fructigena*, *Agricultural University – Plovdiv, Scientific Works*, LXI(2), pp. 209–215.
37. Marinov M., Ganchev D., Prodanova R. (2018), Fungicidal activity of some spirohydantoins and their derivatives towards *Plasmopara viticola, Journal Scientific and Applied Research,* 13, pp. 58–64.

38. Marinova P., Marinov M., Feodorova Y., Kazakova M., Georgiev D., Lekova V., Penchev P., Stoyanov N. (2014), Synthesis, cytotoxicity and antibacterial activity of 3-amino-9'-fluorenespiro-5-hydantoin, *Comptes rendus de l'Académie bulgare des Sciences*, 67(4), pp. 513–518.
39. Marinova P., Marinov M., Feodorova Y., Kazakova M., Slavchev A., Blazheva D., Sarafian V., Nikolova I., Stoyanov N. (2014), Synthesis, characterization, *in vitro* antiproliferative and antimicrobial study of 3-methyl-(9'-fluorene)-spiro-5-(2,4-dithiohydantoin), *Science & Technologies*, IV(1), pp. 112–117.
40. Marinov M., Kostova I., Naydenova E., Prodanova R., Marinova P., Penchev P., Stoyanov N. (2015), Synthesis and antimicrobial activity of new 3-substituted cyclohexanespiro-5-hydantoin derivatives, *University of Ruse "Angel Kanchev" Proceedings*, 54(10.2), pp. 62–67.
41. Magaldi S., Mata-Essayag S., Hartung de Capriles C., Perez C., Colella M. T., Olaizola C., Ontiveros Y. (2004),Well diffusion for antifungal susceptibility testing, *International Journal of Infectious Diseases*, 8(1), pp. 39–45.
42. Valgas C., de Souza S. M., Smânia E. F. A., Smânia Jr. A. (2007), Screening methods to determine antibacterial activity of natural products, *Brazilian Journal of Microbiology*, 38, pp. 369–380.
43. Balouiri M., Sadiki M., Ibnsouda S. K. (2016), Methods for *in vitro* evaluating antimicrobial activity: A review, *Journal of Pharmaceutical Analysis*, 6, pp. 71–79.
44. Bucherer H. T., Lieb V. A. (1934), Über die Bildung substituierter hydantoine aus aldehyden und ketonen. Synthese von hydantoinen, *Journal für Praktische Chemie*, 141, pp. 5–43.
45. Grayshan P. H., Kadhim A. M., Peters A. T. (1974), Heterocyclic derivatives of naphthalene-1,8-dicarboxylic anhydride. Part III. Benzo[k,l] thioxanthene-3,4-dicarboximides, *Journal of Heterocyclic Chemistry*, 11, pp. 33–38.
46. Enchev V., Stoyanov N., Mateva V., Popova J., Kashchieva M., Aleksiev B., Mitewa M. (1999), Copper(II) complexes of spirohydantoins. Synthesis, quantum-chemical, and spectroscopic study, *Structural Chemistry*, 10(5), pp. 381–385.
47. Naydenova E., Pencheva N., Popova J., Stoyanov N., Lazarova M., Aleksiev B. (2002), Aminoderivatives of cycloalkanespirohydantoins: synthesis and biological activity, *Il Farmaco*, 57, pp. 189–194.
48. Naydenova E. D., Todorov P. T., Troev K. D. (2010), Synthesis and characterization of novel cycloalkanespiro-5-hydantoin phosphonic acids, *Phosphorus, Sulfur, and Silicon*, 185, pp. 1315–1320.
49. Jones J. B., Bouzar H., Stall R. E., Almira E. C., Roberts P. D., Bowen B. W., Sudberry J., Strickler P. M., Chun J. (2000), Systematic analysis of xanthomonads (*Xanthomonas* spp.) associated with pepper and tomato lesions, *International Journal of Systematic and Evolutionary Microbiology*, 50, pp. 1211–1219.
50. Potnis N., Timilsina S., Strayer A., Shantharaj D., Barak J. D., Paret M. L., Vallad G. E., Jones J. B. (2015), Bacterial spot of tomato and pepper: diverse *Xanthomonas* species with a wide variety of virulence factors posing a worldwide challenge, *Molecular Plant Pathology*, 16(9), pp. 907–920.
51. *Michielse C. B., Rep M.* (2009), Pathogen profile update: *Fusarium oxysporum*, *Molecular Plant Pathology,* 10(3), pp. 311–324.
52. Guzmán-Guzmán P., Porras-Troncoso M. D., Olmedo-Monfil V., Herrera-Estrella A. (2018), *Trichoderma* species: versatile plant symbionts, *Phytopathology*, available at: https://doi.org/10.1094/PHYTO-07-18-0218-RVW.
53. Qiao J.-Q., Wu H.-J., Huo R., Gao X.-W., Borriss R. (2014), Stimulation of plant growth and biocontrol by *Bacillus amyloliquefaciens* subsp. *plantarum* FZB42 engineered for improved action, *Chemical and Biological Technologies in Agriculture*, available at: https://doi.org/10.1186/s40538-014-0012-2.
54. Borriss R. (2011), *Use of plant-associated Bacillus strains as biofertilizers and biocontrol agents in agriculture*. In: Maheshwari D. (eds) *Bacteria in agrobiology: plant growth responses*, Springer, Berlin, Heidelberg.

Dynamics of mechatronic function modules drives of flow technological lines in food production

Liudmyla Kryvoplias-Volodina, Oleksandr Gavva, Sergii Volodin, Taras Hnativ

National University of Food Technologies, Kyiv, Ukraine

Keywords:

Functional
Module
Packing
Electro-pneumatic
Actuator
Accuracy

Article history:

Received 14.01.2018
Received in revised form 22.05.2018
Accepted 27.12.2018

Corresponding author:

Liudmyla Kryvoplias-Volodina
E-mail: krivoplyas-volodina@ukr.net

DOI: 10.24263/2304-974X-2018-7-4-16

Abstract

Introduction. The tasks were considered, which are related to the working bodies for the artificial food products movement according to the specified movement law and their positioning in the intermediate positions of the kinematic cycle.

Materials and methods. The actuators dynamics characteristics and control system of power part of positional electro-pneumatic actuators were researched. The methods of mathematical and computer modeling, and methods of solving ordinary differential equations and partial differential equations and method of correlation analysis were used.

Results and discussion. The analytical dependences for determining the kinematic parameters of the artificial product movement with the mechanism of collision, which is based on the pneumatic actuator, are obtained. The dynamical model of the actuator is mathematically tested and the movement law of the collision mechanism, which is approximated to the optimal speed, is obtained. To analyze the loading process of the working link of the positional actuator, the model of a generalized control system is used, which is limited by the one full cycle of operation of the functional mechatronic module of the packing machine. Such a model allows to describe the overload process, both in the case of full and partial filling of the working cycle. This is important when packing products in different geometric shapes of consumer packaging, which is typical of modern packaging machines. The simulation model of the actuator is theoretically substantiated and confirmed, which has a number of advantages, unlike the existing structures of positional drives in packaging machines. Calculated difference, during mathematical modeling, of the value of the working time of the output stage of the functional mechatronic module for the processing of the kinematic cycle of the operation of the packaging machine was for the various input parameters of the limit to 7%. The results of the mathematical modeling of dynamics for a positional pneumatic actuator, with the condition of changing the cross section of the exhaust hole, gave the opportunity to obtain the kinematic characteristics of the drive.

Conclusions. The results of mathematical modeling for positional pneumatic actuators with the condition of changing the section of the exhaust hole allowed to track all the kinematic characteristics of the actuator.

Introduction

In recent years, a rather complicated process of optimal control of actuators of technological equipment for food production has been studied by many authors [1-4]. The authors took the various assumptions in order to simplify the mathematical description of the work of tracking and positional actuators [3, 4]. For a long time, this approach was justified, but over time, the productivity of mechatronic functional modules as part of technological equipment has increased significantly. In this connection, many control models of positional actuators with rational kinematic and dynamic parameters have become unacceptable for practical use [19]. Therefore, modulation of the moving process of artificial products by pusher on the basis of a position pneumatic actuator taking into account the real boundary conditions, as well as dynamic processes in the pneumocylinder, is relevant.

The main ways of packing artificial products in polymer films are revealed: the placement of the product in a pre-made package and fastening it with clips; the placement of the product in the sleeve, which is formed from roll packaging material; the placement of the product between two films and the formation of a package with four seams; the wrapping of the product with a polymeric film [8].

The analysis of the existing equipment for the packaging of artificial and small artificial foods, showed the priority of using polymeric packaging materials for a number of economic, environmental and protective parameters [5–7]. There are modules with linear displacement actuators in the composition of the collision mechanisms in the studied packaging machines (PMs), the most common mechatronic functional modules (MFMs) feeding the food product to the packaging area. The main ways of packing artificial products in polymer films are: placing the product in a pre-made package and fastening it with clips; placement of the product in the sleeve, formed from roll packaging material; placement of the product between two films and the formation of a package with four seams; wrapping the product with a polymeric film [8]. FMM layouts, which are using for the packaging of artificial and small artificial products, use commonly-designed functional devices (FDs) with pneumatic or electro-pneumatic actuators for pushing products [9,10]. It should be noted that in some cases, technological operations in packaging machines (movement of artificial products, the formation of a layer of artificial products, delivery of the package) carry out by using a pneumatic actuator [11]. It does not allow using of the single piston motion law when moving artificial products due to their different physical and mechanical properties. The strikes, which arise in the final position in the movement of artificial products, cause loss of their product appearance or the destruction of group units [12]. First of all, it is necessary to take into account, the possibility of practical implementation of this law by a pneumatic actuator, what means the possibility of ensuring a smooth change of all its parameters, when choosing the law of moving an artificial product [13].

The criterion, characterizing the operations of forming the structural elements of the package, can be the law of motion, selected by the condition of the required productivity, which is the most common in MFM packaging machines. It is connected with the work of packing machines, which have their own productivity, and locates at the earlier stages of the technological chain [14,15].

The *aim* is expanding the functionality of food packaging equipment provides the searching for ways to improve the drives of the functional mechatronic modules.

The *tasks* of the study:

- the modeling of piston movement law of the pneumocylinder with an initial difference in air pressure, approximating to the optimal speed. In this case, the loads movement on the fixed flat is considered a collision mechanism with a positional pneumatic actuator.

- using the mathematical modeling to study the cases of smoothing the acceleration function at the moment of disengagement of the driving force, which allows to change smoothly the working parameters of the positional pneumatic actuator.
- creation of the simulation model of the positional actuator, with taking into account the cases of functions smoothing of the of the analogue of speed and analogue of acceleration.
- description of the method of choosing the initial movement stage (in the coordinate x), with taking into account the possible reduction of the actuating mechanism productivity.
- the study of optimal kinematic parameters of the packaging process of artificial food products in packaging machines.
- the development of the mathematical analysis method of the positional electro-pneumatic actuator for working out the modes of operation of the different functional mechatronic modules in a packing machine for artificial food products of the horizontal type.

In addition, it is necessary to set the value of the initial stage of the movement (x coordinate), choosing it in such a way that the initial stage does not have a significant effect on the productivity reduction of the executive mechanism. According to the author, the initial stage should not exceed 10% of the total displacement time of the piston (product), which allows the practical realization of a given law of motion without major errors.

Materials and methods

Materials

The materials were chosen the positional actuators of packaging machines. The aim of the study was chosen the dynamics of electro-pneumatic positional actuators. The analysis of the working bodies motion laws of the initial kinematic link of the collision mechanisms was carried out for the technological schemes of the MFM movement of artificial products and the group (layer) of artificial products into the formed sleeve of the packaging material.

MFM formation characteristics of artificial products packaging

The operations of forming the artificial products packaging are connected to the work of the MFM elements according to the laws of motion, which determine the required productivity of the packaging machine. As an researched positional actuator, for the given layout of Figure 1, MFM was chosen on the basis on pneumo actuator of positional type.

At Figure 1b there is shown with use of the graphs the generalized characteristics of displacement, speed, acceleration for the working output of the MFM. The mathematically illustrated graphs are described in the work [16]. According to the recommendations, we accept the initial conditions for the study of the technical system of the MFM (Figure 1a):

- The collision system, provided by the FMM, works according to the linear modified [17] law;
- The stage of acceleration is limited by the conditions 0<t<0,25T:

$$x = 2x_0\left(\frac{t}{T}\right)^2;\ \dot{x} = 4x_0\frac{t}{T^2};\ \ddot{x} = \frac{4x_0}{T^2}. \quad (1)$$

Deceleration:

$$0{,}75T<t<T;\ x = \frac{4x_0 t}{T} - x - 2x_0\left(\frac{t}{T}\right)^2$$

$$\dot{x} = \frac{4x_0}{T}\left(1-\frac{t}{T}\right);\ \ddot{x} = -\frac{4x_0}{T^2}.$$

Constant motion: 0,25T<t<0,75T;

$$x = \dot{x}t;\ \dot{x} = \frac{x_0}{T};\ \ddot{x} = \text{const}; \quad (2)$$

$$\ddot{x} = \frac{6x_0}{T^2}\left(1-\frac{2t}{T}\right).$$

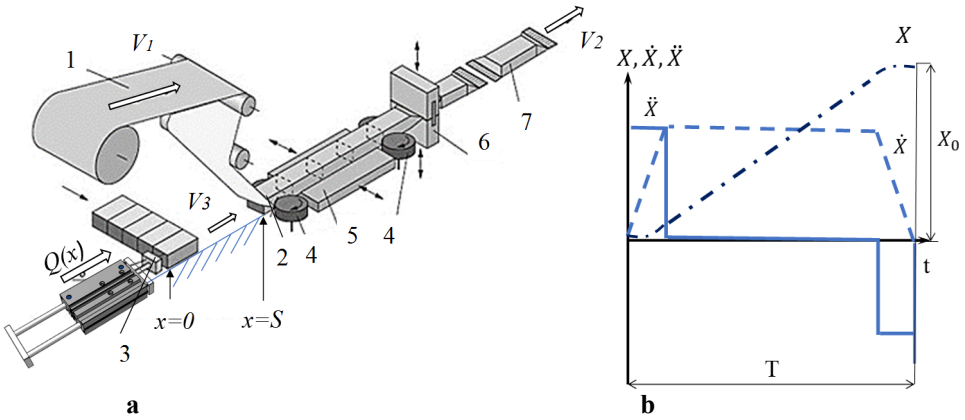

Figure 1. Technological scheme of PM for packing in a three-seam package with the work schedule of the output kinematic link MFM:

1 – FMM supply of packaging material; 2 – FD formation of the semi-sleeve; 3 – FD package formation; 4 – artificial product based on corex; 5 – MFM the formation of the longitudinal seam; 6 – MFM the formation of the longitudinal seams; 7 – FMM forming of welding transverse seams; 8 – FD cutting off surplus shrinkable packaging material; 9 – transport system of withdrawal of finished packaging; 10 – MFM moving products into the sleeve.

The given descriptions of the movement laws of the technological machines [16] of working bodies do not allow us to describe in detail the change in the kinematic characteristics of the working bodies in the arrangement with the electro-pneumatic actuator. Therefore, taking into account Figure 1 (b) and work [16,18], we can formulate research tasks with additional parameters. For such parameters we accept the processes of changing the pressure in the power part of the positional pneumatic actuator. MFM research with taking into account the inertial processes of the power part of the electro-pneumatic actuator is due to the need to supplement information on the operation of the executive mechanisms of automatic machine [16], in particular the packaging machine for the packaging of artificial food products. Well-formed structure of the control system, which also needs to be taken into account in the studies, allows to coordinate the work of all the components of the MFM.

Research methods

Methods of mathematical and computer modeling, methods of solving ordinary differential equations and differential equations in partial derivatives were used to study the dynamics of compressed air in the cavities of the pneumocylinder. In the study of the layout of MFM packaging machines, the theory of automated control of electropneumatic position drives is used.

Results and discussion

The first stage requires the analysis of classical methods for describing the work of the MFM output working links. The graph (Figure 1, B) show the 3 stages of changes in kinematic parameters of the output link. At the real technical systems, according as that the control module is taken into account, the similar graphs can be divided into 4 stages:

- the time of the preparatory period of the forward stroke $t_{I;}$
- the time of the working stroke of the piston t_{II};

- the time of the preparatory period of the reverse stroke t_{III}, which is connected with the time of receipt of the control signal for the operation of the pneumocycler rod;
- the time of piston motion in the reverse direction t_{IV} is determined by a common solution of equations (3) – (5) with the help of the ECM.

The second stage consists of studying the movement of the stem of pneumocylinder, it is the MFM output links. We have chosen the law of the stem movement due to the necessary productivity. This is a special case of the optimal speed of the process of load movement, which allows to achieve maximum productivity of the actuator.

In the implementation of the studied of movement law of the working output link of the MFM (Figure 2), the inertia of the positional electro-pneumatic actuator control system is taken into account. The structure of control of the system (Figure 3) is analyzed, with the condition – to ensure the presence of the driving force Q (acceleration ẍ) in the initial stage of motion.

To compile a mathematical model of the MFM output link, the assumptions are made:

- taking into account the external force on the piston rod until the resistive force Q(x), (Figure 2), does not increase to the value corresponding to the required acceleration ẍ.
- the change in the value of acceleration of the piston and the rod of the pneumocylinder from the maximum to the minimum value is considered at the moment of disengagement of the driving force. It requires an instantaneous increase in pressure in the exhaust flat.

The classic graphs of the movement laws of the working links (Figure 1b) do not take into account the transitional stages of the work of the technical system as part of the control module. Therefore, we have chosen to compile a mathematical model of the work of the initial working link, it is the combined law of the movement of the rod into the electro-pneumatic positional actuator. The graph (Figure 2) describes the working and idle movement of the piston rod in the operation of control elements, it is electromagnetic relays of the control system, the scheme of which is shown on (Figure 4).

Thus, the solution of the problem is reduced to the solution of the optimization problem with initial conditions, that are not equal to zero, followed by smoothing the discontinuous function at the time of switching off the driving force. The movement of the piston of the positional pneumatic actuator (Figure 2) consists of four stages:

Stage I is initial. The using a control signal from electromagnetic relays of an electropneumatic distributor – and the driving force increases ($Q \le Q(x) \le Q_{max}$). The movement law of a piston pneumoscilinder acquires a parabolic form. The work of the working link begins.

Stage II is intensive acceleration. It finishes with the disappearance of the signal of the control electromagnet (first solenoid). The driving force is constant$Q_{max} = const$). The stage condition: Q_{max}- is the maximum driving force, developing by pusher, does not cause deformation of the artificial product.

Stage III is transitional. The using of the electromagnetic relay of the electropneumatic distributor (second solenoid).Driving force decreases ($Q_{max} \ge Q(x) \ge Q$) as a result of the resistance of the compressed air of the rod chamber of the pneumocycler.

Stage IV is characterized by a reverse movement of the rod, which is under the influence of intense deceleration. The stage is completed when the control signal from the second solenoid is turned off.The driving force is zero (Q = 0). It is necessary to ensure the integrity of the load from the pusher. The boundary conditions in this problem are as follows:

$$t = 0;\ \ddot{x} = 0;\ \dot{x} = 0;\ x = 0;\ \ \ddot{x} = \ddot{x}_{IV};\ \dot{x} = 0;\ x = S.$$

where S is the value of the movement of cargo from the initial position to the final; $\ddot{x}_{IV}$ is the value of the load acceleration at the stage of intense deceleration.

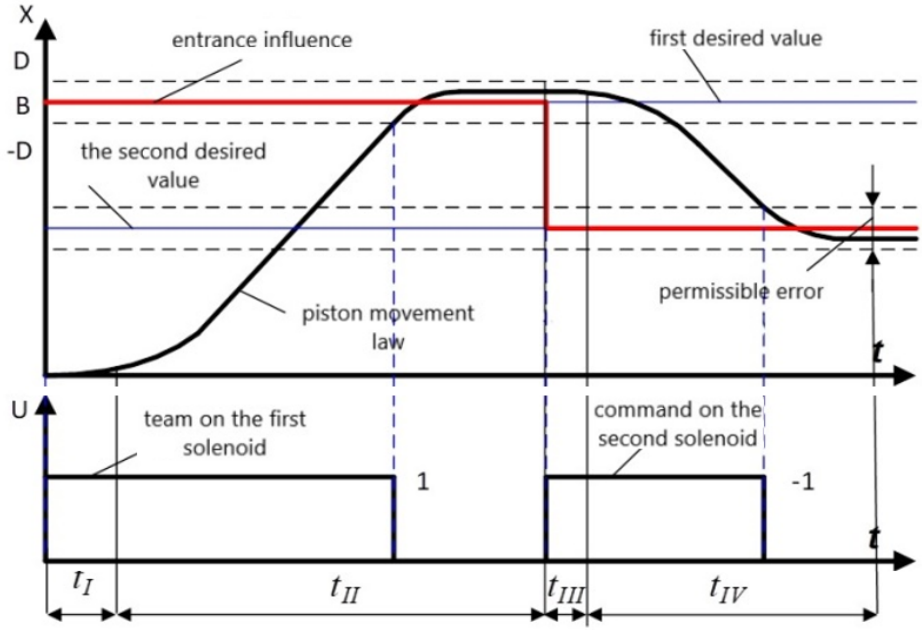

Figure 2. Combined law of motion of the driving link in the MFM positional actuator with taking into account the receipt of control signals from electromagnetic relays of the electropneumatic distributor

According to the equation (4.1), there is no time in final conditions for which the load is moved. This is explained by the fact that during a four-stage mode, the time of movement is determined during the task execution. The variable quantities are set depending on the parameter x, the equation of the piston motion of the pneumatic actuator of two-way action will have the form:

$$m\ddot{x} = p_1(x)F_1\text{-}p_2(x)F_2\text{-}P(x) \quad (3)$$

where m – the mass of the product; p_1, p_2 – pressure of the piston and stomach cavity, $F_{1,2}$ – square of the piston pneumocycline.

We obtain expressions, which characterize the change in pressure as a function of displacement, respectively, for the working and exhaust cavities

$$\frac{dp_1}{dx} = \frac{k}{x_{01}+x}\left[\frac{f_1^e K p_m \sqrt{RT_m}}{F_1}\varphi(\delta_1)\cdot\frac{1}{\dot{x}} - P_1\right] \quad (4)$$

$$\frac{dp_2}{dx} = \frac{k}{S+x_{02}-x}\left[\frac{-(f_2^e K p_2^{\frac{3k-1}{2k}}\sqrt{RT_m})}{F_2 p_m^{(k-1)/2k}}\cdot\frac{1}{\dot{x}}\varphi\left(\frac{\delta_a}{\delta_2}\right) + P_2\right] \quad (5)$$

where k – air adiabatic coefficient, x_{01}, x_{02} – initial and final coordinate of the piston movement, R – gas constant air, T_m – air temperature, p_m – pressure of the pneumatic line; $\varphi(\delta_1)$ – is cost characteristic of the section.

According equation (5), the pressure in the exhaust cavity is:

$$P_2(x) = (P_1(x)F_1\text{-}m\ddot{x}\text{-}P(x))/F_2 \quad (6)$$

After differentiating the $P_2(x)$ function by the variable x, we have:

$$\dot{P}_2(x) = (\dot{P}_1(x)F_1\text{-}m\dddot{x}\text{-}\dot{m}\ddot{x}\text{-}\dot{P}(x))/F_2 \quad (7)$$

According equation (4.4) the effective area of the exhaust hole is

$$f_2^e = \frac{\left[P_2 - \frac{dp}{dx}\frac{S+x_{02}-x}{k}\right]\dot{x}F_2 p_m^{(k-1)/2k}}{kp_2^{(3k-1)/2k}\sqrt{RT_m}\varphi\left(\frac{\delta_a}{\delta_2}\right)} \quad (8)$$

Thus, having the equations (3-8), which are describing the parameters of the positional pneumatic drive depending on the variable x, we can proceed to the definition of the equations characterizing the movement of the moving load on a fixed flat (Figure 3).

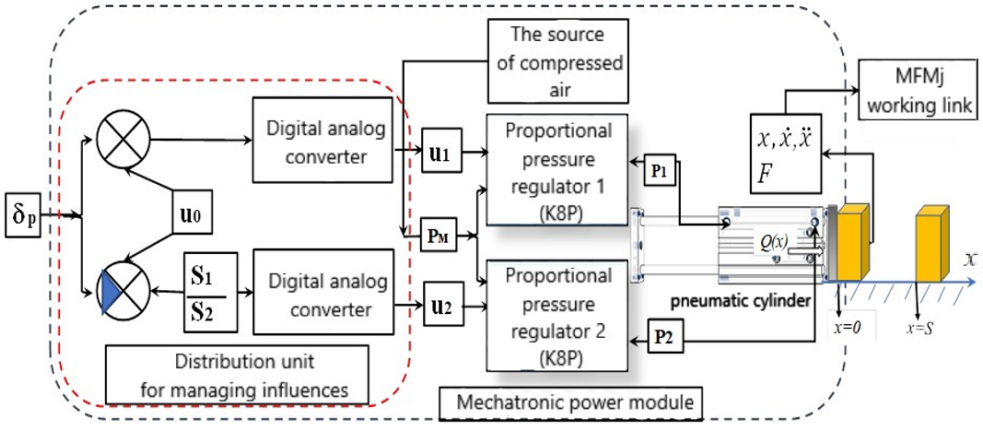

Figure 3. The generalized scheme of the load movement on a fixed flat in the layout with the structural scheme of tracking the piston movement of the pneumocylinder

Figure 3 shows the circuit diagram of the electro-pneumatic positioning actuators of the packing machine. Actuators are built by combining into a single module a pneumocylinder, reliable and inexpensive serial electro-pneumatic distributors of discrete action, precision piston position sensors and a controller that implements the algorithm of digital relay control.

To stop the object at different points, feedback from the continuous action sensor is used that measures the current state of the piston relative to the base value. The pneumomechanical subsystem consists of a piston with a rod, a mechanical control object and equivalent pneumatic springs in the cavities of the pneumocylinder. The control effects, u1 and u2, are on the two pressure control modules, which are implemented programmatically by using the control distribution control block. To achieve high speed drive and obtain the maximum range of force control is advisable to provide a consistent change of effects u1 and u2 in accordance with the equation:

$$\begin{cases} u_1 = u_0 + \delta_p, \\ u_2 = (u_0 + \delta_0) \cdot \frac{S_1}{S_2}. \end{cases} \quad (9)$$

This equation is used the input action of the mechatronic FD δ_p and the reference value u_0, which sets the pressure in the cavities of the pneumocylinder at zero input action, taking into account the difference in the piston area from the rod cavity S_1 and the piston-free cavity S_2. The presence of a MFM with a positional actuator is a distinctive feature of the proposed new structure of the mechatronic FD.

Consider the law of movement of the leading link as a part of the mechatronic FD. It requires:

– to find the time T_{on} of load movement in the optimal speed of the two-stage mode to set the required value of x_{Ik} of load movement at the first stage I in a four-stage mode;

- to determine the equations on the basis of the obtained value x_{Ik}, describing the kinematic parameters of the moving load at first stage in the four-stage mode, and also the final conditions for this stage;
- to consider the load movement as a three-stage and to determine the shutdown time of the driving force and the total time of movement. In this case, the final coordinates for the stages I and III of the three-stage mode of motion coincide with the final coordinates for stages I and IV of the four-stage mode of movement;
- to determine the equations describing the load movement at II and IV stages, and then at III stage for a four-stage mode of motion.

This sequence of tasks is connected with determining the initial and final coordinates of the load movement for each stage and with the searching for integration constants.

The time T_{on} of the load movement at optimal speed in two-step mode (Figure 4, 8, a) is determined by the method [9].

$$T_{on} = \sqrt{\frac{2S}{gf(1-m_c gf/Q)}} \tag{10}$$

where S is value of load movement (piston stroke); m_c is load weight; f is the coefficient of friction between the bearing surface of the load and the displacement flat.

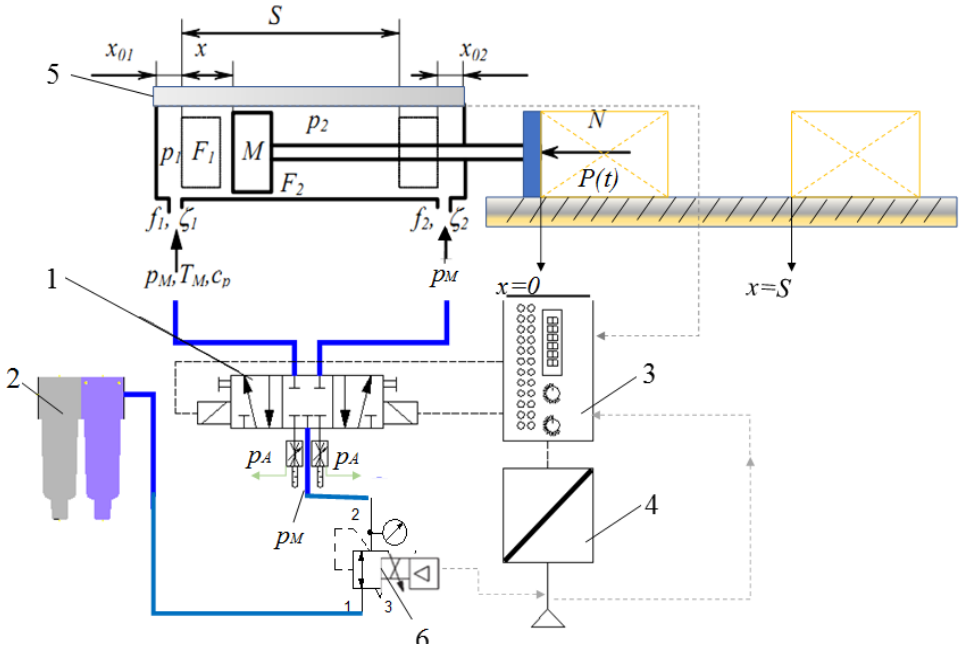

Figure 4. The structured control scheme of the power part of the positional pneumatic actuator with dynamic load:
1 – control divider 5/3 with closed lines in the central position, 2 – air preparation unit, 3 – controller, 4 – control signal converter of the automated control system.

In the Table 1, for ease of use, the equations, describing the kinematic parameters of a moving product (piston) in a four-stage mode, when T and Q_{max} are known.

The changing of parameters of the movement product process on a fixed flat and the operating parameters of the positional actuator when Q_{max} = 20 H; weight of artificial

product m_c =0.5 kg; f = 0.3; S = 0.2 m; $F_1 = 4{,}9 \cdot 10^{-4}$ m^2; $F_2 = 3.77 \cdot 10^{-4}$ m^2;

f_1^e is variable, depending on the diameter of the main pipeline; $P_m = 5 \cdot 10^5$ Pa; $m = m_{gr} + m_p = 0{,}5 + 1{,}5 = 2$ kg, where $m_p = 1{,}5$ – the mass of moving parts of the pneumocylinder; $P_{d.tr} = 20$ N – is the dynamic load of the pneumocylinder is shown in Figure 5.

Table 1

Calculation formulas for determining the kinematic parameters of the moving load by a collision mechanism with a pneumatic actuator in the implementation of the motion law approximating to the optimal velocity

Stage	Calculation formulas
I	Initial conditions: $t = 0;\ x = 0;\ \dot{x} = 0; \ddot{x} = 0$. $\ddot{x}_I = A_1 \cdot \sin(a_1 x)\ , a_1 = \frac{\pi}{2x_{I\text{к}}};$ $A_1 = \ddot{x}_{II} \cdot \dot{x}_I = \sqrt{2 \cdot \frac{A_1}{a_1} \cdot (1 - \cos(a_1 \cdot x))}$ $t_1 = \int_0^{x_{I\text{к}}} \frac{dx}{\sqrt{2\frac{A_1}{a_1} \cdot (1 - \cos(a_1 \cdot x))}}$ Final conditions: $t_{I\text{к}} = t_I;\ \ddot{x}_{I\text{к}} = \ddot{x}_{II};\ x = \dot{x}_{I\text{к}};\ \ddot{x} = x_{I\text{к}}$.
II	Initial conditions: $t_{II\text{н}} = t_1;\ \ddot{x}_{II\text{н}} = \ddot{x}_{II};\ \dot{x}_{II\text{н}} = \dot{x}_{I\text{к}};\ x_{II\text{т}} = x_{I\text{к}}$. $\ddot{x}_{II} = \frac{Q}{m} - g \cdot ƒ;\quad \dot{x}_{II} = \sqrt{\dot{x}^2{}_{I\text{н}} + 2 \cdot (\left(\frac{Q}{m} - g \cdot ƒ\right) \cdot (x - x_{II\text{н}}))};$ $t_{II} = \frac{\dot{x}_{II\text{к}} - \dot{x}_{II\text{н}}}{\frac{Q}{m_c} - g \cdot ƒ}$ Final conditions: $t_{II\text{к}} = t_I + t_I;\ \ddot{x}_{II\text{к}} = \ddot{x}_{II};\ \dot{x} = \dot{x}_{II\text{к}};\ x = x_{II\text{к}}$
III	Initial conditions: $t_{III\text{н}} = t_{II\text{к}};\ \ddot{x}_{III\text{н}} = \ddot{x}_{II\text{к}};\ \dot{x}_{III\text{н}} = \dot{x}_{II\text{к}};\ x_{III\text{н}} = x_{II\text{к}}$ $\ddot{x}_{III} = B_3 + A_3 \cdot \sin(q_3 \cdot x + b_3)$ $A_3 = \frac{\lvert\ddot{x}_{II}\rvert + \lvert\ddot{x}_{IV}\rvert}{2};\ B_3 = \frac{\lvert\ddot{x}_{II}\rvert + \lvert\ddot{x}_{IV}\rvert}{2};\ b_3 = \pi - a_3 * x_\tau$ $a_3 = \frac{0.45 \cdot (p_{2n} + p_{2k}) \cdot k \cdot F_2 - \dot{p}_1 \cdot F_1 (s + x_{02} - x)}{(s + x_{02} - x) \cdot m \cdot A_3}$ $\dot{x}_{III} = \sqrt{2 \cdot (B_3 (x - x_{III\text{н}}) - \frac{A_3}{a_3} \cdot \cos(a_3 \cdot x + b_3) + \frac{x_{II\text{н}}{}^2}{2}}$ $t_{III} = \int_{x_{3\text{к}}}^{x_{3\text{н}}} \frac{dx}{2 \cdot (B_3 \cdot (x - x_{III\text{н}}) - \frac{A_3}{a_3} \cdot \cos(a_3 \cdot x + b_3) + \frac{\dot{x}_{III\text{н}}{}^2}{2}}}$ Final conditions: $t_{III\text{к}} = t_I + t_{II} + t_{III};\ \ddot{x}_{III\text{к}} = \ddot{x}_{IV};\ \dot{x} = \dot{x}_{III\text{к}};\ x = x_{III\text{к}}$
IV	Initial conditions: $t_{IV\text{н}} = t_{III\text{к}};\ \ddot{x}_{IV\text{н}} = \ddot{x}_{IV};\ \dot{x}_{IV\text{н}} = \dot{x}_{III\text{к}};\ x_{IV\text{н}} = x_{III\text{к}}$ $\ddot{x}_{IV} = -g \cdot ƒ\ ;\quad \dot{x}_{IV} = \sqrt{2 \cdot g \cdot ƒ\,(s - x)};\quad t_{IV} = {\dot{x}_{IV\text{н}}}/{g \cdot ƒ}$ Final conditions: $t_{IV\text{к}} = T_r;\ \ddot{x}_{IV\text{к}} = \ddot{x}_{IV};\ \dot{x}_{IV\text{к}} = 0;\ x = s$

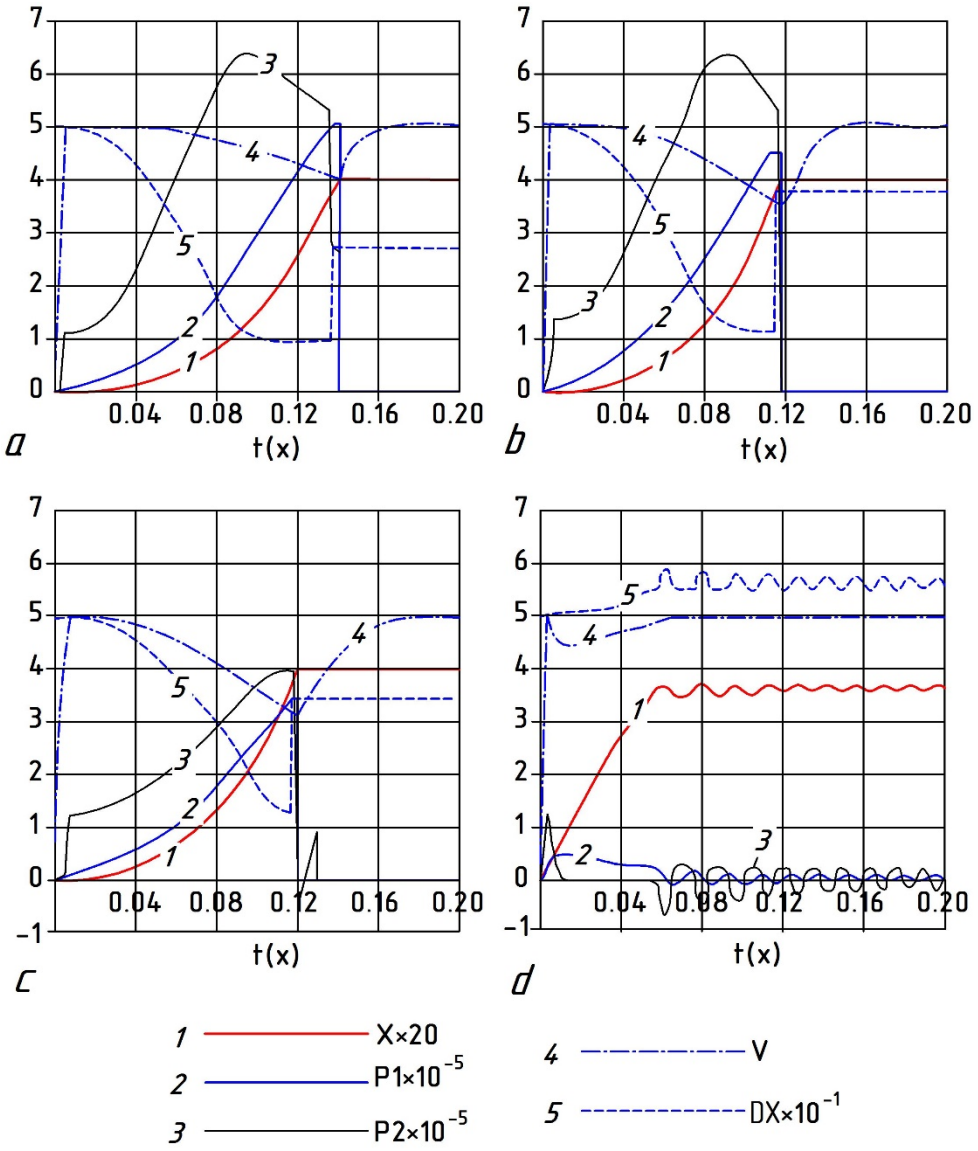

Figure 5. The generalized results of the modeling of the kinematic load and the pressure variation of the working position pneumatic actuator (without taking into account h – the coefficient of viscous friction of the piston in the pneumatic cylinder) with the minimization of the movement time of the artificial product:

a – the diameter of the pipeline is 10mm, $f_1^e = 7.854 \cdot 10^{-5}$ m^2,
b – the diameter of the pipeline is 8 mm, $f_1^e = 5.027 \cdot 10^{-5}$ m^2,
c – the diameter of the pipeline is 6mm , $f_1^e = 2.827 \cdot 10^{-5}$ m^2,
d – the diameter of the pipeline is 4mm , $f_1^e = 1.257 \cdot 10^{-5}$ m^2;

x – the coordinate of the piston movement (m); V – the speed of piston movement (m/s); Dx – the acceleration of piston movement; P_1 – pressure in the piston chamber of the pneumocylinder (Pa); P_2 – the pressure in the rod end of the pneumocylinder (Pa); t – time movement (s).

Thus the resultant of all resistance forces at I, II and III stages of the kinematic links movement:

$$\boldsymbol{P(x) = P_{friction\ force} + (m_c + m_n)\ddot{x} + m_c gf + p_a(F_1 - F_2)} \quad (11)$$

The resultant of all resistance forces at stage IV:

$$\boldsymbol{P(x) = P_{friction\ force} + m_n\ddot{x} + p_a(F_1 - F_2)} \quad (12)$$

Figure 5 shows the graphs of the dependence of kinematic parameters from the time of movement of an artificial product in the implemented mode and the pressure change in the working cavities of the pneumocylinder (the power part of the position actuator).

Conclusion

The output link movement of the experimental MFM, the pneumo-cylinder rod of the electro-pneumatic positional actuator are implemented and mathematically described. The conditions of the initial difference of air pressure are taken into account. The mathematical description of the rod movement law, which is optimal for the speed of action, is obtained. In the obtained results, it is clearly observed that when the exhaust section of the working cylinder of the positional pneumatic actuator is narrowed, the value of the inertial component at stage 4 (deceleration) increases. In addition, given the complexity of the working environment, – compressed air – it is necessary to apply the additional parameters: viscous friction coefficients of the working kinematic pair of piston-rod, resistance coefficients in the exhaust section in the implementation of the fourth stage of motion.

The movement of products on a fixed reference flat by a mechanism of collision with an electro-pneumatic positional pneumatic actuator with consideration of the control system is researched.

The proposed analytical dependences allow:

- to set the working body the law of translational motion, approximating to the optimal speed, without exceeding the maximum permissible dynamic load for the moving load;
- to move the artificial product from the initial position to the final in the shortest possible time for the pneumatic actuator;
- to analyze the existing structures of operating actuators with pneumatic actuators.

References

1. Doherty J., McGinn T. (1988), Automated hybrid package sealing system*, Electronic Manufacturing Technology Symposium,* Fifth IEEE/CHMT International, pp. 183–187.
2. Bogomolov V., Kramskoy A., Kudryavtsev I., Pyatak A., Bondarenko S., Murinets-Markevich B., Plammer M. (2003), K voprosu o vyichislenii pokazatelya politropyi dlya porshnevogo pnevmaticheskogo dvigatelya*, Vestnik HNADU i Severo-Vostochnogo Nauchnogo Tsentra Transportnoy Akademii Ukrainy*, 21, pp. 14–17.
3. Krivts I., Krejnin G. (2006), *Pneumatic Actuating Systems for Automatic Equipment: Structure and Design,* CRC Press Taylor & Francis Group, Boca Raton.
4. Ilyuhin Yu. (2009), *Pozitsionnyie i sledyaschie elektropnevmaticheskie privodyi. Mehatronnyie resheniya Kamotstsi*.
5. Galnaitytė A., Kriščiukaitienė I., Baležentis T., Namiotko V. (2017), Evaluation of Technological, Economic and Social Indicators for Different Farming Practices in

Lithuania, *Economics and Sociology*, 10(4), pp. 189–202, DOI:10.14254/2071-789X.2017/10-4/15
6. Uebing M., Vaughan, N. (1997), On linear dynamic modelling of a pneumatic servosystem*, Proceedings of the FIfth Scandinavian International Conference on Fluid Power SICFP'97*, *vol. 2*, Linkoping.
7. Virvalo T. (2016), Comparing different controllers of electropneumatic position servo, *Proceedings of the Third JHPS International Symposium*, Yokohama.
8. Smaoui M., Brun X., Thomasset D. (2006), *A study on tracking position control of an electro pneumatic system using backstepping design,* Control Eng Pract.
9. Ahn K., Yokota S. (2005), Intelligent switching control of pneumatic actuator using on/off solenoid valves, Mechatron, 15, pp. 683–702, DOI:10.1016/j.mechatronics.2005.01.001.
10. Richard E., Hurmuzlu Y. (2015), A High Performance Pneumatic Force Actuator System, Part 2-Nonlinear Controller Design, *ASME J. Dyn. Syst., Meas., Control*, 122.
11. Shu N., Bone G. (2002), High Steady Acuuracy Pneumatic Servo Positioning System with PVA/PV Control and Friction Compensation, *Proceeding of the IEEE.International Conference on Robotics&Automation*, Washington.
12. Perez-Meneses J. (2003), Dynamic analysis of pneumatically driven mechanisms, *Department of Mechanical Engineering*, University of Guanajuato.
13. Janiszowski K. (2005), Adaptation, modeling of dynamic drives and controller design in servomechanism pneumatic systems, *IEE Proceedings, on Control Theory and Applications*, 151.
14. Janiszowski K., Kuczyński M. (2007), Fast prototyping approach in developing low air consumption pneumatic systems, *Mechatronics*, Springer.
15. Kinyckyi Ya. (2008), *Problems and tests on theory of mechanisms and machines*, Naukova Dumka, Kyiv.
16. Kinyckyi Ya. (2002), *Theory of mechanisms and machines*, Naukova Dumka, Kyiv.
17. Czyżewski A., Smędzik-Ambroży K. (2015), Specialization and diversification of agricultural production in the light of sustainable development, *Journal of International Studies*, 8(2), pp. 63–73, DOI: 10.14254/2071-8330.2015/8-2/6
18. Kinyckyi Ya., Kharzhevskyi V. (2006), *Analytical methods of analysis and synthesis of mechanisms*, KhNU, Khmelnytskyi.
19. Harchenko A. (2008), Razrabotka elektropnevmaticheskih sledyaschih privodov dlya transportnyih robotov na baze mehatronnyih komponentov, *Aktualnyie problemyi zaschityi i bezopasnosti: Trudyi Odinnadtsatoy Vserossiyskoy nauchno-prakticheskoy konferentsii* (1–4 aprelya 2008 g.), Sankt-Prterburg.

Thermal destruction kinetics of coal and solid biomass mixtures

Natalya Dunayevska[1], Yaroslav Zasiadko[2], Taras Shchudlo[1]

1 – Coal Energy Technology Institute of National Academy of Science of Ukraine, Kyiv
2 – National University of Food technologies, Kyiv, Ukraine

Keywords:

Coal
Biomass
Combustion
Kinetics
Donetsk coal basin

Article history:

Received 14.04.2018
Received in revised form 01.07.2018
Accepted 27.12.2018

Corresponding author:

YaroslavZasiadko
E-mail: iaroslav@nuft.edu.ua

DOI:
10.24263/2304-974X-2018-7-4-17

Abstract

Introduction. The work deals with the research on the kinetics of constituent stages of the combustion process of biomass as an individual fuel and as blends with low reactive anthracite coal from the Donetsk Coal Basin.

Materials and methods. The samples of biomass (including the wastes of agricultural and food industries) and Ukrainian from the coal Donetsk Basin were studied by means of non-isothermal TGA. Kinetic studies of the samples was carried out on the Paulik-Paulik-Erdei Q-1000 system derivatograph with the integrated complex of the synchronous data analysis of the STZ 449 Jupiter NETZSCH in the air atmosphere with the heating rate of 20 °C/min within the temperature interval 25–1000 °C.

Results and discussion. Raw data were processed and generalized within differential and integral approaches. It has been shown that the differential method of data processing has to be used coupled with the determination of current normalized values of mass change rate derivative, which presents a serious difficulty. In this respect the integral approach looks more acceptable. Comparison of approximations has been presented. It has been shown that the Coats-Redfern approximation in a form of a series does not increase the approximation accuracy if an increased number of the series members is taken into account. The appropriate range of correlations has been determined by means of the parameter $E/RT>4$ which is valid for the dehumidification and devolatilization regions. For the processes of the coke burnout the correlation of Senum-Yang looks more appropriate.

The obtained set of kinetic constants were used with the appropriate form of the Arrhenius type differential equation and the sample mass loss thermal histories were calculated. The deviation between calculated and experimental values of the sample mass loss does not exceed 10% within a whole temperature range 0–700 K.

Conclusions. The methodology of the constituent stages distinguishing and obtained kinetic constants can be used in engineering calculations of the combustion constituent stages duration and fuel components balance as well as development of process sub models for 3-d simulations.

Introduction

The design of high-performance burners and furnaces should be based on the calculations of the current and local distribution of fuel and oxidant components, the intensity of reactions and heat generation across the device's zones. This, in turn, involves the need to determine the duration of individual stages of the combustion process, comprising in succession: dehydration, volatiles release and coke residue burnout. Thus the knowledge of the adequate values of the kinetic constants of separate stages of the overall burning process of solid fuel becomes critical in the design calculations of burners and furnaces. It should be noted that today the topics of the kinetic studies of solid fuels thermal degradation became an undisputed leader among the research in the field of thermophysics of combustion and multidisciplinary studies on the processing and preparation of solid fuels in the energy sector [1–8]. This is due to the involvement of a variety of biomass types which is used as an alternative fuel in the national energy sectors of countries, both for the purpose of substantially expanding the market of energy resources and with the need to utilize a large amount of solid household waste, waste from the agrarian and food industries [1–7].Wide implementation of co-combustion technologies into the national power sectors renders revitalization effect on the environments, since the said technology allows a significant decrease of harmful substances release primarily into the atmosphere [10]. Knowledge of kinetic parameters becomes especially critical when designing units for co-firing of coal and solid biomass, especially for the pulverized coal combustion, since shredding biomass to the fineness of pulverized coal dust appears cost prohibitive. The technologically attainable sizes of crushed biomass typically surpass typical sizes of coal dust particles by 2–4 orders. Under these circumstances, particular attention should be paid to the proper designing of boiler furnaces and pulverized solid fuel burners to ensure the complete burnout of the coke residue of biomass.

It is obvious that the critical residence time of biomass particles will be determined by the duration of the constituent stages of the overall combustion process, which includes processes of dehydration, release and combustion of volatiles, as well as the burnout of coke residues [4, 5, 11].

Materials and methods

Experimental Materials

The samples of domestic high-ash and low-reactivity coal anthracite grade (type ASHA), pine pellets, wheat straw pellets, soy pellets, saw dust as individual fuels and their blends were investigated. The proportions of coal: biomass 50:50 and 90:10. The data of technical analysis of the studied samples are given in Table 1.

Table 1

Technical analysis of the studied samples

Fuel type	Volatiles (dry) V^d,%	Ash (dry) A^d,%	Moisture W^r,%
Pine Saw Dust 1	82,93	2,90	8,30
Pine Saw Dust 2	83,06	0,90	10,00
Wheat Straw Crushed Pellets	74,52	8,90	9,20
Rape Crushed Pellets	73,08	11,20	9,60
Corn Crushed Pellets	70,55	15,00	10,60
Soy Crushed Pellets	73,82	11,80	11,40
Anthracite Coal (ASHA grade Rus.)	4,690	29,68	1,15

Experimental setup

Kinetic studies of the samples were carried out on the Paulik-Paulik-Erdey Q-1000 system derivatograph with the integrated complex of the synchronous data analysis of the STZ 449 Jupiter NETZSCH in the air atmosphere with the heating rate of 20^0 C/min. in the temperature range 25–1000 °C.

Primary experimental data were obtained in the form of spread sheets, as well as in graphic form. The thermograms of ASH coal and milled pine pellets are shown in Figure 1 and 2. Apparently, the initial data include the curves of the current mass, temperature, mass change rate (the first derivative dm (τ)/dτ) and the rate of mass derivative change (second derivative of mass change in time during the experiment).

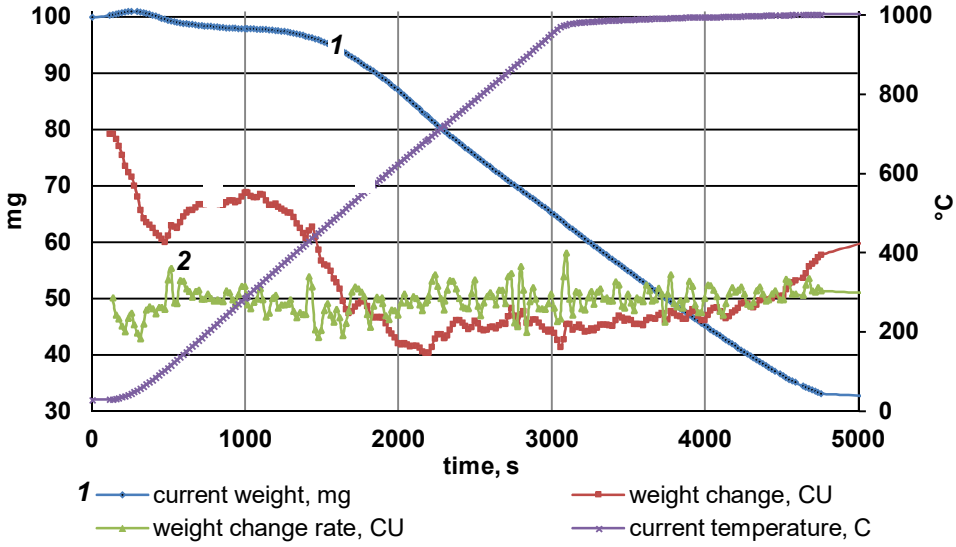

Figure 1. Derivatogravitogram of anthracite coal thermal destruction

The given in Figures 1 and 2 data for two fuels with critically different physical properties have qualitatively similar thermogravitograms which, however, differ considerably. So, assuming that the constituent stages of the general process of thermal destruction (dehydration, volatile yield, coke-coal residue burning) are described by the Arrhenius equation according to the model of the first reaction order, then one should expect a sort of conformity between the sample mass change in time and the character of its derivative [3, 11]. This implies that, if the process can be described by the exponential function and the degree of conversion of a particular component ranges from 0 to 1, then the change of the normalized derivative should be from zero through the local minimum and then back to zero value. The said would hold true if the process has finished completely. If the process is being superseded by the next one, then the derivative of the mass change whilst approaching zero value would not reach it.

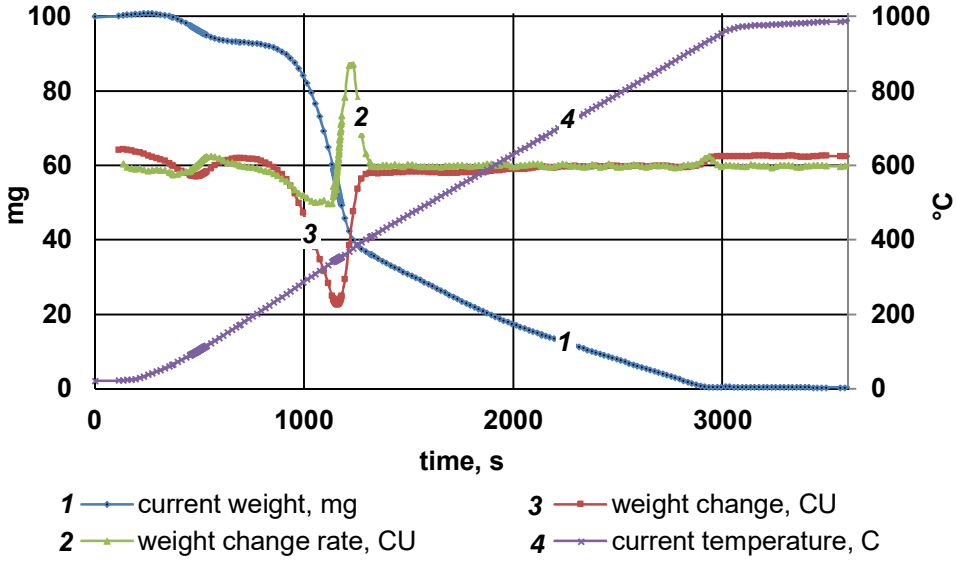

Figure 2. Derivatogravitogram of thermal destruction of pine pellet

This can be clearly seen in Figure 2, line 3 which shows two negative local extremums associated with the two consecutive processes – demoisturization and volatiles release. It should be marked that the derivative line 3 whilst coming back to zero value, nonetheless does not reach it, which signifies overlapping these processes.

In fact, this circumstance is clearly observed for processes only in case of coal biomass mixtures. For anthracite, it seems possible to identify as a complete process only the stage of moisture release, since the first derivative curve clearly shows the trend marked above, Figure1. Unfortunately, the boundary between the stages of volatile yield and the burnout of the coke residue for anthracite cannot be determined at all, since there is neither a change in the mass time change curve, nor a change in the derivative curve past 2000c (600^0 C) can be traced, (see Figure 1). Proceeding from the above, a number of foreign authors tried to analyze the entire process of thermal destruction of coal in the range $200 \div 800^0$ C, as is done in [12], or to correct the constants by choosing the various orders of the reaction, as model fitting methods in [5, 6]. However, the authors [12] provide kinetic equations in two temperature ranges, which indirectly indicate the presence of two distinct processes, and in [4] the whole destruction zone is divided into the region of pyrolysis and the actual burning of coke. This approach was accompanied with the introduction of very complex reaction models. For the pyrolytic region, the authors [4] proposed four separate reactions of the yield of volatile components and two separate reactions for the coke residue burning zone along with the two separate reactions for the oxidation medium.

Initial data of the dewatering process for anthracite, pine pellets and their mixtures are shown in Figure 3.

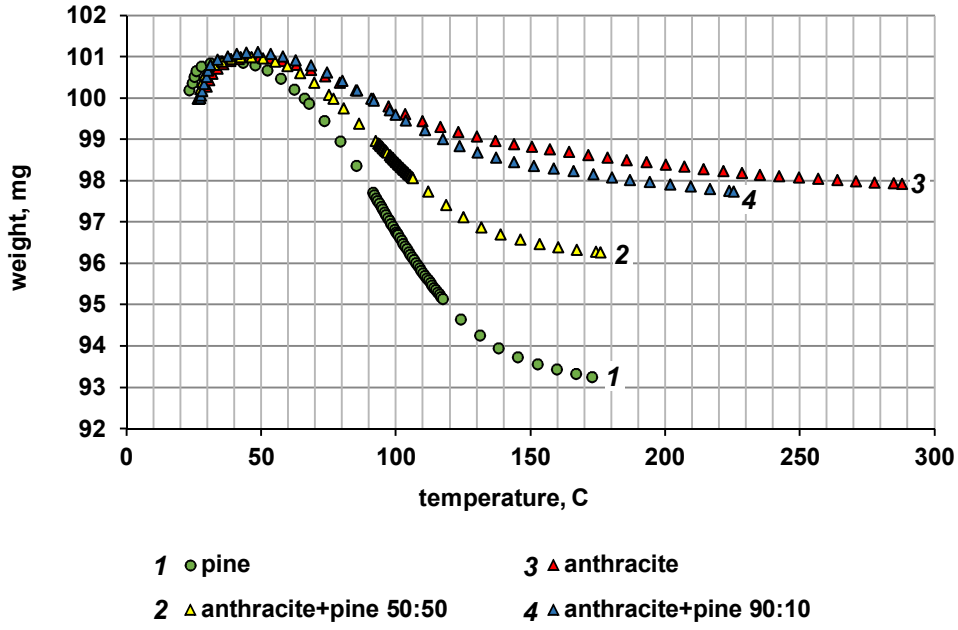

Figure 3. Gravitograms of sample mass change in time at a heating rate 20^0 C/min

For the stage of dewatering, the gravitograms for the significantly different types of fuel vary quantitatively, although they have similar character. For both individual fuels, an initial mass increase is observed, which is explained by the absorption of moisture from air, followed by a decrease in the mass of the sample, the rate of which gradually reaches the maximum, and then – decreases. The mixtures of two heterogeneous fuels show an intermediate nature, shifting towards anthracite as its share in the mixture grows. The comparison of gravitograms and derivatiograms for anthracite and pine pellets is shown in Figure 4 and 5. The given data are obtained under similar conditions in an oxidizing medium at a constant sample heating rate of 20 °C/min. As can be seen from Figure 4, the curve of the derivative of weight change, normalized to the interval from 0 to -1, is characteristic of the derivative of the exponential function, but does not reach the 0-th value at the end of the process, having a specific negative value that testifies to the further progress of the sample mass loss. This may be attributed to the parallel development of the next process which would be the stage of devolatilization.

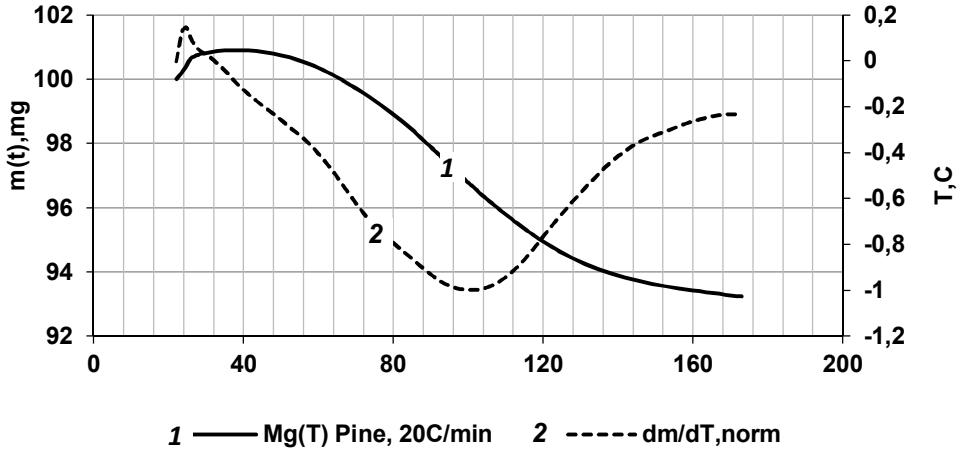

Figure 4. Thermogravitogram and Derivatogram of moisture release at thermal destruction of pine pellets

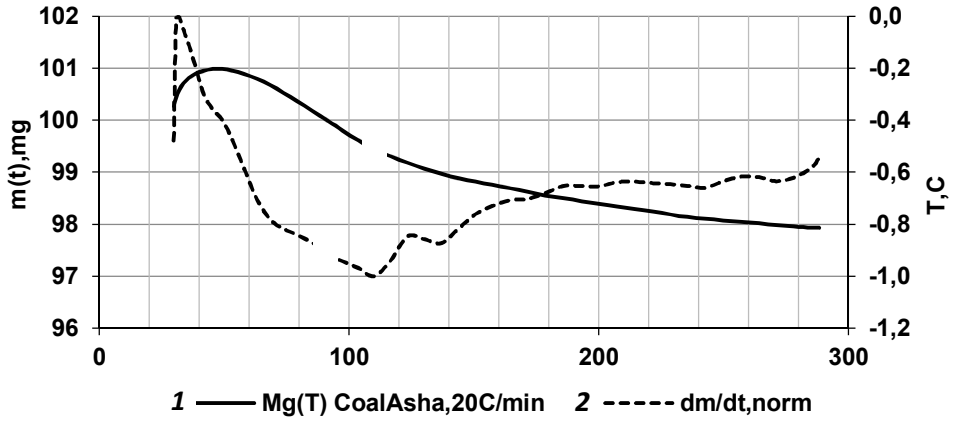

Figure 5. Thermogravitogram and Derivatogram of moisture release at thermal destruction of anthracite coal (ASH)

It is quite probable that such a change in the da/dt curve may be attributed to the beginning of the coke burout. It is wothnoticing, that even a slight share of highly volatile biomass in the mixture causes a noticeable change in the gravitograms and derivatograms profile. In Figure 7, all derivatograms have clear minimal values positioned within a temperature range of 340–350° C. It is also evident that the lower the share of biomass in mixture, the closer the curve approaches "0", which signifies that preceeding process practically approaches its end with the complete exhausting volatiles. Only after this, the coke burnout stars, which is being proven by the following mass loss of samples.

According to the analysis of the primary experimental data the following conclusions may be drawn up:

- the derivatograms and gravitograms of anthracite, biomass and their mixtures differ significantly; for the process of moisture release the curves for all substances retain a

similar trend with a characteristic minimum of derivatograms, after which the da/dt curve approaches the 0 value, which signifies exhaustion of moisture in a sample;
- for all samples of individual fuels and their mixtures the completion of dehydration process coincides with the beginning of the following process of devolatilization, which is proven by the residual values of da/dt not equal to 0;
- the process of volatiles release for biomass and mixtures retain certain similarities insofar all derivatigrams show local minimum, after which the derivatives approach zero, which signifies the completion of the process. For anthracite samples no such trends have been marked, since the derivatogram does not show any marked extremum within a whole range 350–1000 °C;
- the gravitograms and derivatograms of anthracite coal thermal destruction do not allow to identify and separate the processe of volatiles release and coke burnout.

Data analysis and processing

Modern TGA and DTG methods coupled with the application of infrared spectroscopy and differential calorimetry are widely used in almost all physical and technical branches of science [1–3, 10–14], the substances ranged from food products, polymers and solid household wastes, biofuels and fossil fuels were analyzed with these methods. Such diversity caused the need for the development of perfect methods of processing and generalization of experimental data [3, 5, 11, 13-15]. Following [11, 14], it is possible to provide the following classification of analysis methods (see Table 2).

Table2

Main methods of kinetic constants determination [1,12]

Model Methods		Model Free Methods	
Isothermal	**Dynamic**	**Isothermal**	**Dynamic**
Standard	Differential: Freeman-Carrol Coats-Redfern	Friedmann	Kissinger–Akahira–Sunose Flinn-Wall-Ozawa

The advantage of a non-isothermal (dynamic) method is thata single non-isothermal thermogravimetric experiment allows obtaining a set of data related to the sample mass loss as a result of its heating, which in turn, allow calculating the kinetic constants of a process, and thus replaces the receipt and processing of a series of isothermal curves. We used non-isothermal methods of TG analysis for the study of kinetic characteristics of processes of thermal degradation of fuels, including dehydration and volatile yield and coke residue burnout. The dynamic TG analysis is applied with further processing of experimental data by means of one of the following: differential, integral and isoconversional [3,14] methods.
The change in the mass of a solid in a certain process can be mathematically described by one equation, using physical constants and corresponding model functions [2, 3, 11]:

$$\frac{dm(\tau)}{d\tau} = -k \cdot f(m(\tau)) \quad (1)$$

where: $\frac{dm(\tau)}{d\tau}$ - the current at the time of mass of a certain component in the experimental sample; k – constant of the reaction rate; $f(m(\tau))$ – a function that describes a particular reaction model.

The degree of conversion is determined on the basis of taking into account the change in the mass of a sample at the beginning of the process, at the end of the process and at the time (τ):

$$\alpha = (m_0 - m_\tau) / (m_0 - m_\infty), \quad (2)$$

where: m_0 - the initial mass of the sample; m_∞ - sample mass at the end of the process under consideration; m_τ - sample mass at (τ).

It should be borne in mind that the term "conversion" in this case applies exclusively to the process under consideration. That is, in the case of considering the process of moisture release when the particle is heated, it is about the conversion of moisture, while in considering the process of release of volatile – this will mean the conversion of the combustible mass of the sample with the release of combustible gases. The corresponding quantities in (2) relate solely to a particular process. In this case, the difference in the denominator of formula (2) is determined by the value of that component of the fuel involved in the transformation. Obviously, for example for moisture release, it is critical to determine precisely the time of the process beginning, along with precise values of respective masses of components, process completion and the start of the next (release of volatile) process and, accordingly, determining the mass balance of the next reacting component. For dehydration completion, for example, this is the point where the second derivative of the mass change function passes through a zero value in the range 170–200 °C, changing the sign from "+" to "-", that is, where the local reaction rate becomes the minimum value, but would not reach zero precisely, since the final stages of demoisturization coincide with the beginning of the next process.
The constant of the reaction rate is given in the form of the Arrhenius equation:

$$k = A \cdot \exp(-E / RT)$$

where: A – the pre-exponential multiplier, 1/s; E – activation energy, J/mol; R – universal gas star – 8,314 J/(mol·K); T – temperature, K.
Taking into account the Arrhenius equation and (2), equation (1) acquires the form:

$$\frac{d\alpha}{d\tau} = A \cdot \exp(-E / RT) \cdot f(\alpha). \quad (3)$$

A detailed analysis of the methods for applying the equation (2) for processing the experimental data of the TG analysis and the analysis of reaction models is given in [1,3,4,11,12],

When the sample is heated at a constant rate, the dependence of temperature change over time:

$$T = \beta \cdot \tau + C, \quad (4)$$

where β is the heating rate.

Combining (3) and (4) and adopting the first-order reaction model, we obtain

$$\frac{d\alpha}{dT} = -\frac{A}{\beta} \cdot \exp\left(\frac{-E}{RT}\right) \cdot (1-\alpha), \quad (5)$$

or, after logarithm:

$$\ln\left(\frac{\beta}{1-\alpha}\frac{d\alpha}{dT}\right) = -\frac{E}{RT} + \ln A. \quad (6)$$

Equation (6) forms the methodological basis of the differential approach to the kinetic constants determination on the basis of thermogravimetric studies and is the basis of the well-known Friedmann method [9, 14].

Despite its apparent simplicity, the Friedmann method has significant drawbacks related to the need of determining the left side of (6) by the values of current conversion rates and the derivative of the time-varying mass change function. As stated above, the definition of the current conversion rate requires not only the measurement of the current sample mass, but also the determination of the initial content of the component and its total content in the mixture. In many cases gravitograms show initial increase in mass associated with the absorption of moisture when biomass is heated. Moreover, it is often impossible to determine exactly the content of the target component at the end of the process insofar the final stage of the process coincides with the beginning of the consecutive one. The next critical point of this methodology is also the need to scale the value of the derivative $\frac{d\alpha}{dT}$, based on the actual mass loss curve, which becomes extremely complex due to the above mentioned.

In accordance with the integral approach, which has become widespread [7, 9, 14] in recent years, equations (6) is being integrated

$$\beta\int_0^{\alpha}\frac{d\alpha}{1-\alpha}=\beta\cdot Ln(1-\alpha)=-A\int_0^{T}\exp\left(-\frac{E}{RT}\right)dT. \qquad (7)$$

Since the expression on the right side (7) does not integrate analytically, a large number of expressions are proposed for obtaining acceptable approximations, usually in the form of series or rational fractions [6, 10–12, 15]. In [11] it is proposed to apply the method of integration by parts. Having introduced a new variable $x=\frac{E}{RT}$, one obtains. $g(\alpha)=-\frac{AE}{\beta R}\int_{\infty}^{x}\frac{\exp(-x)}{x^2}dx.$ Let us analyze the function $p(x)=\int_{\infty}^{x}\frac{\exp(-x)}{x^2}$ which we then integrate by parts several times:

$$\int_{\infty}^{x}\frac{\exp(-x)}{x^2}dx=\frac{e^{-x}}{x^2}-\int_{\infty}^{x}\frac{2e^{-x}}{x^2}dx,$$

$$\int_{\infty}^{x}\frac{2e^{-x}}{x^3}dx=\frac{-2e^{-x}}{x^3}+\int_{\infty}^{x}\frac{6e^{-x}}{x^4}dx,$$

$$\int_{\infty}^{x}\frac{6e^{-x}}{x^4}dx=\frac{6e^{-x}}{x^4}-\int_{\infty}^{x}\frac{6\cdot 4e^{-x}}{x^5}dx$$

,

or in general:

$$p(x)=\frac{e^{-x}}{x^2}\left(1-\frac{2}{x}+\frac{6}{x^2}-\frac{24}{x^3}+\square\square\square+(-1)^{n-1}\frac{n!}{x^{n-1}}\right).$$

Having taken two members of the series, one obtains the well-known approximation of Coats-Redfern [7], which leads tothe following:

$$Ln\left[\frac{-Ln(1-\alpha)\cdot\beta}{T^2\left(1-\frac{2RT}{E}\right)}\right]=Ln\left(\frac{AR}{E}\right)-\frac{E}{R}\frac{1}{T}. \quad (8)$$

Using n-members of the series leads to the general form of equation:

$$Ln\left[\frac{-Ln(1-\alpha)\cdot\beta}{T^2\left(1+\sum_2^n(-1)^{n-1}\frac{n!}{x^{n-1}}\right)}\right]=Ln\left(\frac{AR}{E}\right)-\frac{E}{R}\frac{1}{T}. \quad (9)$$

The equations (9) and (10) allow determining of the kinetic characteristics based on the results of TG experiments using only the current mass loss data, without resorting to the complicated determination of the mass change derivatives over time.

Recently, a number of the Arrhenius temperature integral approximations have been proposed on the basis of polynomial fractions [6, 13, 15]. The most promising appears the Senum –Yang approximation [11]:

$$p(x)=\frac{e^{-x}}{x^2}\left(\frac{x^4+18x^3+86x^2+96x}{x^4+20x^3+120x^2+240x+120}\right), \quad (10)$$

Having introduced (10) into (7), one obtains

$$Ln\left[\frac{-Ln(1-\alpha)\cdot\beta}{T^2\frac{x^4+18x^3+86x^2+96x}{x^4+20x^3+120x^2+240x+120}}\right]=Ln\left(\frac{AR}{E}\right)-\frac{E}{R}\frac{1}{T}\ . \quad (11)$$

Thus, in general the determination of kinetic constants by either integral or differential methods consists in analyzing correlations in the form Y=f(1/T). Where Y is taken equal: $\ln\left(\frac{1}{1-\alpha}\frac{d\alpha}{dT}\right), \ln\left(\frac{\beta}{T_{\max}^2}\right)$ or right hand side of (8), (9), (11). Experimental data would be approximated by linear function of 1/T with the slope of $\frac{E}{R}$ and an intercept – a function of the frequency factor. Since the correction multipliers in the denominators of (9) and (11) are the functions of the sought values *E* and *A,* the application of (9) and (11) can be utilized through the iterative approach, whereas at first one assumes the values of correction functions in (9,11) equal unity and determines respective values E_1 and A_1, which then are to be used for determination of correction multipliers for equations (9) or (11) and further allow to determine the new paired values of E_2 and A_2. The procedure may be repeated until the stated precision has been reached.

Results and discussion

Data Generalization

The primary data of the derivatograms were processed according to the differential method which allowed determining the temperature ranges and mass loss of the individual stages of samples thermal degradation (Table 3).

Table 3

Temperature ranges and mass loss of individual stages of thermal decomposition of biomass samples

Fuel	Thermal Destruction Stage								
	Dehumidification			Volatiles Release			Coke Burnout		
	Range, °C	Maximum, °C	Mass Loss,%	Range, °C	Maximum, °C	Mass Loss,%	Range, °C	Maximum, °C	Mass Loss,%
Pine Saw Dust 1	27–120	65	7,20	120–416	301	79,80	416–697	n/a	13,00
Pine Saw Dust 2	32–136	56	6,80	136–404	307	77,20	404–610	n/a	16,00
Wheat Straw Pellets	24–187	100	6,18	187–440	290	62,60	440–920	n/a	31,19
Rape Pellets	23–194	103	9,54	194–418	303	57,98	418–872	n/a	32,32
Corn Pellets	24–186	99	9,44	186–416	281	58,02	416–940	n/a	32,51
Soy Pellets	23–161	98	9,23	161–404	294	56,79	404–898	n/a	33,89

As can be seen from the data in Table 3, the coke-ash residue burnout stage reaches a temperature of 1000 °C. For moderate values of the variable x in (9–11), for which the temperature integral was approximated, may decrease to 3–3.5. Since the accuracy of the approximation of the temperature integral (7) depends on the value of the variable and decreases when the values are lower than 5–6, it is necessary to estimate the approximation error and the applicability of the Coates-Redfern method for data processing for the kinetics of burning of the coke residue, that is, at the temperature range greater 600–800 °C. To evaluate the accuracy of the approximation, the integral (7) was calculated numerically in Mathcad and compared with the calculated approximation values. In addition, the 1st, 2nd and 3rd members of the series (10) were taken into account successively. The proposed Senum and Yang equation (13) is also calculated. Comparison of results in the form of the dependence of the relative error module on the parameter x are shown in Figure 6.

As it can be seen from the above, the accuracy of the temperature integral approximation by the series derived above sharply drops down when x lowers below 5. Moreover, since the series is a sign changing one, the accuracy of the approximation does not increase when the number of series members taken into account increases. At the same time the accuracy of the Senum-Yang approximation appears the most reliable even within the range of x lesser than 5.

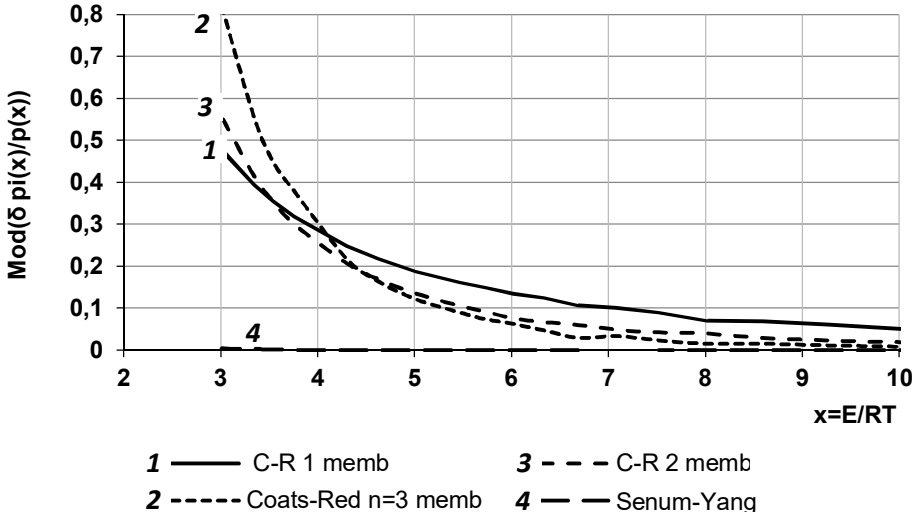

Figure 6. Module of Relative Error of Temperature Integral Series Approximation depending on the number of series members

The character of curves substantiates mentioned above. The divergence between the curves becomes apparent in the region of 1/T lower than 0.0012, which corresponds to the values of x (Figure 6) lesser than 5. At the same time, when approximating data within the lower temperature range, it would be expedient to use the Coats-Redfern method as it is simpler. It should be mentioned specifically that despite a noticeable difference in the values of the apparent activation energies, found from data in Figure7, the respective values of the frequency factor would render the opposite effect, when used in the Arrhenius equation (3) for the calculations of the degree of conversion rate.

Our experimental data processed as shown above by the successive approximations method are presented on Figure 7.

Figure 8 shows a series of data for the dewatering stage for anthracite coal grade, crushed pine pellets and their mixtures. As it is clearly seen, the lines that approximate data for mixtures are localized between such for individual fuels, which is quite natural. Coupled kinetic constants are easily derived from the equations presented in Figure 8. It should be pointed out that all experimental data tend to diverge from the straight lines, which proves that the complex processes of dehumidification, volatiles release and coke burnout can hardly be depicted by the first order reactions. Despite marked above divergence, the determined kinetic constants, being used in calculations by (3) the degree of conversion rate and the history of sample thermal degradation at heating, show their reliability. The results of Mathcad calculations of mass loss curves of heated samples are shown in Figure 9.

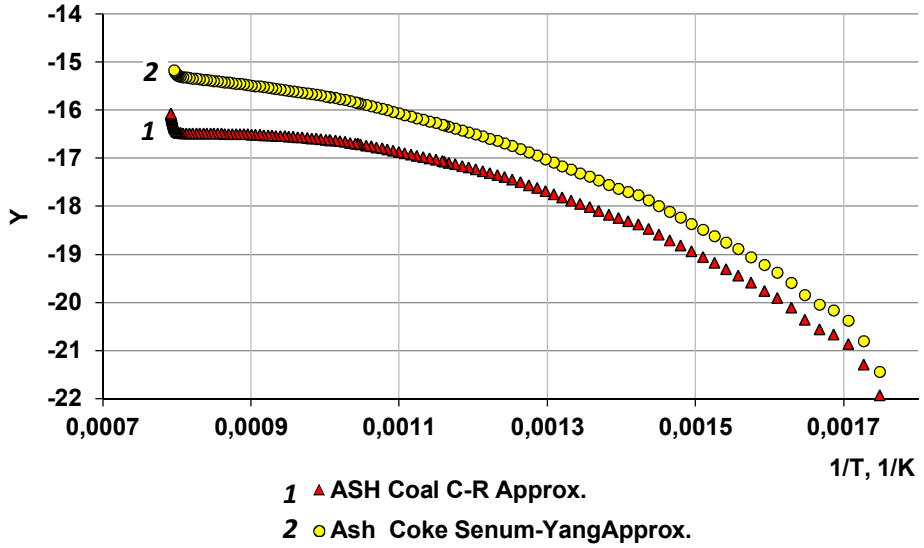

Figure 7. Comparison of data approximated by Coats-Redfern and Senum-Yang methods. Anthracite, coke burnout

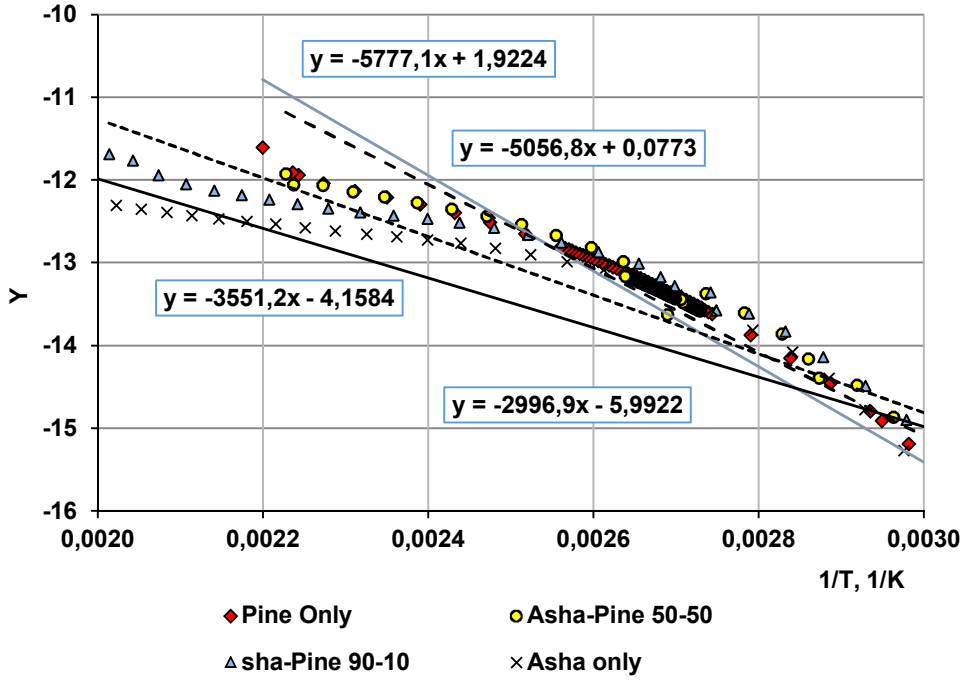

Figure 8. Correlation of Coats-Redfern parameter Y =f(1/T)

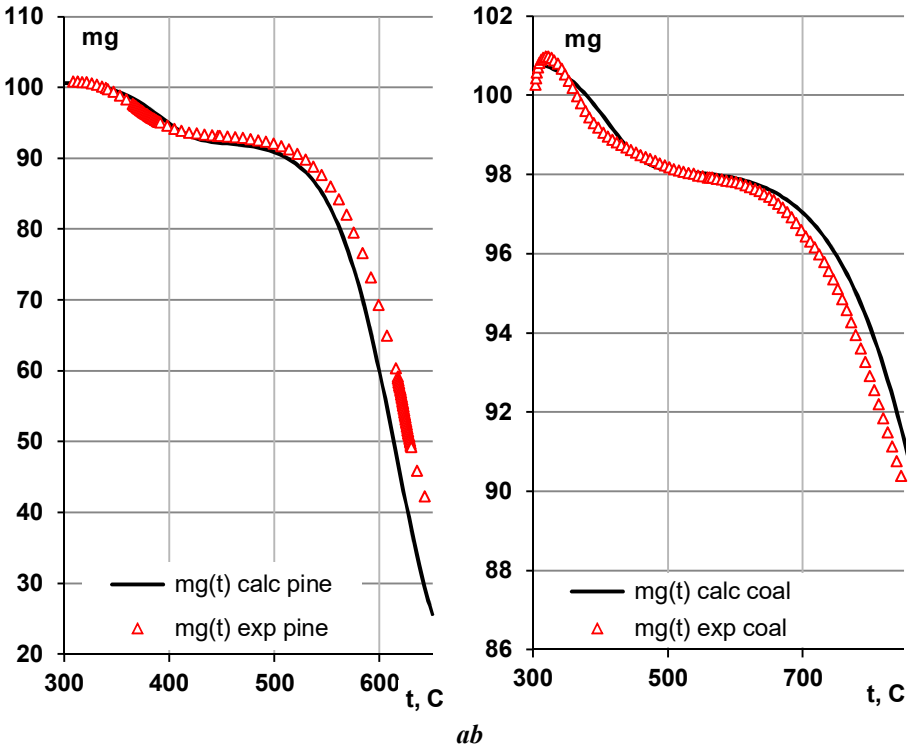

Figure 9. Sample mass loss at thermal destruction curves:
a – pine pellets; b – ASH coal

A system of differential equations $\frac{d\alpha_i}{dT} = \frac{A_i}{\beta} exp(-\frac{E_i}{RT}) \cdot (1-\alpha_i)$ has been solved according to the experimental conditions for dehumidification and devolatilization stages with further determination of current in temperature mass loss curve. As it may be seen, the obtained kinetic constants allow for the calculations of data in close correspondence with experimental data. The obtained kinetic constants are presented in Tables 4 and 5.

Table 4

Kinetic constants for the dehumidification stage (Coal ASH, biomass and mixtures)

Fuel	Frequency Fact., 1/s	Activ. Energy, J/(mol·K)	Temp. Range, °C
ASH Coal	7,432	24917,06	61,6-288,0
Pine Pellet	39483,565	48030,26	46,1-172,9
Straw Pellets	2848,674	40735,27	66,1-166,2
Mix. ASH_Pin50/50	5465,239	42043,06	46,8-176,1
Mix. ASH_Pin90/10	56,4754	29531,06	50,9-225,5
Mix. ASH_Straw90/10	7652,619	45699,56	82,3-185,7

Table 3

Devolatilisation kinetics of ASH coal, biomass and their mixtures

Fuel	Frequency Fact., 1/s	Activ. Energy, J/(mol·K)	Temp. Range, °C
Pine Pellet	20833,67	76562,79	172,9-411,2
Straw Pellets	5,861945	36527,56	166,2-407,6
Mix. ASH_Pin50/50	27603,07	76559,47	176,1-407,1
Mix. ASH_Pin90/10	267478,2	89092,82	225,5-400,6
Mix.ASH_Straw90/10	34136,62	75422,95	185,7-379,9

Conclusions

Detailed investigations of the kinetics of individual stages of solid fuel (coal of the anthracite grade and certain types of solid biomass) thermal destruction have been carried out.

It has been established that the Coats-Redfern method can be used to determine the kinetic constants of the process of dehumidification and volatile release during thermal decomposition of biomass, coal and their mixtures.

It is shown that for the high-temperature processes (burning of the coke residue) a combined method Coats-Redfern and Senum-Yang of iterative approximation should be used.

The obtained kinetic constants allow enough precise calculations of mass loss history of the studied fuels in the determining of the duration of their thermal destruction stages.

The resulting constants can be used in calculations of burners and furnaces.

References

1. Sachin Kumar, Ankit Agrawalla, Singh R.K. (2011), Thermogravimetric Analysis of Groundnut Cake, *International Journal of Chemical Engineering and Applications*, 2(4), pp. 267-281, Available at:http://ijcea.org/papers/115-A621.pdf
2. González J.F., Rayo M.C., Román S., González-garcía C.M., Ledesma B. (2010), Modelling non-isothermal degradation of olive solid waste: influence ofvariables and kinetics, *Proceedings of Third International Symposium on Energy from Biomass and Waste, Venice, Italy*, p. 22.
3. Richard Capart, Lotfi Khezami, Alan K. Burnham (2004), Assessment of various kinetic models for the pyrolysis of a microgranularcellulose, Lawrence Livermore National Laboratory, PaperUCRL-JRNL-201926, p. 29, Available at: https://e-reports-ext.llnl.gov/pdf/304202.pdf
4. Font R., Conesa J.A., Moltor J., Munoz (2009), Kinetics of pyrolysis and combustion of pine needles and cones, *Journal of Analytical and Applied Pyrolysis*, 85(1–2), pp. 276–286, Available at: http://citeseerx.ist.psu.edu/viewdoc/download?doi=10.1.1.822.2174&rep=rep1&type=pdfwww.elsevier.com/locate/jaap
5. Kalita P., Mohan G., Kumar G. Pradeep, Mahanta P. (2009), Determination and comparison of kinetic parameters of lowdensity biomass fuels, *J. Renewable Sustainable Energy*, 1(2), p. 12.

6. Junmeng Cai, Ronghou Liu, Yuanyuan Wang (2007), Kinetic analysis of solid-state reactions: A new integral method for nonisothermal kinetics with the dependence of the pre exponential factor on the temperature ($A=A_0T^n$), *SolidStateSciences*, 9, pp. 421–428.
7. Guida M.Y., Hannioui A. (2016), Evaluation of Reliability of Coats-Redfern and Criado Methods for Kinetics Analysis of Olive Mill Solid Waste and Olive Mill Waste water, *International Journal of Scientific & Engineering Research*, 7(11), pp. 193–204. Available at: https://www.ijser.org/researchpaper/Evaluation-of-Reliability-of-Coats-Redfern-and-Criado-Methods-for-Kinetics-Analysis-of-Olive-Mill-Solid-Waste-and-Olive-Mill-Wastewater.pdf
8. Kharlamova G., Nate S., Chernyak O. (2016), Renewable energy and security for Ukraine: challenge or smart way?, *Journal of International Studies*, 9(1), pp. 88–115, DOI: 10.14254/2071-8330.2016/9-1/7
9. Simionescu M., Albu L. L., Raileanu Szeles M., Bilan, Y. (2017), The impact of biofuels utilisation in transport on the sustainable development in the European Union, *Technological and Economic Development of Economy*, 23(4), pp. 667–686.
10. Jun Han, Dongyi Liu, Linbo Qin, Wangsheng Chen, Futang Xing (2018), A modified temperature integral approximation formula and its application in pyrolysis kinetic parameters of waste tire, *Energy Sources, part A: recovery, utilization, and environmental effects*, 40(2), pp. 220–226.
11. Yunqing Han (2014), *Theoretical study of thermal analysis kinetics, A dissertation submitted in partial fulfillment of the requirements for the degree of Doctor of Philosophy in the College of Engineering at the University of Kentucky,* Lexington, Kentucky, p. 91, Available at: https://uknowledge.uky.edu/me_etds/35
12. Valérie Leroy, Dominique Cancellieri, Eric Leoni, Jean Louis Rossi (2010), Kinetic study of forest fuels by TGA: Model free kinetic approach for the prediction of phenomena, *Thermochimica Acta*, 497, pp.1–6. Available at: https://hal.archives-ouvertes.fr/hal-00547599/document
13. Ji L.Q. (2008), New rational fraction approximating formulas for the temperature integral, *Journal of Thermal Analysis and Calorimetry*, 91(3), p.885–889.
14. Katarzyna Slopiecka, Pietro Bartocci, Francesco Fantozzi (2011), Thermogravimetric analysis and Kinetic study of poplar wood pyrolysis, *Third International Conference on Applied Energy, 16-18 May, Perugia, Italy,* pp. 1687–1698, Available at: http://www.ciriaf.it/ft/File/Pubblicazioni/pdf/1571.pdf
15. Haixiang Chen, Naian Liu (2009), New Approximate Formula for the Generalized Temperature Integral, *AIChE Journal*, 55(7), pp.1756–1770
16. Matheus Poletto, Juliane Dettenborn, Vinícios Pistor, Mara Zeni, Ademir José Zattera (2010), Materials Produced from Plant Biomass. Part I: Evaluation of Thermal Stability and Pyrolysis of Wood, *MaterialsResearch*, 13(3), pp. 375-379, Available at:http://www.scielo.br/scielo.php?script=sci_arttext&pid=S1516-43920100003000016

Genetic algorithm usage for optimization of saturator operation

Volodymyr Polupan, Victor Sidletskyi

National University of Food Technologies, Kyiv, Ukraine

Keywords:

Sugar
Saturation
Control
Automation
Genetic
Algorithm

Article history:

Received 08.06.2018
Received in revised form 20.11.2018
Accepted 27.12.2018

Corresponding author:

Volodymyr Polupan
E-mail:
serunderw@gmail.com

DOI: 10.24263/2304-974X-2018-7-4-18

Abstract

Introduction. It is carried out the research of the optimal control adaptive system of the apparatus of II saturation. Qualitative indexes of the adaptive control system efficiency are defined.

Materials and methods. Adaptive control system of a sugar refinery apparatus of II saturation was studied. Simulation modeling based on classical and hybrid genetic algorithms is used to determine the optimal performance parameters.

Results and discussion. The simulation studies of the quality of functioning of the structural model of the adaptive system of optimal control using the classical genetic algorithm are carried out, as well as the research of the modified genetic algorithm with the addition in the classical algorithm the hybrid functions, namely fmincon, fminsearch patternsearch fminunc.

Adaptive system of optimal control has significantly lower integral quadratic criterion $I = 545$ comparing to the existing one, which integral quadratic criterion $I = 658$. Moreover, control time is also reduced. Adaptive control system requires $T = 109$ s, while existing control system requires $T = 212$ s. Usage of hybrid functions allowed to additionally reduce integral quadratic criterion to $I = 529–541$ and to speed up the system, required time $T = 98–105$ s. Also, a study of the fmincon method without the use of a genetic algorithm was carried out, this model showed a lower execution time T = 88 s, but the value of the integral quadratic criterion I = 604 was higher.

The best results in terms of integral quadratic criterion and time ($I = 529$, $T = 98$ s) were obtained for genetic algorithm combined with *fmincon* hybrid function.

Developed adaptive control system for saturator operation significantly outstands the existing one by all the main indexes. That is why it is highly recommended to replace control system on the sugar refinery with the studied adaptive one.

Conclusions. The novelty of the research results is the scientific substantiation of the feasibility of using classical genetic and hybrid genetic algorithms in the implementation of adaptive optimal control systems.

Introduction

Second saturation apparatus is an unsteady object from the point of view of control – with time flow its parameters unpredictable alter within wide range. Moreover, it works under uncertainty of environment parameters, load and raw material quality. Therefore, there is always a lack of prior information, mathematical models, which describe alterable properties of the objects and environment, do not exist.

Automatic regulators, which were adopted considering initial values of the object parameters, cannot provide sufficient control quality under such conditions. In the last several decades, different improvements for design of control systems were proposed [1–4]. However, the usage of genetic algorithm (GA) in control systems of sugar refinery saturators was not properly studied. Thus, arise a necessity to improve control algorithms and to provide adaptive control system [5, 6].

The objective of this paper is to study the saturator's adaptive control system, which is based on genetic algorithm.

Materials and methods

The second saturation apparatus is a control object, where filtered juice after the first saturation reacts with carbon dioxide. As a result of this reaction calcium salts sediment. The objective of the second saturation optimization is to maximize the sedimentation of calcium salts. Therefore, the amount of calcium ions in the filtered juice must be minimized [7].

The parametric scheme of a control object is shown in Figure 1.

The main material flow in the second saturator is the flow of first saturation filtered juice x_1. Disturbance of z_2 group under normal work conditions has no significant influence on the uniformity of juice flow on the second saturation area.

The more significant is the disturbance of z_3 group. However, alteration of these characteristics takes considerable time. To maintain presets of quantitative indices of second saturation juice (p_1, p_2, p_3) it is necessary to perform control actions u_1, u_2, u_3, u_4. If disturbance of a group z_1 or z_2 is dire, it is necessary to control juice inflow directly.

If the juice level in the collector before the evaporator is considerable or the group z_3 equipment has failed, then juice inflow is limited [8].

The juice pH decrements with the decrement of calcium ions concentration C in the second saturation juice (curve 1 in Figure 2). Hence, considering the pH measurability during the production process, this index is used as a state variable. Moreover, calcium ions concentration and juice pH as well as electrical conductivity X and juice pH (curve 2 in Figure 2) are interrelated with unsteady extreme dependence. The drift of these characteristics has the peculiarity that the minimum of both curves always corresponds to the same value of pH. Considering non-availability of calcium ions concentration sensors, a new criterion of control can be used – electrical conductivity of a saturated juice. Therefore, a control criterion of the second saturation process, considering iterative problem solving, is following:

$$I = \frac{1}{n}\sum_{i=0}^{n-1}\left(pH_{opt.i} - pH_i\right)^2 \to \min \tag{1}$$

where n – number of pH_{opt} determinations at regular intervals Δt during the saturation process $n = TIME/\Delta t$; $TIME$ – saturation process duration [9].

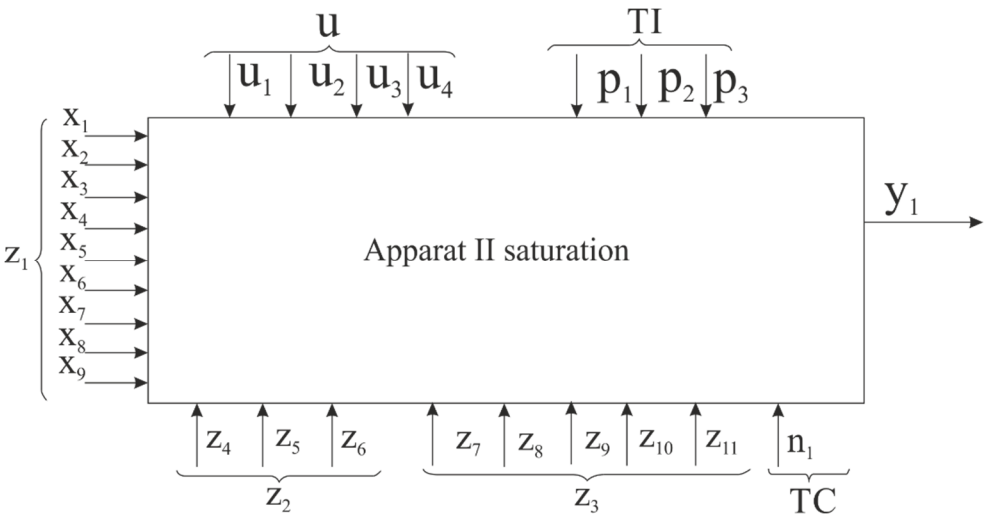

Figure 1. The parametric scheme of a second saturation apparatus:

z_1 – disturbance, caused by the material flow rates alteration of:
- x_1 – first saturation filtered juice, m^3/h;
- x_2 – lime milk, m^3/h;
- x_3 – carbon dioxide, m^3/h;
- x_4 – sulphur dioxide, m^3/h;
- x_5 – filtration sediment, m^3/h;
- x_6 – juice to clear yellow sugar, m^3/h;
- x_7 – evaporated water, m^3/h; in the second saturation apparatus;

y_1 – sulphited juice output rate, m^3/h;

z_2 – disturbance, caused by the alteration of:
- z_4 – carbon dioxide concentration in the saturation gas,%;
- z_5 – lime milk density, g/cm^3;
- z_6 – lime milk contamination,%;

z_3 – disturbance, caused by the alteration of characteristics of:

z_7 – pumps;
- z_8 – heaters;
- z_9 – filters;
- z_{10} – second saturation apparatus;
- z_{11} – equipment serviceability;

TC – technical constrains of n_1 – sulphited juice level in the collector, m;

u – control action to maintain presets of flow rate of:
- u_1 – first saturation filtered juice, m^3/h;
- u_2 – lime milk, m^3/h;
- u_3 – carbon dioxide, m^3/h;
- u_4 – sulphur dioxide, m^3/h;

TI – technological indices:
- p_1 – environment reaction, pH units;
- p_2 – second saturation juice purity,%;
- p_3 – environment reaction of sulphited juice, pH units.

A well-known regression model describes the dependence of the pH value on the consumption of saturation gas (F_{sg}), the temperature of the diffusion juice (T_{dj}), the density of limestone milk (C_{CO2}),the lime milk consumption (F_{CaO}), the density of dry matter (C_{dm}) [17]:

$$pH(F_{sg}, T_{dj}, C_{CO2}, F_{CaO}, C_{dm}) = -15{,}01 - 54{,}123F_{sg} - 34{,}982T_{dj} + 0{,}982C_{CO2} + 6{,}862C_{CP} + 71{,}936F_{CaO} - 3{,}973F_{sg}T_{dj} + 7{,}946F_{sg}C_{CO2} + 28{,}361F_{sg}C_{dm} - 1{,}804F_{sg}F_{CaO} - 1{,}765T_{dj}C_{CO2} - 9{,}082T_{dj}C_{dm} + 4{,}095T_{dj}F_{CaO} + 9.635C_{dm}F_{CaO} - 2.985T_{dj}^2 + 4{,}729F_{sg}^2 + 5{,}028C_{CO2}^2 - 8{,}027C_{dm}^2 + 8{,}941F_{CaO}^2$$

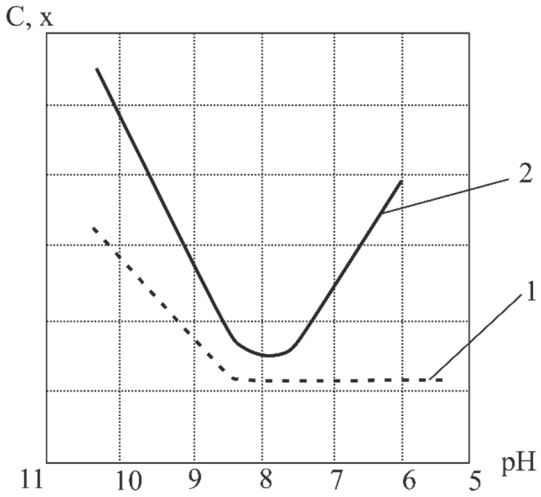

Figure 2

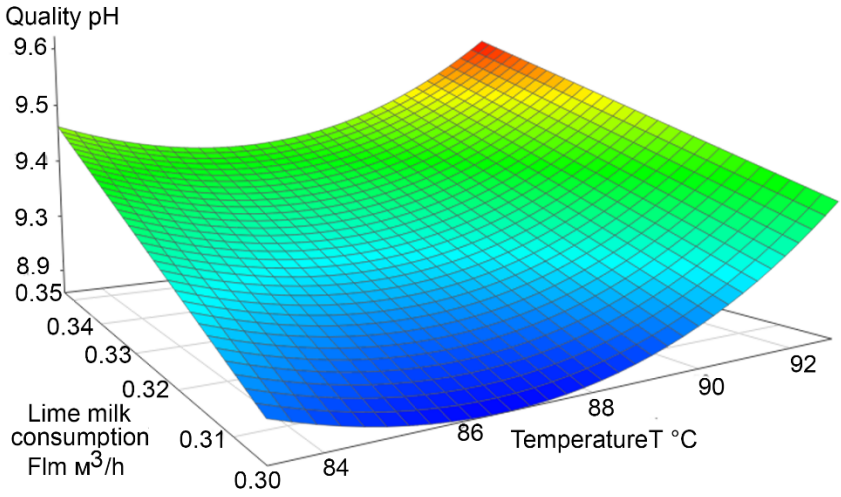

Figure 3. Sensitivity of second saturation qualitative index

Results and discussion

Optimal control system description

A system of optimal control was built to solve the problem, the structural scheme of which is shown in Figure 4. Control Computing Complex (CCC) of the system consists of mathematical model unit (MMU) and optimal control unit (OCU). The former receives information from sensors at regular intervals and defines current state of the saturation process, the latter calculates pH_{opt} and perform a dynamic optimization [10, 11]. Automatic regulator damps the disturbances, which influence the pH of the saturated juice. There are few assumptions considering adaptive system modelling. Firstly, disturbances (measurable and immeasurable) have influence only on the objective function pH extremum drift. Secondly, information collection, processing and output time is considered insignificant, comparing to inertial properties of the object, and thus is neglected.

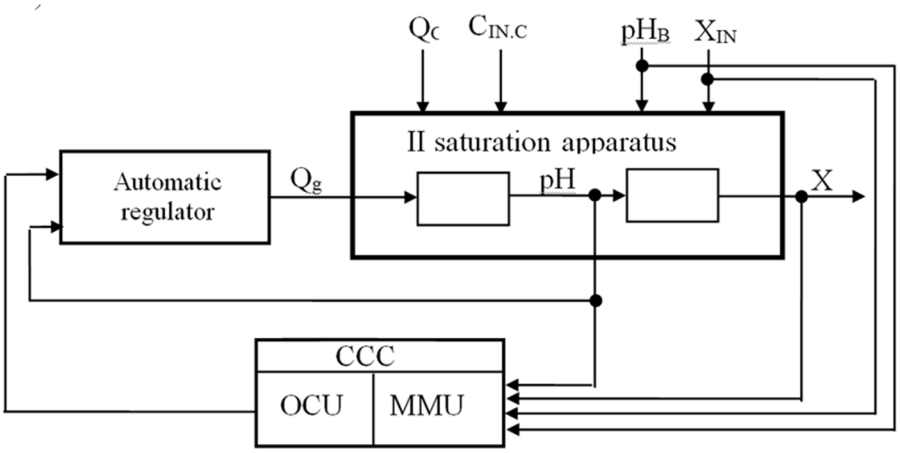

Figure 4. Optimal control system

CCC solves problem of second saturation process control using genetic algorithm (Figure 5).

Genetic algorithm explanation

Genetic algorithm is an evolutionary algorithm of heuristic search, that is used to solve optimization problems by modelling of natural selection, crossover and mutation, which occur during life of living organisms [12]. GA are effectively used to solve multiple-criteria optimization problems. A certain amount of chromosomes determines an individual, which is evaluated with objective function (also known as fitness function). A certain amount of individuals determines population. During the "evolutionary process" genetic material is gathered and the algorithm quickly "moves" towards the vicinity of the optimal solution. The advantages of genetic algorithms include the reliability, the ability to work with discrete and continuous values, GA finds the solution to the problem, without considering all the possible solutions. Genetic algorithms are weakly sensitive to local extrema [12].

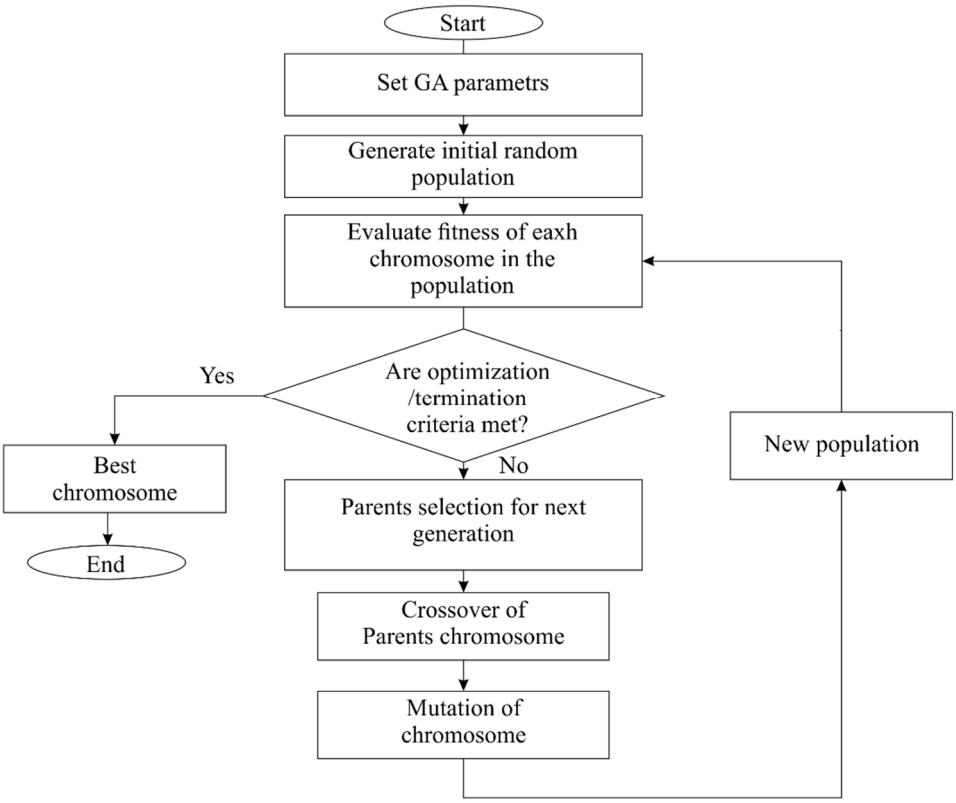

Figure 5. Genetic algorithm

Initial generation of a population consists of many problem solutions (also known as individuals), each with its own set of chromosomes, which is created randomly, usually. Then every problem solution is evaluated with objective function. Therefore, every set of chromosomes has its own fitness value (objective function value), which determines how good each solution to the problem is.

The second generation of a population is created from the selected problem solutions of the initial generation [13]. Usually better problem solutions (better in terms of the objective function) have higher probability to be selected to take part in creation of the second generation. Then the genetic operators, such as crossover and mutation, are applied to the selected problem solutions [14]. As a result, we have second generation. Every problem solution of this generation is also evaluated with objective function. Then this process repeats. Some of the problem solutions are selected to create the third generation, genetic operators are applied to them and so on.

These actions are iterative modelling of evolutionary process, which are repeated until the stop criterion is met. A stop criterion can be:

–global optimal or quasi-optimal solution;

–total amount of the generations created;

–total amount of evolution time.

Thus, one can distinguish the following stages of the genetic algorithm (Figure 5).

1. Objective function formulation.
2. Initial generation creation and its objective function evaluation.

Iterative part.

3. Problem solutions selection.
4. Crossover.
5. Mutation.
6. Objective function evaluation
7. Check if stop criterion is reached.

As one can see it is not necessary to create a perfect initial generation of a population. GA can quite quickly improve the population due to usage of crossover and mutation operators. Initial generation H consist of N problem solutions [15].

Crossover, mutation and selection. Genetic algorithm, usually, use two parent solutions to create one child solution [16]. Different GA have different ways to produce child solutions. The main requirement is that child solution must be able to inherit genes of each parent solution. To produce the next generation only the individuals of the current generation is used.

Control process simulation

The program works as follows:

−initial value *pH_in* is entered before the saturation process start (Figure 6);

−units *a*1 and *b*1 generate values (Figure 6);

−genetic algorithm is used to solve (1) and define optimum (Figure 6);

−during the time $T = 100$ s unit "Dinamic" calculates transition process considering *pH_in* and *pH_opt*. Results are shown in unit "Scope". *pH_opt* is in *pH_opt* array.

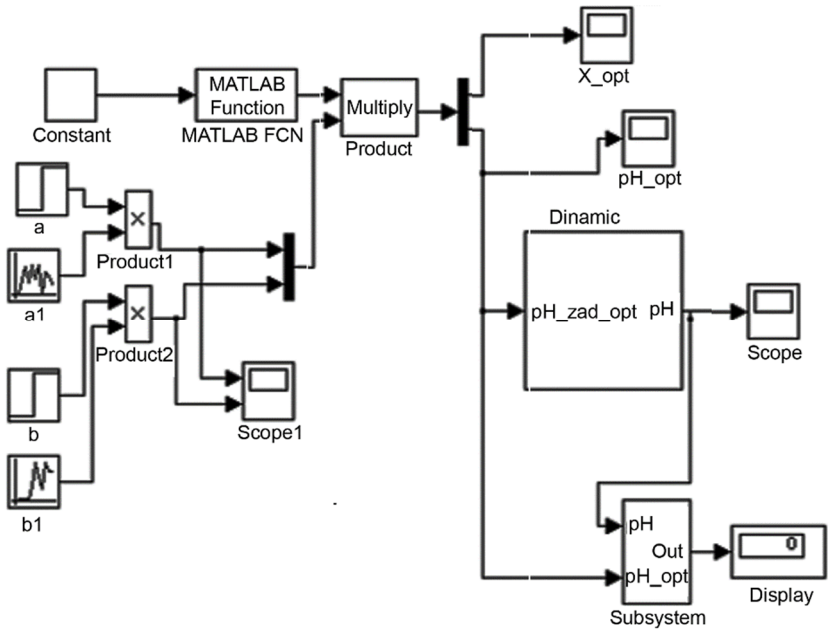

Figure 6. Simulation model

To simplify the dynamic calculation additional unit "Dinamic1" is used. Its inputs are static value of *pH_in* and dynamic value of (*pH_in* + *pH_opt*). Its output forms transition process with duration of 100 s of system time.

Simulation results

Simulation was carried out according to the requirements of the technological process considering different production peculiarities. Values from the sensors were read at a given time. That is initial values. Every simulation was carried out for the existing control system and for the adaptive one. Also, besides classic GA a bunch of hybrid functions were used in addition to GA: *fminsearch*, *patternsearch*, *fminunc*, *fmincon*. Eq. (1) was used to assess control quality. Results are shown in the Table 1.

Table 1

	I		T, c	
Hybrid function	**Existing control system**	**Adaptive control system**	**Existing control system**	**Adaptive control system**
None	658	545	212	109
fminsearch	-	541	-	105
patternsearch	-	536	-	102
fminunc	-	537	-	102
fmincon	-	529	-	98
fmincon without GA	-	604	-	88

As on can see from the table 1, adaptive control system has significantly lower integral quadratic criterion $I = 545$ comparing to the existing one, which integral quadratic criterion $I = 658$. Moreover, control time is also reduced. Adaptive control system requires $T = 109$ s, while existing control system requires $T = 212$ s. Usage of hybrid functions allowed to additionally reduce integral quadratic criterion to $I = 529–541$ and to speed up the system, required time $T = 98–105$ s. The best results in terms of integral quadratic criterion and time ($I = 529$, $T = 98$ s) were obtained for genetic algorithm combined with *fmincon* hybrid function. If control system uses *fmincon* without GA to solve the problem, then it requires even less time $T = 88$ s, however it can find local optimum while losing a global one. Considering this flaw, an adaptive control system must use both GA and *fmincon* hybrid function.

Therefore, the research objective was met and developed adaptive control system for saturator operation significantly outstands the existing one by all the main indexes. That is why it is highly recommended to replace control system on the sugar refinery with the developed adaptive one.

Conclusions

Simulation results confirmed that developed adaptive control system for saturator operation is highly efficient. The best control criterion values of the second saturation process were achieved when classic genetic algorithm was combined with hybrid function *fmincon*.

References

1. Schroder P. (2000), *Intelligent observer and Control Design for Nonlinear Systems*, Springer-Verlag, Berlin.
2. Zinober A. (2003), *Nonlinear and adaptive control*, Springer-Velag, New York.
3. Lucjka N.M. (2005), Syntez optymaljnykh reghuljatoriv dlja system avtomatyzaciji tekhnologhichnykh kompleksiv neperervnogho typu, *Avtomatyka. Avtomatyzacyja. Elektrotekhnycheskye kompleksy i systemy*, 15(1), pp. 148–151.
4. Lisitsin D.V. (2006), Vybor struktury mnogootklikovoi regressionnoi modeli, *Nauchnyi vestnik NGTU*, 22(1), pp. 17–32.
5. Sidlecjkyj V.M., Eljperin I.V., Polupan V.V. (2016), Analiz ne vymirjuvanykh parametriv na rivni rozpodilenogho keruvannja, dlja avtomatyzovanoji systemy, ob'jektiv ta kompleksiv kharchovoji promyslovosti, *Naukovi praci Nacionaljnogho universytetu kharchovykh tekhnologhij*, 22(3), pp. 7–15.
6. Korobiichuk I., Ladanyuk A., Shumyhai D., Boyko R., Reshetiuk V., Kamiński M., (2017), How to Increase Efficiency of Automatic Control of Complex Plants by Development and Implementation of Coordination Control System, *Proceedings International Conference on Systems, Control and Information Technologies SCIT* 2016, vol. 543. Springer, Cham, pp. 189–195.
7. Ladanjuk, A.P., Smitjukh Ja.V., Vlasenko L.O. (2013), *Systemnyj analiz skladnykh system upravlinnja*, NUHT, Kyiv.
8. Cherniavskaia L.I. (2003), *Sakharnaia svekla. Problemy povysheniia tekhnologicheskikh kachestv i effektivnosti pererabotki*, Fitosotsiotsentr, Kyiv.
9. Nelles O. (2001), *Nonlinear system identification*, Springer-Verlag, Berlin.
10. Polupan V.V., Sidlecjkyj V.M. (2017), Struktura avtomatyzovanoji systemy rozshyrenogho keruvannja dlja koordynaciji sumizhnykh stancij cukrovogho zavodu, *Naukovi praci Nacionaljnogho universytetu kharchovykh tekhnologhij*, 23(1), pp. 16–24.
11. Ladanjuk A.P., Zajecj, N.A., Vlasenko L.O., Lucjka N.M. (2006), Koordynacija funkcionuvannja tekhnologhichnykh diljnycj cukrovogho zavodu z urakhuvannjam zadach proghn ozuvannja, Visnyk Vinnycjkogho politekhnichnogho instytutu, 6, pp. 112–115.
12. Lukianenko L.M., Goncharenko I.S., Blonska O.V. (2014), Determination of the optimal placement and capacity of renewable energy sources, *Pratsi Instytutu elektrodynamiky Natsionalnoi Akademii Nauk Ukrainy*, 37, pp. 26–33.
13. Kosakovsky Pond S.L., Frost S.D.W. (2005), Datamonkey: rapid detection of selective pressure on individual sites of codon alignments, *Bioinformatics,* 21, pp. 2531–2533.
14. Posada D., Crandall K.A. (2002), The effect of recombination on the accuracy of phylogeny estimation, *J. Mol. Evol*., 54, pp. 396–402.
15. Burnham K., Anderson D. (2003), *Model selection and multimodel inference*, Springer, New York.
16. Shriner D. (2003), Potential impact of recombination on sitewise approaches for detecting positive natural selection, *Genet. Res.,* 81, pp. 115–121.

Анотації

Харчові технології

Розмір і морфологічні особливості нативних гранул крохмалю різного ботанічного походження

Владімір Літвяк
Науково-практичний центр Національної академії наук Білорусі з продовольства, Мінськ, Республіка Білорусь

Вступ. При розробленні сучасних технологій глибокої переробки рослинної крахмалевмісної сировини найважливішим аспектом є вивчення розмірів і морфологічної структури зерен крохмалю.

Матеріали та методи. Досліджувалися нативні крохмалі: картопляний, кукурудзяний, тапіоковий, пшеничний, рисовий, житній, гороховий, амарантний, ячмінний, сорго, тритикале і вівсяний. Сканувальні електронні мікрофотографії крохмальних зерен були отримані з використанням електронного мікроскопа LEO 1420. Металізація нативних крохмальних препаратів проводилась золотом у вакуумній системі EMITECH K 550X.

Результати і обговорення. Досліджено розміри і морфологічні особливості зерен нативного крохмалю різного ботанічного походження. Основною структурною характеристикою структури нативного крохмалю, що визначає його фізико-хімічні властивості, є зерно крохмалю (гранула). Виявлено велику різноманітність форм крохмальних зерен: правильні і неправильні овальні, округлі та багатогранні. Розміри крохмальних зерен варіювалися в межах 60,0-0,5 мкм. Залежно від середнього розміру крохмалисті зерна можуть розташовуватися в низхідному порядку: картопля (21,7±1,22), жито (21,2± ,36), горох (20,4±2,57), нут (14, 8±0,93), тритикале (13,2±1,75), пшениця (12,4±1,90), сорго (11,0±0,76), ячмінь (10,9±1,15), тапіока (10,6±0,50), кукурудза (9,8±0,42), овес (7,39±0,87), рис (5,3±0,29), амарант (1,1±0,04). Найбільший розмір крохмальних зерен виявлено в картопляному крохмалі, а найменший – в амарантовому. Встановлено, що у 7 нативних крохмалів (сорго, ячмінь, овес, горох, нут, амарант і кукурудза) розподіл крохмальних зерен мономодальний(1-фракційний), у 4 (пшениця, тритикале, картопля і тапіока) – бімодальний (2-фракційний), у 2 (житній і рисовий) – тримодальний (3-фракційний.

Джерело крахмалевмісної сировини й особливості структурної організації нативного крохмалю багато в чому визначають технологічні прийоми, які використовуються для найбільш повного і ощадливого вилучення зерен нативного крохмалю з рослинної клітини.

Основною структурною характеристикою нативного крохмалю, що визначає його властивості, є крохмальне зерно. Особливості розміру і форми крохмальних зерен обумовлюють такі властивості крохмалю: молекулярна маса, кількість зв'язаної вологи, температура желатинізації, співвідношення фракцій крохмалю і щільності їх укладання в кристалічних областях, реологічні характеристики крохмальних клейстерів.

Висновки. Морфологія крохмальних зерен різного ботанічного походження істотно відрізняється за розміром (60,0-0,5 мкм) і формою (округла, овальна,

неправильної форми). Розмір гранул крохмалю є основною структурною характеристикою, що визначає фізико-хімічні властивості крохмальних клейстерів.

Ключові слова: *крохмаль, морфологія, гранула, розмір, форма.*

Хімічний склад і застосування квітів робінії звичайної (*Robinia pseudoacacia* L.)

Станко Станков[1], Хафізе Фідан[1], Таня Іванова[1],
Албена Стоянова[1], Станка Дамянова[2], Микола Десик[3]
1 – Університет харчових технологій, Пловдив, Болгарія
2 – Русенський університет «Ангел Канчев», філія в м. Разград, Болгарія
3 – Національний університет харчових технологій, Київ, Україна

Вступ. Проведено дослідження з метою визначення хімічного складу та біологічної активності квітів робінії, вирощених у Болгарії, та продуктів з них.

Матеріали і методи. Сиропи отримували екстракцією н-гексаном. У сиропах з різною концентрацією визначали хімічний склад за GC-MS, а також вміст поліфенолів, антимікробну та антиоксидантну активність.

Результати і обговорення. Вихід сиропу склав 1,06%. Основні складові сиропу: n-нонакозан (25,18%), н-гептакозан (20,10%), α-ліноленова кислота (5,97%), n-пентакозан (4,98%), пальмітинова кислота (4,92%), диизооктилфталат (4,05%), гексагидрофарнезил ацетон (3,86%), лінолева кислота (3,64%), ізопропилміристат (3,47%), і н-гентриакотан (3,39%). Серед компонентів сиропу найвищий відсоток загальних аліфатичних вуглеводнів – 61,50%. У досліджуваних зразках квітів робінії найбільше таких мінералів: нікелю, міді, кальцію і хрому.

Більш високі значення фенольних сполук виявлено у квітах (0,77 мг GAE/мл), тоді як у сиропі з робінії 60 °Brix – 0,06 мг GAE/мл, сиропі з робінії 70 °Brix – 0,14 мг GAE/мл. Зразки сиропу мають антимікробні властивості щодо патогенних бактерій Salmonella, E. coli і L. monocytogenes.

Висновок. Квіти робінії з огляду на хімічні і біохімічні властивості можуть бути рекомендовані як потенційна сировина для харчової, фармацевтичної та косметичної продукції.

Ключові слова: *робінія звичайна, квітка, екстракт, хімія, склад.*

Вплив технологічних властивостей і режимів обробки на ефективність лущення насіння гороху

Євген Харченко[1], Андрій Шаран[1], Валентин Чорний[1], Олена Єремеєва[2]
1 – Національний університет харчових технологій
2 – Уманський національний університет садівництва

Вступ. Процес лущення зерна гороху є мало дослідженим, через що виникають складнощі моделювання технологічного процесу в цілому. Представлені результати дослідження процесу лущення насіння гороху дають змогу зрозуміти поведінку насіння гороху під час його лущення в машинах з абразивними робочими органами.

Матеріали і методи. Насіння гороху різної крупності та вологості лущили в лабораторній лущильній машині. Продукти лущення очищали в аспіраційному каналі від лузги та мучки, після чого зважували і визначали індекс лущення. Змінюючи

вологість і крупність насіння гороху, швидкість обертання робочого органу лущильної машини, тривалість обробки та коефіцієнт заповнення робочої камери машини, визначали вплив вказаних параметрів на ефективність лущення.

Результати і обговорення. Встановлено, що збільшення тривалості обробки, вологості насіння гороху, швидкості обертання робочих органів і коефіцієнта заповнення робочої камери лущильної машини збільшують ефективність лущення гороху за лінійною залежністю. Збільшення крупності насіння гороху сприяє збільшенню ефективності лущення переважно за рахунок збільшення виходу дрібки. Збільшення крупності зерен призводить до зниження індексу лущення.

Водночас із підвищенням ефективності лущення збільшується і вихід дрібки за рахунок ядра. Зі зростанням вологості насіння гороху вихід дрібки збільшується, якщо порівняти з лущенням сухого гороху. Вихід цілого ядра прямо пропорційний зниженню виходу нелущених зерен. Вихід дрібки також має лінійні залежності при зміні наведених параметрів.

У процесі лущення відбувається зниження зольності ядра, паралельно зменшується і зольність лузги та мучки, що є результатом переходу низькозольних частинок ядра в мучку.

Висновки. Для ефективного лущення насіння гороху необхідно проводити лущення протягом 10–15 с, коефіцієнт заповнення машини повинен бути не менше 0,48. Насіння гороху з абсолютною масою 257 г лущаться краще, ніж насіння гороху з абсолютною масою 213 г.

Ключові слова: *горох, лущення, ядро, зольність, вологість, лузга, мучка, дрібка.*

Визначення біотехнологічних параметрів для культивування молочнокислих бактерій із козячого молока

Ніна Богдан

Науково-практичний інститут садівництва, виноградарства і харчових технологій, Кишинеу, Республіка Молдова

Вступ. Мета дослідження – встановити оптимальні умови культивування для визначення ефективності розвитку молочнокислих бактерій, виділених із козячого молока.

Матеріали і методи. Культивування штамів проводили в стерилізованому середовищі з козячого молока за температури 30±2 °С. Для визначення параметрів було встановлено періодичне культивування в біореакторі Sartorius Biostat® A plus. Кількість клітин молочнокислих бактерій визначали методом підрахунку в чашках.

Результати і обговорення. Повільне зниження pH під час культивування спостерігалося в усіх відібраних штамах. Молочна кислота накопичувалася пропорційно до чотирнадцятої години культивування, що свідчить про інтенсивний розвиток молочнокислих бактерій. Активний розвиток характеризується помірною кислотністю ферментованого молока.

Дані динаміки розвитку штамів і накопичення біомаси в середовищі з козячого молока підтвердили отримання максимальної кількості клітин молочнокислих бактерій lg КУО/г.

Водночас проведено регресійний аналіз значення динаміки pH і життєздатних клітин для точного опису результатів експериментів. Штами CNMN-LB-73, CNMN-LB-74, CNMN-LB-77 і CNMN-LB-78 мають точну лінію регресії в динаміці pH, а

штами CNMN-LB-73, CNMN-LB-74, CNMN-LB-75, CNMN-LB-76 і CNMN-LB-78 – у динаміці розвитку клітин. Стадії розвитку штамів спостерігалися після десятої години культивування. У штамів CNMN-LB-76, CNMN-LB-77, CNMN-LB-79 фаза уповільнення зростання почалася через 12 годин культивування, а у штамів CNMN-LB-73, CNMN-LB-74, CNMN-LB-75, CNMN -LB-78 – через 14 годин. Це підтверджує, що вони більш стійкі до середовища з підвищеною кислотністю, ніж штами, описані іншими авторами, де розмноження клітин спостерігалося до рівня pH 4,7.

Висновки. В умовах періодичного культивування визначені біотехнологічні параметри культивування молочнокислих бактерій із козячого молока. Отримані дані підтвердили важливі біотехнологічні властивості виділених штамів.

Ключові слова: *молоко, коза, кисло-молочний, бактерія, біотехнологія.*

Особливості зміни хімічного складу ягід журавлини болотної у процесі отримання пюре

Віра Оболкіна, Олена Кохан, Іванна Сивній, Ірина Крапивницька
Національний університет харчових технологій, Київ, Україна

Вступ. Проведені дослідження з метою встановлення впливу технологічної обробки процесів бланшування та деаерації на хімічний склад пюре з ягід журавлини болотної.

Матеріали і методи. Досліджували пюре з ягід журавлини болотної, для ідентифікації біофлаваноїдів застосовували методи високоефективної рідинної хроматографії, електронної спектрометрії, газової хроматографії з мас-детектором вихідних і гідролізованих зразків

Результати і обговорення. Встановлено, що внаслідок технологічної переробки ягід журавлини у пюре кількість аскорбінової кислоти зменшилася у 13,5 раза; вміст фенольних речовин у пюре з ягід журавлини становить 983мг%, антоціанів – 160 мг%; збільшується вміст водорозчинного пектину до 3,0%, що пов'язано з частковим гідролізом протопектину, клітковини – 3,1% до масової частки сухих речовин пюре. У пюре з ягід журавлини міститься 36,6% цукрів до масової частки сухих речовин пюре, з них 28,8% є редукуючими глюкозою та фруктозою, збільшення частки яких пов'язане з частковим кислотним гідролізом сахарози під час переробки ягід у пюре.

У пюре виявлено наявність антоціанових сполук, які у вихідному зразку знаходяться в зв'язаному стані з лимонною кислотою, а також монооксикарбоновими кислотами. Ідентифіковано низку органічних кислот: 3-гідроксимасляну кислоту, ферулову кислоту, бурштинову, яблучну, лимонну кислоти. Під час переробки ягід журавлини в пюре в ньому зберігаються природні консерванти, що містяться в свіжій ягоді. Так, у пюре з ягід журавлини міститься бензойна кислота у кількості 122,2 мг% ±15% та наявна невелика кількість сорбінової кислоти – до 2,5 мг% Досліджено позитивний вплив пюре з ягід журавлини на затримку росту дріжджів роду *Candida.*

Висновки. Пюре з ягід журавлини є природним джерелом біологічно-активних речовин та природних консервантів і рекомендується для використання в харчових продуктах функціонального призначення подовженого терміну зберігання.

Ключові слова: *журавлина, пюре, флаваноїд, антоціан, консервант.*

Оптимізація параметрів екстракції поліфенольних антиоксидантів з обезжиреного порошку виноградних кісточок методом відгуку поверхні

Сергій Губський, Максим Лабазов, Ольга Самохвалова,
Наталя Гревцева, Олена Городиська
Харківський державний університет харчування та торгівлі, *Харків, Україна*

Вступ. У дослідженні наведені результати оптимізації умов твердорідинної водної екстракції відходів виноробної промисловості у вигляді знежиреного порошку з виноградної кісточки з метою отримання екстракту з високою антиоксидантною активністю.

Матеріали і методи. Загальну антиоксидантну ємність (TAC) і загальний зміст поліфенольних сполук (TPC) зразків визначали методом кулонометрического титрування в гальваностатичному режимі з електрогенерованим бромом і спектрофотометричним методом за допомогою реактива Folin-Ciocalteu. Експериментальні величини TAC і TPC були представлені в еквіваленті вмісту галової (GAE) на одиницю маси порошку (DW).

Результати і обговорення. Методологію поверхні відгуку (RSM) було використано для пошуку оптимальних умов твердорідинної екстракції фенольних речовин із знежироного порошку виноградної кісточки під впливом трьох факторів: температури (60-100 °C) та часу (90–150 хв) екстракції, співвідношення об'єму розчинника до маси порошку (60–100). Результат показав, що вихід фенольних речовин у зазначених діапазонах становить 1,20–2,64% при величині загальної антиоксидантної ємності 17,71–36,78 мг GAE/г DW. У результаті оптимізаційної процедури було визначено, що при оптимальних умовах (температура 100°C, час екстракції 131 хвилина і співвідношення об'єму екстрагенту до маси порошку 85), була досягнута максимальна TAC екстракту, що дорівнює 37,04 мг GAE/г DW. Величина максимального виходу фенольних речовин 2,646% була отримана при таких умовах: температура 100°C, час екстракції 117 хвилин, співвідношення об'єму екстрагенту до маси порошку 93. При застосуванні оптимізації з двома функціями відгуку TAC і YPC отримано такі оптимальні умови: температура 100°C , час екстракції 123 хвилини та співвідношення об'єму екстрагента до маси порошку 89, при яких величини TAC та YPC дорівнюють 36,91 мг GAE/г DW та 2,633%, відповідно. Валідація отриманих результатів показала їх узгодження в межах 3% з експериментальними величинами.

Висновки. Отримані результати доводять перспективність переробки відходів виноробної промисловості для отримання твердого екстракту з обезжиреного порошку виноградних кісточок як джерела біологічно активних речовин фенольної природи з високим антиоксидантним потенціалом.

Ключові слова: *антиоксиданти, поліфеноли, флавоноїди, кісточки винограду, кулонометрія.*

Холодне пресування у виробництві олії. Огляд

Бюшра Чакалоглу, Васфіє Хазал Озюрт, Семіх Отлуш
Егейський університет, Борнова, Ізмір, Туреччина

Вступ. Метою цього огляду є пояснення принципу роботи установок холодного пресування та обґрунтування ефективності цього способу виробництва олії.

Матеріали і методи. Досліджено виробництво олії з насіння олійних культур методом холодного пресування. Метод холодного пресування порівняно з іншими методами, що використовуються при отриманні олії з насіння олійних культур.

Результати і обговорення. Видобуток олії холодним пресуванням є одним із методів механічного оброблення, який є менш енерговитратним порівняно з іншими, а також екологічно чистим. Метод застосовується у виробництв олії з насіння олійних культур. За допомогою методу холодного пресування можна отримати високоякісні олії за низьких температур. Холодне пресування є екологічно чистим, не потребує використання розчинників. Іншими словами, видобуток олії холодним пресуванням не передбачає ні теплового, ні хімічного оброблення. Методом холодного пресування отримують соєву, соняшникову, рапсову, кукурудзяну, виноградну, конопляну, лляну, рисову, оливкову і гарбузову олії. Крім того, ці олії є цікавими для споживачів завдяки своїй натуральності та безпечності, а також здатності запобігати певним захворюванням і поліпшувати здоров'я людини, оскільки містять велику кількість ліпофільних фітохімічних речовин, зокрема антиоксидантів. Олії мають кращі поживні властивості, ніж рафіновані. Однак метод холодного пресування все ж має недоліки, (низька продуктивність, невідповідність критеріям якості). Олії холодного пресування можуть додаватися до їжі як природні антиоксидантні добавки завдяки фітохімічним властивостям і наявності жирних кислот.

Висновок. У результаті проведеного дослідження визначено переваги і недоліки видобутку олії холодним пресуванням.

Ключові слова: *олія, видобуток, пресування.*

Внутрішні механізми встановлення рівноважного стану водно-спиртових сумішей у технології горілки

Олег Кузьмін[1], Валентина Зубкова[2], Тетяна Шендрік[3],
Юрій Коренець[4], Антон Кузьмін[5], Павло Біленький[1]

1 – Національний університет харчових технологій, Київ, Україна
2 – Університет імені Яна Кохановського в Кельцах, Кельце, Польща
3 – Інститут фізико-органічної хімії та вуглехімії імені Л.М. Литвиненка НАН України, Київ
4 – Донецький національний університет економіки і торгівлі імені Михайла Туган-Барановського, Кривий Ріг, Україна
5 – Національний авіаційний університет, Київ, Україна

Вступ. Досліджено механізм встановлення релаксації водно-спиртових сумішей (ВСС) на основних етапах створення горілки при застосуванні електрохімічної активації (ЕХА) на стадії Na-катіонного зм'якшення технологічної води.

Матеріали і методи. *^{1}H ЯМР* аналіз проводився з використанням: Фур'є *ЯМР* спектрометра Bruker Avance II (400 МГц); спеціального капіляра з ацетоном-d_6; ампул №507-HP високого розділення; дозатора; спирту етилового ректифікованого (СЕР); води пом'якшеної *Na*-катіонуванням; води підготовленої ЕХА; водно-спиртових сумішей (ВСС) із СЕР і пом'якшеної води та води підготовленої ЕХА.

Результати. Досліджено рівноважний стан горілок при створенні ВСС в процесі ЕХА пом'якшеної води *Na*-катіонуванням. Встановлено, що електрохімічні реакції змінюють системи міжмолекулярних взаємодій. Зарядові стани молекул в аноліті та католіті призводять до відмінностей в електронному розподілі, що позначається на хімічних зсувах гідроксильних протонів. Стосовно води пом'якшеної (δ_{H2O}=4.65 м. ч.) аноліт з δ_{H2O}=(4.23; 4.22) м. ч. має зміщення гідроксильного протону в «сильне поле» на Δf=170 Гц, католіт

з δ_{H2O}=(4.56; 4.54) м. ч. має зміщення у «сильне поле» на Δf=40 Гц. Доведено, що ВСС на аноліті (pH=2.43) та спирті етиловому ректифікованому (СЕР) має кисле середовище (pH=3.10), ВСС на католіті (pH=11.08) та СЕР має лужне середовище (pH=11.75). Ці полярні співвідношення концентрацій H_3O^+ до OH^- для аноліту та католіту призводять до перебудови структури в системі спирт/вода. Можна вважати, що протонний обмін прискорюється, при цьому спостерігається один загальний сигнал рухливих протонів $EtOH+H_2O$.

На підставі проведеного дослідження встановлена принципова відмінність поведінки ВСС і горілок, які приготовлені на воді пом'якшеній та воді після обробки ЕХА. Виявлено системи (спирт/вода) зі сталою рівновагою, які характеризуються високою мірою узагальнення протонів, а також характерними для неї швидкостями обміну.

Висновки. Отримані експериментальні дані доводять залежності швидкості і характеру встановлення термодинамічної рівноваги від часу релаксації ВСС. Релаксація відбувається при одночасній стабілізації гідроксильної групи протонів води й етанолу.

Ключові слова: *вода, спирт, суміш, Na-катіонування, електрохімічний, активація, ^{1}H ЯМР, спектроскопія.*

Удосконалення антиоксидантного потенціалу пшеничного борошна і хліба з додаванням лікарських рослин

Іван Дімов[1], Надєжда Петкова[2], Гьоре Наков[3],
Іра Танєва[1], Іван Іванов[2], Вікторія Стамановська[4]

1 – Тракійський університет, Ямболь, Болгарія
2 – Університет харчових технологій, Пловдив, Болгарія
3 – Русенський університет «Ангел Канчев», філія в м. Разград, Болгарія
4 – Бітольський університет «Св. Климент Охрідський», Велес, Македонія

Вступ. Проведене дослідження з метою визначення впливу двох трав'яних сумішей на властивості трав'яного хліба. Встановлено вплив трав на загальний вміст фенолів та антиоксидантну активність трав'яних сумішей, сумішей трав із борошном і трав'яного хліба.

Матеріали і методи. Було використано дві трав'яні суміші (1 – чебрець, материнка і меліса; 2 – чебрець, материнка , меліса і гуньба) з пшеничним борошном для виробництва трав'яного хліба; екстракти зразків оцінювали чотирма методами: ABTS • +, CUPRAC, FRAP і DPPH.

Результати і обговорення. Найбільший загальний вміст фенолів серед усіх досліджених трав містить материнка (30,43 мг GAE/г dw), трав'яна суміш 1 і трав'яна суміш 2 – 19,18 і 17,47 мг GAE/г dw відповідно. У суміші трав'яного борошна і хліба рівень загального вмісту фенолів знаходився в діапазоні від 0,31 до 0,37 мг GAE/г dw. Варто зазначити, що вміст цих біоактивних сполук істотно під час процесу випікання не змінився. Найвищу антиоксидантну активність трав'яних сумішей, сумішей трав'яного борошна і хліба отримували двома з використаних методів – ABTS та FRAP. Найвищий антиоксидантний потенціал продемонстрували рослинна суміш 1, що складалася з трьох трав – 16829,73 мМ ТЕ/100 г dw, тоді як рослинна суміш 2 з чотирма травами – 14693,75 мМ ТЕ/100 г dw. Оцінювання сумішей здійснювалося методом ABTS. Для методу FRAP значення антиоксидантної активності становили:

15997,65 мМ ТЕ/100 г dw для рослинної суміші 1 і 14136,82 мМ ТЕ/100 г dw для рослинної суміші 2.

Висновки. Трави, що додаються в борошно, збільшують загальні фенольні й антиоксидантні значення борошняних сумішей і хліба. Незначні відмінності в антиоксидантних потенціалах спостерігалися для хліба з трьома і чотирма травами.

Ключові слова: *лікарська трава, борошно, хліб, антиоксидант, фенол.*

Дослідження потенціалу штучної нейронної мережі для прогнозування властивостей рафінованого цукрового бурякового соку, отриманого методом електрокоагуляції

Махілех Заріфпоор, Вахід Хакімзадех
Ісламський Азадський університет, Кучанська філія, Кучан, Іран

Вступ. Зважаючи на високий потенціал електрокоагуляції (ЕК) під час видалення зважених часток, а також на високе енергоспоживання при традиційному обробленні, у цьому дослідженні за допомогою штучної нейронної мережі промодельовано процес ЕК для очищення бурякового соку.

Матеріал і методи. В процесі електрокоагуляції досліджено потенціал нейромережі в прогнозуванні мутності, кольоровості та чистоти бурякового соку з різними параметрами: напруга (5, 10 і 15 вольт), pH (6, 7 і 8) і час (постійні інтервали часу від 1 до 60 хв). Моделювання штучної нейронної мережі, яке здійснювалося в програмному забезпеченні Neurosolution V6, застосовувалося для визначення найкращого типу транспортної функції, правил навчання, валідації й тестування на основі їх середньоквадратичних помилок, середніх абсолютних похибок і кореляційних коефіцієнтів. Це дало змогу визначити найкращий тип транспортної функції, правила навчання та застосувати використані значення для навчання, перевірки й тестування на основі їх середньоквадратичних похибок, середньоквадратичних нормалізованих похибок, середніх абсолютних похибок і коефіцієнтів кореляції.

Результати і обговорення. Найкраща нейронна мережа з максимальним коефіцієнтом кореляції для мутності і чистоти отримана в законі Левенберга про навчання і тангенс передачі функції, які включали 8 і 17 нейронів відповідно. Крім того, найкращий коефіцієнт кореляції і менша середня квадратична похибка для моделювання кольоровості, пов'язані з мережею з одним прихованим шаром і 9 нейронами, які вивчаються за законом навчання Левенберга і сигмоподібною передаточною функцією. Моделювання проводилося з різними значеннями даних для навчання, перевірки й тестування. Найкраще прогнозування кореляції для мутності та чистоти отримано, коли 55% даних були використані для навчання, 40% з них – для перевірки та 5% – для тестування, тоді як найкращі відсотки для навчання, перевірки й тестування для прогнозування кольоровості становили 60, 30 і 10 відповідно. Прогнозовані значення моделей мали відповідну кореляцію з експериментальними даними, тому коефіцієнт кореляції з експериментальними даними мутності, кольоровості та чистоти становив, відповідно, 0,999, 0,997 і 0,990. Це дослідження також стосувалося чутливості моделі до вхідних даних. Найбільша чутливість моделі для прогнозування мутності, кольоровості і чистоти була пов'язана з напругою.

Висновок. Модель спрогнозувала мутність, кольоровість і чистоту соку в різних умовах експлуатації, оскільки дані моделювання показали високу кореляцію з експериментальними даними.

Ключові слова: *цукор, буряк, сік, електрокоагуляція, Левенберг, нейронна мережа.*

Розвиток способів розділення у виробництві натуральних ароматизаторів

Наталія Фролова, Анатолій Українець
Національний університет харчових технологій, Київ, Україна

Вступ. Проведені аналітичні та експериментальні дослідження способів розділення природних джерел аромату з отриманням індивідуальних ароматичних речовин. Показано переваги фракційної розгонки та препаративної хроматографії.

Матеріали і методи. Вивчалися ефірні олії змієголовника молдавського та лимона, модельна матриця (суміш терпенових вуглеводнів і їхніх кисневмісних похідних відомого та невідомого складу). Використано методики газохроматографічного аналізу. Окремі фракції цільових ароматичних компонентів отримано препаративною хроматографією.

Результати і обговорення. Вакуумне розділення ефірних олій на фракції за встановленими режимами контролю температури куба та головки,°С відповідно на рівнях: перша фракція – 67–69, 18–24; друга фракція – 112–118, 25–30; третя фракція – 130–135, 32–39; значень тиску, кПа за фракціями: перша – 0,92, друга – 0,62, третя – 0,33; флегмового числа за фракціями: перша – 7:1, друга – 10:1 , третя – 5:1 дає змогуотримувати фракції різного аромату, що значно розширює асортимент натуральних джерел аромату. Також контрольованою фракційною розгонкою проводять детерпенізацію, при якій із ефірної олії видаляються компоненти, які відчутно погіршують органолептичні властивості. Режими детерпенізації лимонної ефірної олії – температура куба та головки, °С відповідно 67–70, 17–19; тиск – 2,64 кПа, флегмове число – 1:3.

Для виділення чистих ароматичних речовин використано препаративну хроматографію з виготовленням спеціальної колонки, підібрано твердий носій – Хромосорб А, нерухому фазу – ПЕГ-6000. Експериментально встановлено ефективні режими процесу – швидкість потоку газу-носія, $см^3$/хв – 85–90; об'єм проби – 0,8–1,0 $см^3$, значення температур , ºС: випарника – 180–250, термостата колонки – 120–200, детектора – 220–250, збірника фракцій – 180–250

Висновок. Розвитком способів розділення є вакуумне фракціонування природних джерел аромату з подальшим препаративним виділенням чистих речовин.

Ключові слова: *ароматизатор, ефірний, олія, хроматографія.*

Механізм жирозв'язування та жироутримання наночастинками харчової добавки на основі подвійного оксиду дво- і тривалентного заліза

Ірина Цихановська[1], Вікторія Євлаш[2], Олександр Александров[1], Тетяна Гонтар[1]
1 – Українська інженерно-педагогічна академія, Харків, Україна,
2 – Харківський державний університет харчування та торгівлі, Харків, Україна

Вступ. Обґрунтовано механізм жирозв'язування та жироутримання наночастинками харчової добавки на основі подвійного оксиду дво- і тривалентного заліза, який представлений моделлю двошарової координації.

Матеріали і методи. Наночастинки харчової добавки на основі оксиду дво- та тривалентного заліза, покриті лінолевою кислотою й нерафінованою соняшниковою олією. Жироутримувальну здатність досліджували за допомогою ІЧ-Фур'є (FTIR) та енергодисперсійної рентгенівської (EDX) спектроскопії, а також методом скануючої електронної мікроскопії (ТЕМ).

Результати і обговорення. Вивчено механізм жирозв'язування та жироутримання наночастинками харчової добавки на основі подвійного оксиду дво- і тривалентного заліза, який представлений моделлю двошарової координації. *Перший адсорбційний шар* утворюється за рахунок електростатичних взаємодій поляризованих груп ліпідів та іонізованих наночастинок харчової добавки і координаційних зв'язків атомів Fe наночастинок харчової добавки з Оксигенами COO^- – групи "гідрофільної головки" ліпіда; *другий адсорбційний шар* – за рахунок електростатичних взаємодій гідрофобних центрів першого адсорбційного шару і вуглеводневих "хвостів" ліпіду.

Поява в ІЧ-спектрах двух нових смуг при: ~1541 $см^{-1}$ і ~1637 $см^{-1}$ підтверджують бідентатну адсорбцію й утворення карбоксилатної групи (–COO–) в композиціях "ліпід-наночастинка харчової добавки".

Мікроскопічними дослідженнями встановлено порядок середнього розміру частинок: для частинок чистої харчової добавки – <d>78±2,36 нм; для частинок добавки, покритих лінолевої кислотою, – <d>80±2,57 нм; для частинок добавки, покритих соняшникової олією, – <d>81±2,93 нм.

Енергодисперсійними рентгенівськими дослідженнями встановлено елементний склад композицій "ліпід-наночастинка харчової добавки": для частинок чистої харчової добавки – Fe 75,5%; O 24, 5%; для частинок добавки, покритих лінолевої кислотою, – Fe 45,6%; O 34, 7%; C 19,7; для частинок добавки, покритих соняшникової олією, – Fe 39,7%; O 36, 7%; C 23,6%.

Висновки. Вперше запропоновано модель двошарової координації для обґрунтування механізму жирозв'язування та жироутримання наночастинками харчової добавки на основі подвійного оксиду дво- та тривалентного заліза.

Ключові слова: *жирозв'язування, жироутримання, оксид заліза, добавка, двошарова координація.*

Антимікробні властивості двох похідних нафтопіранодіону з циклоалканспірогідантоїнами щодо деяких фітопатогенних і корисних мікроорганізмів

Марин Маринов, Младен Найденов, Румяна Проданова
Аграрний університет, Пловдив, Болгарія

Вступ. Досліджені антимікробні властивості двох нафтопірандіонових похідних із циклоалканспірохідантоїнами щодо деяких фітопатогенних і корисних мікроорганізмів

Матеріали і методи. Титульні сполуки отримували згідно з відомою процедурою. Метод дифузії в агарі застосовували для визначення антимікробної активності синтезованих продуктів щодо бактерій і грибів. Використані у дослідженнях вихідні

сполуки (6-бромо-1*H*,3*H*-нафто[1,8-*cd*]піран-1,3-діон, циклоалканспірогідантоїни і похідні нафтопірандіону з циклоалканспірогідантоїнами - 3-(1,3-діоксо-1*H*,3*H*-нафто[1,8-*cd*]піран-6-іл)-1,3-діазаспіро[4.4]нонан-2,4-діон та 3-(1,3-діоксо-1*H*,3*H*-нафто[1,8-*cd*]піран-6-іл)-1,3-діазаспіро[4.5]декан-2,4-діон) синтезовані за описаними в літературі методиками.

Результати і обговорення. Досліджено антимікробну активність вихідних сполук і кінцевих продуктів щодо грибів *Fusarium oxysporum* і *Trichoderma asperellum* Т6, грампозитивної бактерії *Bacillus amyloliquefaciens* 2/7 А і грамнегативної бактерії *Xanthomonas vesicatoria*. Всі речовини (за винятком вихідних спіродидантоїнів) виявляють активність щодо досліджуваних мікроорганізмів. Що стосується досліджених грибів, то фітопатогенні види (*Fusarium oxysporum*) більш чутливі. Ефект відрізняється у випадку з біоконтрольним агентом (*Trichoderma asperellum* Т6). З часом грибок, будучи слабшим, долає інгібувальну дію, зростаючи на вже сформованих зонах інгібування. Продукт 3-(1,3-діоксо-1Н, 3Н-нафто [1,8-cd] піран-6-іл)-1,3-діазаспіро [4,5] декан-2,4-діон найбільш активний щодо фітопатогенних мікроорганізмів, що мають менш слабкий вплив на *Trichoderma asperellum* Т6.

Висновок. Сполуки 6-бромо-1*H*,3*H*-нафто[1,8-*cd*]піран-1,3-діон, 3-(1,3-діоксо-1*H*,3*H*-нафто[1,8-*cd*]піран-6-іл)-1,3-діазаспіро[4.4]нонан-2,4-діон та 3-(1,3-діоксо-1*H*,3*H*-нафто[1,8-*cd*]піран-6-іл)-1,3-діазаспіро[4.5]декан-2,4-діон мають високу біологічну активність щодо всіх тестованих мікроорганізмів.

Ключові слова: *нафтопірандіон, похідна, циклоалканспірохідантоїн, мікроорганізм, фітопатоген, антимікробний.*

Процеси і обладнання

Динаміка позиційних електропневмоприводів функціональних мехатронних модулів потокових технологічних ліній харчових виробництв

Людмила Кривопляс-Володіна, Олександр Гавва, Сергій Володін, Тарас Гнатів
Національний університет харчових технологій, Київ, Україна

Вступ. Розглянуто реалізацію завдань, пов'язаних із синтезом робочих органів для переміщення штучних харчових продуктів за заданим законом руху, та їх позиціювання у проміжних положеннях кінематичного циклу.

Матеріали і методи. Досліджуються динамічні характеристики приводу і система керування силовою частиною позиційного електропневмоприводу. Використані методи математичного та комп'ютерного моделювання, методи розв'язку звичайних диференційних рівнянь та диференційних рівнянь у часткових похідних і метод кореляційного аналізу.

Результати і обговорення. Отримано аналітичні залежності для визначення кінематичних параметрів руху штучного продукту із механізмом зіштовхування на базі пневмоприводу. Математично випробувано динамічну модель приводу й отримано закон руху механізму зіштовхування, наближеного до оптимального за швидкістю. Для аналізу процесу навантаження робочої ланки позиційного приводу використано модель узагальненої системи керування, яка обмежена одним повним циклом роботи функціонального мехатронного модуля пакувальної машини. Отримані

результати розрахунків порівнювались для різних компоновочних рішень досліджуваного приводу з метою удосконалення запропонованих технічних рішень. Розроблена методика математичного аналізу роботи позиційного електропневмоприводу була успішно використана під час відпрацьовування режимів роботи різних функціональних мехатронних модулів у пакувальній машині для штучних харчових продуктів горизонтального типу. Розбіжність розрахованого при математичному моделюванні значення часу робочого ходу вихідної ланки функціонального мехатронного модуля для відпрацьовування кінематичнго циклу роботи пакувальної машини складала для різних вхідних параметрів межі до 7%. Отримані результати моделювання динамічного навантаження і зміни тиску робочого позиційного пневмоприводу підтвердили, що при звуженні вихлопного перерізу робочого циліндра позиційного пневмоприводу збільшується значення інерційної складової на етапі гальмування. Результати математичного моделювання динаміки для позиційного пневмоприводу з умови зміни перерізу вихлопного отвору дали можливість одержати кінематичні характеристики приводу.

Висновки. Отримані результати дають можливість забезпечити робочому органу закон руху, наближений до оптимального за швидкістю дії, не перевищуючи при цьому максимально допустимий для рухомого штучного продукту, і забезпечити потрібну продуктивність пакувальної машини.

Ключові слова: *функціональний, модуль, пакування, електропневмопривод, точність.*

Кінетика термічної деструкції сумішей вугілля і твердої біомаси

Наталія Дунаєвська[1], Ярослав Засядько[2], Тарас Щудло[1]
1 – Інститут вугільних енерготехнологій НАН України, Київ
2 – Національний університет харчових технологій, Київ, Україна

Вступ. Проведені дослідження кінетики складових етапів процесу згоряння біомаси як індивідуально, так і у суміші з низько реакційним вугіллям антрацитової групи Донецького басейну.

Матеріали і методи. Зразки біомаси (включаючи відходи сільськогосподарської та харчової промисловості) та вугілля були вивчені за допомогою неізотермічної термогравіметрії. Кінетичні дослідження зразків проводилися на дериватографі системи Paulik-Paulik-Erdėje Q-1000 з інтегрованим комплексом синхронних аналізів даних STZ 449 JUPITER NETZSCH в атмосферному повітрі з швидкістю нагріву 20 °С/хв. Інтервал температур – 25–1000 °С.

Результати і обговорення. Отримані первинні дані оброблялися й узагальнювалися в рамках диференціальних та інтегральних підходів. Показано, що застосовування диференційного методу обробки даних потребує визначення поточних нормалізованих похідних від швидкості зміни маси зразку, а також балансу компонентів наважки в моменти початку та закінчення процесу, що створює серйозні труднощі. За таких умов інтегральний підхід, застосований для обробки отриманих даних, виглядає більш прийнятним. Представлено порівняння апроксимацій та узагальнення даних за різними методами.

Показано, що застосування апроксимації за методом Коутса-Редферна у вигляді ряду не збільшує точності наближення при врахуванні більшої кількості членів ряду. Допустимі межі застосування методу визначаються величиною E/RT більше 4, що

дійсно для процесів виходу вологи та летких. Для процесу догоряння коксового залишку слід враховувати можливі відхилення та застосовувати метод Сенума-Янга. Отримано сукупність кінетичних констант, які були використані з відповідними диференційними рівняннями типу Арреніуса для розрахунків загальної кривої термодеградації. Відхилення розрахованої поточної маси зразка від визначеної експериментально при нагріві у діапазоні 300–700 К не перевищує 10%, що дає змогу рекомендувати отримані константи для інженерних розрахунків як тривалості окремих стадій процесу, так і балансів компонентів палива у процесі горіння.

Висновки. Методологія виділення окремих стадій процесу й отримані кінетичні константи можуть бути використані для інженерних розрахунків та у вигляді підмоделей для 3-вимірного моделювання процесів горіння твердого палива.

Ключові слова: *вугілля, біомаса, горіння, кінетика, Донецький вугільний басейн.*

Використання генетичного алгоритму для оптимізації роботи сатуратора

Володимир Полупан, Віктор Сідлецький
Національний університет харчових технологій, Київ, Україна

Вступ. Проведені дослідження адаптивної системи оптимального керування роботою апарата ІІ сатурації з метою встановлення кількісних показників ефективності її роботи.

Матеріали і методи. Досліджувалася адаптивна система керування роботою апарата ІІ сатурації цукрового заводу. Для визначення оптимальних параметрів функціонування використано імітаційне моделювання на основі класичних і гібридних генетичних алгоритмів пошуку.

Результати і обговорення. Проведено імітаційні дослідження якості функціонування структурної моделі адаптивної системи оптимального керування з використанням класичного генетичного алгоритму, а також проведено дослідження модифікованого генетичного алгоритму з додаванням у класичний алгоритм гібридних функції, а саме Fmincon і Fminsearch Patternsearch Fminunc**.**

Адаптивна система оптимального керування характеризується суттєво нижчим значенням інтегрального квадратичного критерію $I = 545$ порівняно з наявною на цукровому заводі системою керування, інтегральний квадратичний критерій якої $I = 658$. При цьому час керування також зменшився з $T = 212$ с до $T = 109$ с. Використання гібридних функцій дало змогу додатково знизити інтегральний квадратичний критерій $I = 529–541$ та прискорити роботу системи керування, витрачений час $T = 98–105$ с. Досліджено роботу методу Fmincon без використання генетичного алгоритму, така модель показала нижчий час виконання $T = 88$ с, але вище значення інтегрального квадратичного критерію $I = 604$.

Найкращі результати, за інтегральним квадратичним критерієм і часом керування ($I = 529$, $T = 98$ с), були отримані для генетичного алгоритму разом із гібридною функцією *Fmincon*.

Досліджена адаптивна система керування роботою сатуратора значно випереджає наявну за всіма основними показниками.

Висновки. Новизною результатів досліджень є наукове обґрунтування доцільності використання класичних генетичних і гібридних генетичних алгоритмів під час реалізації адаптивних систем оптимального керування.

Ключові слова: *автоматизація, цукор, сатуратор, генетичний алгоритм.*

Instructions for authors

Dear colleagues!

The Editorial Board of scientific periodical
"**Ukrainian Food Journal**"
invites you for publication of your research results.

Requirements to all texts:
Language – English.
Size of the article – 10–15 pages in Microsoft Word 2003 and earlier versions with filename extension *.doc (!)
Times New Roman, font size 14, 1 line intervals, margins on both sides – 2 cm.

The structure of the article:

1. The title of the article
2. Authors (full name and surname)
3. Institution, where the work has been performed.
4. Abstract (2/3 of a page). The structure of the abstract should correspond to the structure of the article (Introduction, Materials and methods, Results and discussion, Conclusion).
5. Keywords.
6. The main body of the article should contain the following parts:
   - Introduction
   - Materials and methods
   - Results and discussion
   - Conclusion
   - References

   If you need you can add another parts and/or divide them into subparts.
7. The information about the author (Name, surname, scientific degree, place of work, email and contact phone number).

All figures should be made in graphic editor, the font size 14.

The background of the graphs and charts should be only in white color. The color of the figure elements (lines, grid, text) – in black color.
Figures and EXCEL format files with graphs additionally should be submitted in separate files.
Photos are not recommended to be used as graphical materials.

Website of Ukrainian Food Journal: http://ufj.ho.ua

Email for all submissions and other inquiries: ufj_nuft@meta.ua

Шановні колеги!

Редакційна колегія наукового періодичного видання «**Ukrainian Food Journal**» запрошує Вас до публікації результатів наукових досліджень.

Вимоги до оформлення статей

Мова статей – англійська.

Мінімальний обсяг статті – **8 сторінок** формату А4 (без врахування анотацій і списку літератури)**.**

Стаття виконується в текстовому редакторі Microsoft Word 2003, в форматі *.doc.

Для всіх елементів статті шрифт – **Times New Roman**, кегль – **14**, інтервал – 1.

Всі поля сторінки – по 2 см.

Структура статті:

1**.** УДК**.**
2. **Назва статті.**
3. Автори статті (ім'я та прізвище повністю, приклад: Денис Озерянко).
4. *Установа, в якій виконана робота.*
5. Анотація. **Обов'язкова** структура анотації:
   - Вступ (2–3 рядки).
   - Матеріали та методи (до 5 рядків)
   - Результати та обговорення (пів сторінки).
   - Висновки (2–3 рядки).
6. Ключові слова (3–5 слів, але не словосполучень).

Пункти 2–6 виконати англійською і українською мовами.

7. Основний текст статті. Має включати такі обов'язкові розділи:
   - Вступ
   - Матеріали та методи
   - Результати та обговорення
   - Висновки
   - Література.

За необхідності можна додавати інші розділи та розбивати їх на підрозділи.

8. Авторська довідка (Прізвище, ім'я та по батькові, вчений ступінь та звання, місце роботи, електронна адреса або телефон).
9. Контактні дані автора, до якого за необхідності буде звертатись редакція журналу.

Рисунки виконуються якісно. Скановані рисунки не приймаються. Розмір тексту на рисунках повинен бути **співрозмірним** (!) тексту статті. **Фотографії можна використовувати лише за їх значної наукової цінності.**

Фон графіків, діаграм – лише білий. Колір елементів рисунку (лінії, сітка, текст) – чорний (не сірий).

Рисунки та графіки EXCEL з графіками додатково подаються в окремих файлах.

Скорочені назви фізичних величин в тексті та на графіках позначаються латинськими літерами відповідно до системи СІ.

В списку літератури повинні переважати англомовні статті та монографії, які опубліковані після 2000 року.

Правила оформлення списку літератури

В Ukrainian Food Journalвзято за основу загальноприйняте в світі спрощене оформлення списку літератури згідно стандарту Garvard. Всі елементи посилання розділяються **лише комами**.

1. Посилання на статтю:

Автори А.А. (рік видання), Назва статті, Назва журналу (курсивом), Том (номер), сторінки.

Ініціали пишуться після прізвища.

Всі елементи посилання розділяються комами.

1. Приклад:
   Popovici C., Gitin L., Alexe P. (2013), Characterization of walnut (Juglans regia L.) green husk extract obtained by supercritical carbon dioxide fluid extraction, *Journal of Food and Packaging Science, Technique and Technologies,* 2(2), pp. 104–108.

2. Посилання на книгу:

Автори (рік), Назва книги (курсивом), Видавництво, Місто.

Ініціали пишуться після прізвища.

Всі елементи посилання розділяються комами.

Приклад:

2. Wen-Ching Yang (2003), *Handbook of fluidization and fluid-particle systems*, Marcel Dekker, New York.

Посилання на електронний ресурс:

Виконується аналогічно посиланню на книгу або статтю. Після оформлення даних про публікацію пишуться слова ***Available at:*** та вказується електронна адреса.

Приклади:

1. (2013), *Svitovi naukovometrychni bazy*, available at: http://www1.nas.gov.ua/publications/q_a /Pages/scopus.aspx
2. Cheung T. (2011), *World's 50 most delicious drinks [Text]*, Available at: http://travel.cnn.com/explorations/drink/worlds–50-most-delicious-drinks–883542

Список літератури оформлюється лише латиницею. Елементи списку українською та російською мовою потрібно транслітерувати. Для транслітерації з українською мови використовується паспортний стандарт, а з російської – стандарт МВД (в цих стандартах використовуються символи лише англійського алфавіту, без хвостиків, апострофів та ін).

Зручні сайти для транслітерації:

З української мови – http://translit.kh.ua/#lat/passport

З російської мови – http://ru.translit.net/?account=mvd

Додаткова інформація та приклад оформлення статті – на сайті

http://ufj.ho.ua

Стаття надсилається за електронною адресою: ufj_nuft@meta.ua

УДК 663/664

Ukrainian Food Journal публікує оригінальні наукові статті, короткі повідомлення, оглядові статті, новини та огляди літератури.

Тематика публікацій в Ukrainian Food Journal:

Харчова інженерія
Харчова хімія
Мікробіологія
Фізичні властивості харчових продуктів
Якість та безпека харчових продуктів
Процеси та обладнання
Нанотехнології
Економіка та управління
Автоматизація процесів
Упаковка для харчових продуктів

Періодичність виходу журналу 4 номери на рік.

Результати досліджень, представлені в журналі, повинні бути новими, мати чіткий зв'язок з харчовою наукою і представляти інтерес для міжнародного наукового співтовариства.

Ukrainian Food Journal індексується наукометричними базами:
Index Copernicus (2012)
EBSCO (2013)
Google Scholar (2013)
UlrichsWeb (2013)
Global Impact Factor (2014)
Online Library of University of Southern Denmark (2014)
CABI full text (2014)
Directory of Research Journals Indexing (DRJI) (2014)
Universal Impact Factor (2014)
Directory of Open Access scholarly Resources (ROAD) (2014)
European Reference Index for the Humanities and the Social Sciences (ERIH PLUS) (2014)
Directory of Open Access Journals (DOAJ) (2015)
InfoBase Index (2015)
Chemical Abstracts Service Source Index (CASSI) (2016)
Emerging Sourses Citaton Index (2018)

Рецензія рукопису статті. Матеріали, представлені для публікування в «Ukrainian Food Journal», проходять «Подвійне сліпе рецензування» двома вченими, призначеними редакційною колегією: один є членом редколегії і один незалежний учений.

Авторське право. Автори статей гарантують, що робота не є порушенням будь-яких авторських прав, та відшкодовують видавцю порушення даної гарантії. Опубліковані матеріали є правовою власністю видавця «**Ukrainian Food Journal**», якщо не узгоджено інше.

Політика академічної етики. Редакція «Ukrainian Food Journal» користується правилами академічної етики, викладених в роботі Miguel Roig (2003, 2006) "Avoiding plagiarism, self-plagiarism, and other questionable writing practices. A guide to ethical writing". Редакція пропонує авторам статей і рецензентам прямо слідувати цьому керівництву, щоб уникнути помилок у науковій літературі.

Інструкції для авторів та інша корисна інформація розміщені на сайті
http://ufj.ho.ua

Редакційна колегія

Ukrainian Food Journal in 2018. Statistics.

1. Number of the articles

Total number	Original research articles	Review articles
54	52	2

2. Topics of the articles

Food Technology	Biotechnology and Microbiology	Processes and Equipment of Food Production	Economics and Management	Food Safety
33	2	15	3	1

3. Geography of authors

State of authors	Number of the articles	%
Ukraine	34	63,0
Turkey	3	5,6
Bulgaria	2	3,7
Moldova	2	3,7
Lithuania	2	3,7
Georgia	1	1,9
Nigeria	1	1,9
Pakistan	1	1,9
Croatia	1	1,9
Iran	1	1,9
Belarus	1	1,9
States of the author team		
Bulgaria, Macedonia	1	1,9
Bulgaria, Ukraine	1	1,9
Ukraine, Poland	1	1,9
Kazakhstan, Ukraine	1	1,9
Georgia, Ireland	1	1,9
Bangladesh, Japan	1	1,9

Наукове видання

Ukrainian Food Journal

Volume 7, Issue 4
2018

Том 7, № 4
2018

Підп. до друку 27.12.2018 р. Формат 70x100/16.
Обл.-вид. арк. 16.36. Ум. друк. арк. 15.88.
Гарнітура Times New Roman. Друк офсетний.
Наклад 100 прим. Вид. № 19н/18.

НУХТ. 01601 Київ–33, вул. Володимирська, 68

Свідоцтво про державну реєстрацію
друкованого засобу масової інформації
КВ 18964–7754Р
видане 26 березня 2012 року.